

DCE
23

5th DOCTORAL
CONGRESS
IN ENGINEERING

Book of Abstracts



*DCE23 - Symposium on Environmental
Engineering*



Book of Abstracts

of the

Symposium on Environmental Engineering

Editors:

Ana Catarina Silva, Filipe Moisés, Filipe Rocha, Inês Rodrigues,
Isabella Tomasi, Juliana Sá, Miguel Costa, Sara Pardilhó

Porto
June 2023

OUR SILVER SPONSORS



APDL

ADMINISTRAÇÃO DOS PORTOS
DOURO • LEIXÕES • VIANA

ADDVOLT®

This volume contains the peer reviewed and accepted abstracts, presented at the Symposium on Environmental Engineering, of the 5th Doctoral Congress in Engineering – DCE23, held at FEUP-U.Porto, Porto, Portugal, between June 15th and 16th, 2023.

Title: Book of Abstracts of DCE'23 Symposium on Environmental Engineering

Edited by Ana Catarina Silva, Filipe Moisés, Filipe Rocha, Inês Rodrigues, Isabella Tomasi, Juliana Sá, Miguel Costa, Sara Pardilhó

Published by: FEUP Edições

Digital version [Symposium on Environmental Engineering – DCE 2023 \(up.pt\)](#)

First edition June 2023

ISBN. 978-972-752-301-6

This book contains information obtained from authentic sources. Reasonable efforts have been made to publish reliable data information, but the authors, as well as the publisher, cannot assume responsibility for the validity of all materials or for the consequences of their use.

Trademark Notice: Product or corporate names may be trademarks or registered trademarks, and are used only for identification and explanation, without intent to infringe.

Copyright@FEUP and this Book of Abstract

OUR BRONZE SPONSORS



Welcome from Organizing Committee

We want to warmly welcome all participants to the Symposium on Environmental Engineering (SEE), held in the scope of the 5th Doctoral Congress in Engineering (DCE23) hosted at the Faculty of Engineering of the University of Porto (FEUP), Portugal, on the 15th and 16th of June 2023. This Symposium is organised by the PhD students of the Doctoral Program in Environmental Engineering (PDEA) at FEUP, with the support of the professors.

The Symposium covers a wide range of themes in the field of Environmental Engineering, aligned with the UN Sustainable Development Goals. It includes oral and poster presentations distributed mainly on the following topics:

- Water and Waste Management: towards new approaches;
- Clean Air and Energy: becoming accessible for all;
- Sustainability and Innovation: seeking a new future.

It is with great honour that we welcome the Keynote Speakers, who kindly accepted our invitation and elevate the quality of the Symposium:

- Professor Vitor Vasconcelos, an internationally renowned researcher in the field of marine and environmental science, Director of the Interdisciplinary Center of Marine and Environmental Research (CIIMAR), Full Professor at Faculty of Sciences of the University of Porto (FCUP) and Director of the Group of Blue Biotechnology and Ecotoxicology (LEGE lab).
- Eng. Susana Lopes, a senior specialist at LIPOR - *Associação de Municípios para a Gestão Sustentável de Resíduos do Grande Porto* working in the field of waste management, currently leading the new Anaerobic Digestion plant for the biomethane production.

The Symposium Organizing Committee received a total of 45 communications, distributed by 15 oral and 30 poster presentations after peer review of the extended abstracts with the valued support of the Symposium Scientific Committee.

We take this opportunity to acknowledge all authors for their contributions, and the Symposium Scientific Committee, Associate Laboratory ALiCE (integrating the R&D Units LEPABE, LSRE-LCM and CEFT), CERENA and all the other participating institutions for their support.

Porto, June 2023

The Symposium Organizing Committee

Message from the Director of the Doctoral Program in Environmental Engineering at FEUP

The Doctoral Program in Environmental Engineering (PDEA - Programa Doutoral em Engenharia do Ambiente) aims at advanced training in areas of diagnosis, prevention and resolution of environmental problems, considering a multidisciplinary approach.

The fields of specialisation include, but are not limited to: the phenomenological understanding of physical, chemical and/or biological processes that affect the quality of any environmental compartment (surface or groundwater, atmosphere, subsoil and biota) or respective sub-compartment; new industrial practices (green engineering, ecology and industrial symbiosis, environmental nanotechnology) and the use of different forms of renewable energy; the mitigation of environmental problems and development of policies and approaches related to water resources, sanitation, water supply and coastal environments or climate change; among other topics considering the transversal relationship between engineering and sustainability, and methodologies based on the concept of circular economy.

The PDEA students develop their doctoral theses in different departments of FEUP and may perform research studies in its renowned R&D units, promoting excellence in research and technological development, while acquiring transversal skills in communication, scientific ethics, innovation and entrepreneurship. The PDEA curricular component includes course units to develop some of these skills in the first year. At the end of the first year, the work produced during the course unit Thesis Project is presented to the Scientific Committee of the Doctoral Program and a successful completion gives access to the registration in the course unit Thesis, which is developed during the following years in close collaboration with the supervisors.

The PDEA students are encouraged to participate in events such as the DCE series, an opportunity to share their knowledge, and to organise the Symposium on Environmental Engineering of DCE to develop skills related to the organisation of scientific events. The Symposium reached a significant number of registrations and submissions this year, and the renowned Keynote Speakers elevate the symposia by presenting and promoting the discussion of relevant topics covered by environmental engineering.

I am very pleased to congratulate the PDEA students that are organising this edition of the Symposium on Environmental Engineering, for their commitment, perseverance, rigour and smooth organisation, and I am confident that this Symposium at DCE23 will provide a platform for sharing knowledge and discussing ideas making this event a unique experience.

More information about the Doctoral Program can be found at:

https://sigarra.up.pt/feup/en/CUR_GERAL.CUR_VIEW?pv_curso_id=703&pv_ano_lectivo=%202020&pv_origem=CUR

At the Faculty of Engineering of the University of Porto - FEUP, June 2023

Adrián M.T. Silva, Director of the PDEA - Doctoral Program in Environmental Engineering



Welcome from Organizing Committee	1
Message from the Director of the Doctoral Program in Environmental Engineering at FEUP	2
Sponsors	3
Organizing Committee	7
Scientific Committee	7
Symposium Programme – June 15th	8
Symposium Programme – June 16th	9
List of the Symposium Keynote Speakers	12
List of Oral Communications presented in the Symposium on Environmental Engineering	13
OC01. A Three-Dimensional Electrochemical Process Using Cork Granules for the Removal of Sulfamethoxazole and Trimethoprim from Water.....	15
OC02.Effect of temperature on the survival of antibiotic-resistant bacteria and related genes during conventional activated sludge wastewater treatment.....	18
OC03.Techno-economic assessment of microalgal cultures integration in urban wastewater treatment	22
OC04.Overview of volatile methylsiloxanes levels in wastewater.....	25
Acknowledgments.....	27
OC05. Identifying Critical Flood Risk Zones in Ponte da Barca, Portugal: An Objective Approach Using a 2D Hydraulic Model.....	28
OC06.Sustainable production of papaya fruit in catfish aquaponic systems.....	31
OC07.End-of-life tire microplastics: are they safe for users of artificial turf sports facilities?	34
OC08. LCD from waste mobile phones: an environmental- friendly approach to recycle Indium ..	37
OC09. Recycling agro-industrial by-products: kiwi peels as a source of antioxidants to incorporate in cosmetic products	40
OC10. Highly-conductive transparent glass substrates for efficient and scalable photoelectrochemical water splitting.....	43
OC11. Life cycle sustainability assessment of new circular valorisation streams for the next-gen lithium-based energy storage systems	46
OC12. A Tool for Working on Several Dimensions of Sustainability Based on Citizen Science.....	49
OC13. Production of slow-release fertilizers using biochar obtained from vine-canes.....	52
OC14. Potential recovery of phosphorus in the Portuguese urban sector: an opportunity for a critical raw materials supply?.....	55
OC15. One Step Forward to Sustainable Cosmetics	58
List of Posters displayed in the Symposium on Environmental Engineering	61

P01. Microalgal growth in urban wastewater: biomass production with nutrients removal.....	64
P02. Textile Effluent Treatment: from Microalgae Growth to Nutrient Removal.....	67
P03. Microalgae harvesting by flocculation followed by dissolved air flotation: the effect of a natural flocculant concentration and mixing time.....	70
P04. Adsorption capacity of two synthesized biochars and their application in pharmaceuticals removal	73
P05. Removal of Remazol Brilliant Orange dye by chitin beads modified by ionic liquid.....	76
P06. Combined adsorption and electrochemical treatments for the remediation of water containing sulfamethoxazole	79
P07. A novel approach to prepare ZnFe-MOF adsorbent and catalyst: Application in dye and drugs removal from wastewater.....	82
P08. Coagulants derived from chestnut shell and maritime pine bark extracts: preparation and use for textile effluent decolorization	85
P09. Urban Wastewater Resources Recovery - Integration of Nanofiltration and Advanced Oxidation Processes	88
P10. Design and synthesis of spherical Fe _{2.4} Cu ₁ -MOF@PAN for coloured effluent treatment	91
P11. Photocatalytic oxidation of <i>n</i> -decane in the mili-photoreactor NETmix	94
P12. NETmix crystalliser for struvite precipitation: CFD modelling of flow dynamics and distribution.....	97
P13. Photocatalytic H ₂ O ₂ generation and pollutant degradation by nonmetal doped carbon nitride	100
P14. Recycling of printed circuit board (PCB) waste as a catalyst in advanced water treatment .	102
P15. H ₂ O ₂ -assisted photocatalytic degradation of pharmaceuticals in surface waters.....	105
P16. Evaluation of temperature and nitrogen modified activated carbons as catalysts in the ozonation of emerging pollutants.....	107
P17. Generation of sulphate radical through heterogeneous catalysis for wastewater remediation	110
P18. Towards the development of a simple molecularly imprinted electrochemical sensor for the detection of carbamazepine	113
P19. Phytotoxicity Testing of Sewage Sludge and Individual Emerging Contaminants in Agricultural Soil.....	116
P20. CFD Design of a Raceway Pond Reactor: Overall geometry improvement.....	119
P21. CO ₂ /N ₂ separation using PDMS membranes with inorganic filler ZSM-5	122
P22. Automatic monitoring and measurement system for electrodegradation processes.....	125
P23. Evaluation of municipal sewage sludge compliance with Portuguese legislation for its agricultural use.....	128
P24. Incorporation of <i>Moringa oleifera</i> leaf powder and extract in cereal-based foods	131
P25. Tailoring photoelectrochemical stability of tantalum nitride for solar redox flow cells.....	134

P26. Recent advancements in identifying sources of indoor air pollution using continuous monitoring methods	137
P27. Understanding indoor air quality in private dwellings: a case study of Portuguese homes..	140
P28. Impact of PM _{2.5} in schools on asthma-related symptoms	143
P29. Indoor air quality in vehicles: Can low-cost sensors be used as CO ₂ indicators?.....	146
P30. Future shipping emissions – a review	149
Authors index	152

Organizing Committee

Chairs: Adrián Silva | FEUP

Sofia Sousa | FEUP

Arminda Alves | FEUP

Ana Silva | FEUP

Filipe Moisés M. Francisco | FEUP

Filipe Rocha | FEUP

Inês Rodrigues | FEUP

Isabella Tomasi | FEUP

Juliana Sá | FEUP

Miguel Costa | FEUP

Sara Pardilhó | FEUP

Scientific Committee

Chairs: Adrián Silva | FEUP

Sofia Sousa | FEUP

Arminda Alves | FEUP

Cidália Botelho | FEUP

Cristina Vila | FEUP

Francisco Taveira Pinto | FEUP

Joana Dias | FEUP

Maria de Lurdes Dinis | FEUP

Rita Lado | FEUP

Tânia Lopes | FEUP

Vera Homem | FEUP

Vítor Vilar | FEUP

Symposium Programme – June 15th

June 15 th , Thursday	
08:00 - 09:00	Welcoming
09:00 - 09:30	Opening Session (<u>Auditorium</u>)
09:30 - 10:00	Industry keynote lecture
10:00 - 11:00	Round table: "Early Stage Research in Industry"
11:00 - 11:30	Coffee Break (<u>Coffee Lounge</u>)
11:30 - 12:30	Plenary Session: "Sustainable Engineering for an Intelligent World" (<u>Auditorium</u>)
13:00 - 15:00	Lunch (<u>Coffee Lounge</u>) + Poster session (B Corridor) + Workshops
15:00 - 15:10	Welcoming session - Symposium on Environmental Engineering (<u>Room G129</u>) <i>Prof. Adrián Silva and Juliana Sá, FEUP</i>
15:10 - 16:00	Keynote Speaker - Professor Vitor Vasconcelos "Cyanobacteria: impact on water quality and applications in biotechnology" <i>Chaired by Prof. Cidália Botelho and Isabella Tomasi, FEUP</i>
16:00 - 16:30	Oral communications <i>Chaired by Prof. Cidália Botelho and Isabella Tomasi, FEUP</i>
#OC01	A Three-Dimensional Electrochemical Process Using Cork Granules for the Removal of Sulfamethoxazole and Trimethoprim from Water <i>(Paula V. Remor, FEUP)</i>
#OC02	Effect of temperature on the survival of antibiotic-resistant bacteria and related genes during conventional activated sludge wastewater treatment <i>(Sara Ribeirinho-Soares, FEUP)</i>
16:30 - 17:00	Coffee Break (<u>Coffee Lounge</u>)
17:00 - 18:30	Oral communications (<u>Room G129</u>) <i>Chaired by Prof. Vitor Vilar and Inês Rodrigues, FEUP</i>
#OC03	Techno-economic assessment of microalgal cultures integration in urban wastewater treatment <i>(Maria L.F. Nobre, FEUP)</i>
#OC04	Overview of volatile methylsiloxanes levels in wastewater <i>(Fábio Bernardo, FEUP)</i>
#OC05	Identifying Critical Flood Risk Zones in Ponte da Barca, Portugal: An Objective Approach Using a 2D Hydraulic Model <i>(Sayedreza Jafarzadeh, FEUP)</i>
#OC06	Sustainable production of papaya fruit in catfish aquaponic systems <i>(Ounisia Santos, FEUP)</i>

Symposium Programme – June 16th

June 16th, Friday	
08:00 - 09:00	Welcoming
09:00 - 09:40	Keynote Speaker - Eng. Susana Lopes (Room G129) "The waste as a resource" Chaired by Prof. Joana Dias and Miguel Costa, FEUP
09:40 – 10:30	Oral communications Chaired by Prof. Joana Dias and Miguel Costa, FEUP
#OC07	End-of-life tire microplastics: are they safe for users of artificial turf sports facilities? (Tiago Ferreira, FEUP)
#OC08	LCD from waste mobile phones: an environmental- friendly approach to recycle Indium (Márcia A.D. Silva, FEUP)
#OC09	Recycling agro-industrial by-products: kiwi peels as a source of antioxidants to incorporate in cosmetic products (Sandra M. Gomes, FEUP)
10:30 – 11:00	Coffee Break (Coffee Lounge)
11:00 – 11:45	Oral communications (Room G129) Chaired by Prof. Cristina Vila and Filipe Moisés, FEUP
#OC10	Highly-conductive transparent glass substrates for efficient and scalable photoelectrochemical water splitting (Telmo da Silva Lopes, FEUP)
#OC11	Life cycle sustainability assessment of new circular valorization streams for the next-gen lithium-based energy storage systems (Joana R. Gouveia, INEGI)
#OC12	A Tool for Working on Several Dimensions of Sustainability Based on Citizen Science (Daniela Amorim, FEUP)
11:45 – 11:50	Break
11:50 – 12:35	Oral communications (Room G129) Chaired by Prof. Nuno Ratola and Filipe Rocha, FEUP
#OC13	Production of slow-release fertilizers using biochar obtained from vine-canes (Olena Dorosh, ISEP)
#OC14	Potential recovery of phosphorus in the Portuguese urban sector: an opportunity for a critical raw materials supply? (Aias Lima, U. Minho)
#OC15	One Step Forward to Sustainable Cosmetics (Inês Brito, FEUP)
12:35 – 12:45	Closing Session Prof. Sofia Sousa and Ana Silva, FEUP
13:00 - 14:30	Lunch (Coffee Lounge) + Poster Session (B Corridor)
14:30 - 15:30	Award Ceremony (Auditorium)
15:30 – 16:00	Keynote Lecture by Prof. Manuel Heitor
16:00 – 16:30	Closing Session
16:30 – 17:00	Cocktail/Porto d'Honra

Poster Session, 16th of June (13:00 – 14:30 GMT+1)

Water and Waste Management: towards new approaches

- P01. Microalgal growth in urban wastewater: biomass production with nutrients removal #198
(Sara Sousa, Ana F. Esteves, José Carlos Pires, Eva Salgado)
- P02. Textile Effluent Treatment: from Microalgae Growth to Nutrient Removal #204
(Rúben A Martins, Eva M. Salgado, Ana L. Gonçalves, José C. Pires, Ana F. Esteves)
- P03. Microalgae harvesting by flocculation followed by dissolved air flotation: the effect of a natural flocculant concentration and mixing time #212
(Carolina Maia, Larissa Ramos, José CM Pires, Joana A. Loureiro, Maria Carmo Pereira)
- P04. Adsorption capacity of two synthesized biochars and their application in pharmaceuticals removal #347
(Nuria Bernárdez, Emilio Rosales, Marta Pazos, M. Ángeles Sanromán)
- P05. Removal of Remazol Brilliant Orange dye by chitin beads modified by ionic liquid #179
(Salima Benniche, Ariana Pintor, Oumissa Kebiche-Senhadji, Cidália Botelho, Claudia Fontas)
- P06. Combined adsorption and electrochemical treatments for the remediation of water containing sulfamethoxazole #330
(Verónica Poza-Nogueiras, Nuria Bernárdez, Bárbara Lomba, Marta Pazos, M. Ángeles Sanromán)
- P07. A novel approach to prepare ZnFe-MOF adsorbent and catalyst: Application in dye and drugs removal from wastewater #368
(Daniel Terrón, Emilio Rosales, Marta Pazos, M. Ángeles Sanromán)
- P08. Coagulants derived from chestnut shell and maritime pine bark extracts: preparation and use for textile effluent decolorization #191
(Isabella Tomasi, Mafalda Rodrigues, Silvia Santos, Rui Boaventura, Cidália Botelho)
- P09. Urban Wastewater Resources Recovery - Integration of Nanofiltration and Advanced Oxidation Processes #174
(Carla S Santos, Rosa Montes, Rosário Rodil, José B. Quintana, Ana I. Gomes, Vítor J.P. Vilar)
- P10. Design and synthesis of spherical Fe_{2.4}Cu₁-MOF@PAN for coloured effluent treatment #335
(Antía Fernandez-Sanromán, M^a Ángeles Sanromán, Marta Pazos, Emilio Rosales)
- P11. Photocatalytic oxidation of n-decane in the mili-photoreactor NETmix #374
(Sandra M. Miranda, Tatiana Matiazzo, Natan Padoin, Cintia Soares, Tânia F.C.V. Silva, Vítor J.P. Vilar)
- P12. NETmix crystalliser for struvite precipitation: CFD modelling of flow dynamics and distribution #405
(Laura J.R. Cullen, Isabel S. Fernandes, Ricardo J. Santos, Vítor J.P. Vilar)
- P13. Photocatalytic H₂O₂ generation and pollutant degradation by nonmetal doped carbon nitride #409
(Amanda Fujita, André Torres-Pinto, Maria J. Sampaio, Cláudia G. Silva, Joaquim L. Faria, Adrián M.T. Silva)
- P14. Recycling of printed circuit board (PCB) waste as a catalyst in advanced water treatment #404
(Marta A.P. Azevedo, Cátia A.L. Graça, Márcia A.D. Silva, Liliana M. Martelo, Helena M.V.M. Soares, Adrián M.T. Silva)
- P15. H₂O₂-assisted photocatalytic degradation of pharmaceuticals in surface waters #408
(Thalita Tavares, André Torres-Pinto, Cláudia G. Silva, Joaquim L. Faria, Adrián M.T. Silva)
- P16. Evaluation of temperature and nitrogen modified activated carbons as catalysts in the ozonation of emerging pollutants #293
(Cátia A.L. Graça, Riccardo Zema, Carla A. Orge, João Restivo, Juliana Sousa, Manuel F.R. Pereira, Olívia S.G.P. Soares)
- P17. Generation of sulphate radical through heterogenous catalysis for wastewater remediation #346
(Alba Giraldez, Marta Pazos, Ángeles Sanromán)

Water and Waste Management: towards new approaches (continuation)

- P18. Towards the development of a simple molecularly imprinted electrochemical sensor for the detection of carbamazepine #332
(Verónica Poza-Nogueiras, João G. Pacheco, Cristina Delerue-Matos)
- P19. Phytotoxicity Testing of Sewage Sludge and Individual Emerging Contaminants in Agricultural Soil #166
(Ana Sofia Fernandes, Filipe Rocha, Thiago Silva, Vera Homem)
- P20. CFD Design of a Raceway Pond Reactor: Overall geometry improvement #406
(Margarida L.R. Peixoto, Margarida S.C.A. Brito, Ricardo J. Santos, Vítor J.P. Vilar)

Sustainability and Innovation

- P21. CO₂/N₂ separation using PDMS membranes with inorganic filler ZSM-5 #255
(Inês Rodrigues, Lidia Martínez-Izquierdo, Carlos Téllez, Joaquín Coronas, Alirio Rodrigues, Vítor Vilar, Alexandre Ferreira)
- P22. Automatic monitoring and measurement system for electrodegradation processes #349
(Mario Rúa-Pereira, E. Soto, E. Gonzalez-Romero, M. Pazos, E. Rosales, M.A. Sanromán)
- P23. Evaluation of municipal sewage sludge compliance with Portuguese legislation for its agricultural use #324
(Filipe Rocha, Idalina Bragança, Nuno Ratola, Vera Homem)
- P24. Incorporation of *Moringa oleifera* leaf powder and extract in cereal-based foods #314
(Teresa Ferreira, Sandra M. Gomes, Anabela Leitão, Arminda Alves, Lúcia Santos)

Clean Air and Energy: becoming accessible for all

- P25. Tailoring photoelectrochemical stability of tantalum nitride for solar redox flow cells #357
(Filipe Moisés M. Francisco, Paula Dias, Adelio Mendes)
- P26. Recent advancements in identifying sources of indoor air pollution using continuous monitoring methods #310
(Hiten Chojer, P.T.B.S. Branco, F.G. Martins, S.I.V. Sousa)
- P27. Understanding indoor air quality in private dwellings: a case study of Portuguese homes #9
(Adhymaura Silva, Maria C. Pereira, Klara Slezakova)
- P28. Impact of PM_{2.5} in schools on asthma-related symptoms #313
(Juliana P. Sá, Pedro T.B.S. Branco, Maria C.M. Alvim-Ferraz, Fernando G. Martins, Sofia I.V. Sousa)
- P29. Indoor air quality in vehicles: Can low-cost sensors be used as CO₂ indicators? #306
(Ana Catarina T. Silva, Pedro T.B.S. Branco, Sofia I.V. Sousa)
- P30. Future shipping emissions – a review #303
(Rafael A.O. Nunes, Maria C.M. Alvim-Ferraz, Fernando G. Martins, Sofia I.V. Sousa)

Symposium Keynote Speakers



Professor Vitor Vasconcelos
Director of CIIMAR
Keynote Speaker

Thursday, June 15th – 15:00
Room G129 – DEC/FEUP

Cyanobacteria: impact on water
quality and applications in
biotechnology

Professor Vitor Vasconcelos, PhD in Biology at Faculty of Sciences of Porto University (FCUP), is a renowned scientist and researcher in the field of marine and environmental sciences, specializing in cyanobacteria secondary metabolites and their uses: toxins and molecules with biotechnological applications. With an extensive academic background and leadership roles, he is currently Director of CIIMAR - Interdisciplinary Center of Marine and Environmental Research, Full Professor at FCUP and Director of the Group of Blue Biotechnology and Ecotoxicology (LEGE lab). Over the last years, he has been involved in more than 40

projects, being coordinator of national and international research projects. Dr. Vitor Vasconcelos has more than 400 publications in SCI journals in the areas of Toxicology and Biotechnology and has supervised 65 MSC and 25 PhD students. He is also member of the European Marine Board since 2011.



Eng. Susana Lopes
Senior Specialist at LIPOR
Keynote Speaker

Friday, June 16th – 9:00
Room G129 – DEC/FEUP

The waste as a resource

Engineer Susana Lopes has a degree in Environmental Engineering from University of Aveiro and a master's degree in the same area from ESBUC Porto. She has been working in LIPOR since 1999, when she joined to the New Projects Department. In 2010 she took on the position of Director of the Production and Logistics Department; and in mid-2016 she became a Senior Technician in the International Business Office, ensuring at technical level, the promotion and stimulation of cooperation with national and international entities in the Environmental sector. Susana Lopes has been participating in multidisciplinary projects (organic recovery, textile recovery, sustainable

management of CDW, regulations applied to waste), as well as she is trainer at Academia LIPOR. Currently, she is the technical leader for the development of a new factory at LIPOR in Baguim do Monte Complex, namely an Anaerobic Digestion plant to produce biomethane. She is also member of the Board of ECN – European Compost Network.

List of Oral Communications presented in the Symposium on Environmental Engineering

Water and Waste Management: towards new approaches

1. Techno-economic assessment of microalgal cultures integration in urban wastewater treatment - Maria M.L. Nobre, Daniel Tavares, Carolina Fraga, Bruna Oliveira, Mafalda Dias, Sara Mesquita, Catarina Oliveira and José CM Pires
2. A Three-Dimensional Electrochemical Process Using Cork Granules for the Removal of Sulfamethoxazole and Trimethoprim from Water - Paula V. Remor, Sónia Figueiredo, Vítor Jorge Vilar, Cristina Soares, Luísa Correia-Sá and Cristina Delerue-Matos
3. Overview of volatile methylsiloxanes levels in wastewater - Fábio Bernardo, Nuno Ratola, Francisco Sánchez Soberón, Arminda Alves and Vera Homem
4. End-of-life tire microplastics: are they safe for users of artificial turf sports facilities? - Tiago Ferreira, Vera Homem, Francisco-Cereceda-Balic, Ximena Fadic, Arminda Alves, Nuno Ratola
5. LCD from waste mobile phones: an environmental- friendly approach to recycle Indium - Liliana M. Martelo, Márcia A.D. Silva, Hugo A.M. Bacelo
6. Effect of temperature on the survival of antibiotic-resistant bacteria and related genes during conventional activated sludge wastewater treatment - Sara SRS Soares; Olga C. Nunes; Célia M. Manaia; Vítor Jorge Vilar
7. Identifying Critical Flood Risk Zones in Ponte da Barca, Portugal: An Objective Approach Using a 2D Hydraulic Model - Sayedreza Jafarzadeh, Mahdi Alemi, Rodrigo Maia

Sustainability and Innovation: seeking a new future

8. Potential recovery of phosphorus in the Portuguese urban sector: an opportunity for a critical raw materials supply? - Aias Santino Lima, Paulo Ramisio, Sónia Figueiredo, Nídia Caetano
9. Production of slow-release fertilizers using biochar obtained from vine-canes - Olena Dorosh, Cristina Delerue-Matos and Manuela Moreira
10. Life cycle sustainability assessment of new circular valorization streams for the next-gen lithium-based energy storage systems - Joana R. Gouveia, Luís Oliveira, Belmira Neto
11. Sustainable production of papaya fruit in catfish aquaponic systems - Ounísia D Santos, Fernando Sebastião, Luis Cotrim, Judite Vieira, Raul Bernardino, Daniela Vaz, André Fonseca and Maria Rodrigues
12. Recycling agro-industrial by-products: kiwi peels as a source of antioxidants to incorporate in cosmetic products - Sandra M. Gomes, Rita Miranda and Lúcia Santos
13. One Step Forward to Sustainable Cosmetics - Inês Brito, Sara Ferreira and Lúcia Santos
14. A Tool for Working on Several Dimensions of Sustainability Based on Citizen Science - Daniela Amorim, José CM Pires and Fernando G Martins

Clean Air and Energy: becoming accessible for all

15. Highly-conductive transparent glass substrates for efficient and scalable photoelectrochemical water splitting - Telmo da Silva Lopes, Leonardo Rodrigues, Jeffrey Capitão, Dzmitry Ivanou, Paula Dias, Tânia ST Lopes and Adelio Mendes

OC01. A Three-Dimensional Electrochemical Process Using Cork Granules for the Removal of Sulfamethoxazole and Trimethoprim from Water

Paula V. Remor^{1,2,3}, Sónia A. Figueiredo³, Vítor J.P. Vilar^{1,2}, Cristina Soares³, Luísa Correia-Sá³, Cristina Delerue-Matos³

¹LSRE-LCM - Laboratory of Separation and Reaction Engineering – Laboratory of Catalysis and Materials, Faculty of Engineering, University of Porto, Rua Dr. Roberto Frias, 4200-465 Porto, Portugal, (up202010661@edu.fe.up.pt; vilar@fe.up.pt) ORCID 0000-0003-1755-5507; 0000-0003-0943-2144

²ALiCE - Associate Laboratory in Chemical Engineering, Faculty of Engineering, University of Porto, Rua Dr. Roberto Frias, 4200-465 Porto, Portugal.

³REQUIMTE/LAQV, ISEP, Polytechnic of Porto, Rua Dr. António Bernardino de Almeida 431, 4249-015 Porto, Portugal, (saf@isep.ipp.pt; cmdss@isep.ipp.pt; mlsrs@isep.ipp.pt; cmm@isep.ipp.pt) ORCID 0000-0001-8548-2528; 0000-0003-0924-9681; 0000-0003-1135-0260; 0000-0002-3924-776X.

Abstract

The main goal of this study is to develop a safe, sustainable, and cost-efficient solution for contaminants of emerging concern (CECs) removal from water as a polishing treatment that contributes to fulfilling the EU goal of efficient water resources management. The 2D and 3D electrochemical processes were tested for removing two model CECs, sulfamethoxazole (SMZ) and trimethoprim (TMP). Two types of cork granules, a 100% natural sorbent, were used as particulate electrodes in the 3D electrochemical process. The 3D electrochemical process showed a higher ability to remove both CECs than the 2D due to the increase of specific surface area and decrease of mass transfer distance. Moreover, raw cork particles had better results than thermally treated cork particles, especially for SMX.

Author Keywords. Cork, sulfamethoxazole, trimethoprim, electrochemical, wastewater treatment.

 Open Access  Peer Reviewed  CC BY

1. Introduction

The presence of contaminants of emerging concern (CECs), such as pharmaceuticals and personal care products in municipal wastewater treatment plants (WWTPs), is constantly increasing, threatening human health. To prevent the spread of these contaminants in the environment, the use of advanced treatment technologies should be evaluated (Soares et al. 2022).

The electrochemical advanced oxidation processes have been gaining interest lately, namely the three-dimensional (3D) process, in which a third electrode (particulate material) is added to the conventional electrochemical system. The particles of the third electrode act as microelectrodes, increasing the specific surface area, decreasing the distance of mass transfer and consequently improving the efficiency of the process (Correia-Sá et al. 2021).

Various adsorbent materials are used as third electrode particles. Activated carbon is the most common adsorbent, but a circular economy encourages using more sustainable and cost-effective materials. Cork, the outside bark of the cork oak tree (*Quercus suber L.*), is a natural and sustainable material used primarily for wine stoppers production. The manufacturing of cork stoppers generates a considerable quantity of cork byproducts, which can be used as a sustainable sorbent for oil spills management.

In this context, the main goal of this work is to evaluate and compare two types of cork byproducts as particulate electrodes in the 3D electrochemical process to remove two pharmaceuticals commonly present in effluents of WWTPs, sulfamethoxazole (SMX) and trimethoprim (TMP).

2. Materials and Methods

SMX and TMP individual stock solutions were prepared in methanol and stored at -10 °C. For the electrochemical experiments, a Mixed Metal Oxide (MMO) electrode (titanium-coated with RuO₂-IrO₂-TiO₂, 100×20×2 mm) was used as the anode, and stainless steel (STS) electrode (AISI-304, austenitic grade, 100×20×2 mm) was used as the cathode.

Two types of cork particles were used as third electrode: regranulated cork particles- RGC (1.0-2.0 mm) and raw cork particles - RAC (1.0-2.0 mm), both provided by Corticeira Amorim (Portugal). To produce RGC particles, a thermal treatment with water vapor at 380 °C is applied to the RAC particles. Before usage, the RAC granules were washed twice in a 2 h cycle at 60 °C, and both RAC and RGC were dried overnight in an oven at 60 °C.

The 2D and 3D electrochemical experiments were performed in an acrylic cell reactor (2x15x8 cm) with a volume capacity of 240 mL. The inter-electrodes distance was 7.5 cm. The batch experiments employed 150 mL of an aqueous solution with an initial pH of 7, containing 10 mg L⁻¹ of SMZ and TMP, 0.02 M NaCl (as the electrolyte), and were supplied with an airflow of 3000 cm³ air min⁻¹. The current intensity was maintained constant at 0.1 A. For the third electrode (3D experiments), 100 mg of the cork granules (RAC or RGC) were added between the electrodes. Aliquots were taken during the experiments (0, 5 and 10 min) and were filtered through a PTFE membrane filter with a 0.45-µm pore size (Filter-Lab®, Barcelona, Spain) prior to the analysis of SMX and TMP by HPLC-DAD (Shimadzu Corporation, Kyoto, Japan).

3. Discussion

Figure 1 shows the removal of SMX and TMP after 10 minutes using the 2D and 3D electrochemical processes with RAC and RGC particles. For the 2D process, the concentration of SMX and TMP was reduced only by 43% and 30%, respectively. However, the 3D process showed a much higher efficiency than the 2D process, for both cork particles, especially for TMP. The RAC granules achieved complete removal of SMX and TMP, considering the limit of detection of the analytical method. The RGC had a lower capacity for removing SMX than RAC.

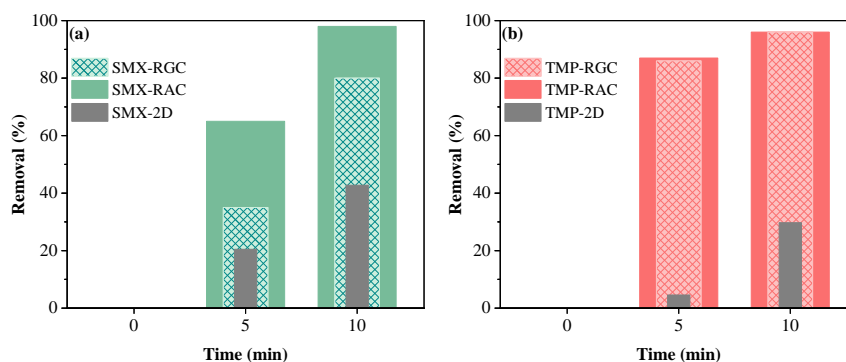


Figure 1: Removal of (a) sulfamethoxazole and (b) trimethoprim with RAC (solid-coloured columns) and RGC (patterned columns) in 3D electrochemical process and 2D electrochemical process (solid-grey columns) as a function of time.

The reaction rate of the 3D process for the removal of TMP was similar for RGC and RAC particles, but faster (around ten times) than the 2D process. For SMX, the RAC had the highest reaction rate, almost six times higher than the 2D process. In addition to the lower efficiency, the energy consumption and the electric energy per order (EE/O) for the 2D process were considerably higher than for the 3D process with RGC and RAC, reaching about 69% and 48% higher values.

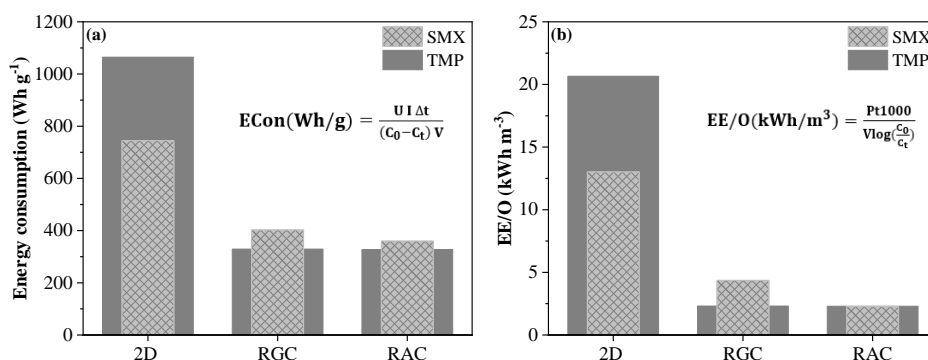


Figure 2: (a) Energy consumption and (b) electric energy per order for the 2D and the 3D processes with RGC and RAC for removal of SMX (patterned columns) and TMP (solid-columns). U - potential difference (V); I - current intensity (A); P - rated power (kW); V - volume of solution (L); t - time (h); C_0 and C_t - initial and instant t concentrations (mol/L).

4. Conclusions

The 3D electrochemical process using cork granules, a byproduct from the cork industry, as a third electrode showed a good performance for removing SMZ and TMP from aqueous solutions. The two types of granules (RGC and RAC) have similar efficiencies in removing TMP. However, for SMX, the RAC granules had the best yields. Besides the higher efficiency, the 3D electrochemical process using RAC also presented lower energy consumption and electric energy per order than the 2D process, indicating its potential for the tertiary treatment of urban wastewaters towards CECs removal.

References

- Correia-Sá, Luísa, Cristina Soares, Olga Matos Freitas, Manuela Maria Moreira, Henri Petrus Antonius Nouws, Manuela Correia, Paula Paíga, et al. 2021. "A Three-dimensional Electrochemical Process for the Removal of Carbamazepine.". In *Applied Sciences* (Switzerland) 11 (14).
- Soares, Cristina, Luísa Correia-Sá, Paula Paíga, Carlos Barbosa, Paula Remor, Olga M. Freitas, Manuela M. Moreira, et al. 2022. "Removal of Diclofenac and Sulfamethoxazole from Aqueous Solutions and Wastewaters Using a Three-Dimensional Electrochemical Process." In *Journal of Environmental Chemical Engineering* 10 (5).

Acknowledgments

This work was financially supported by i) Associate Laboratory for Green Chemistry-LAQV, supported by national funds through FCT/MCTES (UIDB/50006/2020); ii) Project OXI-e3D (POCI-01-0247-FEDER-039882), supported by the Program Portugal 2020, and cofunded by FEDER through POCI and iii) LA/P/0045/2020 (ALiCE), UIDB/50020/2020 and UIDP/50020/2020 (LSRE-LCM), funded by national funds through FCT/MCTES (PIDDAC). P. Remor acknowledges FCT for the Ph.D. grant (SFRH/BD/07543/2020).

OC02.Effect of temperature on the survival of antibiotic-resistant bacteria and related genes during conventional activated sludge wastewater treatment

Sara Ribeirinho-Soares^{1,2*}; Vasco Braga³; Sofia Cabral⁴; Vítor J.P. Vilar^{2,5}; Célia M. Manaia⁶; Olga C. Nunes^{1,2}

¹LEPABE—Laboratory for Process Engineering, Environment, Biotechnology and Energy, Faculdade de Engenharia, Universidade do Porto, Rua Dr. Roberto Frias, 4200-465 Porto, Portugal

²ALiCE – Associate Laboratory in Chemical Engineering, Faculty of Engineering, University of Porto, Rua Dr. Roberto Frias, 4200-465 Porto, Portugal

³Efacec Engenharia e Sistemas SA, Parque Empresarial Arroteia Rua Poente, 4465-591 São Mamede de Infesta, Portugal

⁴ME Water – Manvia Efacec Exploração Técnica Sistemas Ambientais do Minho, Rua Eng. Frederico Ulrich, 4470-605 Maia, Portugal

⁵LSRE-LCM – Laboratory of Separation and Reaction Engineering - Laboratory of Catalysis and Materials, Faculty of Engineering, University of Porto, Rua Dr. Roberto Frias, 4200-465 Porto, Portugal

⁶Universidade Católica Portuguesa, CBQF - Centro de Biotecnologia e Química Fina – Laboratório Associado, Escola Superior de Biotecnologia, Rua de Diogo Botelho 1327, 4169-005 Porto, Portugal

*Presenting author (saramariasoares@hotmail.com) ORCID 0000-0003-2283-8704

Abstract

Understanding the parameters influencing wastewater treatment in terms of bacteria and related ARB&ARGs turnover is crucial to prevent antibiotic resistance accumulation and further proliferation after treated wastewater discharge or reuse. Therefore, this study aimed to determine the effect of temperature on the removal of microorganisms, particularly ARB&ARGs, during wastewater treatment with conventional activated sludge (CAS). Laboratorial CAS systems were installed in an urban wastewater treatment plant (UWWTP) being operated in continuous mode at 10 °C or at ambient temperature, as a control. The remaining operating conditions were set equivalent in test and control systems. Temperature, pH, and dissolved oxygen concentration were continuously monitored. Both the final treated wastewater and the surplus sludge were examined for the prevalence of ARB&ARGs as well as the structure and composition of the bacterial community. Regardless of the operating temperature, the CAS effluents complied with EU Directive 91/271/EEC on the treatment of urban wastewater.

Author Keywords. Temperature, wastewater treatment, antibiotic-resistant bacteria, antibiotic resistance genes

 Open Access  Peer Reviewed  CC BY

1. Introduction

Bacterial antimicrobial resistance was responsible for 1.27 million deaths worldwide in 2019 and its burden is on the rise (Murray et al. 2022). Alongside, the worldwide water crisis is increasing and predicted to affect more than half of the world's population by 2050, being wastewater reuse one of the most promising ways to deal with the water shortage (The United Nations world water development report, 2017). However, it has been reported that treated wastewater, although compliant to current reuse legislation, may still contain biological contaminants like antibiotic-resistant bacteria and related genes (ARB&ARGs) (Moreira et al. 2021). These biological contaminants can lead to resistance accumulation and further proliferation, increasing the risks to human health. UWWTPs are regarded as one of the primary sources of ARGs and ARB environmental dissemination (Manaia et al., 2018). However, studies about the direct influence of the different bio-physico-chemical parameters of the wastewater treatment on the effectiveness of ARB&ARGs removal is lacking. Conventional activated sludge (CAS) is the most employed technology for the secondary treatment of urban wastewaters and has been used in developed countries for over a century (Jankowski et al., 2022). Although CAS process successfully reduces the abundance of bacteria, ARB and ARGs remain in effluents (Jankowski et al., 2022). Temperature, hydraulic retention time (HRT), and sludge retention time (SRT) are the main reported factors in CAS operation that should be addressed to optimize ARB and ARGs reduction in treated wastewater (Meng et al., 2021). It is expected that these factors have a selective effect on ARB, and therefore in ARGs, since they can influence the survival and proliferation of bacteria (Manaia et al., 2018). Therefore, understanding how these parameters influence wastewater treatment in terms of

bacteria turnover and related ARB&ARGs reduction is crucial. The goal of this study was to assess how temperature affects the removal of microorganisms, particularly ARB&ARGs, from wastewater treated with CAS.

2. Materials and Methods

Each CAS system was composed by a cylindrical reactor (6 L) and a clarifier (3 L). Both test (at 10 °C) and control (room temperature) reactors were fed continuously with real wastewater from the UWWTP primary clarifier for 56 days. The mixed liquor of each reactor was stirred continuously at 500 rpm to ensure homogenization and avoid sludge settling. The reactors were aerated in cycles of 1 h promoting a DO concentration of approximately 3 mg O₂/L, followed by 2 h without aeration to promote cycles of aerobic and anoxic conditions to promote nitrogen removal by nitrification and denitrification reactions, respectively, and to remove the biodegradable organic carbon fraction. The combined feed flux was of 5 mL min⁻¹ to achieve a HRT of 20 h. The clarifier allowed the sedimentation of the sludge and the withdrawal of the treated effluent. To ensure a high biomass load in each reactor, 75% of the settled sludge was continuously recycled. Sludge surplus was discarded once a week directly from the bottom of the clarifier resulting in a SRT of 7 days. The reactor and clarifier of the CAS system were maintained at 10 °C. The control CAS system operated at room temperature. The pH, temperature and dissolved oxygen were measured every 10 min throughout the 56 days of continuous operation. To assess the efficiency of each CAS system, the chemical and biological oxygen demand (COD and BOD₅, respectively), total phosphorus, total nitrogen and total and volatile suspended solids concentration (TSS and VSS, respectively) were determined once a week in the feed, mixed liquor, and effluent. Similarly, removal efficiencies of total heterotrophs, enterococci, enterobacteria and *Escherichia coli* were also determined once a week in the feed and effluent using culture-dependent methods. In addition, the abundance of the 16S rRNA and the *int1* genes as well as selected ARGs was determined in the feed, effluent and surplus sludge. To assess possible regrowth during storage of treated wastewater, the same parameters were determined in the effluent and feed after 7 days storage in the dark and room temperature. These parameters were also determined in three independent occasions for the UWWTP effluent, to infer about the scale effect of our CAS systems in the observed results.

3. Discussion

Regardless of the operation temperature (Control CAS at 20.2 ± 3.9 °C and Test CAS at 10.0 ± 0.9 °C) the pH of the mixed liquor of both reactors was 7.3 ± 0.3 (Figure). In Control CAS the average BOD₅ and COD removal was of 94.9 ± 1.2 % and 86.4 ± 2.3 %, respectively (Figure 1). Similarly, in Test CAS the average BOD₅ and COD removal was of 93.8 ± 1.1 % and 86.2 ± 2.7 %, respectively (Figure 2). The average TSS average removal was 93.7 ± 1.9 % for the Control CAS and 93.8 ± 1.6 % for the Test CAS (Figure 3). The effluents of both reactors complied with the European Council's directive on the treatment of urban wastewater (Directive 91/271/EEC) which legislates the maximum values of COD, BOD and TSS for safe treated wastewater disposal (125 mg O₂ L⁻¹, 25 mg O₂ L⁻¹ and 15 mg L⁻¹, respectively). Total phosphorus and nitrogen removal were approximately 46.0 ± 2.0 % and 85.0 ± 1.1 % during treatment with Control CAS and, 42.0 ± 0.9 % and 88.0 ± 2.4 % with Test CAS.

In terms of microbiological load, the log reduction of analyzed cultivable total heterotrophs, enterobacteria, *E. coli* and enterococci was of 2.6 ± 0.5, 1.4 ± 0.5, 1.8 ± 0.5 and 1.7 ± 0.3, respectively, for the Control CAS and of 2.4 ± 0.4, 1.6 ± 0.4, 2.0 ± 0.5 and 1.5 ± 0.3, respectively, for the Test CAS (Figure 3). The 16S rRNA and *int1* genes abundance decreased 1.0 ± 0.4 and 0.8 ± 0.5, respectively during biological treatment in the Control CAS and 0.9 ± 0.5 and 0.6 ± 0.8 in the Test CAS, respectively (Figure 3).

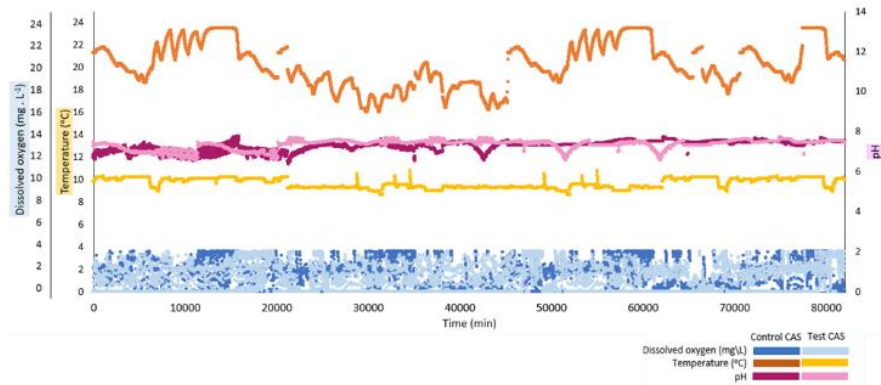


Figure 1: Temperature (°C), pH and dissolved oxygen (mg L^{-1}) inside of Control CAS and Test CAS system reactors.

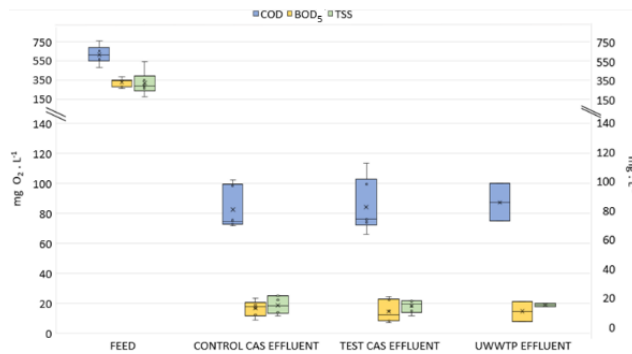


Figure 2: Chemical and biological oxygen demand (COD and BOD₅, $\text{mg O}_2 \text{ L}^{-1}$) and total suspended solids (TSS, mg L^{-1}) in the feed, control CAS effluent, test CAS effluent and UWWTP effluent.

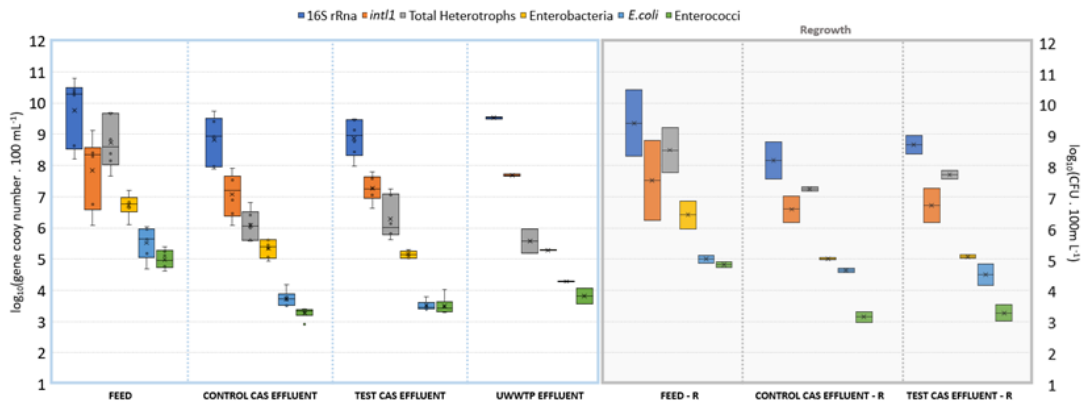


Figure 3: Abundance of 16S rRNA and *int1* genes [\log_{10} (gene copy number 100 mL^{-1})] and of cultivable total heterotrophs, enterobacteria, *E. coli* and enterococci [\log_{10} (CFU 100 mL^{-1})] in the feed and in Control CAS effluent, Test CAS effluent and UWWTP effluent immediately after treatment and the feed and Control and Test CAS effluents after 7 days storage in the dark.

4. Conclusions

The performance of the wastewater treatment was not significantly affected by the operation temperature values that simulate summer and winter in South Europe. Further studies simulating seasonal variations in North Europe and tropical regions will be carried out to conclude on the possible influence of temperature on the dissemination of ARB&ARGs.

References

Jankowski, Paul, Jaydon Gan, Tri Le, Michaela McKennitt, Audrey Garcia, Kadir Yanaç, Qiuyan Yuan, and Miguel Uyaguari-Diaz. 2022. "Metagenomic Community Composition and Resistome

- Analysis in a Full-Scale Cold Climate Wastewater Treatment Plant.” *Environmental Microbiomes* 17 (1): <https://doi.org/10.1186/s40793-022-00398-1>.
- Manaia, Célia M., Jaqueline Rocha, Nazareno Scaccia, Roberto Marano, Elena Radu, Francesco Biancullo, Francisco Cerqueira, et al. 2018. “Antibiotic Resistance in Wastewater Treatment Plants: Tackling the Black Box.” *Environment International* 115 (6): <https://doi.org/10.1016/j.envint.2018.03.044>.
- Meng, Lingwei, Yuzhe Zhao, Xiangkun Li, Yanli Kong, Jingbo Guo, and Mingwei Liu. 2021. “The Effect of Bacterial Functional Characteristics on the Spread of Antibiotic Resistance Genes in Expanded Granular Sludge Bed Reactor Treating the Antibiotic Wastewater.” *Ecotoxicology and Environmental Safety* 225 (12): <https://doi.org/10.1016/j.ecoenv.2021.112714>.
- Moreira, Nuno F.F., Sara Ribeirinho-Soares, Ana Teresa Viana, Cátia A.L. Graça, Ana Rita L. Ribeiro, Nadine Castelhana, Conceição Egas, M.Fernando R. Pereira, Adrián M.T. Silva, and Olga C. Nunes. 2021. “Rethinking Water Treatment Targets: Bacteria Regrowth under Unprovable Conditions.” *Water Research* 201 (8): <https://doi.org/10.1016/j.watres.2021.117374>.
- Murray, Christopher J.L., Kevin Shunji Ikuta, Fablina Sharara, Lucien Swetschinski, Gisela Robles Aguilar, Authia Gray, Chieh Han, et al. 2022. “Global Burden of Bacterial Antimicrobial Resistance in 2019: A Systematic Analysis.” *The Lancet* 399 (10): [https://doi.org/10.1016/S0140-6736\(21\)02724-0](https://doi.org/10.1016/S0140-6736(21)02724-0).
- Nnadozie, Chika F., Sheena Kumari, and Faizal Bux. 2017. “Status of Pathogens, Antibiotic Resistance Genes and Antibiotic Residues in Wastewater Treatment Systems.” *Reviews in Environmental Science and Bio/Technology* 2017 16:3 16 (3): <https://doi.org/10.1007/S11157-017-9438-X>.
- Report, UN Water - The United Nations World Water Development, and undefined 2017. “Wastewater: The Untapped Resource. Facts and Figures.”

Acknowledgments

This work was financially supported by: UIDB/00511/2020 and UIDP/00511/2020 (LEPABE), UIDB/50020/2020 and UIDP/50020/2020 (LSRE-LCM) and LA/P/0045/2020 (ALiCE) funded by national funds through FCT/MCTES (PIDDAC). Sara Ribeirinho-Soares acknowledges the Portuguese Foundation for Science and Technology (FCT) for her PhD grant (PD/BD/05480/2021), financed by national funds of the Ministry of Science, Technology and Higher Education and the European Social Fund (ESF) through the Human Capital Operational Programme (POCH).

OC03. Techno-economic assessment of microalgal cultures integration in urban wastewater treatment

Maria L.F. Nobre^{1,2*}, Daniel Tavares^{1,2}, Carolina Fraga^{1,2}, Bruna Oliveira^{1,2}, Mafalda Dias^{1,2}, Sara Mesquita^{1,2}, Catarina M. Oliveira^{1,2}, José C.M. Pires^{1,2}

¹LEPABE – Laboratório de Engenharia de Processos, Ambiente, Biotecnologia e Energia, Faculty of Engineering, University of Porto, Rua Dr. Roberto Frias, 4200-465 Porto, Portugal



²ALiCE – Associate Laboratory in Chemical Engineering, Faculty of Engineering, University of Porto, Rua Dr. Roberto Frias, 4200-465 Porto, Portugal

*Presenting author (up201806760@up.pt) ORCID [0009-0004-2659-4596](https://orcid.org/0009-0004-2659-4596)

Abstract

Microalgae culturing in municipal wastewater treatment plants (WWTP) can be a solution to lower the effluent's nitrogen (N) and phosphorus (P) concentrations. Additionally, microalgae can facilitate a circular approach to these plants by recycling and reusing material or energetic streams. In this work, a techno-economic assessment of the integration of microalgae culture (*Chlorella vulgaris*) on a northern Portugal WWTP tertiary treatment was performed, resulting in: (i) a 7,377 m³ d⁻¹ treated water flow; (ii) the treatment of 107,736 kg d⁻¹ of sludge; (iii) a required CO₂ flow of 1,667 kg d⁻¹ received from external units, generating income due to carbon credits; (iv) a fertiliser production of 4,330 kg d⁻¹; and (v) 10,874 kWh d⁻¹ of energy production for autoconsumption. Therefore, by integrating this system, the WWTP can achieve yearly gross earnings of approximately 600,000 €.

Author Keywords. Municipal wastewater, wastewater treatment, tertiary treatment, *Chlorella vulgaris*

 Open Access  Peer Reviewed  CC BY

1. Introduction

Due to population growth, increasing demand for resources, such as clean water, exceeds the capacity for natural replenishment. Furthermore, the current take-make-dispose municipal wastewater treatment processes are under tremendous economic and environmental pressure because of high energy consumption, greenhouse gas emissions, and waste generation (Zhang and Liu 2022). As a result, a transition from a linear to a circular economy approach is imperative. This way, the integration of microalgae (e.g., *Chlorella vulgaris*) in municipal wastewater tertiary treatment is an emerging circular solution that can be applied to already existing wastewater treatment plants (WWTP). The cultivation of microalgae removes the nutrients (N and P) present in wastewater, thus decreasing the nutrient load and avoiding eutrophication in the receiving aquatic environment. Moreover, the generated algal biomass can be used to produce biogas by anaerobic digestion. The digestate produced can contribute to an additional value chain as a nutrient-rich fertiliser (Hasport et al. 2022). The present work, schematically represented in Figure , proposes the introduction of a tertiary treatment system with biomass production in open ponds, CO₂ uptake, energy recovery, and sludge valorisation of municipal wastewater in a northern Portugal WWTP. In this study, the economic viability of the proposed process was evaluated.

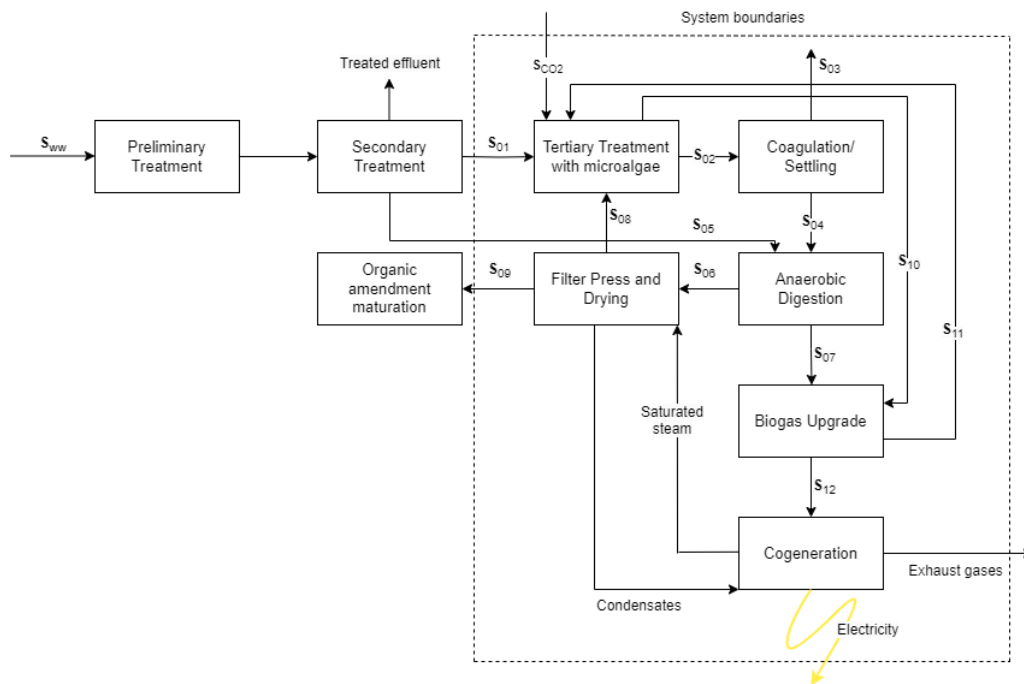


Figure 1: Process flowchart representing the different stages of the process and streams.

2. Materials and Methods

To study the viability of this process, different steps were taken: (i) mass balances to characterise process streams and determine external requirements (such as CO₂); (ii) main equipment design; (iii) energy requirements and production; and (iv) cost and revenue estimation. In this study, assumptions regarding typical wastewater composition, N and P removal efficiencies of primary and secondary treatments, biomass growth kinetics, equipment efficiencies, dimensioning ratios, and specifications were made based on available literature.

3. Results and Discussion

3.1. Mass balances

The process streams (schematically represented in Figure) are characterised in Table 1, according to the performed mass balances.

Streams	Flow rate	Streams	Flow rate
S _{ww}	44,336 m ³ d ⁻¹	S ₀₆	162,591 kg d ⁻¹
S ₀₁	7,235 m ³ d ⁻¹	S ₀₇	1,263 Nm ³ d ⁻¹
S _{CO2}	1,667 kg d ⁻¹	S ₀₈	154 m ³ d ⁻¹
S ₀₂	7,389 m ³ d ⁻¹	S ₀₉	4,330 kg d ⁻¹
S ₀₃	7,377 m ³ d ⁻¹	S ₁₀	758 m ³ d ⁻¹
S ₀₄	11,971 kg d ⁻¹	S ₁₁	758 m ³ d ⁻¹
S ₀₅	107,736 kg d ⁻¹	S ₁₂	1,263 Nm ³ d ⁻¹

Table 1: Mass balances to the process flow streams.

3.2. Economic assessment

An economic analysis was performed to evaluate the process' feasibility, where the fixed capital investment (CapEx), annual production costs (OpEx), and annual revenues were considered. The determined values are presented in Table 2. The fixed capital investment encompasses purchasing major equipment (bioreactors; coagulation tank and mixer; clarifier; anaerobic digester and heat exchanger; absorption columns; combined heat and power unit and filter press), as well as direct and indirect costs; while the annual production costs, which include variable and fixed costs, are related to the coagulant requirements, miscellaneous materials, electricity requirements, repair and maintenance, local taxes and insurance. The annual revenues include the profit from: (i) the CO₂ received from other industries; (ii) the consumption of electrical and thermal energy produced; (iii) the recycling of sludge, since these do not need to be transported to a treatment facility; and (iv) the produced fertiliser.

CapEx	5.9 M€
OpEx	1.3 M€
Annual revenues	1.9 M€
Annual gross earnings	600,000 €

Table 2: Economic parameters (annual) obtained for the proposed process.

The adoption of a more circular approach to WWTP operation, with microalgae cultivation as a tertiary treatment, can result in additional annual gross earnings of approximately 600,000 €.

4. Conclusions

This study presents an economically and environmentally advantageous solution to WWTP operation by integrating microalgae in the tertiary treatment stage. This solution presented benefits related to wastewater treatment, material reuse and energy production, and profits of approximately 600,000 € per year.

References

- Hasport, N., D. Krahe, C. M. Kuchendorf, S. Beier, and U. Theilen. 2022. "The potential impact of an implementation of microalgae-based wastewater treatment on the energy balance of a municipal wastewater treatment plant in Central Europe." *Bioresource Technology* 347: 126695. <https://doi.org/10.1016/j.biortech.2022.126695>.
- Zhang, Xiaoyuan, and Yu Liu. 2022. "Circular economy is game-changing municipal wastewater treatment technology towards energy and carbon neutrality." *Chemical Engineering Journal* 429: 132114. <https://doi.org/10.1016/j.cej.2021.132114>.

Acknowledgements

This work was financially supported by: (i) LA/P/0045/2020 (ALiCE) and UIDB/00511/2020-UIDP/00511/2020 (LEPABE), funded by national funds through FCT/MCTES (PIDDAC); and (ii) Project PhotoBioValue (ref. PTDC/BTA-BTA/2902/2021), funded by FEDER funds through COMPETE2020-Programa Operacional Competitividade e Internacionalização (POCI) and by national funds (PIDDAC) through FCT/MCTES.

OC04. Overview of volatile methylsiloxanes levels in wastewater

Fábio Bernardo^{1,2*}, Nuno Ratola^{2,3}, Francisco Sánchez-Soberón³, Arminda Alves^{2,3}, Vera Homem^{2,3}

¹ LSRE-LCM - Laboratory of Separation and Reaction Engineering – Laboratory of Catalysis and Materials, Faculty of Engineering, University of Porto, Rua Dr. Roberto Frias, 4200-465 Porto, Portugal

² ALiCE - Associate Laboratory in Chemical Engineering, Faculty of Engineering, University of Porto, Rua Dr. Roberto Frias, 4200-465 Porto, Portugal

³ LEPABE - Laboratory for Process Engineering, Environment, Biotechnology and Energy, Faculty of Engineering, University of Porto, Rua Dr. Roberto Frias, 4200-465 Porto, Portugal

*Presenting author (fabiobernardo@fe.up.pt) ORCID 0000-0002-8935-5689

Abstract

In the last decade, volatile methylsiloxanes (VMSs) have come under scrutiny for their potential toxicity, persistence and environmental risk. The aim of this work was to monitor the concentration of seven VMSs (D3, D4, D5, D6, L3, L4 and L5) in wastewater samples collected in a wastewater treatment plant (WWTP) and perform a risk assessment in the discharged effluent. Cyclic VMSs (namely D4, D5, D6) were dominant, with similar concentrations to those found in literature, being D5 the highest, reaching up to 18 $\mu\text{g L}^{-1}$ in the influent. The concentrations decreased along the WWTP stages, reaching up to 0.7 $\mu\text{g L}^{-1}$ for D5, in the effluent. This was mainly due to volatilization and sorption to sewage sludge in the secondary treatment. Most effluent samples did not present environmental risk, however, some indicated minimal risk. Further locations should be assessed to compare VMSs profiles in different regions.

Author Keywords. Volatile Methylsiloxanes; Wastewater; Gas chromatography – mass spectrometry; Environmental Monitoring

 Open Access  Peer Reviewed  CC BY

1. Introduction

Volatile methylsiloxanes (VMSs) are chemically synthesized organic compounds with $-\text{Si}(\text{CH}_3)_2\text{-O}$ units, organized in a linear (Ln) or cyclic (Dn) structure, where “n” is the number of Si atoms (Rücker and Kümmerer, 2014). They have been used for decades in a wide range of industrial processes and commercial applications, especially in the formulations of personal care products (PCPs). After being used, residues of these compounds are discharged down-the-drain, reaching wastewater treatment plants (WWTPs). Several environmental regulators across the world have labeled VMSs as high-volume production chemicals, with their annual global production reaching seven million tons in 2019 (Garside, 2020). They have also been identified as persistent, with the potential to bioaccumulate and be toxic to some aquatic organisms (Bernardo et al., 2023). Recently, the European Union has started to regulate D4 and D5 at less than 0.1% in wash-off PCPs, to prevent their release in harmful concentrations from WWTPs into the surrounding environment, causing a potential threat to the aquatic media (ECHA, 2019).

A 1-year sampling campaign was carried out to study VMSs concentrations in composite wastewater samples collected at a WWTP. All samples were analyzed in duplicate. This work presents an overview of the detected levels of seven VMSs (D3-D6 and L3-L5) using a fast and green extraction approach followed by gas chromatography-mass spectrometry (GC-MS) analysis.

2. Materials and Methods

Four cyclic VMSs (D3, D4, D5, D6) and three linear VMSs (L3, L4, L5) were used in the experiments. Tetrakis(trimethylsilyloxy) silane (M4Q) was selected as internal standard. All standards were purchased from Sigma-Aldrich (St. Louis, MO, USA) with a purity >97%. Stock solutions in *n*-hexane (1.0 g L⁻¹) were initially prepared. From these, mix stock solutions (0.5 and 2.5 mg L⁻¹) were diluted in acetone. The same solvent was used for M4Q (5 mg L⁻¹). To maintain solutions stability, the storage was done at -20 °C in the absence of light. The *n*-hexane ($\geq 95\%$) was purchased from VWR (Fontenaysous-Bois, France) and acetone ($\geq 99.8\%$) from Merck (Darmstadt, Germany). Air Liquide

(Maia, Portugal) supplied both helium (99.999%) and nitrogen (99.999%), for the GC-MS and solvent evaporation, respectively.

3. Results and Discussion

Consumers behaviour in the region served by the WWTP have a direct impact on the levels of VMSs obtained in the influent, since the use of different types of products will induce variability in the results. Overall, three cyclic congeners (D4, D5, D6) were dominant, representing more than 90% of VMSs. The concentration ranges and mean values of linear VMSs were lower than cyclic siloxanes, since cyclic VMSs are more prevalent in the PCPs formulations, which are considered one of the main sources of these compounds. In the influent, D5 and D6 were dominant, with concentrations similar to those found in other WWTPs worldwide. The highest concentrations reached $18 \mu\text{g L}^{-1}$ for D5, $3 \mu\text{g L}^{-1}$ for D6 and $0.9 \mu\text{g L}^{-1}$ for D4, while for linear VMSs, the concentrations were lower than $0.3 \mu\text{g L}^{-1}$. A decrease in VMSs concentrations was observed from influent to effluent, being ascribed to removal along the WWTP, mainly due to volatilization and sorption to sludge. Only D5, L5 and D6 were detected in the effluent, reaching up to $0.7 \mu\text{g L}^{-1}$ for D5, $0.2 \mu\text{g L}^{-1}$ for D6 and $0.02 \mu\text{g L}^{-1}$ for L5. This may be explained by VMSs inherent chemical characteristics, since their volatility decreases when increasing the chain length, reducing their chances to be removed by volatilization during early stages of water treatment. The results also showed that it is important to monitor VMSs concentrations throughout the year to study the effect of climate on the results, since isolated assessments may not truly characterize the conditions and lead to an underestimation of the actual discharge scenario. Toxicity data was collected for VMSs (short- and long-term) to assess environmental risk. According to the risk quotients (RQ), roughly one third of the samples presented minimal risk (RQ between 0.01 and 0.1). However, in WWTPs without secondary treatment or in point discharges with higher loads, the risk may be high enough to cause negative consequences for the environment. Thus, further monitoring is advised. Other locations should also be assessed to compare scenarios of exposure, namely different types of treatment, cities with different population density and different climates.

4. Conclusions

The results seem to indicate that the more volatile congeners, such as D3 and L3, tend to volatilize in the first steps of the treatment, while the more lipophilic (D5, L5, D6) are still present in the final effluent and can therefore be discharged to the aquatic receptor, possibly causing risk, if certain conditions are met (*e.g.*, discharges from illegal sewer connections, river flow droughts, release of untreated combined sewage (bypass) during stormwater events). During wastewater treatment, the most lipophilic VMSs may enter the sludge treatment line, causing major equipment problems when digested, since it promotes their release into the biogas, where the VMSs further convert into microcrystalline silicon dioxide particles, causing internal damage in turbines and cogeneration engines.

References

- Bernardo, F., Alves, A. and Homem, V. 2022. "A review of bioaccumulation of volatile methylsiloxanes in aquatic ecosystems". *Science of the Total Environment*. 153821. Accessed 16 April, 2023. DOI: 10.1016/j.scitotenv.2022.153821
- ECHA (European Chemicals Agency). 2019. "Annex XV Restriction Report. Proposal for Restriction. D4, D5, D6". Accessed 16 April, 2023. <https://echa.europa.eu/-/ten-new-substances-added-to-the-candidate-list>
- Garside, M. 2020. "Silicon – statistics & facts". Accessed 16 April, 2023. <https://www.statista.com/topics/1959/silicon/>

Rücker, C., Kümmerer, K. 2014. "Environmental Chemistry of Organosiloxanes". *Chemical Reviews*. 115(1):466-524. Accessed 9 April, 2021. DOI: 10.1021/cr500319v

Acknowledgments

This work was financially supported by: (i) LA/P/0045/2020 (ALiCE), UIDB/50020/2020 and UIDP/50020/2020 (LSRE-LCM), funded by national funds through FCT/MCTES (PIDDAC); (ii) LA/P/0045/2020 (ALiCE), UIDB/00511/2020 and UIDP/00511/2020 (LEPABE), funded by national funds through FCT/MCTES (PIDDAC); (iii) Project PTDC/ASP-PLA/29425/2017 - POCI-01-0145-FEDER-029425 - funded by FEDER funds through COMPETE2020 – Programa Operacional Competitividade e Internacionalização (POCI) and by national funds (PIDDAC) through FCT/MCTES; (iv) Project PTDC/CTA-AMB/32084/2017 - POCI-01-0145-FEDER-032084- funded by FEDER funds through COMPETE2020 – Programa Operacional Competitividade e Internacionalização (POCI) and by national funds (PIDDAC) through FCT/MCTES; (v) Project "HealthyWaters – Identification, Elimination, Social Awareness and Education of Water Chemical and Biological Micropollutants with Health and Environmental Implications", with reference NORTE-01-0145-FEDER-000069, supported by Norte Portugal Regional Operational Programme (NORTE 2020), under the PORTUGAL 2020 Partnership Agreement, through the European Regional Development Fund (ERDF); (vi) PhD Grant PD/BD/137758/2018 – Fábio Bernardo, supported by FCT PhD programme, under the Portugal 2020 Partnership Agreement and European Social Fund (ESF); (vii) National funds through FCT – Fundação para a Ciência e a Tecnologia, I.P., under the Scientific Employment Stimulus - Individual Call - CEECIND/00676/2017 (Vera Homem). The authors wish to express their gratitude to the wastewater treatment entity that participated in this study.

OC05. Identifying Critical Flood Risk Zones in Ponte da Barca, Portugal: An Objective Approach Using a 2D Hydraulic Model

Sayedreza Jafarzadeh¹, Mahdi Alemi¹, Rodrigo Maia¹



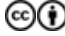
¹Departamento de Engenharia civil, Faculdade de Engenharia, Universidade do Porto, Rua Dr. Roberto Frias, 4200-465 Porto, Portugal

*Presenting author (up202003222@edu.fe.up.pt) ORCID 0000-0001-8681-5865

Abstract

During the last few decades, climate change, urbanization, and ecological concerns are all driving the need for flood management strategies. Human activity in floodplains is inevitable with much development in flood-prone areas. The objectives of this research are based on assessment of critical flood risk zones with the two-dimensional (2D) hydraulic (Iber+) model in the river Lima basin, Ponte da Barca, Portugal. 2D overland simulations were conducted to visualize the effects of an urban flood event in 2016. The model was evaluated with photos taken at control areas during the flood event on 12th-13th Feb 2016 and for 100 years return period streamflow series. The impact of the Vada river tributary on the water depth, at the Ponte da Barca station, is also considered. The results show a decrease in water depth in the Ponte da Barca station, when the Vada river backwater effect during floods is not considered.

Author Keywords. Flood management strategies, Flood characteristics, Two-dimensional hydraulic model, Hydrodynamic model.

 Open Access  Peer Reviewed  CC BY

1. Introduction

Climate change is increasingly threatening Europe's ecosystems and biodiversity, with floods being recognized as significant hazards (Bruwier et al. 2018) (Chen, Leandro, and Djordjević 2015). Urban centers, including Ponte da Barca, Portugal, face challenges due to inadequate drainage systems and expanding impervious surfaces. To address these concerns, this study utilizes a two-dimensional hydraulic model to identify areas at high risk of flooding (Teng et al. 2017) and assess the influence of the Vada river tributary downstream of Ponte da Barca, specifically focusing on analyzing the backwater effect on water elevation in order to understand its impact. By providing valuable insights, the findings contribute to the development of effective flood management strategies, minimizing adverse impacts on the community and environment. This research supports the ongoing paradigm shift towards proactive risk reduction and mitigation in flood management, crucial in the face of climate change.

2. Materials and Methods

This study employed a two-dimensional hydraulic model to analyze flooding in Lima river basin near Ponte da Barca. The objectives included understanding flow dynamics, defining water levels and paths during flooding, identifying flood-contributing zones along the riverbanks, determining areas directly affected by flooding, and assessing the influence of the Vada river tributary on water depth at the Ponte da Barca hydrometric station. The study utilized a high-resolution picture in the Iber+ software to define the study area's geometry and incorporated bridge piers for improved accuracy. Flow hydrographs were derived from rainfall records, and an unstructured mesh with 719,578 cells was used. Elevation data came from a 2m resolution Digital Elevation Model (DEM). The simulation covered a 52-hour period (4 hours for warming up), including the reported flood event in February 2016, and results were saved at hourly intervals for comparison with measured flow data at the Ponte da Barca station.

3. Discussion

The hydraulic model simulations in this study provided valuable insights into the characteristics of flooding in Ponte da Barca. Various features of the model were used to present the results, including water depth, water elevation, and water velocity (Pinho et al. 2015). These parameters

allowed for a detailed understanding of the areas affected by each flood event. The study utilized data from the flood event that occurred in the river Lima basin from February 12th to 13th, 2016, as reported by SNIRH. The inlet flow for the Vada river was assigned as 3.5% of the Lima River streamflow. Benchmark points were defined at the Ponte da Barca hydrometric station with specific coordinates. The results illustrate the temporal variation of water depth changes over a duration of 187,200 seconds.

For model validation, the upstream flood discharge of the Lima River was assigned as 3,022 m³/s for a period of 5 hours (18,000 seconds) (Bussi and Ortiz 2016). This discharge corresponded to the peak flow with a return period of 100 years, as reported by APA (APA 2014) for the selected reach of the Lima River. Assigning 5 hours of discharge allowed for steady flow at the final time step of the simulation. The concept of return period corresponding to the probability of an event to occur, a flood with a return period of 100 years has a 1% chance of occurrence each year. However, the cumulative probability is much greater considering the exposure to the risk over multiple years. The calculated water elevation by the final model at the benchmark point was 24.77 m. This value was compared to two historical values at the benchmark location, which were reported as 24.42 m in 1987 and 24.25 m in 1909. These comparisons provide an indication of the accuracy and reliability of the model's predictions.

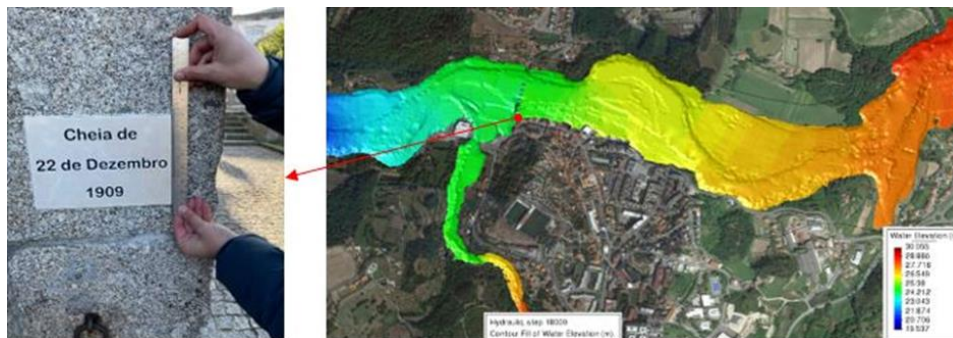


Figure 1-Historical Water elevation benchmark- Model water elevation for return period of 100 years

The validation of the hydraulic model has shown good of river flow results for flood events and a good representation of the areas affected by these flood events. The final step was to focus on the Vada river's effect in the water depth in the Ponte da Barca station. For this purpose, the inlet flow of the Vada River was considered null. Two simulations with no inflow from the Vada River were made to see how it can affect the results for the flood event occurred 12th-13th Feb 2016 and for the peak flow with return period of 100 years, as follows:

1. Inlet flow with a maximum of 1100 m³/s on 12th-13th Feb 2016 in Lima River (with no streamflow in Vada river) shows a decrease in the average water depth equal to 8 cm for 52 hours.
2. Simulation of a 100 years of return period inflow of 3022 m³/s: the water depth goes down for 12 cm (with no Vada River inflow).

4. Conclusions

In conclusion, the findings from the hydrodynamic model applied to the Ponte da Barca region within the river Lima basin highlight its effectiveness in accurately simulating and determining various flood characteristics, including water depth, water elevation, and the areal extent of the affected area. This contributes significantly to our understanding of flooded regions during extreme events.

This study further concludes that the presence of the Vada river, which joins the Lima River downstream of Ponte da Barca, has the potential to significantly influence water levels during severe flooding. The consequences of this phenomenon are particularly pronounced in agricultural areas, leading to substantial damage to crops. Additionally, while the impact on residential land is

currently limited, the projected increase in urbanization within this vicinity suggests that more land may soon be subject to settlement.

References

- APA. 2014. "Elaboration of Specific Cartography on Flood Risk for Mainland Portugal".
- Bruwier, M., A. Mustafa, D. G. Aliaga, P. Archambeau, S. Ercicum, G. Nishida, X. Zhang, M. Piroton, J. Teller, and B. Dewals. 2018. "Influence of Urban Pattern on Inundation Flow in Floodplains of Lowland Rivers." *Science of the Total Environment* 622–623: 446–58. <https://doi.org/10.1016/j.scitotenv.2017.11.325>.
- Bussi, G, and E Ortiz. 2016. "Using Post-Flood Surveys and Geomorphologic Mapping to Evaluate Hydrological and Hydraulic Models : The Flash Flood of the Girona River (Spain) in 2007." *JOURNAL OF HYDROLOGY*. <https://doi.org/10.1016/j.jhydrol.2016.04.039>.
- Chen, Albert S, Jorge Leandro, and Slobodan Djordjević. 2015. "Urban Water Journal Modelling Sewer Discharge via Displacement of Manhole Covers during Flood Events Using 1D/2D SIPSON/P-DWave Dual Drainage Simulations." <https://doi.org/10.1080/1573062X.2015.1041991>.
- Pinho, José, Rui Ferreira, Luís Vieira, and Dirk Schwanenberg. 2015. "Comparison Between Two Hydrodynamic Models for Flooding Simulations at River Lima Basin." *Water Resources Management* 29 (2): 431–44. <https://doi.org/10.1007/s11269-014-0878-6>.
- Teng, J., A. J. Jakeman, J. Vaze, B. F.W. Croke, D. Dutta, and S. Kim. 2017. "Flood Inundation Modelling: A Review of Methods, Recent Advances and Uncertainty Analysis." *Environmental Modelling and Software* 90: 201–16. <https://doi.org/10.1016/j.envsoft.2017.01.006>.

Acknowledgments

This work is scientifically supported by Dr. Mahdi Alemi and Professor Rodrigo Maia in Hydraulic Water Resource and Environment Group of the Civil Engineering Department at the University of Porto.

OC06.Sustainable production of papaya fruit in catfish aquaponic systems

Ounísia Santos^{1,2*}, Fernando Sebastião^{1,2}, Luís Cotrim^{1,2}, Judite Vieira^{1,2}, Raul Bernardino^{1,2}, Daniela Vaz^{1,2}, André Fonseca³, Maria Rodrigues³

¹ LSRE-LCM - Laboratory of Separation and Reaction Engineering – Laboratory of Catalysis and Materials, Polytechnic of Leiria, 2411-901 Leiria, Portugal

² ALiCE - Associate Laboratory in Chemical Engineering, Faculty of Engineering, University of Porto, Rua Dr. Roberto Frias, 4200-465 Porto, Portugal


³ School of Technology and Management, Polytechnic of Leiria, 2411-901 Leiria, Portugal

*Presenting author (ounisia.santos@ipleiria.pt) ORCID 0000-0001-5007-5252

Abstract

Aquaponic systems are a sustainable solution to overcome poor water and nutrient management in the agricultural sector. Given the growing commercial interest in papaya (*Carica papaya*) fruit, an aquaponic system was used to study productivity. The system was monitored to assess plants' growth and health status, water quality, and greenhouse environmental conditions. Crop productivity shows promising results since the quantity and quality of the fruit are quite satisfactory. Improved water and nutrient use efficiency was obtained, and the values were in the adequate range for growing plants. Challenges to sustainability center around balancing the aquaponic system to maximize production outputs to satisfy the demand for papaya fruit.

Author Keywords. Sustainability, Water Management, Aquaponics, Papaya (*Carica papaya*), African catfish (*Clarias gariepinus*)

 Open Access  Peer Reviewed  CC BY

1. Introduction

Urban development and agriculture are the main reasons for the increasing pressure on freshwater resources. Agriculture usage represents 69% of global freshwater, and usually, water for food production is used inefficiently (United Nations 2021). Solutions that aim for more efficient water management in the agricultural sector, inducing water reuse and soil conservation, are an alternative to conventional agriculture (Tomasi et al. 2014). Aquaponic systems are a promising solution, defined as a soilless agriculture system that synergistically combines two food production systems (aquaculture and hydroponics), in a more sustainable and symbiotic environment where nutrients and water are kept in recirculation (Maucieri et al. 2017). In these systems, nutrients for plant growth are produced through fish excretion as a result of feeding and are transformed by the action of bacteria (Lennard and Leonard 2004).

The African catfish (*Clarias gariepinus*) is one of the most popular fish species in aquaponics (Pinho et al. 2021), due to its fast growth, eating habits (omnivorous), and tolerance to environmental stress (Adeshina et al. 2021). Papaya (*Carica papaya*) is one of the most grown tropical fruits and has become an important commercial fruit crop worldwide, due to its high productivity, nutritional value, and functionality. Papaya ripe fruit is rich in vitamins A and C, folate, as well as calcium, and its juicy fruit with a sweet flavour is very appreciated (Zhou et al. 2021).

Thus, this research aimed to study a more sustainable and innovative option to produce papaya fruits, to satisfy the high demand and evaluate tree productivity and improvements in the aquaponics systems.

2. Materials and Methods

The study was conducted in a greenhouse at the academic facilities of the Polytechnic of Leiria, city of Leiria (latitude 39°44'37" N longitude 8°48'25" O and 33 m altitude above sea level), using an integrated aquaponic system comprising a fish-rearing tank; a drum filter linked to a sedimentation tank; a biofilter for nitrification; a deep water culture (DWC) hydroponic unit for plant production and a sump tank. The system had a water volume capacity of 6450 L under permanent aeration and constant recirculation with an estimated hydraulic residence time (HRT) of 2.4 h. The fish tank contained 7 African catfish varying in length 77.6 ± 6.0 cm (body weight: 3.64 ± 0.34 kg), fed with a commercial feed twice a day at 100 g/day.

Tank and DWC unit water physicochemical parameters such as pH, oxidation-reduction potential (ORP), dissolved oxygen (OD), temperature (T), electric conductivity (EC), and total dissolved solids (TDS), were measured daily with a multiparameter probe (Edge HI2030/HI763100, Hanna Instruments, Italy). Additional water parameters such as ammonium (NH₄⁺), nitrite (NO₂⁻), nitrate (NO₃⁻), and phosphate (PO₄³⁻) concentrations, were measured weekly according to standard methods.

Papaya seedlings were obtained from commercial enterprises and 14 plants were transplanted into the system on May 2nd, 2022. Currently, after almost a year, the growth of the papaya trees is no longer significant, but the fruits are still developing and started to ripen in March 2023. Plant survival, health status, and morphology were analysed according to several parameters (height, stem diameter, number of fruits, and sanity) once a month assessing growth and overall look.

Greenhouse air temperature and relative humidity were measured hourly with a LogTag HAXO-8 (LogTag, New Zealand).

3. Results

Monitorization data from May 2nd, 2022, to March 28, 2023, were used to assess the performance of aquaponic systems.

3.1. Aquaponic system

Results of water parameters measured in the fish tank and DWC unit showed that values of pH, ORP, DO, T, TDS, and EC, were similar within the system with adequate values for fish production. Ammonium and nitrite concentrations were adequate for fish production (Thangam 2014), given the rapid conversion by nitrifying bacteria. Nitrates and phosphates were available for plant uptake in high concentrations because of fish feeding and metabolism (Table).

	pH	ORP	DO (mg/L)	EC (µS/cm)	TDS (mg/L)	T (°C)	NH ₄ ⁺ (mg/L)	NO ₂ ⁻ (mg/L)	NO ₃ ⁻ (mg/L)	PO ₄ ³⁻ (mg/L)
Fish tank	6.17	81.4	7.37	1401	787	22.1	0.12	0.15	494	35.4
DWC unit	6.16	80.0	5.85	1396	788	22.0	0.11	0.15	492	35.3

Table 1: Average values of water parameters in the fish tank and DWC unit during plant growth

3.2. Crop productivity

The results of plant monitoring showed that after 3 months in the systems, some started exhibiting signs of disease such as burnt leaves or stiffness loss, and 4 of them didn't adapt to the system. Plants started flowering within 3 months and produced an average of 10 fruits per plant which remain in the maturation phase. After an 8-month growing period, the plant's average height was 105.25±48.38 cm, and the average stem diameter measured at the base of the plant was 6.33±3.34 cm. Due to lower temperatures and high humidity in the winter period plants showed signs of stress such as leaves loss and fungal contamination.

4. Conclusions

Challenges to sustainability center around balancing the aquaponic system, maximizing production outputs by controlling conditions such as temperature, light, and humidity, and assuring optimal growth. These systems could ensure more local production to satisfy the high demand for papaya, thus reducing the associated carbon footprint.

References

- Adeshina, Ibrahim, Lateef O Tihamiyu, Musa I Abubakar, Oluwafunmike O Ogundayomi, and Ojo Adesanmi. 2021. "Effects of Dietary *Mitracarpus Scaber* Leaves Extract on Growth, Physiological, Antioxidants, and Mucosal Immune Profiles of North African Catfish, *Clarias Gariepinus*, and Resistance against *Edwardsiella Tarda* Infection." *Trop Anim Health Prod* 53 (6): 541. <https://doi.org/https://doi.org/10.1007/s11250-021-02989-5>.
- Lennard, Wilson A, and Brian V Leonard. 2004. "A Comparison of Reciprocating Flow versus

- Constant Flow in an Integrated, Gravel Bed, Aquaponic Test System." *Aquacult Int* 12: 539–53. <https://doi.org/https://doi.org/10.1007/s10499-004-8528-2>.
- Maucieri, Carmelo, Carlo Nicoletto, Ranka Junge, Zala Schmautz, Paolo Sambo, and Maurizio Borin. 2017. "Hydroponic Systems and Water Management in Aquaponics: A Review." *Ital J. Agron* 13 (1). <https://doi.org/10.4081/ija.2017.1012>.
- Pinho, Sara M, Luiz H David, Fabiana Garcia, Karel J Keesman, Maria Célia Portella, and Simon Goddek. 2021. "South American Fish Species Suitable for Aquaponics: A Review." *Aquacult Int* 29 (4): 1427–49. <https://doi.org/https://doi.org/10.1007/s10499-021-00674-w>.
- Sikawa, Daniel C, and Amararatne Yakupitiyage. 2010. "The Hydroponic Production of Lettuce (*Lactuca Sativa* L) by Using Hybrid Catfish (*Clarias Macrocephalus* × *C. Gariepinus*) Pond Water: Potentials and Constraints." *Agric. Water Manag.* 97 (9): 1317–25. <https://doi.org/https://doi.org/10.1016/j.agwat.2010.03.013>.
- Thangam, Y. 2014. "Effect of Acute and Sublethal Toxicity of Nitrite to Fresh Water Fish *Cirrhinus Mrigala*." *Int.J.Sci. Eng* 5: 789–95.
- United Nation. 2021. "The United Nations World Water Development Report 2021: 'Valuing Water.'" UNESCO: Paris, France. <https://unesdoc.unesco.org/ark:/48223/pf0000375724/PDF/375724eng.pdf.multi>.
- Zhou, Ziwei, Rebecca Ford, Ido Bar, and Chutchamas Kanchana-Udomkan. 2021. "Papaya (*Carica Papaya* L.) Flavour Profiling." *Genes* 12 (9): 1416. <https://doi.org/https://doi.org/10.3390/genes12091416>.

Acknowledgments

Authors acknowledge funding by FCT/MCTES (PIDDAC): LA/P/0045/2020 (ALICE), UIDB/50020/2020, and UIDP/50020/2020 (LSRE-LCM).

OC07. End-of-life tire microplastics: are they safe for users of artificial turf sports facilities?

Tiago Ferreira^{1,2*}, Vera Homem^{1,2}, Francisco-Cereceda-Balic³, Ximena Fadic³, Arminda Alves^{1,2}, Nuno Ratola^{1,2}

¹LEPABE – Laboratory for Process Engineering, Biotechnology and Energy, Faculty of Engineering, University of Porto, Rua Dr. Roberto Frias, 4200-465 Porto, Portugal

²ALiCE – Associate Laboratory in Chemical Engineering, Faculty of Engineering, University of Porto, Rua Dr. Roberto Frias, 4200-465 Porto, Portugal

³Centre for Environmental Technologies (CETAM) and Department of Chemistry, Universidad Técnica Federico Santa María, Valparaíso, Chile;

*Presenting author (tferreira@fe.up.pt) ORCID 0009-0006-7720-0731

Abstract

In recent years, the extensive use of recycled rubber granulate (crumb rubber) in artificial turf football fields has been raising concern on the scientific community due to the numerous hazardous substances that have been detected in this matrix (e.g., carcinogenic polycyclic aromatic hydrocarbons, plasticizers and heavy metals). Volatile methylsiloxanes, being mass-produced chemicals with a broad scope of day-to-day applications, are ever-present in the environment, and as such the possibility of its presence in crumb rubber was contemplated in this work, especially given the recent inclusion of this material in the domain of microplastics. A total of 135 crumb rubber samples from various countries were analyzed in parallel with 12 samples of alternative infill materials, with volatile methylsiloxanes being detected in all of them (from 2 to up to 5,100 ng.g⁻¹). In spite of this, the exposure risk to football players and field workers was found to be negligible.

Author Keywords. End-of-life tires, crumb rubber, volatile methylsiloxanes, microplastics, human exposure.

 Open Access  Peer Reviewed   CC BY

1. Introduction

Upon the end of its life cycle, tires are often recycled in the form of crumb rubber (CR) that can be applied as infill in artificial turf. The external part of a tire is comprised of synthetic rubber, fillers and reinforcement metals, while minor constituents include vulcanization additives (ECHA 2017). However, its gradual degradation process may lead to the formation of impurities that are potentially harmful to humans, among which are carcinogenic polycyclic aromatic hydrocarbons (PAHs) and heavy metals. Volatile methylsiloxanes (VMSs) are a class of low-molecular weight siloxanes that are used in a large number of formulations, including personal-care products (PCPs), silicone components, lubricants, paints and fabric softeners (Perry and Kayatin 2017). Out of all VMSs, D4, D5 and D6 – the most abundant species (ECHA 2019) – were identified as highly persistent and bioaccumulative substances (ECHA 2018). Although they are not plastics from a material perspective, the rubber granules applied in artificial turf fields are made from a synthetic polymer. Thus, they now fall into the category of microplastics, making them potential transport vectors of environmental pollutants (Arienzo *et al.* 2021).

All things considered – the large-scale production of siloxanes, the widespread use of VMSs in various consumer and industrial products, their persistence in the environment and, lastly, the microplastic nature of CR – this work was based on the hypothesis that VMSs may, in fact, be present in this material and potentially cause harm to the artificial turf sports facilities users and workers.

2. Materials and Methods

The analysis of the cyclic siloxanes (cVMSs) D3, D4, D5 and D6, and linear siloxanes (lVMSs) L3, L4 and L5 was carried out by an ultrasound-assisted extraction with 1:1 (v/v) Hex:DCM, followed by a QuEChERS clean-up step and finalized with GC-MS instrumental analysis and quantification.

3. Results and Discussion

The results corroborated the initial hypothesis that VMSs are present in CR, since they were detected in all 135 samples (from which 128 belonged to artificial turf fields and 7 were taken directly from commercial packages, meaning that they had not suffered any prior use). Total VMS levels ranged from 2 to 215 ng.g⁻¹ in the field samples and from 90 to almost 5,100 ng.g⁻¹ in the commercial samples. The globally higher concentration of the latter indicates possible VMS volatilization. The measured VMS levels were lower than those reported for other organic microcontaminants in CR – Figure .

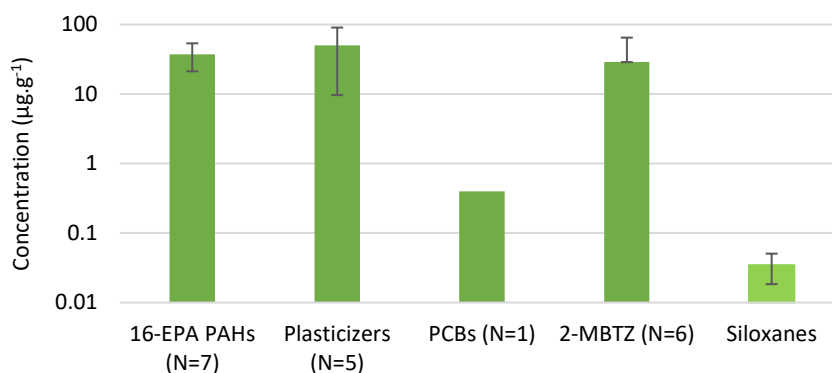


Figure 1: Concentration (µg.g⁻¹) of volatile methylsiloxanes in crumb rubber vs. other organic microcontaminants (logarithmic scale, base 10).

Statistical tests were applied to infer the influence of certain independent variables in the VMS levels. Indoor fields were found to have higher VMS levels (due to not being exposed to sunlight and possibly failing to have adequate ventilation in some cases), while there was also a gradual decrease of the VMS concentration over time. The country and granulometry did not manifest a significant statistical impact. In terms of alternative infill materials, cork showed the lowest VMS content (which was also lower than the one of CR), corroborating previous studies that highlighted (for other organic microcontaminants) this material as a safer alternative to CR (Armada et al. 2022; Celeiro et al. 2021).

Translating these results to a human exposure assessment, oral and dermal VMS exposure doses were estimated for football players and field workers – based on the methodology developed by Peterson et al. 2018. The oral pathway was found to be the primary exposure route (maximum total exposure of 20 ng.kg⁻¹.year⁻¹), nevertheless its magnitude was decidedly insufficient to cause any alarming health implications – using as a benchmark the European Chemicals Agency’s derived no-effect levels (DNEL) of 1.35×10⁹ and 1.83×10⁹ ng.kg⁻¹.year⁻¹ for D4 and D5, respectively (ECHA 2022).

4. Conclusions

The present work was pioneer in targeting VMSs in crumb rubber, providing a reliable and robust analytical method for this purpose. The presence of this class of microcontaminants was confirmed, nonetheless the measured VMS levels and/or the exposure parameters were not significant enough to question the safety of artificial turf fields regarding VMS exposure.

References

- Arienzo et al. 2021. ‘The Dual Role of Microplastics in Marine Environment: Sink and Vectors of Pollutants’. *Journal of Marine Science and Engineering* 9 (6): 642. <https://doi.org/10.3390/jmse9060642>.
- Armada et al. 2022. ‘Global Evaluation of the Chemical Hazard of Recycled Tire Crumb Rubber Employed on Worldwide Synthetic Turf Football Pitches’. *Science of The Total Environment* 812 (March): 152542. <https://doi.org/10.1016/j.scitotenv.2021.152542>.

- Celeiro et al. 2021. 'Evaluation of Chemicals of Environmental Concern in Crumb Rubber and Water Leachates from Several Types of Synthetic Turf Football Pitches'. *Chemosphere* 270 (May): 128610. <https://doi.org/10.1016/j.chemosphere.2020.128610>.
- ECHA. 2017. 'Rubber Granules Evaluation'. (Ver 1.01), 120 p. https://echa.europa.eu/documents/10162/17220/annexes_to_axv_report_rubber+granules_en.pdf/f3cc9f58-8ab3-8e4a-0258-51466817f0fd.
- ECHA. 2018. 'Draft Minutes of the 60th Meeting of the Member State Committee (MSC-60) 12-14 June 2018'. https://echa.europa.eu/documents/10162/2200413/msc-60_minutes_en.pdf/f407b9e7-78a4-966d-cc51-9d36b8c7ee3e?t=1551257817661.
- ECHA. 2019. 'Annex XV Restriction Report - proposal for a restriction', 91 p. https://echa.europa.eu/documents/10162/13641/rest_d4d5d6_axvreport_en.pdf/c4463b07-79a3-7abe-b7a7-5c816e45bb98.
- ECHA. 2022. 'Decamethylcyclopentasiloxane - Toxicological Information' (Last accessed in March 2023). <https://echa.europa.eu/pt/brief-profile/-/briefprofile/100.007.969>.
- Perry et al. 2017. 'The Incidence and Fate of Volatile Methyl Siloxanes in a Crewed Spacecraft Cabin' <https://ntrs.nasa.gov/citations/20170010355>.
- Peterson et al. 2018. 'Comprehensive Multipathway Risk Assessment of Chemicals Associated with Recycled ("crumb") Rubber in Synthetic Turf Fields'. *Environmental Research* 160 (January): 256–68. <https://doi.org/10.1016/j.envres.2017.09.019>.

Acknowledgments

This work was financially supported by: (i) Projects LA/P/0045/2020 (ALICE – Associated Laboratory in Chemical Engineering) and UIDB/00511/2020 and UIDP/00511/2020 (LEPABE – Laboratory for Process Engineering, Environment, Biotechnology and Energy), funded by national funds through FCT/MCTES (PIDDAC); (ii) Project SAFEGOAL (PTDC/EQU-EQU/28101/2017; POCI-01-0145-FEDER-028101), funded by FEDER through COMPETE2020—Programa Operacional Competitividade e Internacionalização (POCI) and by national funds (PIDDAC) through FCT/MCTES; (iii) Project REDES179166, funded by CONICYT – Comisión Nacional de Investigación Científica y Tecnológica (Chile) and Project FOVI210064, funded by the Chilean National Agency for Research and Development (ANID); (iv) V. Homem thanks national funds through FCT, under the Scientific Employment Stimulus-Individual Call - CEECIND/00676/2017. The authors wish to thank the help of the volunteers that helped in the collection of the samples.

OC08. LCD from waste mobile phones: an environmental- friendly approach to recycle Indium

Liliana M. Martelo¹, Márcia A.D. Silva^{1,2}, Hugo A.M. Bacelo,¹ Margarida M.S.M. Bastos²,
Helena M.V.M. Soares¹

¹REQUIMTE/LAQV, Departamento de Engenharia Química, Faculdade de Engenharia, Universidade do Porto, Rua Dr. Roberto Frias, 4200-465 Porto, Portugal


²LEPABE, Departamento de Engenharia Química, Faculdade de Engenharia, Universidade do Porto, Rua Dr. Roberto Frias, 4200-465 Porto, Portugal

Abstract

The main aim of this work was to recover indium (In) from the liquid crystal display (LCD) screen as the major targeted metal due to its worldwide scarcity that makes it a critical metal.

The current recycling process leads to significant losses of In and does not take into account the presence of toxic substances, the liquid crystals. To make the recycling process more efficient, the separation of the several layers of the LCD screen is crucial. This separation allows the isolation of the ITO substrate, where In is more concentrated. After layer separation, an acid leaching process assisted by microwave was able to extract 99.01% of all In. To purify the recovered In, ion-exchange technology using a bispicolylamine chelating resin (specifically, M4195 resin) allowed to purify In from other contaminants resulting in an eluate containing In with a purity of 92 %.

Author Keywords. Recycling waste of mobile phones, Combined physical and chemical processes, Recovery of Indium, Microwave-assisted leaching, Ion-Exchange Technology

 Open Access  Peer Reviewed  CC BY

1. Introduction

Mobile phones (MPs) screens are usually made of Liquid Crystal Display (LCD). An LCD consists in two clear glass panels coated with indium-tin oxide (ITO) and sandwiched between them are the liquid crystals (LCs). A polymeric film (PF) is used to bind the glass panels and other structures together. Several studies have shown the metal constitution from multiple brands of waste MPs . In 2019, the worldwide consumptions of Indium (In) was 110 Mt and the production of LCD constitutes almost 80% of it. According to the Global E-Waste Monitor, in 2020, 6.7Mt of screens were disposed; therefore, there is a huge opportunity for recycling these equipments and recovering In, which is considered a critical metal according to the European Union.

Currently, the standard recycling process for LCD screens involves mechanical crushing or pyrolysis as an initial step. However, this method shreds both hazardous (such as, LCs) and valuable recyclable (such as, In) materials together, resulting in a low recovery rate. Additionally, in the context of a circular economy, it is essential to target the recovery of glass and plastics from LCD screens to close the recycling loop. Unfortunately, these fractions are often disregarded.

To tackle this problem, an innovative hybrid strategy combining physical and chemical processes was developed by us that allows, for the first time, recovering In efficiently together with other components (plastic component and glass substrate) from LCDs through a nearly zero-waste and circular approach.

2. Materials and Methods

Several brands and models of smartphones were collected from local collectors and, after manually dismantling of the cell phones, the screens were removed from the remaining components of the cell phones.

Subsequently, the screens were cut, and the resultant pieces immersed in a solution of water and ethyl acetate (in a ratio of 5:1) inside a low-pressure reactor for 1 hour at 180 °C. This process allowed the detachment of the PF from the ITO substrate and the LCs remained dissolved in the aqueous media. Next, the recovery of In from the ITO glass was carried out using microwave-assisted soft acid leaching conditions. This involved subjecting the ITO substrate to a solution of 0.25 M of hydrochloric acid (HCl), with a solid/liquid ratio of 1/5, and three cycles of 30 seconds each at a power of 840 W.

The purification of In from the HCl leachate was performed using the DOWEX M4195 (referred as M4195) resin purchased from Sigma Aldrich.

Then, the pH of the leachate was adjusted to 2 ± 0.1 using concentrated sodium hydroxide (NaOH) solution and used as inlet solution for continuous mode adsorption assays in a glass chromatographic column filled with a packed bed of M4195 resin (0.75 g) and a volume of 0.845 mL at a flow rate of 0.5 mL/min. Elution of the target metal (In) was performed using sulphuric acid (H_2SO_4) 0.25 mol/L solutions, which were prepared from analytical grade H_2SO_4 (95%).

Metal concentrations were measured by atomic absorption spectroscopy with flame atomization (AAS-FA) in a Perkin Elmer AAnalyst 400 (Norwalk, CT, USA) or an Analytik JenaA NovAA350 (Konrad-Zuse, Germany) spectrometers using acetylene (Cu, Fe, In and Zn) or nitrous oxide (Al and Sn) flame.

3. Results and discussion

3.1. Pre-treatment to dismantle the LCDs screen

To retrieve In from LCDs, an initial step is required to isolate all the layers that make up the display of a MP. As this material is fragile and prone to breaking, an alternative to physical and mechanical methods has been opted for; a combination of water and ethyl acetate (5:1) was used not only to separate the various layers but also to dissolve the LCs due to its solubilizing properties.

3.2. Recovery of Indium by microwave assisted acid leaching followed by ion-exchange

The extraction of the target metal, In, was carried out by microwave-assisted leaching being different HCl concentrations tested. The highest extraction of In (99.04%) was obtained using 0.5M HCl; however, using half of the HCl concentration (0.25M), an In extraction yield of similar magnitude (98.81%) was achieved. When compared to the literature, the use of the microwave proves to be more efficient in terms of time, energy consumption, and quantity of reagents used. Together with In, which was extracted almost totally, other metals were also extracted. A leachate constituted by Al (33.5 %), Fe (5.2 %), Sn (0.9 %), Zn (4.0 %) and Cu (2.4 %) was achieved where In represented 54% of the metal content in solution. So, to purify it from the other metal contaminants, a continuous mode adsorption-elution technique using a bispicolylamine chelating resin (M4195 resin) was selected.

The adsorption curve of the metals from the leachate through the M4195 resin evidenced the following order of affinity: $\text{Cu (II)} > \text{In (III)} > \text{Zn (II)} > \text{Fe (II)} \approx \text{Al (III)}$, which is similar to the metal affinity reported by Grinstead, et al. Considered the metal composition of the leachate, it is expected that, besides In, other metals, namely, Cu and Zn, are also adsorbed to the resin. Using a flow rate of 0.5 min./L, the breakthrough capacity of the resin for In was observed after 540 minutes. After this time, the ratio between the metal concentration in the raffinate and in the inlet was > 1 for Al and Fe evidencing that the bed of the resin at least contains Cu, In, Sn and Zn. Aiming to achieve a purified eluate containing In, its selective elution using 0.25 M H_2SO_4 solution was attempted to avoid Cu, Sn and Zn elution. An eluate containing In with a purity of 92% was obtained. Although M4195 was never used to purify In, when comparing to other resins used for this purpose (such as Diphonix, or Methylene crosslinked calixarene carboxylic acid resins), it is clear that it has a higher capacity of adsorption and presents good ability to purify In over other metals.

4. Conclusions

A new process combining physical and chemical methods to recycle In from LCDs is presented. This strategy proved to be efficient in different aspects. Starting by delaminating the various LCD layers, plastics are easily separated from the films and the most polluting components, the LCs, leaving the ITO substrate totally available for subsequent recovery of In from it. After a microwave-assisted leaching, 98.81% of In was leached under mild acid (0.25 M HCl) conditions and a multi-metal leachate containing In (54%) plus Al (33.5 %), Fe (5.2 %), Sn (0.9 %), Zn (4.0 %) and Cu (2.4 %) was achieved. The bispicolylamine chelating (M4195) resin was chosen to purify In in a continuous adsorption mode. Although this resin has never been used for this purpose, it proved to be efficient over a long period of time at a high flux and for a higher concentration of In (when compared to other resins for the same purpose) and showed a good selectivity to In over the other base metals, namely, for Al, Fe, and Sn. The high affinity of the resin to In resulted in an increase of the purity of In up to 92 %. Overall, this process allows to recover every part of the LCD (including plastics and LC) and recover In with an overall yield of 90.09% and a purity of 92%.

References

- K. Zhang, Y. Wu, W. Wang, B. Li, Y. Zhang, and T. Zuo, "Recycling indium from waste LCDs : A review," *Resources, Conservation and Recycling*, vol. 104. Elsevier, pp. 276–290, Nov. 01, 2015. Doi : 10.1016/j.resconrec.2015.07.015.
- K. Winans, A. Kendall, and H. Deng, "The history and current applications of the circular economy concept," *Renewable and Sustainable Energy Reviews*, vol. 68. Elsevier Ltd, pp. 825– 833, Feb. 01, 2017. Doi : 10.1016/j.rser.2016.09.123.
- D. Pradhan, S. Panda, and L. B. Sukla, "Recent advances in indium metallurgy : A review," *Mineral Processing and Extractive Metallurgy Review*, vol. 39, no. 3. Taylor and Francis Inc., pp. 167–180, May 04, 2018. Doi : 10.1080/08827508.2017.1399887.
- Gabriel, A. P., Giordani, B. B., Kasper, A., & Veit, H. M. (2018). Indium extraction from lcd screens. *Detritus*, 3(September), 43–46. <https://doi.org/10.31025/2611-4135/2018.13704>
- R. R. Grinstead, "Selective absorption of copper, nickel, cobalt and other transition metal ions from sulfuric acid solutions with the chelating ion exchange resin XFS 4195," *Hydrometallurgy*, vol. 12, no. 3, pp. 387-400, 1984/07/01/ 1984.
- A. W. Trochimczuk, E. P. Horwitz, and S. D. Alexandratos, "Complexing Properties of Diphonix, a New Chelating Resin with Diphosphonate Ligands, Toward Ga(III) and In(III)," *Separation Science and Technology*, vol. 29, no. 4, pp. 543-549, 1994/02/01 1994.
- B. B. Adhikari, M. Gurung, H. Kawakita, and K. Ohto, "Solid phase extraction, preconcentration and separation of indium with methylene crosslinked calix[4]- and calix[6]arene carboxylic acid resins," *Chemical Engineering Science*, vol. 78, pp. 144-154, 2012.

Acknowledgments

This work is financially supported by national funds through the FCT/MCTES (PIDDAC), under the project PTDC/CTA-AMB/3489/2021

OC09. Recycling agro-industrial by-products: kiwi peels as a source of antioxidants to incorporate in cosmetic products

Sandra M. Gomes^{1,2*}, Rita Miranda³, Lúcia Santos^{1,2}

¹LEPABE - Laboratory for Process Engineering, Environment, Biotechnology and Energy, Faculty of Engineering, University of Porto, Rua Dr. Roberto Frias, 4200-465 Porto, Portugal

²ALiCE - Associate Laboratory in Chemical Engineering, Faculty of Engineering, University of Porto, Rua Dr. Roberto Frias, 4200-465 Porto, Portugal


³FEUP - Faculty of Engineering, University of Porto, Rua Dr. Roberto Frias, 4200-465 Porto, Portugal

*Presenting author (scgomes@fe.up.pt); ORCID [0000-0001-9654-2899](https://orcid.org/0000-0001-9654-2899)

Abstract

Kiwi peels are a highly produced agro-industrial by-product, which is generally discarded in landfills. To give a new purpose to this by-product, kiwi peels extract was obtained using a solid-liquid extraction, with an extraction yield of 46 %, and its antioxidant and antimicrobial properties were tested. The total phenolic content (TPC) was around 52 mg gallic acid equivalents (GAE)/g, and the antioxidant capacity was higher for ABTS in comparison to DPPH. The extract also presented antibacterial activity against *S. aureus*. These results indicate that skincare products could be a sustainable option for the use of kiwi peels. Its valorization could be an important step towards a circular economy, giving proper use to all the bioactive compounds present in it.

Author Keywords. Agro-industrial by-products; Phenolic compounds; Natural antioxidants; Sustainability; Circular economy

 Open Access  Peer Reviewed  CC BY

1. Introduction

Food production and processing, necessary to satisfy the needs of the growing population of the world, generates large amounts of agro-industrial residues every year (UNEP 2021). These by-products present several consequences at both environmental and socio-economic levels. Food residues are generally discarded in landfills where they are left to decompose, which contributes to the emission of greenhouse gases, impairing the environment (Torres-León et al. 2018). Agro-industrial by-products are generally rich in bioactive compounds that present interesting biological properties. Kiwi peels (KP), for example, are rich in phenolic compounds, vitamins, flavonoids, and polyphenols, presenting numerous biological activities such as antioxidant and antimicrobial capacity (Sanz et al. 2021). Taking into consideration the composition of KP, the extracts obtained from this by-product can be incorporated into different products, namely cosmetic ones. This strategy can generate products with potential biological benefits, where natural compounds can be used in substitution of synthetic ones. Also, it contributes to minimising the environmental problems associated with agro-industrial residues and to a circular economy model (A.M. Silva et al. 2021). Therefore, the use of antioxidant compounds from natural sources contributes to the production of value-added products in a sustainable manner.

2. Materials and Methods

To obtain natural antioxidants from agro-industrial by-products, kiwis were acquired in local supermarkets. The fruit was washed and dried with a paper towel. The peels were removed and then lyophilised to completely remove the water. Finally, the peels were grounded using a coffee grinder. After the pre-treatment of the samples, phenolic-rich extracts were obtained from the kiwi peels. For that, a solid-liquid extraction method with a Soxhlet apparatus was performed for 2 h, using ethanol as solvent, in a sample-to-solvent ratio of 1:20 (m/V). The solvent was evaporated using a rotary evaporator and then by submitting the samples to a constant stream of nitrogen (2 mbar). The total phenolic content (TPC) and antioxidant and antimicrobial activities of the extract were evaluated. The TPC was analysed using the Folin-Ciocalteu method, where the sample solution (1 g/L in ethanol) was incubated with water, Folic-Ciocalteu reagent and sodium carbonate (333.3 g/L in water) for 2 h and the changes in the absorbance were analysed at 750 nm. The results were expressed in gallic acid equivalents (GAE) using a gallic acid calibration curve (A.M.T. Silva et al.

2007). The radical scavenging activity was studied using both 2,2-diphenyl-1-picrylhydrazyl (DPPH) and 2,2-azinobis (3-ethyl-benzothiazolin-6-sulfonic acid) (ABTS) methods. Briefly, in the DPPH method, the sample solution (8.0 – 1.5 g/L in ethanol) was incubated with DPPH radical solution (150 µM/L in ethanol) for 40 minutes and the absorbance was analysed at 515 nm (Bobo-García et al. 2015). In the ABTS method, the sample solution (2.5 – 0.1 g/L in ethanol) was incubated with ABTS radical solution for 15 minutes and the absorbance was analysed at 734 nm (Xiao et al. 2020). In both methods, the percentage of inhibition of the radical was calculated and the IC₅₀ values were determined. Finally, the antibacterial activity was evaluated against *E. coli*, *S. aureus* and *S. epidermis* bacteria using the disk diffusion method. After 24 h of incubation at 37 °C, the inhibition halos were measured.

3. Discussion

In this work, phenolic-rich extracts were obtained using a solid-liquid extraction, with an extraction yield of (45.77 ± 2.82) %. Ethanol was the solvent used due to its polarity and because it is a compound Generally Recognized As Safe (GRAS). The results obtained from the extract characterization are expressed in Table 1.

TPC (mg GAE/g)	IC ₅₀ (mg/L)		<i>E. coli</i>	d _{halo} (mm)	
	DPPH	ABTS		<i>S. aureus</i>	<i>S. epidermidis</i>
51.90 ± 4.47	222.89 ± 11.74	57.79 ± 4.24	ND	8.0 ± 0.8	ND

Table 1: Characterization of the phenolic-rich extract obtained from kiwi peels. TPC: total phenolic content; GAE: gallic acid equivalents; IC₅₀: extract concentration necessary to inhibit 50% of the radical; DPPH: 2,2-diphenyl-1-picrylhydrazyl; ABTS: 2,2-azinobis (3-ethyl-benzothiazolin-6-sulfonic acid); ND: not detected

Kiwi peels (KP) extract presented a total phenolic content (TPC) of around 52 mg GAE/g. This value can be associated with the presence of certain compounds, such as protocatechuic acid, caffeic acid, rutin, or quercetin. The TPC value obtained in the present study is similar to the ones found in the literature (Lee et al. 2012; Guthrie et al. 2020). Regarding the DPPH and ABTS assays, KP extract was able to inhibit both radicals. The IC₅₀ value was significantly higher for DPPH, meaning that the necessary concentration of extract to inhibit 50% of the respective radical is higher for DPPH. Considering the antibacterial capacity, it was observed that KP extract could inhibit the growth of *S. aureus*, but no inhibition halos were detected for *E. coli* or *S. epidermidis*. Literature reports demonstrated that the antibacterial activity of the extract is a dose-dependent mechanism (Alim et al. 2019). Therefore, higher extract concentrations can be tested to evaluate the potential antibacterial capacity against *E. coli* and *S. aureus*. The biological properties demonstrated by the extract makes it an interesting ingredient to be incorporated into cosmetic formulations.

4. Conclusions

This work aimed to evaluate the biological properties of kiwi peels extract and evaluate their potential use as a natural preservative in cosmetic products. The obtained extract presented antioxidant activity against both ABTS and DPPH radicals and was able to inhibit the growth of *S. aureus*. The results of this study demonstrate the potential of these extracts to be used as a natural source of phenolic compounds. Their incorporation in cosmetic formulations, such as moisturizing creams, can create a value-added product that allies the sustainability with a circular economy model.

References

- Alim, A., T. Li, T. Nisar, D. Ren, et al. 2019. "Antioxidant, antimicrobial, and antiproliferative activity-based comparative study of peel and flesh polyphenols from *Actinidia chinensis*." *Food Nutr Res* 63. <https://doi.org/10.29219/fnr.v63.1577>.
- Bobo-García, G., G. Davidov-Pardo, C. Arroqui, P. Vírveda, et al. 2015. "Intra-laboratory validation of microplate methods for total phenolic content and antioxidant activity on polyphenolic extracts, and comparison with conventional spectrophotometric methods." *J Sci Food Agric* 95 (1): 204-9. <https://doi.org/10.1002/jsfa.6706>.

- Guthrie, Francesca, Yiting Wang, Natasha Neeve, Siew Young Quek, et al. 2020. "Recovery of phenolic antioxidants from green kiwifruit peel using subcritical water extraction." *Food and Bioproducts Processing* 122: 136-144. <https://doi.org/10.1016/j.fbp.2020.05.002>.
- Lee, Min-Young, Mi-So Yoo, Yoo-Jeong Whang, Yoo-Jeong Jin, et al. 2012. "Vitamin C, Total Polyphenol, Flavonoid Contents and Antioxidant Capacity of Several Fruit Peels." *Korean Journal of Food Science and Technology* 44 (5): 540-544. <https://doi.org/https://doi.org/10.9721/kjfst.2012.44.5.540>.
- Sanz, V., L. López-Hortas, M. D. Torres, and H. Domínguez. 2021. "Trends in kiwifruit and byproducts valorization." *Trends in Food Science & Technology* 107: 401-414. <https://doi.org/10.1016/j.tifs.2020.11.010>.
- Silva, Adrián M. T., Ekaterini Nouli, Nikolaos P. Xekoukoulotakis, and Dionissios Mantzavinos. 2007. "Effect of key operating parameters on phenols degradation during H₂O₂-assisted TiO₂ photocatalytic treatment of simulated and actual olive mill wastewaters." *Appl Catal B* 73 (1): 11-22. <https://doi.org/10.1016/j.apcatb.2006.12.007>.
- Silva, Ana Margarida, Paulo C. Costa, Cristina Delerue-Matos, Piotr Latocha, et al. 2021. "Extraordinary composition of *Actinidia arguta* by-products as skin ingredients: A new challenge for cosmetic and medical skincare industries." *Trends in Food Science & Technology* 116: 842-853. <https://doi.org/10.1016/j.tifs.2021.08.031>.
- Torres-León, Cristian, Nathiely Ramírez-Guzman, Liliana Londoño-Hernandez, Gloria A. Martinez-Medina, et al. 2018. "Food Waste and Byproducts: An Opportunity to Minimize Malnutrition and Hunger in Developing Countries." *Frontiers in Sustainable Food Systems* 2 (52). <https://doi.org/10.3389/fsufs.2018.00052>.
- UNEP. 2021. *Food Waste Index Report 2021*. (Nairobi, Kenia: UN Environment Programme). <https://www.unep.org/resources/report/unep-food-waste-index-report-2021>.
- Xiao, Fan, Tao Xu, Baiyi Lu, and Ruihai Liu. 2020. "Guidelines for antioxidant assays for food components." *Food Front* 1 (1): 60-69. <https://doi.org/10.1002/fft2.10>.

Acknowledgments

This work was financially supported by LA/P/0045/2020 (ALiCE), UIDB/00511/2020 and UIDP/00511/2020 (LEPABE), funded by national funds through FCT/MCTES (PIDDAC).

OC10. Highly-conductive transparent glass substrates for efficient and scalable photoelectrochemical water splitting

Telmo da Silva Lopes^{1,2*}, Leonardo Rodrigues^{1,2,3}, Jeffrey Capitão^{1,2}, Dzmitry Ivanou^{1,2}, Paula Dias^{1,2}, Tânia Lopes^{1,2}, Adélio Mendes^{1,2}

¹LEPABE -Laboratory for Process Engineering, Environment, Biotechnology and Energy, Faculty of Engineering, University of Porto, Rua Dr. Roberto Frias, 4200-465 Porto, Portugal;

²ALiCE – Associate Laboratory in Chemical Engineering, Faculty of Engineering, University of Porto, Rua Dr. Roberto Frias, 4200-465 Porto, Portugal;




³CONSTRUCT-LFC, Department of Civil Engineering, Faculty of Engineering, University of Porto, 4200-465 Porto, Portugal

*Presenting author (up201306016@edu.fe.up.pt) ORCID (0000-0002-5623-5031)

Abstract

The wide implementation of solar energy harvesting and conversion technologies is dependent on efficient energy storage solutions that tackle sunlight's biggest challenge: intermittency. Photoelectrochemical (PEC) cells use semiconductor-based photoelectrodes to directly convert irradiation into storable energy vectors like hydrogen. Despite the scientific achievements in the development of efficient materials, there is a generalized lack of knowledge on upscaling challenges. One such challenge is the high ohmic resistances imposed by the transparent conductive oxides commonly used in the preparation of photoelectrodes. This work addresses this challenge by demonstrating the potential of using highly-conductive fluorine-doped tin oxide (FTO) lines as efficient and cheap current collectors for PEC applications. 25-cm² α -Fe₂O₃ photoelectrodes were prepared via ultrasonic spray pyrolysis on substrates with FTO patterns optimized by computational simulations. The best-performing sample displayed a photocurrent density 15 % higher than the one observed for a collector-less reference, with stable performance for 100 h continuous operation.

Author Keywords. Energy storage, solar fuels, photoelectrochemical cells, photolithography, transparent conductive oxide, ultrasonic spray pyrolysis, upscaling, hematite photoelectrode

 Open Access  Peer Reviewed  CC BY

1. Introduction

Harvesting energy directly from sunlight represents the most desirable pathway for meeting society's energy needs in a carbon-neutral way (Walter *et al.* 2010). Photoelectrochemical (PEC) water splitting (WS) is a promising technology that directly converts solar energy into clean and storable hydrogen (H₂) (Dias and Mendes 2017). Green H₂ is often referred to as the energy vector of the 21st century, finding applicability in power-generating and industrial applications, the latter as a chemical feedstock for H₂-to-X. In the last decades, most PEC-WS research efforts have focused on developing new semiconductor-based photoelectrodes engineered to reach solar-to-hydrogen conversion efficiencies above the required 10 % for commercial applications (Dias and Mendes 2017). Nonetheless, few or no attempts have been made to develop effective and innovative strategies to upscale highly efficient small-size photoelectrodes while keeping efficiency, stability, and low-cost milestones. Those three criteria are crucial to accelerate the implementation of PEC systems in the market. Photoelectrodes with photoactive areas beyond 10 cm² have their performance severely limited due to the high ohmic losses that are imposed by the transparent conductive oxides (TCOs) commonly used as substrates/current collectors (Vilanova, Lopes, and Mendes 2018). To tackle this challenge, this work proposes the use of highly conductive fluorine-doped tin oxide (FTO) lines as stable current collectors for low-resistivity transparent glass substrates. The lines were fabricated by photolithography-assisted ultrasonic spray pyrolysis (USP), and their width and geometry were optimized using a computational simulator until substrate conductivity and transparency were maximized. Ultrathin 25 cm² hematite (α -Fe₂O₃) photoelectrodes prepared using these substrates, demonstrated a photocurrent-density of *ca.* 0.46 mA-cm² (1.45 V_{RHE}), *ca.* 15 % higher than films deposited on regular FTO substrates. This optimised large-area photoelectrode remained stable for more than 100 h.

2. Materials and Methods

2.1. Ultrasonic spray pyrolysis deposition of FTO and ultrathin bare α -Fe₂O₃ films

FTO-coated glass substrates were masked by spraying a heat-resistant ink solution; the collector design pattern was produced by selectively ablating the mask layer using pulse laser ablation (355

nm·ns). The samples were then placed on a hot plate, below an ultrasonic spray nozzle, and FTO was grown following a procedure similar to the one described elsewhere (Pinheiro *et al.* 2023). Bare $\alpha\text{-Fe}_2\text{O}_3$ ultrathin films were then prepared also by USP, adapting a procedure previously optimised by this research team (Vilanova, Lopes, and Mendes 2018).

3. Discussion

To understand the influence of the thickness and geometry/pattern of the current collectors on the resistivity of $5 \times 5 \text{ cm}^2$ FTO-coated glass substrates, a DC conductivity model in COMSOL Multiphysics® was developed. All studied current collector designs considered: (1) an initial FTO-coated glass substrate with a resistivity of $7 \Omega \text{ sq}^{-1}$; FTO current collectors with (2) *ca.* $5 \mu\text{m}$ of height; and (3) covering only *ca.* 15 % of the total substrate area. Following a stepwise procedure, the width and distance between features on the current collectors was optimised to meet the previously discussed criteria. Afterwards, a two probe resistance simulation was performed using an electric current physics module. In simple terms, it was assumed that a current density of $1 \text{ mA}\cdot\text{cm}^{-2}$ was generated at the centre of each pattern feature. Afterwards, the current reaching a ground probe on the edge of the substrate was used to estimate the overpotential resulting from the substrate resistivity – Figure a. The overpotential contours displayed in square, triangle, and honeycomb patterned current collectors can be found in Figure b, as well as those simulated for a reference sample with no current collectors.

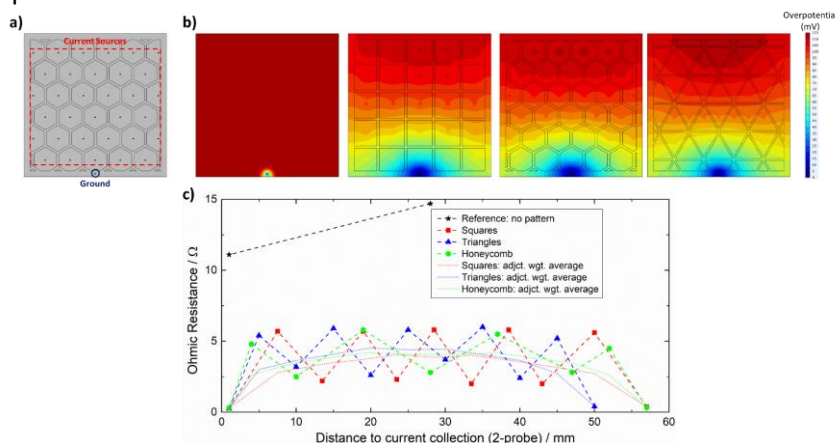


Figure 1: Two-probe resistance simulation: a) location of current sources and ground, b) simulated results for various optimized current collector patterns; c) experimental two-probe resistance test validation.

To validate the theoretical model used for conductivity optimization, two-probe resistance measurements (Keithley 2425-C SourceMeter) were performed on the FTO-coated glass substrates after photolithography-assisted USP of the three current collector patterns under analysis. Similarly to what was observed in the simulations, compared with a collector-less FTO-coated reference substrate, a great increase of conductivity (or decrease of overpotential) is observed for samples displaying the designed current collectors. Among the three patterns studied, the square-shaped geometry guarantees a better current extraction distribution – Figure b/c. To understand if an increased substrate conductivity leads to a higher PEC performance towards water oxidation, bare $\alpha\text{-Fe}_2\text{O}_3$ ultrathin films were deposited on these substrates and characterised by J - V measurements following a procedure described elsewhere (Vilanova, Lopes, and Mendes 2018) - Figure a. The current collector pattern labelled as “Square” yields the highest photocurrent at $1.45 \text{ V}_{\text{RHE}}$ (*ca.* $0.46 \text{ mA}\cdot\text{cm}^{-2}$), followed by the “Triangle” and “Honeycomb” samples, as observed in the simulations. This noteworthy value represents a roughly 15 % increase compared to the photocurrent density observed for the collector-less reference. In a long-term stability test, the square-patterned $\alpha\text{-Fe}_2\text{O}_3$ sample maintained the photogenerated current for more than 100 h - Figure b.

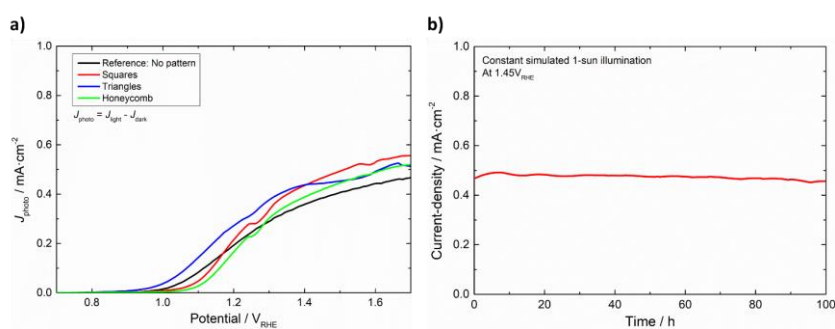


Figure 2: a) J - V characteristics of bare α - Fe_2O_3 ultrathin film photoelectrodes prepared using the various substrates; b) long-term stability test performed on the sample with Square-patterned current collectors.

4. Conclusions

The main objective of this work was to design, fabricate and characterize FTO lines as stable current collectors for low-resistivity transparent glass substrates for PEC-WS. To improve the design of efficient line-shaped current collector patterns, DC conductivity simulations were conducted and experimentally validated. The aim was to maximize substrate conductivity while minimizing any loss in the photoactive area. The 25 cm² square-patterned α - Fe_2O_3 photoelectrode displayed a photocurrent density of *ca.* 0.46 mA·cm⁻², which was 15 % higher than that observed for a collector-less reference. Remarkably, the FTO current-collector was stable for more than 100 h under continuous PEC operation with simulated sunlight, surpassing any previously reported current collector's stability by over 10-fold. This demonstration validates the concept of using highly-conductive FTO lines as efficient and cheap current collectors for PEC applications, avoiding the use of expensive and prone-to-corrosion metallic materials.

References

- Dias, Paula, *et al.* 2017. "Hydrogen Production from Photoelectrochemical Water Splitting." In *Encyclopedia of Sustainability Science and Technology*, edited by Robert A. Meyers, 1-52. New York, NY: Springer New York.
- Pinheiro, X. L., *et al.* 2023. "Design of experiments optimization of fluorine-doped tin oxide films prepared by spray pyrolysis for photovoltaic applications." *Ceramics International* 49 (8):13019-13030. doi: <https://doi.org/10.1016/j.ceramint.2022.12.175>.
- Vilanova, António, *et al.* 2018. "Large-area photoelectrochemical water splitting using a multi-photoelectrode approach." *Journal of Power Sources* 398:224-232. doi: <https://doi.org/10.1016/j.jpowsour.2018.07.054>.
- Walter, Michael G., *et al.* 2010. "Solar Water Splitting Cells." *Chemical Reviews* 110 (11):6446-6473. doi: 10.1021/cr1002326.

Acknowledgments

T.S.L., P.D. and T.L. are grateful to FCT for funding (references: SFRH/BD/147426/2019, CEECIND/02862/2018, and CEECIND/02385/2021, respectively). L.R. acknowledges project BlueWoodenHouse (POCI-01-0247-FEDER-047157). This work has received funding from: i) Project ASAPFuels - PTDC/EQU-EQU/4225/2021 funded by FEDER, through COMPETE2020 and by national funds, through FCT; ii) 2SMART (NORTE-01-0145-FEDER-000054) supported by (NORTE 2020), under the PORTUGAL 2020 Partnership Agreement, through the ERDF; and by iii) LA/P/0045/2020 (ALiCE), iv) UIDB/00511/2020 and v) UIDP/00511/2020 (LEPABE), funded by national funds through FCT/MCTES (PIDDAC).

OC11. Life cycle sustainability assessment of new circular valorisation streams for the next-gen lithium-based energy storage systems

Joana R. Gouveia¹, Luís Oliveira¹, Belmira Neto^{2,3,4}

¹INEGI – Instituto de Ciência e Inovação em Engenharia Mecânica e Engenharia Industrial, Campus da FEUP, Rua Dr. Roberto Frias 400, 4200-465 Porto, Portugal, (jrgouveia@inegi.up.pt) ORCID [0000-0002-6833-9540](https://orcid.org/0000-0002-6833-9540), (loliveira@inegi.up.pt) ORCID [0000-0003-2180-0376](https://orcid.org/0000-0003-2180-0376)

²LEPABE – Laboratory for Process Engineering, Environment, Biotechnology and Energy, Faculty of Engineering, University of Porto, Rua Dr. Roberto Frias, 4200-465 Porto, Portugal (belmira.neto@fe.up.pt) ORCID [0000-0003-0572-4211](https://orcid.org/0000-0003-0572-4211)




³ALiCE – Associate Laboratory in Chemical Engineering, Faculty of Engineering, University of Porto, Rua Dr. Roberto Frias, 4200-465 Porto, Portugal

⁴DEMM – Department of Metallurgical and Materials Engineering, Faculty of Engineering, University of Porto, Rua Dr. Roberto Frias, 4200-465 Porto, Portugal

Abstract

This paper presents a project thesis aimed at assessing sustainability dimensions for the novel solid-state lithium-ion batteries. The focus is on the improvements that can be made concerning the environmental, economic and social performance of the current and future designs of solid-state batteries. The structure of the proposal is as follows: an overall analysis of solid-state battery critical raw material requirements regarding secondary sourcing and potential sustainability gains; then the development of battery cell eco-design guidelines based on current and upcoming directives on battery design; a techno-economic analysis on future battery market demand based on the growth of EV sales up to 2050; and finally a life cycle sustainability assessment on alternative recovery processes for lithium through waste streams. The proposed work aims to contribute with scientific advances for the sustainable development of the European lithium battery market.

Author Keywords. Lithium-ion batteries, solid-state batteries, sustainability, lithium, circularity.

 Open Access  Peer Reviewed  CC BY

1. Introduction

The increase of electric mobility has provided an alternative to road transport. Electric vehicles (EV) are recognised as crucial for reducing road emissions and energy demand (IEA 2022b; 2021). However, with the expected exponential growth in EV market sales (Tsiropoulos, Tarvydas, and Lebedeva 2018), the trajectory of electric mobility has come to a crossroads, as the cost for the main resources used in battery manufacturing is likely to continue to growth at a steady pace and the demand for larger production volumes is increasing (Fleischmann et al. 2021; IEA 2022a). Along with the rising costs is the public awareness of the environmental and social impacts associated with battery manufacturing and the need for end-of-life handling, especially the impacts from the extraction and processing of lithium (Li) (together with other critical materials), which is used as an electrolyte material for EV batteries.

It is of a pivotal importance to ensure that the critical raw materials (CRM) that are present in todays, and future, lithium-ion batteries (LIB) are recovered at the end of its life. However, current recycling processes have not suffered any significant changes over the years and, with the upcoming entry of new LIBs generations, such as solid-state batteries (SSB), it is necessary to ensure that these will undergo an effective recycling pathway.

Future European regulations on batteries, are expected to establish mandatory sustainability requirements (European Parliament 2022; European Commission 2020), namely for material demand, costs, battery performance and second-life applications. So far, these intentions have not yet been put into regulatory action.

The attempt to a robust transition towards circularity requires the quantification of the sustainability aspects of potential alternatives for CRM sourcing. The evaluation of the economic, environmental, and social dimensions will provide a stronger liability to the transitions towards potential sustainable gains and assist in determining the best performing solutions for the relevant stakeholders integrating the battery value-chain.

2. Materials and Methods

The project thesis is anchored to the European project RELiEF: Recycling of Lithium from Secondary Raw Materials and Further – which aims to develop new recovery processes of lithium from several secondary streams, with the final purpose of producing high-value lithium battery-grade materials and components.

As such, the work proposed in this project thesis aims to conduct extensive research on the several aspects that influence the future battery value chain regarding its environmental, economic and social performance, addressing material criticality, eco-design, and economic market trends for the novel solid-state battery, with a final focus on potential sustainability gains from recovering lithium from waste streams, for integration into higher value streams.

These gaps will be addressed in this project thesis, shown in Table , with the research questions and the objectives to be attained within each one of the phases of the PhD project.

	Research Question	Objective
1	Are the existing recovery and recycling pathways (pyro, hydrometallurgy and complementary) suitable for the new lithium based SSB (4th generation)?	To analyse current recycling technologies for their adaptability for the successful recycling of SSB designs, and provide new pathways for the identified technological gaps;
2	Which are the best practices for a sustainable design of cells used for the SSB regarding its key operational conditions?	To establish the best practises for the sustainable design of SSB, based on key performance indicators for all life cycle phases
3	What is the expected market volume demand of LIBs in 2050 considering the expected EV market sales? Will the expected LIB production for EV allow to respond to the 2050 climate goals of the Paris Agreement? What are the most promising sources for lithium from alternative recovery pathways?	To determine the most promising alternative pathways for lithium sourcing, based on future market trend analysis
4	Which are the main sustainability aspects (assessed through the economic, environmental, and social impacts) for the previously identified most promising pathways for recovering lithium from secondary waste-stream sources?	To analyse the sustainability of the identified pathways regarding their environmental, economic, and social performance, and compare with current lithium conventional extraction and production processes.

Table 1: Research questions and main objectives.

Table outlines the methodologies to be used in the response to each research question (RQ). In terms of the structure, each RQ will correspond to a chapter of the PhD project thesis.

RQ#	Methodologies and approaches	Chapter
RQ1	• Literature analysis	<i>Recovery and recycling pathways for the new generation of lithium based SSB</i>
RQ2	• Eco-design, by determining the main environmental aspects and requirements for advanced environmental and economic performance without hindering the technical performance.	<i>Best practises for a sustainable design of SSB cells</i>
RQ3	• Lean curve method, an approach for cost estimation and economic assessment, based on market projections for demands of EVs. • Prospective Life Cycle Assessment (p-LCA), to determine the environmental effects of the integrations of these new lithium streams in road transport GHG emissions and match them with the Paris Climate Agreement targets for 2050	<i>Techno-economic analysis of foreseen lithium value chains by 2050</i>

RQ4	<ul style="list-style-type: none"> Life Cycle Sustainability Assessment Framework, to analyse in a life cycle perspective the performance of lithium recovery pathways from secondary streams, applying life cycle assessment (LCA), life cycle costing (LCC) and social life cycle assessment (S-LCA). 	<i>Life cycle sustainability assessment of circular lithium production processes models</i>
------------	--	---

Table 2: Main methodologies to be applied in each research question and correspondent chapter

3. Conclusions

The PhD thesis is expected to contribute to the scientific community through advances in life cycle studies for strategic and sustainable developments for the lithium battery market.

References

- European Commission. 2020. "Proposal for a Regulation of the European Parliament and of the Council Concerning Batteries and Waste Batteries, Repealing Directive 2006/66/EC and Amending Regulation (EU) No 2019/1020" 0353 (2019). <https://eur-lex.europa.eu/legal-content/EN/TXT/?uri=CELEX%3A52020PC0798>.
- European Parliament. 2022. "Plenary – March I 2022," no. December 2020: 2022.
- Fleischmann, Jakob, Dorothee Herring, Friederike Liebach, and Martin Linder. 2021. "Unlocking Growth in Battery Cell Manufacturing for Electric Vehicles." <https://www.mckinsey.com/business-functions/operations/our-insights/unlocking-growth-in-battery-cell-manufacturing-for-electric-vehicles>.
- IEA. 2021. "Net Zero by 2050: A Roadmap for the Global Energy Sector." *International Energy Agency*, 224.
- IEA. 2022a. "Electric Cars Fend off Supply Challenges to More than Double Global Sales – Analysis - IEA." 2022. <https://www.iea.org/commentaries/electric-cars-fend-off-supply-challenges-to-more-than-double-global-sales>.
- IEA. 2022b. "Transport – Topics - IEA." 2022. <https://www.iea.org/topics/transport>.
- Tsiropoulos, Ioannis, Dalius Tarvydas, and Natalia Lebedeva. 2018. *Li-Ion Batteries for Mobility and Stationary Storage Applications - Scenarios for Costs and Market Growth*. Luxembourg: Publications Office of the European Union. <https://doi.org/10.2760/8717>.

Acknowledgments

This work was supported by the European Union's Horizon Europe research and innovation program through the RELiEF project (grant n° 101069789). This work was financially supported by LA/P/0045/2020 (ALiCE), UIDB/00511/2020 and UIDP/00511/2020 (LEPABE), funded by national funds through FCT/MCTES (PIDDAC).

OC12. A Tool for Working on Several Dimensions of Sustainability Based on Citizen Science

Daniela Amorim^{1,2*}, Fernando G. Martins^{1,2}, José C.M. Pires^{1,2}

¹LEPABE – Laboratory for Process Engineering, Environment, Biotechnology and Energy, Faculty of Engineering, University of Porto, Rua Dr. Roberto Frias, 4200-465 Porto, Portugal

²ALiCE – Associate Laboratory in Chemical Engineering, Faculty of Engineering, University of Porto, Rua Dr. Roberto Frias, 4200-465 Porto, Portugal

*Presenting author (up200906501@edu.fe.up.pt) ORCID (0000-0002-8439-5331)

Abstract

Sustainability is a theme that reaches everyone in companies and organisations, where it must also be worked on every day through small actions. This work presents a tool to allow everyone to analyse their performance in terms of sustainability and to trace actions for continuous improvement in daily life. The tool presents indicators in four dimensions of sustainability: social, economic, environmental and global analysis. Based on the answers of 357 people, consumerism, fair value of products, and a balanced career are the three indicators with low score. The most voted indicator for improvement by women was the consumerism and for men was the balanced career. The results by age are different and correspond to the different times of life, with older people selecting career issues.

Author Keywords. Sustainability, Citizen Science, Improvement, Environment, Social, Economic, Global.

Open Access Peer Reviewed CC BY

1. Introduction

Sustainability is a topic that is currently the focus of companies and other organisations but also of governments. Therefore, it needs to be worked with all citizens to fulfil the current challenges and achieve the desired improvements.

To meet their goals, companies, the other organisations and the governments need to engage and empower all people on the issue of sustainability. As this is a challenge, the Citizen Science method can facilitate the dissemination of information and engagement, as it is a method to engage people in science through individual results, opinions and participation on a voluntary basis (European Union, 2023).

The tool *Sustentablarte* is based on four groups of four indicators which allow the performance of each individual in the environmental, social, economic and global areas to be verified by scoring from 1 to 8 values in each of the 16 indicators (Amorim, 2023). Global indicators have been considered that allow looking at the topic of sustainability in a macro way in people's daily lives (Steven et al., 2022). This tool allows ordinary citizens to evaluate their daily performance in terms of sustainability, allowing them to make different decisions in their daily lives, leading to continuous improvement in a simple and intuitive way. (Amorim, 2023). Each part has four indicators that allow characterise and evaluate each dimension (Figure 1), where each indicator has its own explanation so that the citizen can understand whether to select one or eight.

Each column begins at value one and ends at value eight, as shown in Figure 3, providing a clear image of which areas are in greater deficit in that person's daily life.

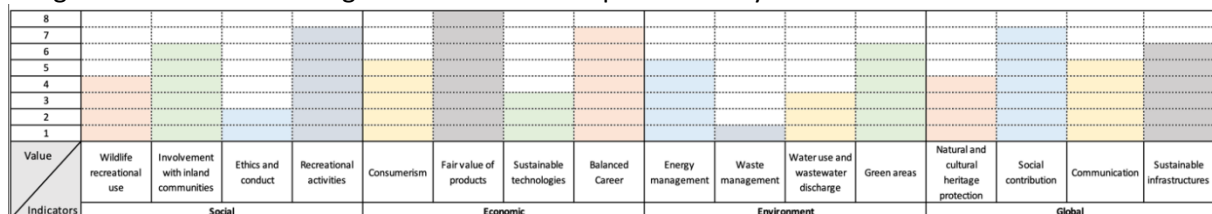


Figure 3: Tool with the filling done in example mode.

This study aims to test the tool *Sustentablarte* on the basis of citizen science to understand how the population performs by age group and gender in the 16 indicators of this tool.

2. Materials and Methods

A sequential mixed-method approach, which combines the benefits of qualitative and quantitative analyses, was implemented in “Sustentablarte” (Amorim, 2023).

For this study, the methodology was carried out in two phases:

- Phase 1 – Sample selection;
- Phase 2 – Data collection and analysis;

With these two phases, it is possible to know the compliance status of each person with the selected indicators.

2.1. Phase 1 – Sample selection

The sample for this study was selected following the Citizen Science methodology, where each person decides to participate on a voluntary basis. To this end, two forms of participation were created, the purchase of the sustainability diary, which included this tool or participation in lectures or workshops where this tool was carried out with the support of the team. The sending of the results was voluntary.

2.2. Phase 2 – Data collection with people

The data collection was carried out on people over the age of 16 and was intended to be carried out at events where its completion could be followed up.

During seven months (September 2022 until March 2023), the tool was carried out with people in seminars, lectures, and workshops where it was possible to compile several data and guide all these people in filling it in.

In academic terms no distinction was made from the sample as the aim would be to characterise the general population on a voluntary basis.

3. Results and Discussion

During the seven months, 357 people filled in the tool (Table), from which we obtained the data in Figure . It is possible to see that only three indicators - consumerism, fair product value, and balanced career - scored at value one, and three indicators did not score at value eight - ethics and conduct, fair product value, and social contribution.

		Age				Total
		<18 years	18-25 Years	26-40 Years	>40 Years	
Gender	Woman	13	57	117	76	263
	Men	3	17	41	33	94

Table 1: Sample characterisation

Another indicator that differs from the others is green areas, where all people voted from five, which shows the level of importance of these areas for the people who made up the sample.

When analysing the indicators by gender, the indicator most voted for by women with the value 1 is consumerism and for men it is a balanced career. In terms of age, the younger age groups have better scores in the environmental area, while the two older groups have better scores in the economic group.

		Age				
		<18 years	18-25 Years	26-40 Years	>40 Years	
Gender	Women	Consumerism(1)	Consumerism (1)	Balanced Career (1)	Consumerism (1)	Worst score
		Waste management (7)	Waste management (8)	Green areas (8)	Energy management (8)	Best score
	Men	Recreational activities (2)	Balanced Career (1)	Balanced Career (1)	Consumerism (1)	Worst score
		Waste management (7)	Waste management (8)	Green areas (8)	Energy management (7)	Best score

Table 2: Analysis of results according to age by gender, showing the worst and best results in each parameter

Overall, it can be seen that most of the scores are in the core values, such as shown in Figure .

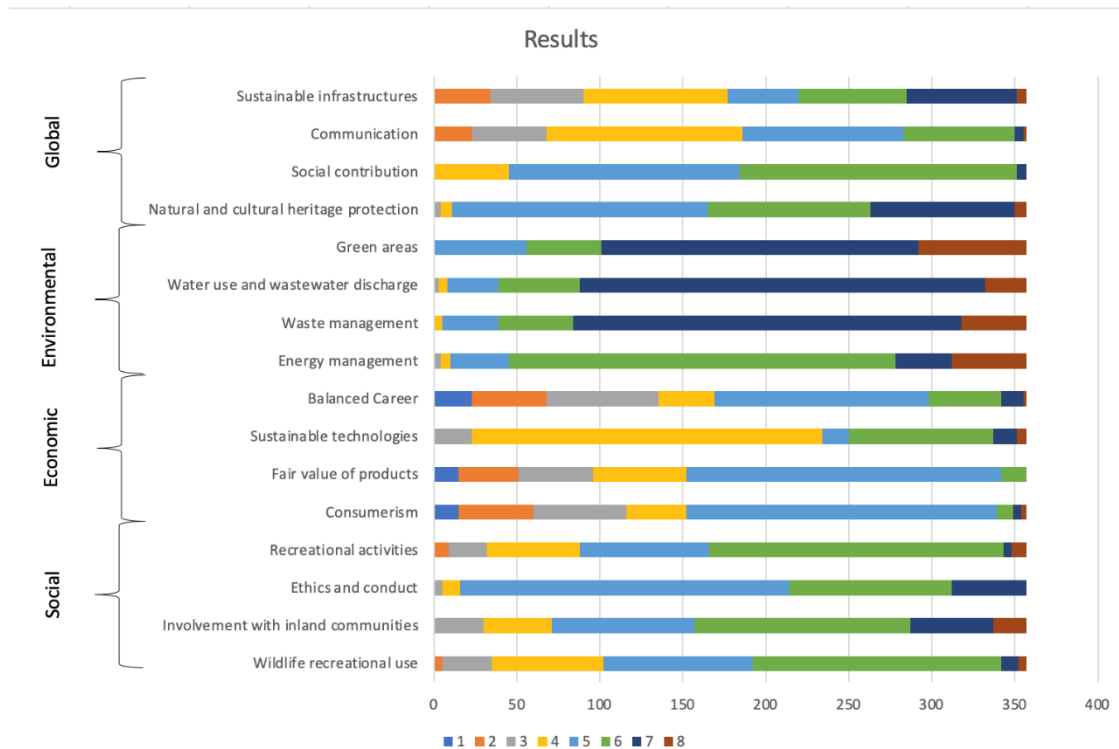


Figure 2: Results obtained from 357 people from September 2022 to March 2023.

With these results, it is possible to see that most people scored in values five and six (Table), which shows some concern with the indicators, but with room for improvement.

Indicators score	1	2	3	4	5	6	7	8
Relative Frequency	1%	3%	7%	14%	27%	26%	18%	4%

Table 3: Percentage of answers by indicator score out of 5712 answers.

4. Conclusions

In this analysis, it is possible to relate these groups of indicators to the consumption pattern and the origins of the products consumed in Portugal, since consumerism and the value of products are closely related and appear here as major points of improvement.

This point shows how people feel about their standard of living, but also indicates that there may be major points of demand from citizens when shopping in the future.

You can also see a lot of room for improvement in these indicators in the people who made up this sample since 52% of the people voted five or lower.

References

- Amorim, D. (2023). *Sustentável(mente)*. Cordel d' Prata.
- European Union. (19 de 04 de 2023). *eu-citizen.science*. Obtido de citizen.science: <https://eu-citizen.science>
- Steven, G., Muhammad, S., Roopali, M., & Jon, M. (2022). Sustainable management education and an empirical five-pillar model of sustainability. *The International Journal of Management Education*, Vol 20.

Acknowledgements

This work was financially supported by LA/P/0045/2020 (ALiCE) and UIDB/00511/2020-UIDP/00511/2020 (LEPABE), funded by national funds through FCT/MCTES (PIDDAC).

OC13. Production of slow-release fertilizers using biochar obtained from vine-canecan

Olena Dorosh^{1*}, Cristina Delerue-Matos¹, Manuela M. Moreira¹




¹ REQUIMTE/LAQV, Instituto Superior de Engenharia do Porto, Instituto Politécnico do Porto, Rua Dr. António Bernardino de Almeida, 431, 4249-015 Porto, Portugal

*Presenting author (olena.dorosh@graq.isep.ipp.pt) ORCID 0000-0002-5713-9041

Abstract

Biochar incorporation into the soil positively affects its physicochemical properties and can be used to obtain slow-release fertilizers (SRFs), that allow to control the dose of nutrients available for plant's uptake. Biochar characteristics may be engineered in order to meet the soil necessities. In the present work four different biochars were produced from vine-canecan: one without any kind of modification, one modified physically with a flux of CO₂ and other two chemically modified with AlCl₃ and MgCl₂. The results obtained indicate that the biochars obtained from vine-canecan are able to adsorb N, mainly at acidic pH values, and posteriorly could be used as plant fertilizers. The best adsorption results corresponded to 14.11 and 12.14 mg of N/g of biochar for the pristine biochar and the one modified with AlCl₃, respectively.

Author Keywords. Biochar, vine-canecan, slow-release fertilizers, nutrients and soil.

 Open Access  Peer Reviewed  CC BY

1. Introduction

Biochar is a carbon-rich porous material produced by thermal conversion of biomass at elevated temperatures and under an inert atmosphere (Tomczyk, Kondracki, and Szewczuk-Karpisz 2022). It has been gaining increased attention over the past years due to its properties, such as large surface area, presence of functional groups attached to its surface and high adsorption capacity (Wang et al. 2022). These properties make biochar a promising material for the incorporation into the soil as a corrective/fertilizer (Komnitsas and Zaharaki 2016). Another characteristic that makes this material so interesting and sustainable is that it can be prepared from agricultural and animal wastes, forest biomass and sewage sludge (Tomczyk, Kondracki, and Szewczuk-Karpisz 2022; Komnitsas and Zaharaki 2016). The biomass used and the pyrolysis conditions applied influence greatly the final material's physicochemical properties (Kazemi Shariat Panahi et al. 2020).

Considering the benefits of incorporating biochar into the soil and the necessity of replacing conventional fertilizers, the idea of producing slow-release fertilizers (SRFs) prepared from biochars has emerged (Khan et al. 2021). These SRFs would solve one of the main problems associated with the use of conventional fertilizers which is the overdosage, since they delay the nutrient availability for plant uptake after application and diminish the loss into the environment (Khan et al. 2021). As a matter of fact, a large percentage of the nutrients present in the conventional fertilizers, end up being leached, runoff and washed away (Wang et al. 2022). The main challenge encountered today for the production of SRFs from biochars are the insufficient textural parameters or low content of surface functional groups that cannot adsorb the desired quantities of nutrients (Tomczyk, Kondracki, and Szewczuk-Karpisz 2022). To overcome this obstacle, biochar engineering, through physical and chemical modifications, can be employed, since it allows achieving biochar properties that are optimum for specific applications and/or under certain conditions (Kazemi Shariat Panahi et al. 2020). Physical modifications include ball milling, gas or steam activation, and microwaves (Kazemi Shariat Panahi et al. 2020). Chemical modifications are performed using acids, bases, salts, polymers, or oxidation by hydrogen peroxides (Tomczyk, Kondracki, and Szewczuk-Karpisz 2022). The goal of this work was to produce biochars from vine-canecan, an agro-industrial residue, to be used as SRFs loaded with nitrogen, phosphorus, and potassium. Physical and chemical modifications were tested in order to compare their adsorption efficiency with the pristine biochar.

2. Materials and Methods

Vine-canecan of the Touriga Nacional variety were kindly provided by Sogrape and used as the raw material to produce the biochars. Biochar (B) was produced in an industrial oven from Ibero Massa Florestal (Portugal): 20 min of heating, 1 h of holding at 400 °C, without gas supply, and cooling

until room temperature. The physically modified biochar was produced under the same conditions described above but with a flow of CO_2 of 30 mg/L. While to produce the chemically modified biochars, 30 g of milled vine-canecan were mixed with 200 mL of an AlCl_3 (30 g/L) and MgCl_2 (200 g/L) solution were stirred overnight. After drying the mixtures, the vine-canecan were pyrolyzed applying the same conditions as used by Ibero Massa Florestal. All the biochars were then crushed using a mortar, sieved to a particle size smaller than 100 μm , and stored in closed plastic bags until further use.

To investigate the effects of pH on NO_3^- removal, 0.5 g of biochar were added to 50 mL of a NaNO_3 (50 mg/L) solution and the solutions pH were adjusted to values ranging between 2 and 13 with 0.1 M HCl or 0.1 M NaOH. After 24 h of stirring, the samples were filtered with a 0.22 μm nylon syringe filter and the amount of N still present in the solution was measured using a total nitrogen analyzer. The same was done for a commercial biochar (BC) in order to compare with the ones obtained from vine-canecan.

3. Discussion

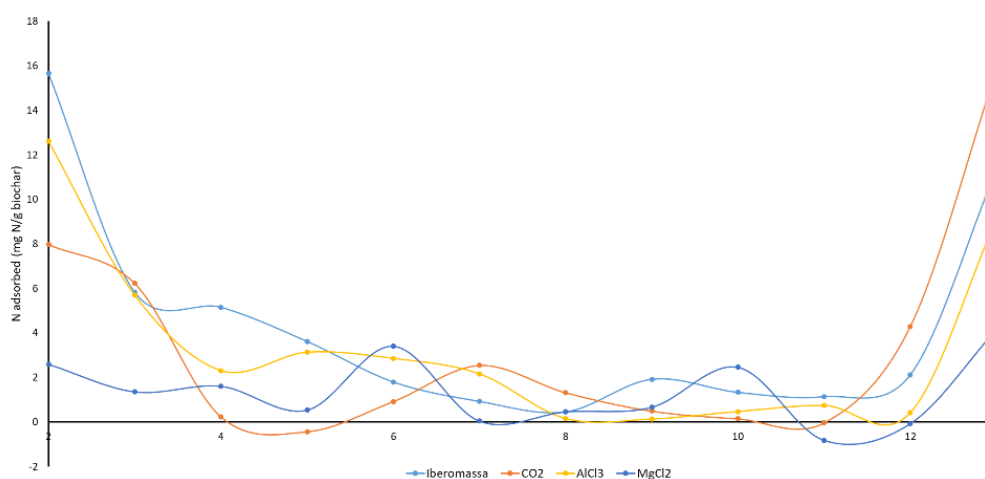


Figure 4: Adsorption of N in function of pH by biochar prepared from vine-canecan without modifications (B), biochar prepared from vine-canecan with flow of CO_2 (BCO₂) and biochar prepared from vine-canecan impregnated in AlCl_3 (BA AlCl_3) and MgCl_2 (BM MgCl_2).

The biochars adsorption efficiency was studied at pH values ranging from 2 to 13 and as it can be observed on Figure 4, all biochars adsorbed higher amounts of N at acidic and basic pH values, which was already expected considering that biochars are charged samples. The pristine biochar, the chemically modified with AlCl_3 and physically modified with CO_2 presented the highest adsorption values, corresponding to 15.40, 12.61 and 15.79 mg of N/g of biochar, respectively. At some pH values, the opposite seemed to occur and N naturally present in the biochar was released to the solution. Work is being developed in order to determine the adsorption kinetics and isotherms of N. Afterwards, the same studies will be performed for K and P.

4. Conclusions

Preliminary results show that vine-canecan can represent an environmentally friendly solution to produce SRFs loaded with N, as it would add economic value to an underutilized residue and at the same time produce bio-based fertilizers from organic sources and solve the problem of nutrients leaching.

References

Kazemi Shariat Panahi, Hamed, Mona Dehghani, Yong Sik Ok, Abdul Sattar Nizami, Benyamin Khoshnevisan, Solange I. Mussatto, Mortaza Aghbashlo, Meisam Tabatabaei, and Su Shiung Lam. 2020. "A Comprehensive Review of Engineered Biochar: Production, Characteristics, and

- Environmental Applications.” *Journal of Cleaner Production* 270: 122462. <https://doi.org/10.1016/j.jclepro.2020.122462>.
- Khan, Hamza Ahmad, Salman Raza Naqvi, M. Taqi Mehran, Asif Hussain Khoja, M. Bilal Khan Niazi, Dagmar Juchelková, and Abdulaziz Atabani. 2021. “A Performance Evaluation Study of Nano-Biochar as a Potential Slow-Release Nano-Fertilizer from Wheat Straw Residue for Sustainable Agriculture.” *Chemosphere* 285 (June). <https://doi.org/10.1016/j.chemosphere.2021.131382>.
- Komnitsas, Kostas A., and Dimitra Zaharaki. 2016. “Morphology of Modified Biochar and Its Potential for Phenol Removal from Aqueous Solutions.” *Frontiers in Environmental Science* 4 (APR): 1–11. <https://doi.org/10.3389/fenvs.2016.00026>.
- Tomczyk, Agnieszka, Bartosz Kondracki, and Katarzyna Szewczuk-Karpisz. 2022. “Chemical Modification of Biochars as a Method to Improve Its Surface Properties and Efficiency in Removing Xenobiotics from Aqueous Media.” *Chemosphere* 312 (P1): 137238. <https://doi.org/10.1016/j.chemosphere.2022.137238>.
- Wang, Chongqing, Dan Luo, Xue Zhang, Rong Huang, Yijun Cao, Gonggang Liu, Yingshuang Zhang, and Hui Wang. 2022. “Biochar-Based Slow-Release of Fertilizers for Sustainable Agriculture: A Mini Review.” *Environmental Science and Ecotechnology* 10: 100167. <https://doi.org/10.1016/j.ese.2022.100167>.

Acknowledgments

This work was financially supported by the Fundação para a Ciência e a Tecnologia (FCT) / the Ministério da Ciência Tecnologia e Ensino Superior (MCTES) through national funds (Portugal) [UIDB/50006/2020, UIDP/50006/2020, LA/P/0008/2020]. Olena Dorosh (2021.05322.BD) is thankful for her Ph.D. grant financed by FCT/MCTES. Manuela M. Moreira (CEECIND/02702/2017) is thankful for her contract financed by FCT/MCTES—CEEC Individual Program Contract and to REQUIMTE/LAQV. The supply of the vine-canes is acknowledged to Sogrape, S.A.

OC14. Potential recovery of phosphorus in the Portuguese urban sector: an opportunity for a critical raw materials supply?

Aías Lima^{1*}, Paulo Ramisio¹, Sónia Figueiredo^{2,3}, Nídia Caetano^{3,4,5}

¹ Centre for Territory, Environment and Construction, University of Minho, Campus de Azurém, 4804-533 Guimarães, Portugal

² LAQV/REQUIMTE – Laboratório Associado para a Química Verde/Rede de Química e Tecnologia, Instituto Superior de Engenharia do Porto, Rua Dr. António Bernardino de Almeida 431, 4249-015 Porto, Portugal (saf@isep.ipp.pt) ORCID 0000-0001-8548-2528

³ Instituto Superior de Engenharia do Porto, Rua Dr. António Bernardino de Almeida 431, 4249-015 Porto, Portugal

⁴ LEPABE - Laboratory for Process Engineering, Environment, Biotechnology and Energy, Faculty of Engineering, University of Porto, Rua Dr. Roberto Frias, 4200-465 Porto, Portugal (nsc.isep.ipp.pt) ORCID 0000-0002-2185-6401


⁵ ALiCE - Associate Laboratory in Chemical Engineering, Faculty of Engineering, University of Porto, Rua Dr. Roberto Frias, 4200-465 Porto, Portugal

*Presenting author (1180080@isep.ipp.pt); ORCID 0000-0002-1656-2281

Abstract

Phosphorus (P), which plays an important role in the food sector, is facing a global shortage. It has been identified as one of the materials at risk of scarcity, and in 2014 it was declared as a critical raw material by the European Union. Studies indicate that the only way to close the P loop in the European Union is to recycle P from waste streams back into the food chain. In Portugal, the loss of P after wastewater treatment and landfilling has considerable value, motivating the evaluation of recovery and potential recovery of phosphorus. In addition, sludge from wastewater treatment plants (WWTP), which represents a specific flow of this sector, was also identified as having a high potential for P recovery. This work presents a preliminary assessment of the circularity of phosphorus in the urban cycle and the corresponding technical and political issues involved.

Author Keywords. Agricultural fertilizers, Circular economy, Phosphorus, Valorization potential, WWTP sludge

 Open Access  Peer Reviewed  CC BY

1. Introduction

Studies indicate that the only way to close the phosphorus (P) loop in the European Union is to recycle this nutrient from waste streams back into the food chain. P plays an important role as agricultural fertilizer for food production, and it is facing a global shortage, having been identified as one of the materials at risk of scarcity, and in 2014 it was declared as a critical raw material by the European Union (Blankestijn, 2019).

The Urban Wastewater Treatment Directive (Directive 91/271/EEC, 1991) and its recent proposal for revision, the Waste Framework Directive (Directive 2008/98/EC, 2008), as well as the new EU Fertilizing Product Regulation (Regulation (EU) 2019/1009, 2019), within the framework of the EU Circular Economy Package (COM98, 2020), all point to increase recycling efforts, to improve resource efficiency, and to strengthen biowaste management. These directives have been reformulated to consider nutrients recovered from wastes as raw materials. Also, the specification of valued materials for raw material sources has been provided by the European Fertilizing Product Regulation, contributing to closing nutrient cycles within the EU member states (Garske et al., 2020).

Experimental studies have already proved the significance of P recovery from wastewater, which could enable the provision of supplementary fonts to fertilizer stocks, indicating that P recycling from different EU waste streams can potentially meet up to 30% of national demand (El Wali et al., 2019). The Global Compendium of Phosphorus Recovery from Sewage/Sludge/Ash (2019), points out that no environmental protection measure would have been implemented without law enforcement, especially when it leads to additional costs, since the legal framework is tailored for the existing *status quo* and is very slow in adapting to future challenges. The re-definition of *End-of-Waste* criteria is a tough process, but also a prerequisite to enable value chains to bridge the gap

between recovery and recycling. Most of the technologies can also be adapted and applied in anaerobic digesters in landfills.

Portugal, according to Van Dijk et al. (2016) ranks third among European countries with the highest concentration of phosphorus in agricultural soils (13.2 kg P/ha-year), thus having significant potential to reduce imports of phosphate fertilizers, and/or to market the recovered P, to countries with a lower nutrient balance.

This research focuses on estimating the potential value of P recovery in the Portuguese waste and wastewater sectors by characterizing and evaluating the circularity of phosphorus within its production and consumption chain, based on demographic, spatial, and economic data.

2. P in wastewater and solid waste in Portugal - potential for resources recovery

Golroudbary et al. (2020) found that some countries (in which Portugal is included) would not improve their decisions related to phosphorus recovery and use, concluding that reuse policies represent a higher limitation than resource recovery technologies.

Based on recent data concerning P present in WWTP sludge, provided by the Portuguese waste and water reports (ERSAR, 2023), and in solid waste, according to the *Code of good agricultural practices* (2018), and expanding the analysis to P consumption in agricultural soils (INE, 2021), it is possible to conclude that the potential for P recovery through the solid waste and wastewater sectors would be sufficient to supply all P soil demand, as depicted in Figure , and even to explore its commercial value as a recovered raw material.

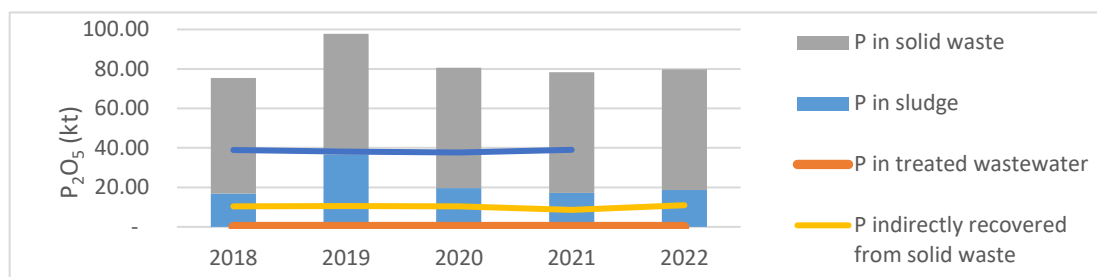


Figure 1: Evolution of P content in wastewater and solid waste (2018-2022)

According to the *Decreto Lei Nº. 276/2009*, which regulates sludge management and its use in agricultural soils, even after its recovery, the reuse of P still faces some challenges, related to sludge and soil characteristics, the dependence on spatial and climate conditions, suggesting the need for a strategic sludge plan management. However, nutrient products resulting from the crystallization of phosphorus, having the possibility of being used as fertilizers, must pass through the scrutiny of the national regulations related to the fertilizer market.

3. Conclusions

This study constitutes an initial approach to the implementation of phosphorus circularity and the promotion of the circular economy through its valorization. From the work carried out, it can be concluded that the wastewater and waste sectors have great potential for enhancing phosphorus recovery throughout their life cycle. Portugal, in addition to presenting a great potential for P recovery, presents a considerably favorable soil P balance, which would generate a surplus of recovered P, that can be valued.

References

- Blankesteyn M., 2019. "From measuring to removing to recovering phosphorus in water management in the Netherlands: Challenges for science-based innovation". *Science of the Total Environment*, 666:801–811. Accessed 22 May 2023. DOI: 10.1016/j.scitotenv.2019.02.230
- Code of Good Agricultural Practices, 2018. ENVIRONMENT AND AGRICULTURE, FORESTS AND RURAL DEVELOPMENT. Offices of the Secretaries of State for the Environment and Forestry and Rural Development. Portugal, 2018. (in Portuguese) Accessed 22, May 2023. <https://files.dre.pt/2s/2018/02/025000000/0413204170.pdf>

- COM98, 2020. Communication from the Commission to the European Parliament (2020). A new Circular Economy Action Plan. Accessed 22, May 2023. <https://www.un.org/sustainabledevelopment/sustainable-consumption-production/>
- Decreto-Lei No. 276/2009, of October 2, 2009. Ministry of the Environment, Spatial Planning, and Regional Development. *Diário da República* n.º 192/2009, Series I of 2009-10-02, pages 7154 – 7165. (in Portuguese) Accessed 22 May, 2023. <https://dre.pt/dre/detalhe/decreto-lei/276-2009-490974>
- Directive 2008/98/EC of the European Parliament and of the Council of 19 November 2008 on waste and repealing certain Directives (Text with EEA relevance). (n.d.). Accessed 22 May 2023. <https://eur-lex.europa.eu/legal-content/EN/TXT/?uri=celex%3A32008L0098>
- Directive 91/271/EEC of the European Parliament and of the Council, of 21 May 1991, concerning urban waste-water treatment. N. L. 135/40. (1991). Accessed 22 May 2023. <https://eur-lex.europa.eu/legal-content/EN/TXT/?uri=celex%3A31991L0271>
- El Wali M., Golroudbary S. R., and Kraslawski A., 2019. “Impact of recycling improvement on the life cycle of phosphorus”. *Chinese Journal of Chemical Engineering*, 27(5): 1219–1229. Accessed 22 May 2023. DOI: 10.1016/j.cjche.2018.09.004
- ERSAR, 2023. RASARP Annual report of the water and waste sector, Volume 2 - Economic and financial characterization of services. Portugal, 2018, 2019, 2020, 2021, 2022. (in Portuguese) Accessed 22 May 2023. <https://www.ersar.pt/pt/site-publicacoes/Paginas/edicoes-anuais-do-RASARP.aspx>
- Garske B., Stubenrauch J., Ekardt and F., 2020. “Sustainable phosphorus management in European agricultural and environmental law”. *Review of European, Comparative & International Environmental Law*, 29(1):107–117. Accessed 22 May 2023. DOI: 10.1111/reel.12318
- Global compendium on phosphorus recovery from sewage/sludge/ash, 2019. lead agent: Kompetenzzentrum Wasser Berlin (Germany) and p-rex® environment (Germany). Accessed 22 May 2023. <https://www.vesiyhdistys.fi/wpcontent/uploads/2019/12/GWRCPhosphorusCompendiumFinalReport2019-March-20.pdf>
- Golroudbary S. R., El Wali M., and Kraslawski A., 2020. “Rationality of using phosphorus primary and secondary sources in circular economy: Game-theory-based analysis”. *Environmental Science & Policy*, 106:166–176. Accessed 22 May 2023. DOI: 10.1016/j.envsci.2020.02.004
- National Institute of Statistics - Agricultural Statistics: 2021. Lisbon: INE, 2021. (in Portuguese) Accessed 22 May 2023. <https://www.ine.pt/xurl/pub/210756829>. ISSN 0079-4139. ISBN 978-989-25-0265-6
- Regulation (EU) 2019/1009 of the European Parliament and of the Council, 2019. laying down rules on the making available on the market of E. fertilizing products and amending R. (EC) N. 1069/2009 and (EC) N. 1107/2009 and repealing R. (EC) N. 2003/2003. (2019). Accessed 22 May 2023. <https://eur-lex.europa.eu/legal-content/EN/TXT/?uri=celex%3A32019R1009>
- Van Dijk K. C., Lesschen J. P., and Oenema O., 2016. “Phosphorus flows and balances of the European Union member states”. *Science of the Total Environment*, 542:1078–1093. Accessed 22 May 2023. DOI: 10.1016/j.scitotenv.2015.08.048

Acknowledgments

We would like to thank the financial support of the Foundation for Science and Technology (FCT)/Ministry of Science, Technology and Higher Education for the Ph.D. scholarship grant with the reference 2022.12500.BD to CTAC (UIDB/04047/2020), ALiCE (LA/P/0045/2020), LEPABE (UIDB/00511/2020 and UIDP/00511/2020), CIETI (UIDB/04730/2020), and LAQV/REQUIMTE (UIDB/50006/2020, UIDP/50006/2020, and LA/P/0008/2020).

OC15. One Step Forward to Sustainable Cosmetics

Inês Brito^{1,2*}, Sara M. Ferreira^{1,2}, Lúcia Santos^{1,2}

¹LEPABE—Laboratory for Process Engineering, Environment, Biotechnology and Energy, Faculty of Engineering, University of Porto, Rua Dr. Roberto Frias, 4200-465 Porto, Portugal



²ALiCE—Associate Laboratory in Chemical Engineering, Faculty of Engineering, University of Porto, Rua Dr. Roberto Frias, 4200-465 Porto, Portugal

*Presenting author (up201806661@edu.fe.up.pt) ORCID [0009-0008-2057-3478](https://orcid.org/0009-0008-2057-3478)

Abstract

The use of water in personal care products and their packaging consisting mainly of plastic are two major problems of the Cosmetic Industry, imposing the need to develop sustainable cosmetics. On the other hand, it is reported in literature that by-products of the catering and agricultural sector are rich in phenolic compounds with bioactive properties, namely high antioxidant capacity, suggesting the possibility to incorporate them in cosmetic formulations. In that regard, the purpose of this work is the development of a sustainable formulation of solid shampoo, incorporating extracts from mango peel to act as antioxidant, contributing to a circular economy. The characterization of the extracts revealed the presence of several phenolic compounds and a strong antioxidant capacity. The following stage is the performance evaluation of the solid shampoo after the incorporation of the extracts.

Author Keywords. Solid shampoo, mango peel, phenolic compounds, antioxidant.

 Open Access  Peer Reviewed  CC BY

1. Introduction

One of the great issues associated with the Cosmetic Industry is the amount of plastic generated for the packaging of personal care products used by the worldwide population, more specifically, shampoo. This results in increased waste, greenhouse gas emissions and pollution of waterways, due to plastic incineration and its high decomposition time. Furthermore, commercial shampoos contain a high water content to dilute the mixture, imposing a serious problem since this resource is getting scarcer (Aguar et al. 2022, 35, 39).

Therefore, the Cosmetic Industry needs to adopt innovative sustainable practices. For instance, solid cosmetics are a good alternative to commercial products. Because of their anhydrous formulation, the use of water is substantially reduced, as well as the amount of packaging. Additionally, since the formulation is more concentrated, anhydrous products last longer than conventional products and have a higher shelf life (Aguar et al. 2022, 41).

On the other hand, it has been shown in literature that by-products from the agriculture and catering sectors, such as seeds or peels, are rich in phenolic compounds (Capanoglu, Nemli, and Tomas-Barberan 2022, 6793), which are secondary metabolites produced by plants to defend itself from exposure to stress conditions (Tungmunnithum et al. 2018, 95). Due to their antioxidant capacity, they have the potential to be incorporated in cosmetic formulations.

Hence, the purpose of this work is the development of a natural shampoo bar formulation, incorporating extracts from by-products of a local restaurant, more specifically mango peel (MP), and evaluate the possibility of being a replacement for commercial antioxidants. In this way, the saving and the recovery of natural resources, as well as the reduction of waste, would be accomplished, contributing to a circular economy.

2. Materials and Methods

For the extraction of the phenolic compounds from mango peel of the Palmer variety, it was performed a solid-liquid extraction, using a Soxhlet extractor and ethanol as solvent. For the evaluation of the antioxidant potential of the extract, it was performed the Total Phenolic Content (TPC), the DPPH (2,2-diphenyl-1-picrylhydrazyl) and the ABTS (2,2-azinobis (3-ethyl-benzothiazolin-6-sulfonic acid)) assays. For the identification and quantification of the phenolic compounds, it was performed high-performance liquid chromatography coupled to diode array detection (HPLC-DAD), according to the method described in Ferreira, Gomes, and Santos (2023, 2052).

3. Discussion

In Table are the results of the characterization of the mango peel extract.

Characterization of the Mango Peel Extract		
	TPC ($\text{mg}_{\text{GAE}} \cdot \text{g}^{-1}_{\text{extract}}$)	12.2 ± 0.8
DPPH	IC_{50} ($\text{mg}_{\text{extract}} \cdot \text{L}^{-1}$)	53.0 ± 3.4
ABTS	TEAC ($\text{mg}_{\text{Trolox}} \cdot \text{g}^{-1}_{\text{extract}}$)	323.7 ± 23.9
HPLC-DAD		
Compound Identified	Concentration ($\text{mg} \cdot \text{g}_{\text{extract}}^{-1}$)	
Catechin	97.4	
Chlorogenic Acid	50.6	
Quercetin	114.2	
Rosmarinic Acid	185.3	

The results are expressed as mean \pm standard deviations of 4 independent measurements. TPC: total phenolic content; GAE: gallic acid equivalents; IC_{50} : the concentration of extract necessary to inhibit 50% of DPPH radical; TE: Trolox equivalents; TEAC: Trolox equivalent antioxidant capacity; HPLC-DAD: high-performance liquid chromatography coupled to diode array detector.

Table 1: Results of the total phenolic content and antioxidant capacity of the mango peel extract and compounds identified by HPLC-DAD.

The total phenolic content of the extract was inferior to the literature values (Suleria, Barrow, and Dunshea 2020, 1212), however, that can be associated with the use of a different extraction method. Additionally, the variety and growing conditions of the fruit may interfere with the composition of the peel, and consequently with the TPC of the extract.

Concerning the antioxidant capacity, the obtained IC_{50} value indicates that the MP extract is a strong antioxidant, according to literature (Fitrasyah et al. 2021, 199). Previous studies have reported the presence of the compounds listed in Table 1 in MP extracts, except for rosmarinic acid, which was the main phenolic compound found in this study. As mentioned previously, such difference may be related to the differing extraction conditions and variety of the fruit.

Before the incorporation of the antioxidants in the solid shampoo, it was made several attempts to develop an ideal formulation, which is presented in Table . Initially, Phase A and Phase B, were melted separately at 80 °C. Afterwards, the two phases were mixed until obtaining a homogenous solution and Phase C, D and E were added.

The following step is to incorporate the MP extract in the formulation and evaluate its potential as an antioxidant. Additionally, several tests will be executed on the solid shampoo over a period of 6 weeks to evaluate the organoleptic and physiochemical properties, the ability to remove dirt from the hair, the degree of oxidation as well as the thermal stability.

Phase	Ingredient	Function	% (w/w)
A	Sodium Cocoyl Isethionate	Primary Surfactant	65
	Coco Glucoside	Secondary Surfactant	20
B	Beeswax	Consistency adjustment	7
	Shea Butter	Emollient	5
	Panthenol	Humectant	1
C	Essential Oil	Fragrance	1
D/E	Tocopherol/ Lactic Acid	Commercial Antioxidant/ Buffer	1/ 0.05

Table 2: Formulation of the developed solid shampoo bar.

4. Conclusions

The results of the characterization of the MP extract revealed that the extract is a promising alternative to the commercial antioxidants used in cosmetic formulations. This suggests that by-products from the catering sector may be reused to develop value-added cosmetics. With the base

formulation for the solid shampoo, the following step is to incorporate the MP extract in the formulation and evaluate its antioxidant potential, as well as the performance.

References

- Aguiar, Joana B., *et al.* 2022. "Water sustainability: A waterless life cycle for cosmetic products." *Sustainable Production and Consumption* 32: 35-51. <https://doi.org/10.1016/j.spc.2022.04.008>.
- Capanoglu, Esra, *et al.* 2022. "Novel Approaches in the Valorization of Agricultural Wastes and Their Applications." *Journal of Agricultural and Food Chemistry* 70 (23): 6787-6804. <https://doi.org/10.1021/acs.jafc.1c07104>.
- Ferreira, Sara M., *et al.* 2023. "A Novel Approach in Skin Care: By-Product Extracts as Natural UV Filters and an Alternative to Synthetic Ones." *Molecules* 28 (5): 2037-2058. <https://doi.org/10.3390/molecules28052037>.
- Fitriyasyah, Siti Ika, *et al.* 2021. "Analysis of Chemical Properties and Antioxidant Activity of Sambiloto (*Andrographis paniculata* Nees.) Leaf Tea Formula as a Functional Drink in Preventing Coronavirus Diseases and Degenerative Diseases." *Open Access Macedonian Journal of Medical Sciences (OAMJMS)* 9 (A): 196-201. <https://doi.org/10.3889/oamjms.2021.5872>.
- Suleria, Hafiz AR, *et al.* 2020. "Screening and characterization of phenolic compounds and their antioxidant capacity in different fruit peels." *Foods* 9 (9): 1206-1232. <https://doi.org/10.3390/foods9091206>.
- Tungmunnithum, Duangjai, *et al.* 2018. "Flavonoids and other phenolic compounds from medicinal plants for pharmaceutical and medical aspects: An overview." *Medicines* 5 (3): 93-109. <https://doi.org/10.3390/medicines5030093>.

Acknowledgments

This work was financially supported by: LA/P/0045/2020 (ALiCE), UIDB/00511/2020 and UIDP/00511/2020 (LEPABE) and funded by the project S4Hort_Soil&Food – Sustainable practices for Soil health & horticultural products quality improvement in the Entre Douro e Minho Region, with reference NORTE-01-0145-FEDER-000074, co-financed by the European Regional Development Fund (ERDF), through the North Portugal Regional Operational Programme (NORTE2020), under the PORTUGAL 2020 Partnership Agreement.

Sara M. Ferreira would like to thank the Portuguese Foundation for Science and Technology (FCT) for her PhD grant (2022.10910.BD).

List of Posters displayed in the Symposium on Environmental Engineering

Water and Waste Management: towards new approaches

1. Microalgal growth in urban wastewater: biomass production with nutrients removal - Sara Sousa, Ana F. Esteves, José Carlos Pires, Eva Salgado #198
2. Textile Effluent Treatment: from Microalgae Growth to Nutrient Removal - Rúben A. Martins, Eva M. Salgado, Ana L. Gonçalves, José C. Pires, Ana F. Esteves # 204
3. Microalgae harvesting by flocculation followed by dissolved air flotation: the effect of a natural flocculant concentration and mixing time. - Carolina Maia, Larissa Ramos, José C.M. Pires, Joana A. Loureiro, Maria Carmo Pereira. #212
4. Adsorption capacity of two synthesized biochars and their application in pharmaceuticals removal. - Nuria Bernárdez, Emilio Rosales, Marta Pazos, M. Ángeles Sanromán. #347
5. Removal of Remazol Brilliant Orange dye by chitin beads modified by ionic liquid. - Salima Benniche, Ariana Pintor, Ounissa Kebeche-Senhadji, Cidália Botelho, Claudia Fontas. #179
6. Combined adsorption and electrochemical treatments for the remediation of water containing sulfamethoxazole. - Verónica Poza-Nogueiras, Nuria Bernárdez, Bárbara Lomba, Marta Pazos, M. Ángeles Sanromán. #330
7. A novel approach to prepare ZnFe-MOF adsorbent and catalyst: Application in dye and drugs removal from wastewater - Daniel Terrón, Emilio Rosales, Marta Pazos, M. Ángeles Sanromán #368
8. Coagulants derived from chestnut shell and maritime pine bark extracts: preparation and use for textile effluent decolorization - Isabella Tomasi, Mafalda Rodrigues, Sílvia Santos, Rui Boaventura, Cidália Botelho #191
9. Urban Wastewater Resources Recovery – Integration of Nanofiltration and Advanced Oxidation Processes - Carla S. Santos, Rosa Montes, Rosário Rodil, José Quintana, Ana I. Gomes, Vítor J.P. Vilar #174
10. Design and synthesis of spherical Fe_{2.4}Cu₁-MOF@PAN for coloured effluent treatment. - Antía Fdez-Sanromán, M^a Angeles Sanromán, Marta Pazos, Emilio Rosales #335
11. Photocatalytic oxidation of *n*-decane in the mili-photoreactor NETmix. - Sandra M. Miranda, Tatiana Matiazzo, Natan Padoin, Cíntia Soares, Tânia F.C.V. Silva, Vítor J.P. Vilar. #374
12. NETmix crystalliser for struvite precipitation: CFD modelling of flow dynamics and distribution - Laura J.R. Cullen, Isabel S. Fernandes, Ricardo J. Santos, Vítor J.P. Vilar #405

13. Photocatalytic H₂O₂ generation and pollutant degradation by nonmetal doped carbon nitride - Amanda Fujita, André Torres-Pinto, Maria J. Sampaio, Cláudia G. Silva, Joaquim L. Faria, Adrián M.T. Silva #409
14. Recycling of printed circuit board (PCB) waste as a catalyst in advanced water treatment - Marta A.P. Azevedo, Cátia A.L. Graça, Márcia A.D. Silva, Liliana M. Martelo, Helena M.V.M. Soares, Adrián M.T. Silva #404
15. H₂O₂-assisted photocatalytic degradation of pharmaceuticals in surface waters - Thalita Tavares, André Torres-Pinto, Cláudia G. Silva, Joaquim L. Faria, Adrián M.T. Silva #408
16. Evaluation of temperature and nitrogen modified activated carbons as catalysts in the ozonation of emerging pollutants - Cátia A.L. Graça, Riccardo Zema, Carla A. Orge, João Restivo, Juliana Sousa, M. Fernando R. Pereira, O. Salomé G.P. Soares #293
17. Generation of sulphate radical through heterogenous catalysis for wastewater remediation. - Alba Giráldez, Marta Pazos, Ángeles Sanromán #346
18. Towards the development of a simple molecularly imprinted electrochemical sensor for the detection of carbamazepine. - Verónica Poza-Nogueiras, João G. Pacheco, Cristina Delerue-Matos #332
19. Phytotoxicity Testing of Sewage Sludge and Individual Emerging Contaminants in Agricultural Soil. - Ana Sofia Fernandes, Filipe Rocha, Thiago Silva, Vera Homem. #166
20. CFD Design of a Raceway Pond Reactor: Overall geometry improvement. Margarida L.R. Peixoto, Margarida S.C.A. Brito, Ricardo J. Santos, Vítor J.P. Vilar #406

Sustainability and Innovation: seeking a new future

21. CO₂/N₂ separation using PDMS membranes with inorganic filler ZSM-5 - Inês Rodrigues, Lidia Martínez-Izquierdo, Carlos Téllez, Joaquín Coronas, Alírio Rodrigues, Vítor Vilar, Alexandre Ferreira. #255
22. Automatic monitoring and measurement system for electrodegradation processes – M. Rúa-Pereira, E. Soto, E. González-Romero, M. Pazos, E. Rosales, M.A. Sanroomán #349
23. Evaluation of municipal sewage sludge compliance with Portuguese legislation for its agricultural use - Filipe Rocha, Idalina Bragança, Nuno Ratola, Vera Homem - #324
24. Incorporation of *Moringa oleifera* leaf powder and extract in cereal-based foods - Teresa Ferreira, Sandra M. Gomes, Anabela Leitão, Arminda Alves, Lúcia Santos #314

Clean Air and Energy: becoming accessible for all

25. Tailoring photoelectrochemical stability of tantalum nitride for solar redox flow cells - Filipe Moisés M. Francisco, Paula Dias, Adélio Mendes #357

26. Recent advancements in identifying sources of indoor air pollution using continuous monitoring methods. – H. Chojer, P.T.B.S Branco, F.G. Martins, S.I.V. Sousa. #310
27. Understanding indoor air quality in private dwellings: a case study of Portuguese homes. - Adhymaura Silva, Maria C. Pereira, Klara Slezakova. #9
28. Impact of PM_{2.5} in schools on asthma-related symptoms. - Juliana P. Sá, Pedro T.B.S. Branco, Maria C.M. Alvim-Ferraz, Fernando G. Martins, Sofia I.V. Sousa #313
29. Indoor air quality in vehicles: Can low-cost sensors be used as CO2 indicators? - Ana Catarina T. Silva, Pedro T.B.S. Branco, Sofia I.V. Sousa - #306
30. Future shipping emissions – a review. - Rafael A.O. Nunes, Maria C.M. Alvim-Ferraz, Fernando G. Martins, Sofia I.V. Sousa. #303

P01. Microalgal growth in urban wastewater: biomass production with nutrients removal

Sara Sousa^{1,2*}, Ana F. Esteves^{1,2,3}, José Carlos Pires^{1,2}, Eva Salgado^{1,2}

¹ LEPABE- Laboratório de Engenharia de Processos, Ambiente, Biotecnologia e Energia, Faculty of Engineering, University of Porto, Rua Dr. Roberto Frias, 4200-465 Porto, Portugal

² ALiCE - Associate Laboratory in Chemical Engineering, Faculty of Engineering, University of Porto, Rua Dr. Roberto Frias, 4200-465 Porto, Portugal


³ LSRE-LCM - Laboratory of Separation and Reaction Engineering - Laboratory of Catalysis and Materials, Faculty of Engineering, University of Porto, Rua Dr. Roberto Frias, 4200-465 Porto, Portugal

*Presenting author (up201806617@up.pt)

Abstract

Microalgae technologies have emerged as a viable option for treating wastewater with distinct characteristics. This work aims to study the performance of the microalga *Chlorella vulgaris* in the tertiary treatment of wastewater, evaluating its growth and contaminants removal. Microalgae were able to grow and remove nutrients from secondary effluents supplemented with 1% (M1) and 5% (M5) digestate from sludge anaerobic digestion. Nitrogen removal efficiencies of 100% were observed in both cases. In M1, the phosphorus concentration was negligible by the end of the assay. In terms of growth and nutrient removal, the results for assay M1 were more favourable than M5, complying with the new maximum limits for nutrient discharge.

Author Keywords. Microalgae; Nutrients removal; Urban effluents; Wastewater bioremediation.

 Open Access  Peer Reviewed  CC BY

1. Introduction

Since the beginning of the 19th century, world population growth and the consequent industrial development have caused an increase in the global average temperature and the amounts of wastewater discharged into waterways (NASA, 2013). Some compounds present in these discharges, namely nitrogen (N) and phosphorus (P), are responsible for harmful effects on aquatic environments, particularly eutrophication (Zhu et al., 2019). Therefore, it is necessary to regulate effluent discharge at values that reflect the assimilative capacity of the medium (Qv et al., 2023). The current European Urban Wastewater Treatment Directive (EU Directive 91/271/EEC) will be revised with more stringent discharge limits for P and N (0.5 mg_P/l or 90% P removal; 6 mg_N/l or 85%N removal) (European Commission 2022), and wastewater treatment plants (WWTP) should be adapted to treat contaminated urban effluents up to these values. Previous studies have confirmed the ability of microalgae to perform bioremediation of wastewater by removing pollutants such as N, P, pathogens, and heavy metals (Xiao and Zheng 2016). Moreover, microalgae such as *Chlorella* have been shown to be rather tolerant to contamination by toxic compounds (Abdelfattah et al., 2023). Microalgae technologies have appeared as an alternative for removing contaminants from various effluents and at different stages of the treatment process (Tam and Wong 1996). These systems have economic and environmental advantages (You et al., 2022). This work aims to study the ability of the microalga *Chlorella vulgaris* to perform the tertiary treatment of wastewater, assessing its growth and contaminants removal.

2. Materials and Methods

Secondary effluent from a WWTP was supplied with 1% (M1 assay) and 5% (M5 assay) mixture (v/v) of digestate from sludge anaerobic digestion and used to culture microalgae. Three independent experiments were performed for each of these conditions. Three types of controls were analyzed: (i) a negative control (effluent mixture without microalgae) exposed to light for each mixture (C-M1 and C-M5); (ii) a negative control under dark conditions for each mixture (CE-M1 and CE-M5); and (iii) a positive control (microalgal culture in OECD modified medium, C+). The experiments were conducted in batch mode for 11 days using 1-L photobioreactors maintained at room temperature under continuous light supply ($201 \pm 26 \mu\text{mol m}^{-2} \text{s}^{-1}$) and agitation through aeration. Once a day,

the temperature was monitored, and the pH was adjusted to 7 by carbon dioxide injection. Daily samples were collected to evaluate microalgal growth and the removal of ammonium-nitrogen (NH₄-N), nitrate-nitrogen (NO₃-N), and phosphate-phosphorus (PO₄-P) from the wastewater. Microalgal cell counts were performed using a Neubauer counting chamber. NH₄-N and NO₃-N were quantified using the Spectroquant Ammonium Kit Test and the Brucine method, respectively. PO₄-P concentration was determined following the methodology presented by Lee et al. (2009).

3. Results and Discussion

3.1. Microalgae growth

The results demonstrate that microalgae were able to grow in both effluent mixtures. However, the specific growth rate was slightly higher ($0.34 \pm 0.01 \text{ d}^{-1}$) in the M1 assay than in the M5 assay ($0.28 \pm 0.03 \text{ d}^{-1}$). The average biomass productivity was similar in M1 and M5 (3.0 ± 0.6) $\times 10^3$ and (2.7 ± 0.2) $\times 10^3 \text{ cells mL}^{-1} \text{ d}^{-1}$. While in M1 the microalgal adaptation phase was only apparent until day 4, in the case of M5, the lag phase was visible until day 7. At the end of day 11, microalgal cell concentration was still increasing in assay M5.

3.2. Removal of nitrogen

In M1 and M5 assays, the NO₃-N concentration was below the detection limit throughout the assays. The initial NH₄-N concentration in M1 and M5 was 65 ± 2 and $91 \pm 2 \text{ mg}_N \text{ L}^{-1}$, respectively. In M1, the NH₄-N removal was complete by day 7, while in M5 the removal was complete only by day 9. In C-M1 and C-M5, the NH₄-N removal was noticeable but considerably lower by days 7 and 9 than in M1 and M5, respectively. On the other hand, in the dark negative control, the removal efficiency after 11 days was only 53 ± 2 and $49 \pm 4 \%$ in CE-M1 and CE-M5, respectively, lower than the values observed for C-. This difference can be explained by the growth of native microalgae on the effluent due to light exposure and, consequently, photosynthetic activity.

3.3. Removal of phosphorus

The initial PO₄-P concentration was 9.0 ± 0.3 , 14 ± 1 and $10.0 \pm 0.1 \text{ mg}_P \text{ L}^{-1}$ in M1, M5, and C+, respectively. In M1, the phosphate removal was complete on day 11, presenting a similar removal efficiency as in C+. In CE-M1, it has no PO₄-P removal, while in C-M1 the removal efficiency was only $56 \pm 2\%$. On the other hand, in M5, at the end of the experiment, the removal percentage was $52 \pm 2\%$. Thus, the microalgal culture in the 5% mixture ended the assay with a phosphate concentration of $7.4 \pm 0.6 \text{ mg}_P \text{ L}^{-1}$. Although, in C-M5, the final PO₄-P concentration was similar to this value ($7.7 \pm 0.2 \text{ mg}_P \text{ L}^{-1}$), the removal efficiency was lower slightly lower ($42 \pm 5\%$). In CE-M5, the removal efficiency was only $19 \pm 6\%$. These results obtained for this parameter highlight the activity of the cultivated microalgae.

4. Conclusions

Based on the results presented, it can be stated that microalgae were able to grow and remove nutrients from both effluent mixtures tested. However, the results were more satisfactory in the case of the mixture with a smaller amount of digestate. Although in the M5 assay the final effluent did not respect the future maximum discharge limit, the final effluent from the M1 assay conforms with the legislation limits for nitrogen and phosphorus.

References

- EPA. "Method 352.1: Nitrogen, Nitrate (Colorimetric, Brucine) by Spectrophotometer." EPA Washington, DC, USA, 1971.
- NASA (National Aeronautics and Space Administration). 2013. "NASA finds 2012 sustained long-term climate warming trend". Accessed 22 February, 2023 <https://www.nasa.gov/topics/earth/features/2012-temps.html>
- Zhu, S., L. Qin, P. Feng, C. Shang, Z. Wang and Z. Yuan. 2019. "Treatment of low C/N ratio wastewater and biomass production using coculture of *Chlorella vulgaris* and activated sludge in a batch photobioreactor". In *Bioresource Technology* 274, 315-320. ELSEVIER.

- Qv, M., D. Dian, D. Liu, Q. Wu, C. Tang, S. Li and L. Zhu. 2023. "Towards advanced nutrient removal by microalgae-bacteria symbiosis system for wastewater treatment". In *Bioresource Technology* 370, 128574. ELSEVIER.
- European Commission. 2022. "Annexes to the Proposal for a Directive of the European Parliament and of the Council concerning urban wastewater treatment (recast)". Brussels.
- Funtes, J.L., I. Garbayo, M. Cuaresma, Z. Montero, M. González-del-Valle and C. Vílchez. 2016. "Impact of Microalgae-Bacteria Interactions on the Production of Algal Biomass and Associated Compounds". In *Marine Drugs*, 14, 100.
- Abdelfattah, A., S. S. Ali, H. Ramadan, E. I. El-Aswar, R. Eltawab, S. Ho, T. Elsamahy, S. Li, M. M. El-Sheekh, M. Schagerl, M. Kornaros and J. Sun. 2023. "Microalgae-based wastewater treatment: Mechanisms, challenges, recent advances, and future prospects". In *Environmental Science and Ecotechnology* 13, 100205. ELSEVIER
- You, X., L. Yang, X. Zhou and Y. Zhang. 2022. "Sustainability and carbon neutrality trends for microalgae-based wastewater treatment: A review". In *Environmental Research* 209, 112860. ELSEVIER.
- Li, X., W. Li, J. Zhai; H. Wei, Q. Wang. 2019. "Effect of ammonium nitrogen on microalgal growth, biochemical composition and photosynthetic performance in mixotrophic cultivation". In *Bioresource Technology* 273, 368-376. ELSEVIER.
- Lee, B.-H., S.-Y. Park, Y.-S. Heo, S.-S. Yea, D.-E. Kim. 2009. "Efficient Colorimetric Assay of RNA Polymerase Activity Using Inorganic Pyrophosphatase and Ammonium Molybdate". In *Bulletin of the Korean Chemical Society* 30, pp 2485-2488. DOI: 10.5012/bkcs.2009.30.10.2485

Acknowledgements

This work was financially supported by: (i) LA/P/0045/2020 (ALiCE) and UIDB/00511/2020-UIDP/00511/2020 (LEPABE), funded by national funds through FCT/MCTES (PIDDAC); and (ii) Project PhotoBioValue (ref. PTDC/BTA-BTA/2902/2021), funded by FEDER funds through COMPETE2020-Programa Operacional Competitividade e Internacionalização (POCI) and by national funds (PIDDAC) through FCT/MCTES. A.F. Esteves and E.M. Salgado thank FCT for the financial support of their work through the FCT PhD Research Scholarships 2020.05477.BD and 2021.07412.BD, respectively.

P02. Textile Effluent Treatment: from Microalgae Growth to Nutrient Removal

Rúben A. Martins^{1,2*}, Eva M. Salgado^{1,2}, Ana L. Gonçalves^{1,2,3}, José C. Pires^{1,2}, Ana F. Esteves^{1,2,4}

¹ LEPABE- Laboratório de Engenharia de Processos, Ambiente, Biotecnologia e Energia, Faculty of Engineering, University of Porto, Rua Dr. Roberto Frias, 4200-465 Porto, Portugal

² ALiCE - Associate Laboratory in Chemical Engineering, Faculty of Engineering, University of Porto, Rua Dr. Roberto Frias, 4200-465 Porto, Portugal

³ CITEVE - Technological Centre for the Textile and Clothing Industries of Portugal, Rua Fernando Mesquita, 2785, 4760-034 Vila Nova de Famalicão, Portugal

⁴ LSRE-LCM - Laboratory of Separation and Reaction Engineering - Laboratory of Catalysis and Materials, Faculty of Engineering, University of Porto, Rua Dr. Roberto Frias, 4200-465 Porto, Portugal




*Presenting author (up201806410@fe.up.pt)

Abstract

Textile production generates significant amounts of polluted wastewater that requires adequate treatment before discharge. Conventional treatment processes are the most common; while they are efficient, they also have numerous disadvantages. Microalgae technologies seem to be a promising alternative, capable of treating effluents and generating valuable products. In this study, an experimental setup lasting 10 days used microalgae (*Chlorella vulgaris*) and a textile effluent from a Portuguese company to evaluate both biomass growth and nutrient removal. The microalga was able to grow in the textile wastewater with a specific growth rate of

0.199 d⁻¹, and nutrient removal efficiencies of 73.3%, 95.9%, and 91.8% for NO₃-N, NH₄-N, and PO₄-P, respectively, were observed.

Author Keywords. Microalgae, Textile effluent, Wastewater treatment, Nutrient removal.

Open Access  Peer Reviewed   CC BY

1. Introduction

The textile industry is one of the oldest longstanding human industries in the world, producing thousands of tons of products every year. Among the textile process steps, the coloration step, in which a dye gives the desired color to the fiber, is commonly pointed to as one of the least environmentally friendly steps of the entire production process. During this step, depending on the used dye and the affinity of the fiber, coloration consumes between 50 to 240 L of water per kg of finished textile product in addition to high energy consumption. Alongside big volumes of water, according to previous studies, 10 to 25% of all the dye being used does not adhere to the fiber, and 11 to 16% is still present in the wastewater (Khan, et al. 2022). Textile effluents also feature bad odors, chemical oxygen demand and biochemical oxygen demand values above the established discharge limits, a high number of suspended solids and heavy metals in their composition (Mostafa 2015). Therefore, it is of the most importance that these effluents are treated before being discharged to reduce their potentially hazardous effects on the environment. Similar to other wastewaters, textile effluents follow the same treatment guidelines consisting of a sequence of physical, chemical, and biological treatments divided into primary, secondary and tertiary treatment. Despite their efficiency, these methods have notable downsides that are worth pointing out: (i) high energy consumption; (ii) require extensive treatment plants; and (iii) generate unwanted by-products with no market value that are likely destined to end up on a landfill, further increasing the economic and environmental costs of the treatment process. Considering these limitations, it is important to research and develop eco-friendly alternatives to conventional treatment methods that can achieve the same or better efficiency rates while generating by-products with commercial value. Textile wastewater treatment using microalgae has been pointed out as a potential solution for this problem. Microalgae are photosynthetic microorganisms with quick growth rates and high resistance to adverse environmental conditions. These microorganisms can consume the nitrogen and phosphorous available in wastewater, producing biomass while

treating the effluent. After the treatment, microalgae biomass can be used for bioenergy applications, pigment extraction (chlorophyll a and b and carotenoids), and as a biofertilizer. This study aims to evaluate the efficiency of using microalgae for textile wastewater treatment.

2. Materials and Methods

To test the viability of textile effluent treatment using microalgae, an experiment was conducted using *Chlorella vulgaris* and textile wastewater provided by a Portuguese company. The experimental setup was as follows: six 1-L borosilicate flasks at room temperature connected to air pumps to promote agitation; a continuous light source with an intensity of $200 \mu\text{mol m}^{-2} \text{s}^{-1}$. Two flasks were negative controls (effluent without microalgae exposed to light, C-, and under dark conditions, CE-), one was a positive control (C+, where microalgae grew in an ideal growth medium, OECD), and three were triplicates of a mixture of *C. vulgaris* and textile effluent (E assay). The experimental run was set to last a total of 10 days. Temperature and pH were monitored every workday using an electrochemical analyzer, with the pH of each flask being adjusted to 7 with a CO₂ stream. Optical density (OD) was also measured every workday through a spectrophotometer, set to a 680 nm wavelength, to measure microalgae growth throughout the experiment. Samples for nitrate-nitrogen (NO₃-N), ammonium-nitrogen (NH₄-N) and phosphate-phosphorous (PO₄-P) concentration measurements were collected on days 0, 1, 2, 3, 6, 8 and 10. NO₃-N quantification followed the brucine method (EPA 1971). PO₄-P were quantified as described by Lee, Park et al. (2009) and the NH₄-N quantification was done with the Spectroquant Ammonium Kit Test.

3. Results and Discussion

Initial effluent characterization showed a NO₃-N, PO₄-P and NH₄-N concentration of 0 mg L^{-1} , 5.12 mg L^{-1} and 6.8 mg L^{-1} , respectively. Microalgae cannot consume P in the absence of N; as such, it was necessary to supplement the effluent with NO₃-N. Following a molar ratio of 5:1 (N:P), as used in a previous study, 70.25 mg of NaNO₃ was added per liter of effluent. The microalgal growth and nutrient consumption were evaluated at the end of the experiment. Microalgae in C+ grew at a specific growth rate of $0.355 \pm 0.005 \text{ d}^{-1}$, and in E assay, grew at a growth rate of $0.20 \pm 0.01 \text{ d}^{-1}$. Microalgae were expected to grow at a lower rate in E assay, since an adaptation phase occurred, and the initial nutrient concentration was lower compared to C+ assay. C- and CE- showed no changes in OD throughout the experiment, and thus it is possible to conclude that there were no native microalgae in the effluent provided. Average productivity shows results on par with the specific growth rate. Microalgal productivity in C+ assay ($77 \pm 1 \text{ mg d}^{-1} \text{ L}^{-1}$) was higher than E assay ($45 \pm 2 \text{ mg d}^{-1} \text{ L}^{-1}$). Nutrient consumption analysis shows that microalgae were able to consume the nitrogen and phosphorous available in the effluent. After 10 days, in E assay, the microalgae consumed $75.63 \pm 0.03 \%$ of the initial NO₃-N concentration, $96.0 \pm 0.3 \%$ of the NH₄-N and $91.83 \pm 0.02 \%$ of the PO₄-P available. In the C+ assay, a NO₃-N and PO₄-P removal of $97.2 \pm 0.5 \%$ and $95.4 \pm 0.3 \%$ were observed, respectively. Overall, *C. vulgaris* can simultaneously grow and treat textile wastewater. It is worth mentioning that in both C- and CE- assays, a reduction in phosphorous content of $25.88 \pm 0.02 \%$ occurred, indicating that there was some microorganism in the effluent that could consume phosphate-phosphorous and could be competing with *C. vulgaris*. The discharge limit established by the European Union for sensitive areas for nitrogen and phosphorous is 10 mg L^{-1} and 1 mg L^{-1} , respectively (Directive 91/271/EEC). The textile effluent provided already had less than 10 mg L^{-1} of nitrogen. Also, the PO₄-P concentration was below 1 mg L^{-1} after one day of treatment with microalgae. In short, despite the experiment running for 10 days, the effluent provided is, by law, ready to be discharged after only one day of treatment. Textile effluents can have various compositions with higher nutrient concentrations than the ones reported in this study. In those cases, microalgal treatment is expected to have an even higher impact.

4. Conclusions

This experiment evaluated microalgae growth and removal efficiency of NO₃-N, NH₄-N and PO₄-P by *C. vulgaris* in textile wastewater. The effluent treatment using microalgae was effective, showcasing 75.63 ± 0.03 % removal of NO₃- N, 96.0 ± 0.3 % removal of NH₄-N and 91.83 ± 0.02 % removal of PO₄-P, and providing a specific growth rate of 0.20 ± 0.01 d⁻¹. Additionally, after one day, the effluent already possessed the necessary quality defined by the European Union, in regards to nitrogen and phosphorous concentration, to be properly discharged without serious environmental damage.

References

- Khan, A. A., et al. (2022). "Recent progress in microalgae-derived biochar for the treatment of textile industry wastewater." *Chemosphere*: 135565.
- Mostafa, M. (2015). "Waste water treatment in textile Industries-the concept and current removal technologies." *Journal of Biodiversity and Environmental Sciences* 7(1): 501-525.
- EPA (Environmental Protection Agency) Washington, DC, USA. 1971. "Method 352.1: Nitrogen, Nitrate (Colorimetric, Brucine) by Spectrophotometer".
- Lee, B.-H., et al. (2009). "Efficient colorimetric assay of RNA polymerase activity using inorganic pyrophosphatase and ammonium molybdate." *Bulletin of the Korean Chemical Society* 30(10): 2485-2488.
- European Union. Directive 1991/271/EEC—Directive of the European Council oh 21 May 1991 concerning urban wastewater treatment. J. Eur. Commun. 1991, 34, 40.

Acknowledgments

This work was financially supported by: (i) LA/P/0045/2020 (ALiCE) and UIDB/00511/2020-UIDP/00511/2020 (LEPABE) funded by national funds through FCT/MCTES (PIDDAC); and (ii) Project PhotoBioValue (ref. PTDC/BTA-BTA/2902/2021), funded by FEDER funds through COMPETE2020-Programa Operacional Competitividade e Internacionalização (POCI) and by national funds (PIDDAC) through FCT/MCTES. A.F. Esteves and E.M. Salgado thank FCT for the financial support of their work through the FCT PhD Research Scholarships 2020.05477.BD and 2021.07412.BD, respectively.

P03. Microalgae harvesting by flocculation followed by dissolved air flotation: the effect of a natural flocculant concentration and mixing time

Carolina Maia^{1,2*}, Larissa Ramos³, José C. M. Pires^{1,2}, Joana A. Loureiro^{1,2}, Maria Carmo Pereira^{1,2}

¹LEPABE—Laboratory for Process Engineering, Environment, Biotechnology and Energy, Faculty of Engineering, University of Porto, Rua Dr. Roberto Frias, 4200-465 Porto, Portugal

²ALiCE—Associate Laboratory in Chemical Engineering, Faculty of Engineering, University of Porto, Rua Dr. Roberto Frias, 4200-465 Porto, Portugal

³Instituto de Recursos Naturais, Universidade Federal de Itajubá, Itajubá 37500-903, Brazil

*Presenting author (up201704692@edu.fe.up.pt) ORCID 0000-0002-5031-9218

Abstract

Microalgae are a potential source of several value-added compounds, including products that can be used to produce biofuels. However, the harvesting process must be optimized before their application on a large scale. Using flocculation followed by dissolved air flotation (DAF) as harvesting techniques has raised great interest since these methods are one of the most cost-effective processes to concentrate the microalgae's solid content. This study explored the effect that the concentration of chitosan, an organic natural flocculant, and the slow (20 rpm) mixing time have on the harvesting efficiency of the microalga *Chlorella vulgaris*. The best conditions for microalgae harvesting were obtained with the addition of 50 mg/L of chitosan and without slow mixing.

Author Keywords. Chitosan, *Chlorella vulgaris*, Dissolved air flotation, Flocculation, Harvesting, Microalgae.

 Open Access  Peer Reviewed  CC BY

1. Introduction

Microalgae are photosynthetic microorganisms that are effective at converting solar energy into triglycerides, which can be utilized to produce biofuels like biodiesel, bioethanol and others (Laamanen et al., 2016; Machado et al., 2022). In addition, they also accumulate high-value products like vitamins, pigments, and antioxidants. However, the microalgae harvesting procedure must be improved for its widespread use to be commercially feasible. The harvesting process accounts for 20–30% of costs being a critical challenge due to: (i) diluted cultures; (ii) small microalgae cell size; and (iii) negative surface charge. It is therefore necessary to research a practical harvesting method that considers energy efficiency, allows the recycling of nutrients and water, eliminates the use of toxic chemicals, and leaves a small footprint.

Flocculation followed by sedimentation or flotation is one of the most cost-effective processes that can concentrate the solid content up to 2-7% (Laamanen et al., 2016). In this method, inorganic or organic substances that have flocculant activity are used to form flocs, for example, by adsorption and surface charge neutralization (Machado et al., 2022). Contamination is a severe problem with this method since flocculants end up in the harvested biomass, reducing the product's quality (Demir-Yilmaz et al., 2023). To overcome this problem, applying natural-based organic flocculants has aroused interest. Chitosan, a residue from the seafood industry, is the most widely used biopolymer for microalgae harvesting since it is an abundant natural organic flocculant, biodegradable, presents low toxicity, and does not contaminate the biomass (Laamanen et al., 2016). Chitosan easily binds to microalgae, changing their surface charge, their zeta potential, and forming flocs since it has a high density of cationic charges that are electrostatically attracted to the negatively charged surface of microalgae, promoting their flocculation (Laamanen et al., 2016; Machado et al., 2022).

After flocculation, microalgae can be harvested by sedimentation or flotation (Demir-Yilmaz et al., 2023; Laamanen et al., 2016). Flotation is preferable to sedimentation because it allows for shorter retention times and more efficient harvesting, producing a thicker concentrate due to the gravitational drainage of water from the foam. This technique involves the attachment of small air bubbles to the destabilized microalgae flocs, which leads them to rise to the surface and

concentrate. In dissolved air flotation (DAF), 5-15% of the water that has gone through separation is recycled and pressurized in the 400-650 kPa range. The harvesting process occurs as the water depressurizes back to atmospheric pressure, releasing bubbles in the range of 10-100 μm .

Considering all of this, this study aims to optimize the harvesting of the microalga *Chlorella vulgaris* by combining flocculation and dissolved air flotation methods. For this purpose, the impact of chitosan concentration and mixing time on the harvesting process was investigated.

2. Materials and Methods

2.1. Flocculation Assays

A chitosan solution (deacetylation degree $\geq 75\%$ from Sigma–Aldrich St. Louis, MO, US) was prepared by mixing 200 mg of the natural compound powder with 20 mL of 0.1 M HCl for one hour. To create a chitosan solution with 2 mg/mL, the fully dissolved mixture was diluted to 100 mL by adding distilled water.

A *Chlorella vulgaris* solution with an optical density at 680 nm (OD_{680}) of 0.32 (= 141 mg/L) was used. The flocculation assays were performed in batch mode using the Jar test equipment with six stirrers and fluorescent lights to monitor floc development. All experiments were conducted at room temperature (aprox. 20 °C) using 500 mL of microalgae in 800 mL beakers. After adding chitosan, the suspension was stirred at 150 rpm for 3 min and then at 20 rpm for 15 min. Different chitosan concentrations and slow (20 rpm) mixing times were employed.

2.2. Dissolved Air Flotation Assays

The DAF experiments were carried out using a flotation kit that includes a pressurization chamber and a graduated cylinder with a working volume of 1 L. In the pressure chamber, water was saturated at a pressure of 4.5 kp/cm² (441 kPa). The flotation procedure occurred in the graduated cylinder, where the pressured liquid was mixed with the suspensions from the flocculation assays at a recirculation ratio of 15%. Due to the addition of water from the pressure chamber, the microalgae solution after the flotation experiments was diluted; therefore, the dilution factor was calculated, and the optical density at 680 nm was multiplied by it to obtain the correct value after DAF (OD_i). To determine the harvesting efficiency (η) (Equation 1), the OD_{680} before flocculation (OD_i) was also calculated (Machado et al., 2022). These measurements were performed in a UV-vis spectrophotometer.

$$\eta (\%) = \frac{OD_i - OD_f}{OD_i} \times 100 \quad (1)$$

3. Results and Discussion

The addition of a flocculant, such as chitosan, is essential to occur flocculation and for an efficient harvesting process. In the absence of chitosan and for the lowest concentrations studied (10, 20 and 30 mg/L), these methods were not able to harvest microalgae (< 20%). The addition of chitosan at concentrations of 40 and 50 mg/L resulted in harvesting efficiencies of $55.5 \pm 0.7\%$ and $72.5 \pm 0.5\%$, respectively. Nevertheless, the harvesting efficiency dropped to $18.7 \pm 0.4\%$ when the chitosan concentration reached 60 mg/L. To understand these results, dynamic light scattering (DLS, Malvern ZetaSizer apparatus, Malvern Instruments Ltd., Malvern, UK) was used to determine the zeta potential of the microalgae. It was observed that as the zeta potential approached zero, the harvesting efficiency increased. In fact, the zeta potential was closer to zero ($+1.62 \pm 0.05$ mV) with the addition of 50 mg/L of chitosan. To study the influence of slow mixing time, a concentration of 50 mg/L was defined. When there was no slow mixing, the harvesting efficiency was $72.2 \pm 1.3\%$. Furthermore, this efficiency was also obtained after 15 min of slow mixing. The harvesting efficiency dropped to $53.6 \pm 8.4\%$ when the slow mixing duration was extended to 20 min. Therefore, the slow mixing time has no positive effects on microalgae harvesting and can be skipped. In this study, it was also observed that the harvesting efficiency is dependent on the zeta potential; hence, the chitosan concentration must be optimized to promote the neutrality of this parameter's value.

Otherwise, the microalgae remain stable in the medium, do not adhere to the bubbles released in the DAF, and the harvesting efficiency decreases.

4. Conclusions

The current work shows the potential of merging two techniques (flocculation and DAF) for microalgae harvesting; nevertheless, before the procedure is able to be widely used, various parameters need to be optimized. In this work, different chitosan concentrations and different slow mixing times were analyzed to find the optimal conditions for *Chlorella vulgaris* harvesting. It was found that chitosan must be present in the medium, but not in excess, for the zeta potential of the microalgae to approach zero mV and for the procedure to be effective. Furthermore, the time spent in the slow mixing step did not improve the harvesting process. In this study, to obtain the highest harvesting, 50 mg/L of chitosan should be added to the medium, and slow mixing is not necessary.

References

- Demir-Yilmaz, Irem, Malak Souad Ftouhi, Stéphane Balayssac, Pascal Guiraud, Christophe Coudret, and Cécile Formosa-Dague. "Bubble Functionalization in Flotation Process Improve Microalgae Harvesting." *Chemical Engineering Journal* 452 (2023): 139349. <https://doi.org/10.1016/j.cej.2022.139349>.
- Laamanen, Corey A, Gregory M Ross, and John A Scott. "Flotation Harvesting of Microalgae." *Renewable and Sustainable Energy Reviews* 58 (2016): 75-86. <https://doi.org/10.1016/j.rser.2015.12.293>.
- Machado, Cláudia A, Ana F Esteves, and José CM Pires. "Optimization of Microalgal Harvesting with Inorganic and Organic Flocculants Using Factorial Design of Experiments." *Processes* 10, no. 6 (2022): 1124. <https://doi.org/10.3390/pr10061124>.

Acknowledgments

This work was financially supported by: (i) LA/P/0045/2020 (ALiCE) and UIDB/00511/2020-UIDP/00511/2020 (LEPABE) funded by national funds through FCT/MCTES (PIDDAC); (ii) Project PhotoBioValue (ref. PTDC/BTA-BTA/2902/2021), funded by FEDER funds through COMPETE2020-Programa Operacional Competitividade e Internacionalização (POCI) and by national funds (PIDDAC) through FCT/MCTES; and (iii) project "HyGreen&LowEmissions", with the reference NORTE-01-0145-FEDER-000077, supported by Norte Portugal Regional Operational Programme (NORTE 2020), under the PORTUGAL 2020 Partnership Agreement, through the European Regional Development Fund (ERDF).

P04. Adsorption capacity of two synthesized biochars and their application in pharmaceuticals removal

Nuria Bernárdez^{1*}, Emilio Rosales¹, Marta Pazos¹, M. Ángeles Sanromán¹

¹Department of Chemical Engineering, University of Vigo, Campus As Lagoas-Marcosende, Vigo, Spain

*Presenting author (nuria.bernardez@uvigo.gal) ORCID 0009-0003-5210-7977

Abstract

This research has focused on the study of two synthesized biochars, named as high (BCH) and low temperature (BLC), to verify their adsorption capacity for pharmaceuticals. Initially, both biochars were physically and chemically characterised. In addition, zero charge point (pH_{zcp}) was determined in order to know the adsorbents charge surface as a function of pH. Then, the adsorption potential of the biochar was ascertained by selecting two pharmaceutical contaminants with a different chemical speciation: sulfamethizole (SMZ) and fluoxetine (FLX). In this context, a removal of 63% and 100% was achieved in FLX for BCH and BCL, respectively. The performance of SMZ was substantially lower attaining 9% and 5% after 60 min of contact. Therefore, the biochars adsorption capacity has demonstrated a significant dependence on pH, proving being highly effective for positively charged pollutants.

Author Keywords. Adsorption, Biochar, Chemical Speciation, Fluoxetine, Sulfamethizole.

 Open Access  Peer Reviewed  CC BY

1. Introduction

The presence of emerging contaminants or micro-pollutants in diverse environmental settings is becoming a widespread global concern. Several compounds from pharmaceuticals and personal care products, show a high persistence and bioaccumulation, and although they are commonly found at trace levels, they may pose a significant threat to human health and aquatic organisms (Ahmed and Hameed 2018).

The release of these compounds to the environment by different routes, including ineffective treatment in wastewater treatment plants (WWTP), require the development of alternative treatments for effluents containing such contaminants. Different methods have been reported as effective in the removal of these kind of micro-pollutants, nevertheless, some of these procedures involve high operating costs and unpredictable intermediates formation. In this framework, adsorption processes have been shown as an efficient alternative for removing micro-pollutants through an economical and simple technique (Sotelo et al. 2014), with a wide range of operating design.

This technique is based on the use of an adsorbent for the removal of the pollutants. The most used adsorbent is activated carbon, however, several low-cost alternative material, such as hydrochar or biochar materials, have been reported. In this study, two synthesized biochars have been proposed, characterized and evaluated through adsorption studies.

2. Materials and Methods

Biochar characterization.

Two biochars, BCH and BCL, were synthesized from biomass wastes in a tubular furnace (Aero-360) and consequently characterized. Distribution of functional groups on the adsorbent surface was determined by Fourier-transform infrared spectroscopy (FTIR). Carbon, nitrogen, hydrogen, and sulfur content was quantified by elemental analysis, and metals presence was measured by inductively coupled plasma mass spectrometry (ICP-MS) and microwave plasma atomic emission spectroscopy (MP-AES) techniques. Finally, surface morphology was studied through scanning electron microscopy (SEM).

Zero charge point of both biochars was also determined by immersing 1 g of adsorbent in 0.1 M NaNO_3 solutions at different pH. Suspensions were kept under shaker agitation (150 rpm) at 25 °C and final pH was measured after 24 h.

Sulfamethizole and fluoxetine adsorptions.

Adsorption capacity of biochars was tested suspending 10 g/L of adsorbent in 0.1 L of 10 ppm contaminant solution, being SMZ and FLX the model pollutants. SMZ concentration was measured by a UV-Vis spectrophotometer (Thermo Fisher Genesys M-150) at 262 nm and FLX was measured through HPLC, according to the method reported by Escudero-Curiel et al. (2021). The kinetic study was performed and assessed by pseudo-first and pseudo-second-order kinetics.

3. Discussion

Initially, different techniques have been used to characterize both adsorbents. Chemical properties of the biochars were analysed by FTIR spectrometry showing similar profiles and functional groups for BCH and BCL, except for a greater carbonate groups presence in BCL. The elemental analysis showed that the percentages of carbon and nitrogen were slightly higher in the case of BCH compared to BCL. Concerning metal presence, a significant transition metal content was detected in both samples, providing them with interesting properties for other micro-pollutant removal processes. Regarding SEM analysis, a similar morphology of heterogeneous porous structure has been shown in both biochars. Adsorbents characterization was completed by determining the pH_{zcp} , located at pH 7.8 for BCH and 7.7 for BCL.

Based on microspecies distribution of pharmaceuticals at natural pH (6.31 for FLX and 6.29 for SMZ), the FLX was found as positive species, while SMZ was mainly in negative species. In this context, biochars adsorption capacity for pollutants showed different behaviour (Figure).



Figure 1: SMZ (red) and FLX (green) removal after 1 h and 24 h of treatment.

It was observed that FLX uptake after 60 min of treatment was 5 times higher than that of SMZ in case of BCH, while this difference increased to 10 times in case of BCL. This trend was kept during the following 24 h of treatment.

The high elimination in case of FLX indicated that at working pH, which was lower than pH_{zcp} , both adsorbents presented a negatively charge surface, favouring biochar-pharmaceutical electrostatic interactions. This hypothesis was also contrasted based on the SMZ removal, since there would be an electrostatic repulsion due to the same polarity of adsorbent and pollutant.

Finally, adsorption kinetics for FLX were studied. Given the promptness with which the steady state was reached, especially for BCL, both models showed a good fit, but this was slightly better on pseudo-second-order kinetics (Table).

Adsorbent	q_e (mg/g)	k_2 (g/(mg min))	R^2
BCH	7.664	0.588	0.9956
BCL	10.192	1.699	0.9975

Table 1: Kinetic parameters of FLX adsorption treatment.

where q_e is the amount of pollutant adsorbed per gram of biochar at equilibrium and k_2 is the pseudo-second-order kinetic constant.

This behaviour revealed that contaminant removal was conducted by a chemical adsorption or chemisorption process, resulting from the bonds formed between the adsorbent surface and the pharmaceutical.

4. Conclusions

In this study, the adsorption capacity of BCH and BCL was evaluated for two emerging pollutants, FLX and SMZ. Results showed significant improvement in the removal of pollutant with a positive microspecies distribution for both biochars at working pH, giving rise to a process governed by chemisorption phenomena.

Consequently, both adsorbents could be used for environmental purposes, being possible to improve their performance through the study of modifications in their properties.

References

- Ahmed, MJ, and BH Hameed. 2018. "Removal of emerging pharmaceutical contaminants by adsorption in a fixed-bed column: A review". *Ecotoxicology and Environmental Safety* 149: 257-266. Accessed 24 April, 2023. DOI: [10.1016/j.ecoenv.2017.12.012](https://doi.org/10.1016/j.ecoenv.2017.12.012).
- Sotelo, José Luis, Gabriel Ovejero, Araceli Rodríguez, Silvia Álvarez, José Galán, and Juan García. 2014. "Competitive adsorption studies of caffeine and diclofenac aqueous solutions by activated carbon". *Chemical Engineering Journal* 240: 443-453. Accessed 25 May, 2023. DOI: [10.1016/j.cej.2013.11.094](https://doi.org/10.1016/j.cej.2013.11.094)
- Escudero-Curiel, Silvia, Valeria Acevedo García, M^a Ángeles Sanromán and Marta Pazos. 2021. "Eco-approach for pharmaceutical removal: Thermochemical waste valorisation, biochar adsorption and electro-assisted regeneration". *Electrochimica Acta* 389: 138694. Accessed 20 April, 2023. DOI: [10.1016/j.electacta.2021.138694](https://doi.org/10.1016/j.electacta.2021.138694)

Acknowledgments

Grant PDC2021-121394-I00 and PCI2022-132941 funded by MCIN/AEI/ 10.13039/501100011033 and by the "European Union NextGeneration EU/PRTR" and Xunta de Galicia, and the European Regional Development Fund (ED431C 2021-43).

P05. Removal of Remazol Brilliant Orange dye by chitin beads modified by ionic liquid

Salima Benniche^{1*}, Ariana Pintor^{2,3}, Ounissa Kebiche-Senhadj¹, Cidalia Botelho^{2,3}, Claudia Fontas⁴

¹Laboratoire des Procédés Membranaires et de Techniques de Séparation et de Récupération (LPMTSR), Faculty of Technology- University of Bejaia, 06000 Bejaia, Algeria.

²Laboratory of Separation and Reaction Engineering – Laboratory of Catalysis and Materials (LSRE-LCM), Department of Chemical Engineering, Faculty of Engineering, University of Porto, Rua Dr. Roberto Frias, 4200-465 Porto, Portugal.

³ALiCE - Associate Laboratory in Chemical Engineering, Faculty of Engineering, University of Porto, Rua Dr. Roberto Frias, 4200-465 Porto, Portugal



⁴Department of Chemistry, University of Girona, C/Maria Aurèlia Capmany 69, 17003 Girona, Spain.

*Presenting author (salima.benniche@gmail.com)

Abstract

Organic pollutants such as dyes present a serious issue for the environment. The present work aimed to investigate the elimination of Remazol Brilliant orange 3 R from synthetic colored solutions using chitin and chitin bead modified by Aliquat 336 (Ch-A336). The capacity of chitin toward the removal of Remazol Brilliant Orange 3R (RBO-3R) (reactive orange 16) has been enhanced by the incorporation of Aliquat-336 in the matrix of the chitin beads. The results of adsorption of RBO-3R by Ch-A336 indicate that the pseudo-second order kinetic model fitted well the adsorption data. Furthermore, the adsorption equilibrium is well described by the Langmuir isotherm model, with the maximum adsorption capacity calculated to be 151 mg/g. The capacity of adsorption of RBO-3R by Ch-A336 is 3 times greater than the adsorption capacity of the neat chitin on the range of pH 2-9 under the same experimental conditions.

Author Keywords. Chitin, Aliquat336, adsorption, azo dyes, Reactive orange 16.

 Open Access  Peer Reviewed  CC BY

1. Introduction

Textile industries discharge huge amounts of wastewater contaminated with hazardous substances, including dyes. These dyes, which are often recalcitrant, are known to be carcinogenic and mutagens and affect both the environment and human health. Many approaches have been developed to eliminate these substances from industrial effluents and adsorption has been reported as a simple, economical, and effective method (Senthil Kumar and Saravanan 2017; Holkar et al. 2016). Ionic liquids and biopolymers received great interest in the field of water treatment during the last two decades, and the two materials can also be combined to develop new sorbents with high efficiency and performance (Ayati et al. 2019).

In the present work, chitin beads modified by Aliquat 336 were prepared and applied for the removal of a reactive dye RBO-3R (azo dye) in synthetic solutions prepared using distilled water.

2. Materials and Methods

2.1. Materials

Chitin, tricaprylylmethylammonium chloride (Aliquat-336, $C_{10}H_{18}N_2O_2$, Sigmaaldrich 95%), LiCl (biochem, 98 %), N,N-dimethylacetamide (biochem chemopharma, 98%), RBO-3R (DyStar textilfarben) were used for adsorbent elaboration and for preparation of solutions.

2.2. Preparation of modified chitin beads (chitin-A336) and adsorption tests

The chitin solution was prepared by dissolving 1 g of chitin in (DMAc+ LiCl 5%(V/V)). Aliquat 336 is added to prepare the Ch-A336 beads. The microspheres were formed by pouring the Ch-DMAc LiCl/A336 solution dropwise into a distilled water bath. The beads were filtered, washed with distilled water and dried.

For the batch adsorption tests, RBO-3R solutions were prepared by diluting a stock dye solution of 1000 mg/L and putting it in contact with a quantity of adsorbent in a rotary shaker. The RBO-3R dye concentration was determined by UV-Vis spectrophotometry at 494 nm.

3. Discussion

3.1. Effect of pH

The effect of pH was evaluated for both adsorbents under the same experimental conditions, the results show that the adsorption capacity of Ch-A336 is independent of pH, while the capacity of chitin beads decreases with the increase of pH.

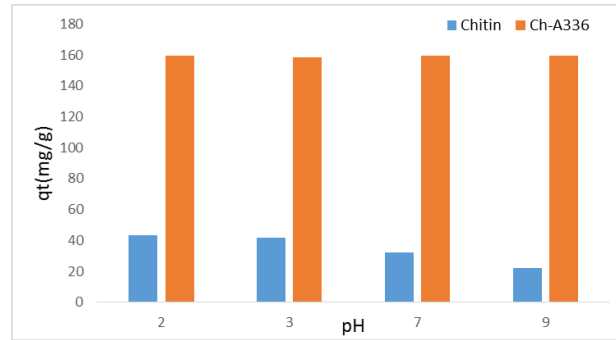


Figure 1: The effect of pH on the removal of RBO-3R onto the Chitin and Ch-A336 beads. Dosage= 0.025g/25 mL of dye solution, T = 20 °C, 20 rpm, pH = 2,5,7,9

3.2. Kinetics and Isotherms

As shown in Figure 2, the adsorption equilibrium is reached after 16 hours for RBO-3R. The 'pseudo second order' kinetic model fits well the experimental data, so the process is governed by chemisorption.

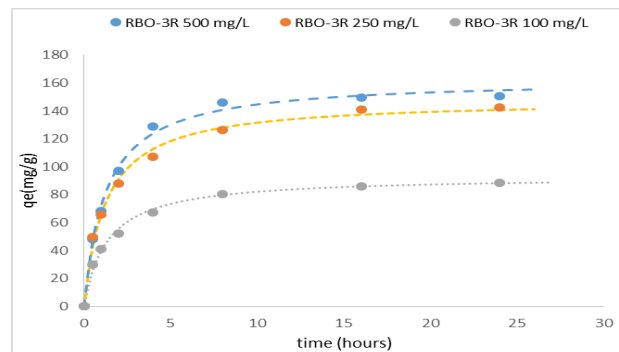


Figure 2: Pseudo-second-order kinetics for adsorption of RBO-3R onto the Chitin-A336 beads. Dosage 0.025g/25 mL of dye solution, pH = 2, 20 rpm, T = 20 °C

The Langmuir model describes better the experimental data, with a correlation coefficient of 0.998, so we conclude that the adsorption of RBO-3R takes place by forming a single layer of adsorbate on a perfectly homogeneous surface. The maximum capacity of chitin-A336 beads towards RBO-3R is 151 mg/g, this result is competitive with results obtained using other adsorbents in the literature (Hassan and Carr 2018).

Parameters	q_{\max} (mg/g)	K_L (L/mg)	R^2
RBO-3R	151	0.119	0.998

Table 1: Parameters of Langmuir adsorption isotherm model

4. Conclusions

The capacity of Ch-A336 beads to remove RBO-3R is 3 times greater than the capacity of pure chitin beads.

The Chitin-A336 beads were found to be a good adsorbent, effective for the removal of RBO-3R, and could be easily separated by decantation after the adsorption process.

References

- Ayati, Ali, Sara Ranjbari, Bahareh Tanhaei, and Mika Sillanpää. 2019. 'Ionic Liquid-Modified Composites for the Adsorptive Removal of Emerging Water Contaminants: A Review'. *Journal of Molecular Liquids* 275 (February): 71–83. <https://doi.org/10.1016/j.molliq.2018.11.016>.
- Hassan, Mohammad M., and Christopher M. Carr. 2018. 'A Critical Review on Recent Advancements of the Removal of Reactive Dyes from Dyehouse Effluent by Ion-Exchange Adsorbents'. *Chemosphere* 209: 201–19.
- Holkar, Chandrakant R., Ananda J. Jadhav, Dipak V. Pinjari, Naresh M. Mahamuni, and Aniruddha B. Pandit. 2016. 'A Critical Review on Textile Wastewater Treatments: Possible Approaches'. *Journal of Environmental Management* 182 (November): 351–66. <https://doi.org/10.1016/j.jenvman.2016.07.090>.
- Ranjbari, Sara, Bahareh Tanhaei, Ali Ayati, and Mika Sillanpää. 2019. 'Novel Aliquat-336 Impregnated Chitosan Beads for the Adsorptive Removal of Anionic Azo Dyes'. *International Journal of Biological Macromolecules* 125: 989–98.
- Senthil Kumar, Ponnusamy, and Anbalagan Saravanan. 2017. '11 - Sustainable Wastewater Treatments in Textile Sector'. In *Sustainable Fibres and Textiles*, edited by Subramanian Senthilkannan Muthu, 323–46. The Textile Institute Book Series. Woodhead Publishing. <https://doi.org/10.1016/B978-0-08-102041-8.00011-1>.

Acknowledgments

This work received partial financial support from the Erasmus mobile up program awarded by the University of PORTO. This work was financially supported by LA/P/0045/2020 (ALiCE), UIDB/50020/2020 and UIDP/50020/2020 (LSRE-LCM), funded by national funds through FCT/MCTES (PIDDAC). A. Pintor acknowledges her Junior Researcher contract by FCT (CEECIND/01485/2017).

P06. Combined adsorption and electrochemical treatments for the remediation of water containing sulfamethoxazole

Verónica Poza-Nogueiras^{1*}, Nuria Bernárdez¹, Bárbara Lomba¹ Marta Pazos¹, M. Ángeles Sanromán¹




¹BIOSUV research group, Department of Chemical Engineering, University of Vigo, As Lagoas-Marcosende, 36310 Vigo, Spain

*Presenting author (vpzoa@uvigo.gal) ORCID [0000-0002-7869-3850](https://orcid.org/0000-0002-7869-3850)

Abstract

In this work, low-cost commercial biochar was immobilized on alginate. The resulting composite was tested as adsorbent for the removal of antibiotic sulfamethoxazole (SMX) from water. Firstly, assays on Erlenmeyer flasks proved the capacity of the biochar-alginate beads to adsorb SMX and demonstrated that the adsorption capacity of the biochar was not reduced due to the immobilization. Then, the combination of adsorption and anodic oxidation treatments was performed on a 0.5 L reactor. A synergistic effect was observed when combining both treatments, with a boost removal of SMX attained compared with the treatments applied alone.

Author Keywords. Antibiotic, water remediation, biochar, alginate beads, electrochemical regeneration, anodic oxidation.

 Open Access  Peer Reviewed  CC BY

1. Introduction

Antibiotics are among the most frequently reported water pollutants. Given the risk of producing antimicrobial resistance, the development of efficient processes for their elimination is imperative (Akhil et al. 2021). Among the diverse treatment alternatives, adsorption is one of the most attractive; yet, the high cost of the adsorbent materials and the further need to regenerate the spent adsorbent are drawbacks to be tackled. In this context, the research focus has shifted to the use of low-cost adsorbents obtained from agricultural and forestry wastes, while at the same time investigating more efficient regeneration processes, such as electrochemical treatments, for the recovery of the spent adsorbents (Zhou et al. 2021). An interesting option is to combine the adsorption and regeneration steps on the same treatment. With this in mind, the aim of this work is to immobilize a biochar on alginate and to assess the feasibility of using it on a combined adsorption and anodic oxidation (AO) treatment for the removal of the antibiotic sulfamethoxazole (SMX).

2. Materials and Methods

2.1. Reagents and adsorbent preparation

SMX (analytical grade), anhydrous sodium sulphate and calcium chloride were supplied by Sigma-Aldrich. Sodium alginate was provided by Analema. All aqueous solutions were prepared with Milli-Q water (18.2 MΩ cm). The commercial biochar, obtained from forestry wastes, was purchased from Carvão Zero (Portugal).

Biochar was immobilized in alginate, forming biochar-alginate beads. Initially, commercial biochar was grinded and sieved (particles < 0.5 mm). Then, 4 g of the obtained powder were dispersed in 0.2 L of an alginate solution (1% and 3% w/v concentrations of alginate were tested). Afterwards, the resulting mixture was dropped into an agitated 0.58 M CaCl₂ solution to produce the crosslinking and form the biochar-alginate beads. The beads were left for 1 h in that hardening solution and then they were washed and stored at 4°C in water.

2.2. Experimental setup and equipment

Initial adsorption assays were carried out in 0.25L Erlenmeyer flasks, using 0.05 L of a 50 mg/L SMX solution at natural pH and different adsorbent dosages. Erlenmeyer flasks were introduced in a shaker at 150 rpm and 25°C.

Subsequent anodic oxidation and combined treatments were carried out in a rectangular reactor with a 0.5 L-capacity, using a solution containing 50 mg/L of SMX and 0.01 M of Na₂SO₄ as supporting electrolyte at natural pH, 54 g of biochar-alginate beads, a Ni foam cathode and a graphite anode (both 23.5 cm²). 10 V were applied with a power supply and the solution was constantly aerated at a flow of 1 L/min (which contributed to the mobility of the adsorbent). The removal of SMX was determined by measuring the absorbance at 263 nm with a Genesys M-150 UV-Vis spectrophotometer (Thermo Fisher).

3. Discussion

3.1. Flask adsorption assays

Firstly, the point of zero charge pH of the biochar-alginate beads was determined to be 7.3, quite similar to the powder of biochar (point of zero charge pH: 7.5). The adsorption assays were performed at natural pH (*ca.* 5.8), on which the adsorbent surface is positively charged whereas the pollutant ($pK_{a1} = 1.9$, $pK_{a2} = 5.6$) is partially at its anionic state, which can contribute to the SMX adsorption.

Two different alginate concentrations (1% and 3% w/v) were tested for the immobilization of biochar and the manufactured adsorbent beads were used in adsorption assays with a biochar-alginate composite dosage of 2.5 g. A higher uptake was obtained for the adsorbents prepared with the 1% w/v alginate solution (0.17 vs. 0.10 mg/g); hence, that concentration was selected for the subsequent assays. Afterwards, the effect of different adsorbent dosages was analyzed (Figure). For comparison purposes, an adsorption experiment using 0.4 g of biochar powder (equivalent to the amount of biochar present in 10 g of the biochar-alginate beads) was also carried out. As observed, quite similar SMX removals were obtained when comparing the equivalent biochar dosage in the powder and beads configurations. Considering that the immobilization of biochar on alginate allows overcoming the issues of working with a powder and provides an easier recovery of the adsorbent from the solution, the composite adsorbent was chosen for the subsequent treatment assays at the reactor.

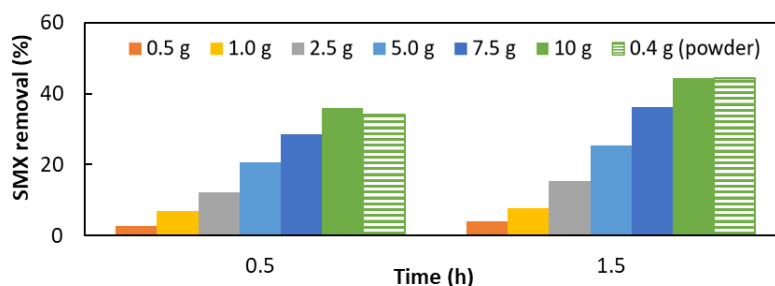


Figure 1: SMX removal using different dosages of adsorbent: 0.5-10 g of biochar-alginate beads and 0.4 g of biochar powder.

3.2. Combined adsorption and electrochemical treatments

Once the adsorption capacity of SMX on the biochar-alginate beads has been demonstrated at Erlenmeyer flasks, the removal of the pollutant combining those adsorbents with an AO treatment was assessed at an electrochemical reactor (Figure). As observed, the removal of SMX attained after 2 h of treatment when AO or adsorption assays were applied alone was much lower than the reduction of the pollutant obtained when combining both processes. This synergistic effect may be explained by the fact that the oxidation of the pollutant provided by the electric field contributes to the continuous regeneration of the adsorbent, while at the same time, the adsorption process concentrates the pollutant on the adsorbent, facilitating its oxidation.

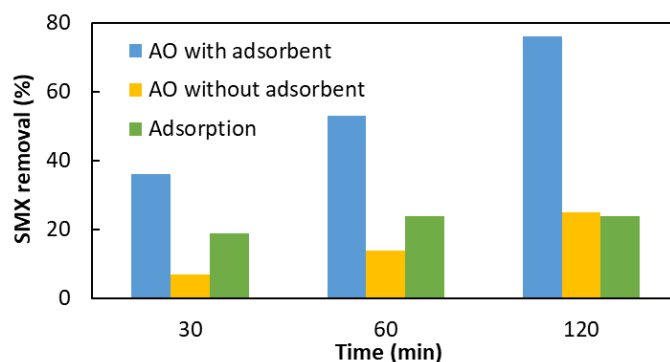


Figure 2: Treatment of SMX by means of adsorption, AO and the combination of both treatments.

4. Conclusions

The results obtained demonstrate the viability of using an immobilized biochar on alginate to adsorb the antibiotic SMX, providing an easy-to-handle adsorbent and overcoming the operation issues of working with powder adsorbents. Additionally, the synergistic effect of combining adsorption and AO treatments has been proven. Future work will involve the optimization of operational parameters and evaluation of the treatment in continuous mode.

References

- Akhil, Dilipkumar, Divya Lakshmi, Senthil P. Kumar, Dai Viet N. Vo, and Ashokkumar Kartik. 2021. "Occurrence and removal of antibiotics from industrial wastewater". *Environmental Chemistry Letters* 19:1477-1507. DOI: 10.1007/s10311-020-01152-0.
- Zhou, Wei, Xiaoxiao Meng, Jihui Gao, Haiqian Zhao, Guangbo Zhao, Jun Ma. 2021. " Electrochemical regeneration of carbon-based adsorbents: a review of regeneration mechanisms, reactors, and future prospects". *Chemical Engineering Journal Advances* 5: 100083. DOI: 10.1016/j.ceja.2020.100083.

Acknowledgments

This research was funded through the join 2019-2020 Biodiversa & Water JPI joint call for research proposals, under the BiodivRestore ERA-Net COFUND programme with the Project PCI2022-132941 funded by MCIN/AEI /10.13039/501100011033. Authors also acknowledge the grant PDC2021-121394-I00 funded by MCIN/AEI/ 10.13039/501100011033 and by the "European Union NextGenerationEU/PRTR" and Xunta de Galicia, and the European Regional Development Fund (ED431C 2021-43).

P07. A novel approach to prepare ZnFe-MOF adsorbent and catalyst: Application in dye and drugs removal from wastewater

Daniel Terrón^{1*}, Emilio Rosales¹, Marta Pazos¹, M. Ángeles Sanromán¹



¹Department of Chemical Engineering, University of Vigo, Isaac Newton Building, Campus As Lagoas Marcosende 36310, Vigo, Spain.

*Presenting author (daniel.terron@uvigo.gal) ORCID [0009-0009-4240-5181](https://orcid.org/0009-0009-4240-5181)

Abstract

Advanced Oxidation Processes (AOPs) are becoming of interest to the scientific community, as a viable and efficient option for the removal of emerging pollutants. In this context, AOPs require a suitable catalyst to carry out a radical reaction, which is responsible for degrading the pollutants. In recent years, new materials such as metal-organic frameworks (MOFs), capable of adsorbing pollutants into their pores and acting as catalysts in oxidation processes have stood out. In our study, a ZnFe-MOF is synthesised by solvothermal one-step method and used as adsorbent and/or catalyst for sulphate or hydroxyl radical generation processes. Tests with dye Rhodamine B as a model organic pollutant show promising results, being able to completely degrade it in 90 min for the hydroxyl radical process and 120 min for the peroxymonosulphate activated system. Finally, a trial tested with the drug Fluoxetine showed an elimination higher than 80% in 900 min.

Author Keywords. Emerging pollutants, drugs, wastewater, Advanced oxidation processes, AOPs, Metal-Organic Frameworks, ZnFe-MOF, Rhodamine B, Fluoxetine.

 Open Access  Peer Reviewed  CC BY

1. Introduction

Conventional treatments in a water treatment plant, which are based on a physical and biological approach, were not designed for these unidentified contaminants that we call emerging contaminants. Some of these contaminants, as well as pharmaceuticals or dyes, can have negative effects on human health and have become a threat to the water purification network, as due to their recalcitrant nature they are very difficult to remove by these methods (Lama *et al.* 2022). Among the processes developed to solve this problem, advanced oxidation processes emerge as a viable option that, together with the appropriate catalyst, are capable of removing these pollutants. In this context, Metal-Organic Frameworks (MOFs) appear as a suitable catalyzer to the AOPs processes thanks to their iron content (Fdez-Sanromán, *et al.* 2022), being stable in water and able to be reused in several treatment cycles.

In our research, two metals such as Zn and Fe are combined to form MIL-MOF powder which is used as a catalyst in AOPs for the removal of model organic pollutants such as Rhodamine B or Fluoxetine. The selected AOPs are based on the action of hydroxyl radicals (heterogeneous Fenton, electroFenton) or sulphate radicals by activation of peroxymonosulphate (PMS).

2. Materials and Methods

2.1. Materials

Terephthalic acid (H₂BDC), iron (III) chloride hexahydrate and zinc nitrate hexahydrate were used to synthesize ZnFe-MOF. N-N, Dimethylsulfamide (DMF) was used as the reaction solvent and ethanol (CH₃CH₂OH, 99%) was used to wash it, following the reagents used for similar synthesis in the cited research (Shi *et al.* 2022).

2.2. Methods

Bimetallic ZnFe-MOF solvothermal synthesis: ZnFe-MOF was synthesized following the referenced method (Shi *et al.* 2022).

Material characterization: The ZnFe-MOF was characterized using XRD (XPert Pro 3) and FTIR (Nicolet 6700) analysis (CACTI University of Vigo) to investigate the effect of the crystalline structure and functional groups on advanced oxidation processes (AOPs).

Degradation and reuse tests: For testing the efficacy of the ZnFe-MOF, simulated water samples containing Rhodamine B at a concentration of 100 ppm and fluoxetine at a concentration of 10 ppm were used. Two different methods were employed to degrade the pollutants: the first method involved activating PMS with a concentration of 0.6 mM by the MOF to generate sulfate radicals, while the second method involved mixing the solution with H₂O₂ at a concentration of 32 mM and the MOF to generate hydroxyl radicals. The effectiveness of the ZnFe-MOF was evaluated in a range of 0.5-3.2 mM for both pollutants. The mixtures were stirred and samples were taken at various intervals for analysis. For Rhodamine B tests, samples were taken at 5, 15, 30, 45, 60 and 90 minutes, while for fluoxetine assays, samples were taken at 5, 15, 30, 60, 260, 390 and 900 minutes. Samples of Rhodamine B were centrifuged and analyzed using a spectrophotometer (at 554 nm) without interference, while fluoxetine samples were filtered and analyzed using high-performance liquid chromatography (HPLC) (Escudero-Curiel *et al.* 2023). For reuse tests, the ZnFe-MOF pellet from a previous test was resuspended in a new simulated polluted water sample containing 100 ppm of Rhodamine B after being centrifuged.

3. Discussion

3.1. Material characterization

ZnFe-MOF powder obtained after synthesis is shown in Figure . This material was subjected to FTIR analysis (as shown in Figure). The analysis revealed strong bands that corresponded to the C=O, -COO, C-O, and C-H bending vibrations of the benzene ring (at 1503-1656, 1391, 1017, and 749 cm⁻¹, respectively). The analysis also confirmed that the Zn and Fe metal ions were correctly coordinated with H₂BDC to form MIL-MOF crystals, as evidenced by the observed bands at 528 cm⁻¹ and 560 cm⁻¹, respectively (Shi *et al.* 2022).



Figure 1: Orange-red coloured ZnFe-MOF powder.

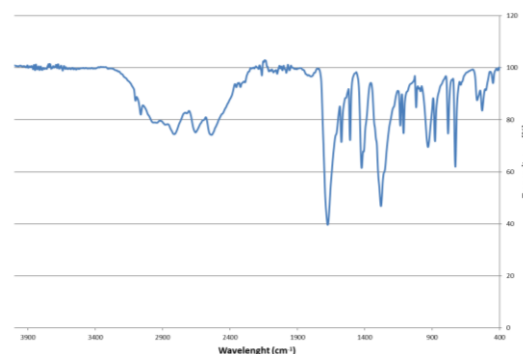


Figure 2: Orange-red coloured ZnFe-MOF powder.

3.2. Degradation of Rhodamine B by using radical-based treatment

Hydroxyl radicals: ZnFe-MOF is an excellent catalyst able to achieve complete degradation within 90 min. On the other hand, the dye adsorption levels are only able to reduce the concentration by up to 70% in the same time frame, with less than 5% for the H₂O₂ control.

Sulfate radicals: The inclusion of ZnFe-MOF as a catalyst in the PMS activation method enhances the process, leading to an 84% reduction in water contaminant within 60 min. This is a significant improvement compared to the PMS control or MOF adsorption experiments, which only achieved 58% or 61% reduction in the same time frame, respectively.

During the fluoxetine test, it was observed that ZnFe-MOF continues to function as a PMS catalyst. At a concentration of 0.45mM, successfully removing the entire dose of the drug was achieved within 900 min.

3.3. Reuses

The properties of the catalyst are maintained even after three cycles in the Fenton process, resulting in 100% degradation. However, in the fourth cycle, there is a decline in performance. The reusability of the catalyst follows the same trends observed previously, where the adsorption rate slows down, and its catalytic ability is gradually affected with each reuse.

4. Conclusions

The results of the treatment of AOPs, using the novel synthesised ZnFe-MOF as catalyst, have been promising, managing to degrade a model organic pollutant such as Rhodamine B in 90 min under hydroxyl radical process, and a drug such as Fluoxetine in 900 min under a PMS/ZnFe-MOF activated system.

References

- Escudero-Curiel, S., Penelas, U., Sanromán, M.Á., Pazos, M. 2021. "An approach towards Zero-Waste wastewater technology: Fluoxetine adsorption on biochar and removal by the sulfate radical" *Chemosphere* 268, art. no. 129318.
- Fdez-Sanromán, A., Pazos, M., Sanroman, A. 2022. "Peroxymonosulphate activation by Basolite® F-300 for *Escherichia coli* disinfection and Antipyrine degradation" *International Journal of Environmental Research and Public Health*, 19 (11), art. no. 6852.
- Lama, G., Mejjide, J., Sanromán, A., Pazos, M. 2022. "Heterogeneous Advanced Oxidation Processes: Current approaches for wastewater treatment" *Catalysts* 12, no. 3: 344.
- Shi, Y., Wang, L., Dong, S., Miao, X., Zhang, M., Sun, K., Zhang, Y., Cao, Z., Sun, J. 2022. "Wool-ball-like BiOBr@ZnFe-MOF composites for degradation organic pollutant under visible-light: Synthesis, performance, characterization and mechanism" *Optical Materials*. 131, art. no. 112580.

Acknowledgments

This research has been financially supported by MCIN / AEI /10.13039/501100011033 Project PID2020-113667GB-I00 and Xunta de Galicia, and the European Regional Development Fund (ED431C 2021-43).

P08. Coagulants derived from chestnut shell and maritime pine bark extracts: preparation and use for textile effluent decolorization

Isabella Tomasi^{1,2*}, Mafalda Rodrigues³, Sílvia Santos^{1,2}, Rui Boaventura^{1,2}, Cidália Botelho^{1,2}

¹ LSRE-LCM - Laboratory of Separation and Reaction Engineering – Laboratory of Catalysis and Materials, Faculty of Engineering, University of Porto, Rua Dr. Roberto Frias, 4200-465 Porto, Portugal

² ALiCE - Associate Laboratory in Chemical Engineering, Faculty of Engineering, University of Porto, Rua Dr. Roberto Frias, 4200-465 Porto, Portugal

³ Chemical Engineering Bachelor Program, Department of Chemical Engineering, Faculty of Engineering, University of Porto, Rua Dr. Roberto Frias, 4200-465 Porto, Portugal

*Presenting author (up201702301@up.pt) ORCID 0000-0001-9259-8422

Abstract

Plant extracts have been investigated as promising precursors of natural coagulants/flocculants. Vegetable residues, such as chestnut shell and maritime pine bark, can be used as rich sources of tannins. Tannins exhibit anionic behavior in an aqueous solution but could be chemically modified to acquire a positive charge and promote coagulation activity. The cationization of tannin extracts can be achieved through the Mannich reaction, involving an aldehyde and an amine. In this work, chestnut shells and pinus bark tannin extracts were cationized. The resulting biocoagulants were evaluated on coagulation/flocculation assays. Both coagulants could remove more than 96% of color from a simulated dyehouse effluent.

Author Keywords: Coagulation, cationization, tannins, natural coagulants.

 Open Access  Peer Reviewed  CC BY

1. Introduction

Coagulation/flocculation (CF) is frequently employed for textile wastewater remediation. Textile effluents contain a wide range of chemicals (dyes, salts, bases, auxiliary chemicals) that can harm the environment if not properly treated (Lopes et al., 2019). Conventional coagulants such as aluminium and ferric salts, and synthetic polymers are commonly applied, despite being expensive, easily affected by pH, and responsible for potentially toxic sludge. To overcome these disadvantages, coagulants derived from natural materials have gained recognition. Tannins are considered promising precursors for coagulants/flocculants (Tomasi et al., 2022). Most colloids in water are negatively charged, as are the phenolic tannin groups. Therefore, tannins should be chemically modified to acquire cationic character and coagulation properties. The *Mannich* reaction has been used to cationize tannins. It consists of a tannin reaction with formaldehyde and ammonium chloride, primary or secondary amines (Arismendi et al., 2018). One of the procedures to carry out the aminomethylation consists of preparing the Mannich solution (iminium ion formation) and its later interaction with tannins (Quamme & Kemp, 1985). In this work, chestnut shell (CS) and maritime pine bark (PB) extracts were cationized and applied as tannin-based coagulants to remove color from a synthetic textile wastewater. These waste materials are generated in furniture, pulp and paper, and chestnut processing activities, and are commonly discarded, used as a soil conditioner, or for energy recovery, despite their valorization potential.

2. Materials and Methods

2.1. Tannin Extracts and Chemical Modification

CS and PB extracts were obtained through microwave-assisted and solid-liquid techniques, respectively, using water as solvent. Tannin extracts were dissolved in hot water (55-65 °C). The Mannich solution was obtained by refluxing ammonium chloride with commercial formaldehyde solution (37 % wt.) for 3 h. This solution was then slowly added to the tannin mixture, and the reaction was performed for 5h (CS) and 2.5h (PB) at 85 °C, under slow stirring. The products were diluted to 10.00 mL with distilled water. Two cationization tests (Table) were performed for each

extract, using different amounts of formaldehyde (conditions adapted from the literature on other tannin sources). CS₁, CS₂, PB₁, and PB₂ products were obtained.

Test	Tannin dissolution		Mannich solution		Ref
	H ₂ O (mL)	NH ₄ Cl (g)	CH ₂ O solution (mL)		
1	1.2	0.40	3.2		(Arismendi et al., 2018)
2	2.5	0.40	1.8		(Quamme & Kemp, 1985)

Table 1: Mannich reaction conditions considering 1 g of tannin extract

2.2. Jar Test

A synthetic dyehouse wastewater was prepared using a Sirius Blue K-CFN dye, sodium chloride, and sodium bicarbonate (80, 2.5, and 1 g/L, respectively). CF assays were conducted at pH 8, using a jar test apparatus. PB and CS were tested and compared to Tanfloc SG (TF; a commercial coagulant derived from Black Wattle), and aluminium sulfate (AS). The minimum coagulant dosages were determined first, followed by the optimal coagulant dosages. CF assays consisted of coagulant addition, followed by rapid (150 rpm, 3 min) and slow mixing stages (20 rpm, 15 min), and settling (15 min). Turbidity and blue color removal (absorbance at 571 nm) were evaluated. Clarified samples (with no blue color) were also analyzed for color using the Pt/Co scale. The effect of adding a flocculant (*Magnafloc*) at the slow mixing stage was studied.

3. Results

Preliminary CF experiments showed that CS₁ and PB₂ did not present relevant coagulation abilities. Results obtained for PB₁, CS₂, TF, and AS are presented in Figure . Optimum coagulant dosages, considered the minimum values that provided maximum color removals (all above 96%), were determined as 550, 750, 190 and 360 mg/L, respectively for PB₁, CS₂, TF, and AS. Considering the amount of coagulant needed for almost total decolorization, the tannin commercial coagulant presented the best performance. To achieve similar efficiencies, much higher dosages are required for other coagulants. It is worth of note that optimum dosages found for AS and PB₁ are the minimum ones that provided flocs formation. Clarified effluent samples (no blue color) were filtered and analyzed in the Pt/Co scale to evaluate “yellow shades.” AS coagulant provided the lowest residual color (< 20 units), whereas the organic coagulants generated levels of 28 (TF) and 100 units (PB₁ and CS₂). Floc size was only assessed visually. Even though, quite low turbidity levels were measured in the supernatant (mostly < 16 NTU), showing flocs with good settling properties. Flocculant addition was tested but has only improved floc size for TF, with slightly reduction of turbidity observed. The addition of Magnafloc can be then disregarded.

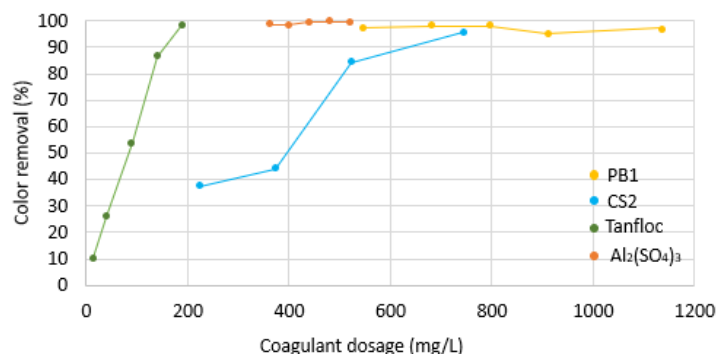


Figure 1: Color removal percentages obtained in jar tests for the treatment of a simulated textile wastewater using different coagulants and coagulant dosages.

4. Conclusions

Two successful coagulants were generated from chestnut shell and pine bark through Mannich reaction. The results show that cationization conditions are sensitive to the tannin source. Coagulation-flocculation-sedimentation experiments show that both coagulants are effective on

decolorization of textile effluents. At the same dosages, PB derived coagulant was more efficient than the CS coagulant. Lower AS or TF coagulant are however required to find the same efficiency. Considering that the work is still exploratory, and the extraction and cationization are yet to be optimized, the results here obtained seem to be promising.

Acknowledgments

This work was financially supported by LA/P/0045/2020 (ALiCE), UIDB/50020/2020 and UIDP/50020/2020 (LSRE-LCM), funded by national funds through FCT/MCTES (PIDDAC). Isabella T. Tomasi and Sílvia C. R. Santos acknowledge doctoral and postdoctoral scholarships (respectively, BD/11977/2022 and SFRH/BPD/117387/2016), awarded by FCT.

References

- Arismendi, W. A., Ortiz-Ardila, A. E., Delgado, C. V., Lugo, L., Sequeda-Castañeda, L. G., & Celis-Zambrano, C. A. (2018). Modified tannins and their application in wastewater treatment. *Water Science and Technology*, 78. <https://doi.org/https://doi.org/10.2166/wst.2018.336>
- Lopes, E. C., Santos, S. C. R., Pintor, A. M. A., Boaventura, R. A. R., & Botelho, C. M. S. (2019). Evaluation of a tannin-based coagulant on the decolorization of synthetic effluent. *Journal of Environmental Chemical Engineering*, 7(3). <https://doi.org/https://doi.org/10.1016/j.jece.2019.103125>
- Quamme, J. E., & Kemp, A. H. (1985). *STABLE TANNIN BASED POLYMER COMPOUND* (USA Patent No. 4558080).
- Tomasi, I. T., Machado, C. A., Boaventura, R. A. R., Botelho, C. M. S., & Santos, S. C. R. (2022). Tannin-based coagulants: Current development and prospects on synthesis and uses. *Science of the Total Environment*. <https://doi.org/https://doi.org/10.1016/j.scitotenv.2022.153454>

P09. Urban Wastewater Resources Recovery - Integration of Nanofiltration and Advanced Oxidation Processes

Carla S. Santos^{1,2*}, Rosa Montes³, Rosário Rodil³, José B. Quintana³, Ana I. Gomes^{1,2}, Vítor J.P. Vilar^{1,2}

¹LSRE-LCM – Laboratory of Separation and Reaction Engineering – Laboratory of Catalysis and Materials, Faculdade de Engenharia da Universidade do Porto, Rua Dr. Roberto Frias, 4200-465 Porto, Portugal (up201604254@edu.fe.up.pt) ORCID [0000-0003-3985-134X](https://orcid.org/0000-0003-3985-134X)

²ALiCE – Associate Laboratory in Chemical Engineering, Faculdade de Engenharia da Universidade do Porto, Rua Dr. Roberto Frias, 4200-465 Porto, Portugal

³Department of Analytical Chemistry, Institute of Research on Chemical and Biological Analysis (IAQBUS), Universidad de Santiago de Compostela, Spain

* presenting author (up201604254@edu.fe.up.pt) ORCID ([0000-0003-3985-134X](https://orcid.org/0000-0003-3985-134X))

Abstract

The change in the state of water resources has become an issue of global importance and the reuse of urban wastewater (UWW) represents a promising solution to the problem of water scarcity. The combination of membrane filtration and advanced oxidation processes contribute to an increase in UWW quality. In this work, a tube-in-tube membrane photoreactor is applied for the removal of contaminants of emerging concern present in reverse osmosis (RO) and nanofiltration (NF) concentrates using the UV-C/Persulfate process. For both concentrates, diclofenac (anti-inflammatory), iopromide (x-ray contrast) and sulfamethoxazole (antibiotic) presented high levels of removal ($\geq 70\%$), while carbamazepine, irbesartan (angiotensin II blocker) and melamine (flame retardant) shown to be resistant (removals $< 25\%$).

Author Keywords. Nanofiltration, Reverse Osmosis, Advanced Oxidation Processes, Urban Wastewater, Concentrate, Contaminants of Emerging Concern

 Open Access  Peer Reviewed  CC BY

1. Introduction

Wastewater reuse represents a promising solution to water scarcity problems in various fields of application, particularly in the agricultural sector, for which water supply accounts for more than 70% of demand. However, conventional technologies in wastewater treatment plants (WWTPs) are not sufficient to remove a wide range of pollutants. For this reason, advanced treatments are required for effluent recovery. One promising method to improve effluent quality is membrane filtration, especially, reverse osmosis (RO) and nanofiltration (NF). However, the application of the RO or NF process generates an unavoidable concentrated stream, referred to as concentrate or retentate, which is generally characterized by high levels of inorganic salts, refractory organic substances, and trace micropollutants. To reduce the pollutant load of the concentrate streams, specific methodologies have been applied such as advanced oxidation processes. One example is the combination of UV radiation and oxidants, generating powerful reactive oxygen species (ROS). The tube-in-tube membrane photoreactor, proposed by Vilar et al. (2020), allows the integration of different mechanisms for ROS generation within a single unit operated in continuous flow mode. In this reactor, a tubular ceramic ultrafiltration membrane provides a uniform distribution of the oxidant through multiple dosing points along its entire length. In this research, the tube-in-tube membrane photoreactor was employed for the removal of contaminants of emerging concern (CECs) present in RO and NF concentrates by applying UV-C radiation and persulfate (UV-C/PS). The physicochemical characteristics of the treated concentrates were also evaluated so that they can be safely discharged of in aquatic systems.

2. Materials and Methods

A membrane filtration pilot, integrating RO or NF membranes (RE 4040-BE or NE 4040-70, respectively), was installed in a municipal WWTP in Northern Portugal. The influent was collected downstream of the second clarifier, stored in a 1 m³ capacity feed tank and pumped to the RO/NF unit via an EFAFLU pump. The produced concentrate was reintroduced into the feed tank (concentration factor ≈ 2.7). Afterwards, a sample of the concentrate and permeate was collected

at the outlet of the membrane module and stored until use. The concentrate was filtered through a sand filtration system in order to minimize the amount of solids.

A tube-in-tube membrane photoreactor system, with partial recirculation of the effluent with a ratio $Q_R/Q_F = 27.5/2.5$ L/h (where "R" stands for recirculation flow rate and "F" the feed flow rate) was used for the treatment of the concentrate samples. The system was operated with a residence time of 3.4 min, corresponding to an accumulated UV-C dose of 3.8 kJ per liter of concentrate. A stock solution of oxidant ($[S_2O_8^{2-}, PS] = 254,4$ mM; pH = 3,7) was pumped ($Q_{PS} = 0,2$ mL min⁻¹) through the lumen side of the membrane, permeating the pores until reaching the annular reaction zone ($[PS] = 1.2$ mM) where the concentrate to be treated flows. The analysis of the CECs in the water samples (Table 1) was performed in an Acquity UPLC® liquid chromatograph interfaced to a XEVO TQD® triple quadrupole mass spectrometer equipped with an electrospray interface (ESI) from Waters (Milford, MA, USA).

Parameters	Units	UWW	RO		UWW	NF	
			C	P		C	P
Conductivity	μS cm ⁻¹	1387	5700	430	1079	2315	874
Chemical Oxygen Demand (COD)	mg L ⁻¹	130	195	12.5	70	206	1.2
Dissolved Organic Carbon (DOC)	mg L ⁻¹	16.2	48	7.1	13.1	51	0.9
Dissolved Inorganic Carbon (DIC)	mg L ⁻¹	61.5	178	34.9	50	65	41.5
Total Suspended Solids (TSS)	mg L ⁻¹	64.5	52	2.7	31.5	1.2	1.5
Chloride (Cl ⁻)	mg L ⁻¹	132	689	26.9	159	232	152
Nitrite (NO ₂ ⁻)	mg L ⁻¹	13.8	25.2	4.2	8.1	18.8	2.0
Sulfate (SO ₄ ²⁻)	mg L ⁻¹	58	315	0.3	57	298	1.1
Nitrate (NO ₃ ⁻)	mg L ⁻¹	19.2	9.9	0.4	5.8	19.1	0.1
Phosphate (PO ₄ ³⁻)	mg L ⁻¹	14.4	14	<0.03	10.6	43.1	0.7
Sodium (Na ⁺)	mg L ⁻¹	109	855	<0.02	124	422	99
Ammonium (NH ₄ ⁺)	mg L ⁻¹	43.6	223	64.4	5.5	54.2	118
Potassium (K ⁺)	mg L ⁻¹	24.1	196	2.4	25.4	84.3	20.4
Magnesium (Mg ²⁺)	mg L ⁻¹	7.0	36.0	15.6	5.2	99.0	1.9
Calcium (Ca ²⁺)	mg L ⁻¹	32.7	128	0.1	28.5	11.6	13.2
Melamine (MLN)	μg L ⁻¹	4.6	20.5	0.7	3.0	10.5	<0.35
Diuron (DRN)	μg L ⁻¹	0.1	0.2	<0.02	0.2	0.2	0.2
Carbamazepine (CBZ)	μg L ⁻¹	2.0	2.4	<0.02	0.9	3.4	0.3
Carbamazepine 10,11-epoxide (CBZ-EPX)	μg L ⁻¹	0.3	0.5	<0.04	0.5	2.8	0.4
Bisoprolol (BSPL)	μg L ⁻¹	0.8	1.3	<0.02	0.6	1.3	0.3
Losartan (LSTN)	μg L ⁻¹	1.8	3.6	<0.11	0.6	1.5	<0.11
Irbesartan (ISTN)	μg L ⁻¹	3.1	4.2	<0.04	2.0	3.0	<0.04
Diclofenac (DCF)	μg L ⁻¹	2.6	6.5	<0.15	1.8	7.8	<0.15
Iopromide (IOP)	μg L ⁻¹	12.7	18.6	<0.32	3.8	17.9	<0.32
Sulfamethoxazole (SMX)	μg L ⁻¹	0.7	0.8	<0.03	0.3	3.5	<0.02
Venlafaxine (VLX)	μg L ⁻¹	2.2	2.4	<0.02	0.8	2.0	0.4

Table 1 : Characterization of the UWW, RO and NF concentrate (C) and permeate (P).

3. Discussion

RO and NF were able to achieve a permeates with high quality, enabling its use for irrigation of crops, accordingly to the Regulation (EU) 2020/741 – Annex 1. Regarding the treatment of the concentrate streams from RO and NF, similar CECs removals were obtained (Figure 1). The CECs that showed greater degradation were DCF, IOP and SMX. These compounds are known to exhibit high photodegradability, as evidenced by their high molar absorptivity ($\epsilon_{254} > 10^3$) and quantum yields (Φ_{254}). In turn, CBZ, ISTN and MLN were the contaminants with the lowest levels of removal, followed by BSPL and VLX. The highly stable organic compound MLN has been shown to be resistant to direct degradation by hydroxyl radicals (OH[•]) requiring the generation of sulfate radicals (SO₄^{•-}), although the reported reaction constant with SO₄^{•-} is relatively low ($k \approx 10^5$, Maurino et al. 2016).

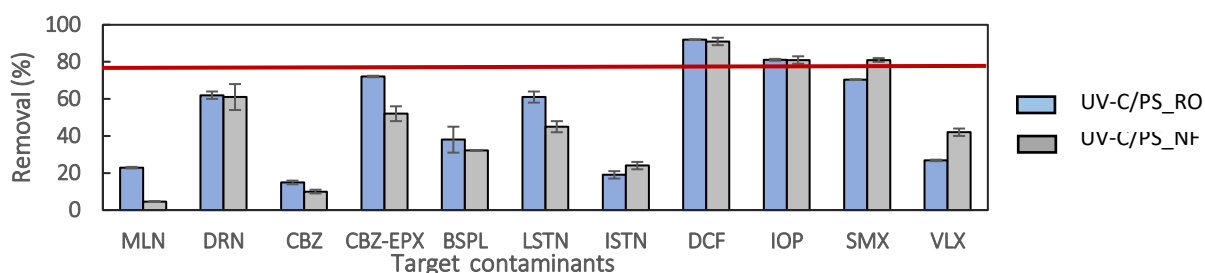


Figure 1: Removal (%) of the CECs in the photo-treated RO and NF concentrates.

According to the final physicochemical characteristics of the treated concentrates (Table 2), it can be concluded that these cannot be discharged into the surface water since, although they comply with the legally required TSS and BOD values (35 mg L^{-1} and 25 mg L^{-1} , respectively), the COD value is higher than the maximum allowable (125 mg L^{-1}) (according with the Council Directive 91/271/EEC).

Concentrate	pH	COD	DOC	DIC	TSS	CBO ₅
	-	mg L ⁻¹	mg L ⁻¹	mg L ⁻¹	mg L ⁻¹	mg L ⁻¹
RO	8.1	174	46	172	34	<5
NF	7.6	143	54	54	20	<5

Table 2: Main physicochemical characteristics of the RO/NF concentrates after treatment.

4. Conclusions

Membrane filtration allows to obtain a permeate with very good quality, with low amounts of CECs, allowing its reuse for crop irrigation. A low footprint membrane photoreactor was applied in this work to promote the application of the UV-C/PS oxidative process. DCF, IOP and SMX were successfully removed while MLN, CBZ and ISTN showed high resistance to the oxidative process in both concentrates under study. Additional tests are being carried out to ensure that the treated concentrate can be discharged safely into the receiving environment.

References

- Maurino, Valter, Marco Minella, Fabrizio Sordello, and Claudio Minero. 2016. "A proof of the direct hole transfer in photocatalysis: The case of melamine." *Applied Catalysis A: General* 521:57-67. doi: <https://doi.org/10.1016/j.apcata.2015.11.012>.
- Vilar, Vítor J. P., Pello Alfonso-Muniozgueren, Joana P. Monteiro, Judy Lee, Sandra M. Miranda, and Rui A. R. Boaventura. 2020. "Tube-in-tube membrane microreactor for photochemical UVC/H₂O₂ processes: A proof of concept." *Chemical Engineering Journal* 379:122341. doi: <https://doi.org/10.1016/j.cej.2019.122341>.

Acknowledgments

This work was financially supported by LA/P/0045/2020 (ALiCE), UIDB/50020/2020 and UIDP/50020/2020 (LSRE-LCM), funded by national funds through FCT/MCTES (PIDDAC) and (iii) project SERPIC, Aquatic/0002/2020, funded by ERA-NET-European Research Area networks through the FCT.

P10. Design and synthesis of spherical $Fe_{2.4}Cu_1$ -MOF@PAN for coloured effluent treatment

Antía Fdez-Sanromán^{1*}, M^a Ángeles Sanromán¹, Marta Pazos¹, Emilio Rosales¹

¹ CINTECX, Universidade de Vigo, Department of Chemical Engineering, Campus Universitario As Lagoas—Marcosende, 36310 Vigo, Spain

*Presenting author (antia.fernandez.sanroman@uvigo.gal) ORCID 0000-0001-7485-3055

Abstract

In this study, several bimetallic FeCu-MOFs were synthesized varying the Fe:Cu ratio. These catalysts were tested in the degradation of Rhodamine B through the activation of peroxymonosulfate (PMS). $Fe_{2.4}Cu_1$ -MOF demonstrated the best degradation levels and the effect of PMS/ $Fe_{2.4}Cu_1$ -MOF ratio was studied. With the aim to avoid the operational problem of the small particle size and facilitate its recovery $Fe_{2.4}Cu_1$ -MOF immobilized on polyacrylonitrile spheres were prepared. The experimental design was carried out to acquire the most efficient operational conditions. Three independent variables (PMS concentration, catalyst dosage, time) and the decolorization as response were selected. Based on the results, it was determined a maximum degradation of 80.92% at 2.5 mM of PMS, 1.1 g/L catalyst dosage and time 89 min. In addition, under these conditions, the so-prepared catalyst maintained its activity in several cycles without loss of activity. So, it proved to be a feasible catalyst for the removal persistent contaminants.

Author Keywords. Advanced Oxidation Processes, Immobilisation, Metal-Organic Framework, Rhodamine B removal.

 Open Access  Peer Reviewed  CC BY

1. Introduction

In the textile, cosmetic, paper and plastic industries, synthetic dyes are widely used, and these compounds can cause serious environmental problems when discharged directly. Typical wastewater treatment plants cannot degrade most of these pollutants and generate large volumes of sludge, resulting in secondary pollution (Mahmoodi et al. 2019). For this reason, different treatments have been developed, including Advanced Oxidation Processes (AOP).

AOPs are based on the generation of non-selective radicals with high oxidizing power, such as hydroxyl and sulfate radicals. To obtain these radicals, peroxymonosulfate (PMS) activation using transition metals is the most significant. Due to the meaningful advantages that heterogeneous catalysts provide, they are increasingly used today. These advantages include the easy recovery of the catalyst and the ability to operate in both batch and flow systems. Among the heterogeneous catalysts, Metal-Organic Frameworks (MOF), which are a class of porous, crystalline materials with a broad range of applications, stand out. These MOFs were initially synthesized with a single metal at the centre of the structure. Nowadays, there are studies that reinforce the catalytic properties of MOFs by adding one or more metals to the structure. Therefore, the aim of this work is to synthesize several bimetallic MOFs and study their catalytic activity and potential application for remediation of coloured effluents, such as Rhodamine B, by immobilisation on polyacrylonitrile (PAN) spheres.

2. Materials and Methods

Synthesis of Fe_xCu_y -MOF: Several MOFs (Fe_1Cu_1 , $Fe_{0.5}Cu_1$, $Fe_{1.7}Cu_1$, $Fe_{2.4}Cu_1$) were synthesized by a solvothermal process with small modifications of the described by Fu et al. (2022) using different Fe:Cu ratios.

Synthesis of the $Fe_{2.4}Cu_1$ -MOF on PAN spheres: The process was developed in two steps. Initially, the PAN spheres were produced according to the procedure described by Mahmood and Waisi (2021). Then, the synthesis of $Fe_{2.4}Cu_1$ -MOF was carried out following the procedure described above with the spheres added to the metal solutions before adding it to the hydrothermal reactor obtaining the new catalyst $Fe_{2.4}Cu_1$ -MOF@PAN.

Characterization of synthesized catalysts: Scanning Electron Microscopy (SEM) was performed on a JEOL JSM-6700F equipped with an Energy Dispersive X-rays spectroscopy (EDS) Oxford Inca Energy

300 SEM. For the crystallographic analysis, the X-ray diffraction (XRD) was made on a Siemens D5000 diffractometer (C.A.C.T.I., University of Vigo, Vigo, Spain).

Rhodamine B degradation: In all the experiments, the degradation of the dye at initial concentration of 10 ppm was performed on a volume of 50 mL. In the tests to select the FeCu-MOF, a concentration of 1 mM PMS and 0.25 g/L of FeCu-MOF were employed. To determine the most effective catalyst, different concentrations of PMS (1, 2 and 2.5 mM) and catalyst (0.25 and 0.5 g/L) were applied.

Experimental design: a Response Surface Methodology with Central Composite Face-Centered experimental (RSM CCF-C) design matrix were applied to design the experiments. To investigate the operating parameters three main variables were selected: time (10-90 min), Fe_{2.4}Cu₁-MOF@PAN concentration (0.3 - 1.2 g/L) and PMS (1.5-2.5 mM) as factors that may potentially affect the response function, which is dye decolourisation. Statistical analysis of the model was performed to evaluate the analysis of variance (ANOVA) using Design Expert® 8.0.0 software (Stat-Ease Inc., Minneapolis, USA).

3. Discussion

As results of the synthesis procedures four different MOFs have been obtained (Fe₁Cu₁, Fe_{0.5}Cu₁, Fe_{1.7}Cu₁, Fe_{2.4}Cu₁) and characterized for their physical, chemical, and morphological properties. From the FeCu-MOF characterization by XRD and SEM, it has been confirmed that they have been properly synthesized, as it can be seen in the Figure .

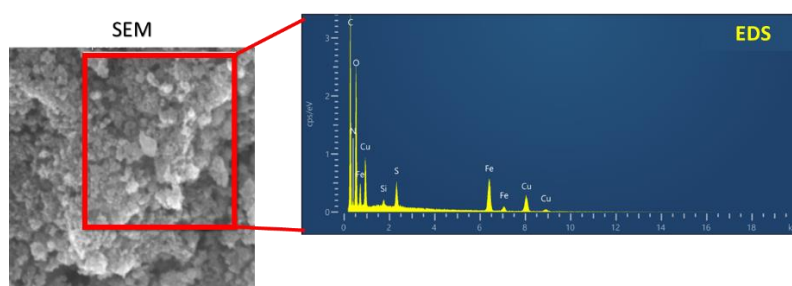


Figure 1: SEM image of Fe_{1.7}Cu₁-MOF, with EDS analysis of this section of the image.

Figure 1 confirms that iron is 1.7 times more abundant than copper. According to SEM images, all MOFs synthesized had a rod-like shape, primarily differing in size. Compared to Fe_{0.5}Cu₂-MOF, Fe_{2.4}Cu₁-MOF has a 320 μm difference in size.

Their ability for PMS activation capacity was analysed under natural pH conditions. It was observed that increasing the amount of iron in the bimetallic catalyst improves Rhodamine B degradation under the same conditions. Therefore, Fe_{2.4}Cu₁ was selected as the best candidate to be immobilized in PAN spheres, designated Fe_{2.4}Cu₁-MOF@PAN.

The immobilization was carried out and the results were also analysed by SEM and EDS. The results showed the growth of the selected MOF in the spheres. Then, the catalytic capability of Rhodamine B degradation by PMS activation via Fe_{2.4}Cu₁-MOF@PAN was then studied and optimized by RSM CCF-C. A total of 20 experiments were carried out in this study, including six replicates at the central point. In this case, the empirical quadratic model fitted well to the experimental data. The ANOVA analysis demonstrated that the model was highly significant, and all variables had a significant effect on Rhodamine B degradation. In addition, the predicted R² was in reasonable agreement with the adjusted R². Thus, the model can reflect properly the experiments and the expression correlating the variables and response was attained. Based on this the optimization of the process was carried out. From the model optimization, the maximum pollutant degradation at 2.5 mM PMS and 89 min with 1.1 g/L Fe_{2.4}Cu₁-MOF@PAN was 80.92% which was validated experimentally.

As aforementioned, the capability of the immobilized catalyst of being reused and to maintain its catalytic effect is also an important issue. To analyze the reusability and stability of Fe_{2.4}Cu₁-MOF@PAN, successive degradation cycles were performed. After five cycles under these

conditions, Fe_{2.4}Cu₁-MOF@PAN showed a reduction of less than 5% in Rhodamine B removal efficiency probing a good mechanic and catalytic properties.

4. Conclusions

In conclusion, a Fe_{2.4}Cu₁-MOF with high catalytic capacity have been synthesized that can be supported on spheres of PAN to facilitate the operation in flow systems. This Fe_{2.4}Cu₁-MOF@PAN retains all their properties and can be reused in successive cycles keeping its activity. Consequently, continuous flow processes can benefit from its high stability in decontamination of wastewater.

References

- Fu, Ao, Zhibin Liu, and Zhirong Sun. 2022. "Cu/Fe Oxide Integrated on Graphite Felt for Degradation of Sulfamethoxazole in the Heterogeneous Electro-Fenton Process under near-Neutral Conditions." *Chemosphere* 297. DOI: 10.1016/j.chemosphere.2022.134257.
- Mahmood, Ola Abd Al-Qader, and Basma I Waisi. 2021. "Crystal Violet Dye Removal from Aqueous Water Using Polyacrylonitrile Precursor Beads." *Materials Today: Proceedings* 42: 2185–92. <https://doi.org/https://doi.org/10.1016/j.matpr.2020.12.303>.
- Mahmoodi, Niyaz Mohammad, Mina Oveisi, Ali Taghizadeh, and Mohsen Taghizadeh. 2019. "Novel Magnetic Amine Functionalized Carbon Nanotube/Metal-Organic Framework Nanocomposites: From Green Ultrasound-Assisted Synthesis to Detailed Selective Pollutant Removal Modelling from Binary Systems." *Journal of Hazardous Materials* 368: 746–59. DOI: 10.1016/j.jhazmat.2019.01.107.

Acknowledgments

This research has been financially supported by Project PID2020-113667GBI00, funded by MCIN/AEI/10.13039/501100011033 and Xunta de Galicia, and the European Regional Development Fund (ED431C 2021-43). Also, Antía Fdez-Sanromán thanks Ministerio de Ciencia e Innovación (PRE2021-098540) for her predoctoral fellowship.

P11. Photocatalytic oxidation of *n*-decane in the mili-photoreactor NETmix

Sandra M. Miranda^{1, 2*}, Tatiana Matiazzo³, Natan Padoin³, Cíntia Soares³, Tânia F. C. V. Silva^{1, 2}, Vítor J.P. Vilar^{1, 2}

¹ LSRE-LCM - Laboratory of Separation and Reaction Engineering – Laboratory of Catalysis and Materials, Faculty of Engineering of the University of Porto (FEUP), Rua Dr. Roberto Frias, 4200-465 Porto, Portugal

² ALiCE - Associate Laboratory in Chemical Engineering, Faculty of Engineering, University of Porto, Rua Dr. Roberto Frias, 4200-465 Porto, Portugal ³ Laboratory of Materials and Scientific Computing (LabMAC), Department of Chemical and Food Engineering, Federal University of Santa Catarina (UFSC), Florianópolis, SC, Brazil

*Presenting author (sandra.miranda@fe.up.pt) ORCID [0000-0003-2614-059X](https://orcid.org/0000-0003-2614-059X)

Abstract

This study focuses on the photocatalytic degradation of *n*-decane in the gas phase, using a NETmix mili-photoreactor illuminated by UVA LEDs. To assess the influence of the illumination on the walls and base of the network of chambers and channels inside the NETmix, two mili-photoreactors with different depths (1 and 3 mm) were used. Several experiments were performed to evaluate different loads of TiO₂ under back-side (BSI) and front-side (FSI) illumination mechanisms for both mili-photoreactors. Besides, Reynolds number (*Re*) was increased from 53 to 1174 to improve the mixing degree inside the mili-photoreactor; for that, feed flow rates (*Q_{feed}*) from 0.67 to 15 L min⁻¹ were considered. A Computational Fluid Dynamics (CFD) modeling was used to oversee the velocity flow profile inside the reactor and complement/analyze *n*-decane single-pass oxidation.

Author Keywords. Advanced Oxidation Processes; Photocatalysis; VOCs; Air Decontamination; Process intensification; NETmix mili-photoreactor; CFD

 Open Access  Peer Reviewed  CC BY

1. Introduction

Poor indoor air quality and related health problems have been pointed out as one of the worldwide priority concerns (Billionnet et al. 2011). Volatile organic compounds (VOCs), common chemical contaminants, such as hydrocarbons (toluene, benzene, *n*-decane), ketones, and organochlorine compounds, are one of the leading causes of sick building syndrome (Jiang et al. 2014). The intensification of heterogeneous photocatalytic processes, through the minimization of mass and photon transfer limitations, using an innovative mili-photoreactor, NETmix, towards indoor air treatment has been considered a promising strategy for the abatement of pollutants as VOCs (da Costa Filho et al. 2017).

2. Materials and Methods

The catalyst employed in the experiments was the commercial benchmark TiO₂ (P25 - Aeroxide®) from Evonik Degussa Corporation. *n*-decane (C₁₀H₂₂) with a purity greater than 95% was used to study the photocatalytic oxidation process. Heterogeneous photocatalysis was performed using a mili-structured photoreactor, based on NETmix technology, irradiated by UVA light-emitting diodes (UVA-LEDs). The lab-scale prototype contains four main sections: feed generator; mili-photoreactor; illumination systems; photoreactor feed/exit stream analysis by a master gas chromatographic analysis system with a flame ionization detector. The NETmix mili-photoreactor comprise a back stainless-steel slab where small sized chambers and channels are imprinted and a frontal borosilicate glass. The sealing is done by mechanical compression and O-rings and incorporates multi-inlet injection points along the reactor. The catalyst was sprayed over channels and chambers (front-side illumination (FSI) mechanism) or over one side of the borosilicate glass (back-side illumination (BSI) mechanism).

3. Discussion

For both configurations, different amounts of TiO₂ nanoparticles were tested. Therefore, the remaining experiments were carried out with loadings of: 75 mg (1.35 mg cm⁻²) for BSI mechanism; 200 mg (NETmix-1) and 400 mg (NETmix-3), which correspond to 2.17 mg cm⁻² and 2.42 mg cm⁻², respectively, for FSI mechanism. Figure 5 illustrates the effect of the Reynolds number on the *n*-

decane degradation and mineralization over TiO₂-P25 film for NETmix milli-photoreactors with different depths (1 and 3 mm). Higher Re is a consequence of higher feed flow rate (Q_{feed}). By increasing the Q_{feed} , the contact between *n*-decane molecules and the catalyst surface decreases as consequence of the lower residence time. However, a higher degree of mixing improves mass transfer. For the NETmix-3, a ~11-fold increase in Q_{feed} (Re 53 to 587) led to a decrease of ~1.7-/1.8-fold in the *n*-decane degradation, for FSI/BSI mechanism. However, the same increase in Q_{feed} led to an increase of ~6.7-fold in the reaction rate for both mechanisms, since a higher organic load per minute imply that more molecules are available to be converted (Figure a). It is visible that the FSI mechanism presents a higher *n*-decane degradation/mineralization when compared with the BSI mechanism, as the catalyst's surface area is higher; however, lower than expected. Inside the channels the flow is parallel, but in the chambers it is chaotic, favouring dead volume formation and small recirculation zones (Figure b).

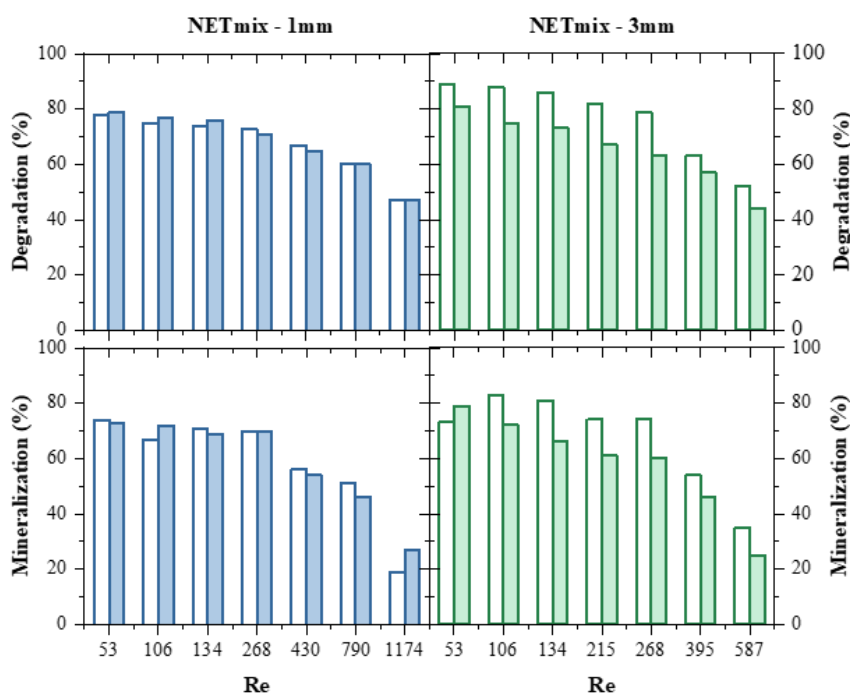


Figure 5: Effect of Reynolds number on *n*-decane degradation and mineralization at steady-state conditions (298 K and 1 bar): $C_{dec,feed} = 6.4 \times 10^{-4} \text{ mol m}^{-3}$ and RH = 10% for: FSI (open columns) and BSI (closed columns) mechanisms.

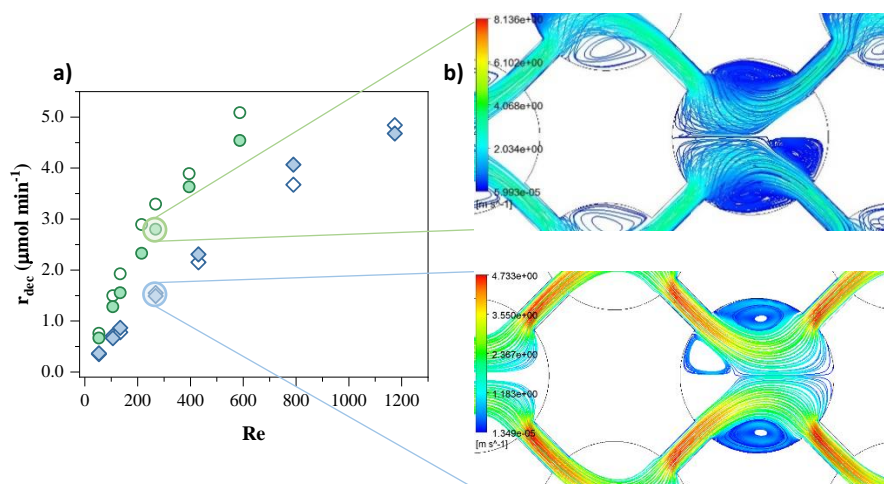


Figure 2: a) Reaction rate for: FSI (open symbols) and BSI (closed symbols) mechanisms with 3 mm (○, ●) and 1 mm (◇, ◇). Measured at steady-state conditions (298 K and 1 bar): $C_{dec,feed} = 6.4 \times 10^{-4} \text{ mol m}^{-3}$ and RH = 10%. b) Top view of the velocity flow profile inside the channels and chambers of both NETmix.

4. Conclusions

Higher single-pass removal efficiencies were achieved by reducing the feed flow rate. For both reactors, the illumination mechanism, BSI or FSI, did not play a relevant role in the reaction rate for *n*-decane degradation at gas phase. The increase in the photocatalytic reaction rate for both illumination mechanisms was not proportional to the increase in catalyst surface per reactor volume, since FSI mechanism is 1.7 times greater for NETmix-1 and 3 times greater for NETmix-3 than BSI mechanism.

References

- Billionnet, C., E. Gay, S. Kirchner, B. Leynaert, and I. Annesi-Maesano. 2011. "Quantitative assessments of indoor air pollution and respiratory health in a population-based sample of French dwellings." *Environ Res* 111 (3): 425-34. <https://doi.org/10.1016/j.envres.2011.02.008>.
- da Costa Filho, Baturai M., Ana L. P. Araujo, Gabriela V. Silva, Rui A. R. Boaventura, Madalena M. Dias, José C. B. Lopes, and Vítor J. P. Vilar. 2017. "Intensification of heterogeneous TiO₂ photocatalysis using an innovative micro-meso-structured-photoreactor for *n*-decane oxidation at gas phase." *Chemical Engineering Journal* 310: 331-341. <https://doi.org/https://doi.org/10.1016/j.cej.2016.09.080>.
- Jiang, Zhi, MingXia Chen, Jianwei Shi, Jian Yuan, and Wenfeng Shangguan. 2014. "Catalysis Removal of Indoor Volatile Organic Compounds in Room Temperature: From Photocatalysis to Active Species Assistance Catalysis." *Catalysis Surveys from Asia* 19 (1): 1-16. <https://doi.org/10.1007/s10563-014-9177-8>.

Acknowledgments

This work was financially supported by LA/P/0045/2020 (ALiCE), UIDB/50020/2020 and UIDP/50020/2020 (LSRE-LCM), funded by national funds through FCT/MCTES (PIDDAC). Sandra M. Miranda gratefully acknowledge FCT for their PhD research fellowship, SFRH/BD/119915/2016. Tânia F.C.V. Silva acknowledge the FCT Individual Call to Scientific Employment Stimulus 2017 (CEECIND/01386/2017).

P12. NETmix crystalliser for struvite precipitation: CFD modelling of flow dynamics and distribution

Laura J. R. Cullen^{1,2*}, Isabel S. Fernandes^{1,2}, Ricardo J. Santos^{1,2}, Vítor J. P. Vilar^{1,2}

¹Laboratory of Separation and Reaction Engineering – Laboratory of Catalysis and Materials

(LSRE-LCM), Faculty of Engineering, University of Porto, Rua Dr. Roberto Frias, 4200-465 Porto, Portugal

²ALiCE – Associate Laboratory in Chemical Engineering, Faculty of Engineering, University of

Porto, Rua Dr. Roberto Frias, 4200-465 Porto, Portugal

*Presenting author (up201806139@edu.fe.up.pt)

Abstract

This work proposes the use of the NETmix reactor to produce sustainable phosphorus-nitrogen-based fertilisers from the liquid-fraction of digestates. In this sense, Computational Fluid Dynamics (CFD) tools were used to evaluate the flow distribution inside this reactor, as well as its flow dynamics, when operating with different flow regimes in each inlet. A simplified NETmix geometric model was used to reduce the computational time of dynamic tracer experiments for various asymmetric inlet flowrates. Time-averaged flowrates in each channel were computed to represent the flowrate variation along the NETmix channels. In addition, the velocity magnitudes in the x and y -directions in the centre of downstream chambers were determined so as to study the dynamic behaviour of the flow inside this reactor from turbulent scales energy distribution.

Author Keywords. NETmix, struvite, CFD, tracer experiments, flow distribution, turbulence.

 Open Access  Peer Reviewed  CC BY

1. Introduction

Phosphorus is a key element for plant growth, and is abundantly present in soils in the form of insoluble inorganic and organic compounds. However, since plants only have access to approximately 20% of this nutrient, the use of natural or synthetic fertilisers becomes necessary to ensure proper crop growth (Prasad and Chakraborty 2019). Synthetic fertilisers are usually made from phosphate rocks. In recent years, there has been a growing concern regarding the non-renewability of these resources and their evident depletion worldwide, as a result of intensification of agricultural practices and a poor management of organic P resources (Alewell et al. 2020). Thus, it has become necessary to recycle and recover this element so that its use becomes more sustainable.

Wastewater is known to be a great source of nutrients, such as nitrogen (N) and phosphorus (P). These effluents, before being discharged, are subject to several treatment processes in wastewater treatment plants. P is usually removed from the liquid fraction of a side-stream generated during anaerobic digestion, called the digestate (Di Capua et al. 2022). This recovery can be done through a crystallisation process, in which N and P precipitate in the form of an insoluble mineral called struvite with the addition of magnesium (Mg) salts (Di Capua et al. 2022). There are other alternative P recovery methods, like adsorption and electrochemical precipitation, but these are still premature from a scientific point of view. Moreover, although some crystallisation-based technologies already exist, they are not economically feasible (Achilleos, Roberts, and Williams 2022).

This work pretends to evaluate the performance of the NETmix reactor for the production of struvite from wastewater effluents through crystallisation with Computational Fluid Dynamics (CFD) tools. NETmix is a patented static mixer consisting of a network of cylindrical mixing chambers interconnected by prismatic channels. This mixer is known for its great mixing capacities above a critical Reynolds number ($Re_c = 200$), above which a chaotic laminar flow is achieved (Torres 2017). Two main aspects were studied in this reactor, namely the flow distribution and flow dynamics.

2. Materials and Methods

Two-dimensional dynamic tracer experiments were simulated in ANSYS/Fluent 2022 R2. Both working fluids (water and tracer) assumed the properties of water at 20 °C: density of 998.2 kg·m⁻³ and viscosity of 1.003 mPa.s. The continuity and the Navier-Stokes equations were solved during the simulations assuming an incompressible and isothermal flow. A reduced geometric model of NETmix, the 2D ExtendedNUB, was used, in which periodic boundary conditions are considered at the sidewalls. The ExtendedNUB geometry can be seen in Figure 6, in which surfaces and characteristic dimensions are identified.

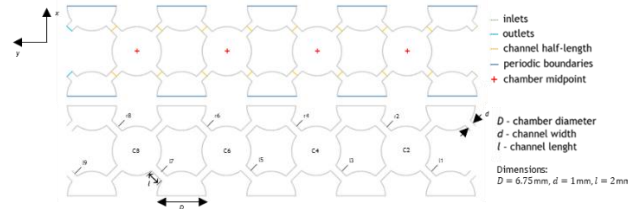


Figure 6. (a) Surfaces of the 2D ExtendedNUB geometry and (b) characteristic dimensions and identification of channels and chambers. Letters ‘r’ and ‘l’ indicate the right and left-hand side channels.

The flow inside the NETmix reactor was simulated for asymmetric flowrates at the two inlets. A steady laminar regime was set on the right-hand side inlet (tracer input) and a self-sustained fully developed chaotic regime on the left-hand side inlet (water input). This was done by defining a Reynolds number larger and lower than Re_c in the right inlet (Re_1) and in the left inlet (Re_2), respectively. The objective was to predict the performance of this reactor when mixing a dilute stream with the nutrients to be precipitated (the digestate liquid fraction) and a stream with a high concentration of Mg. The simulations were run for ten passage times, τ .

3. Discussion

Regarding flow distribution, the time-averaged volumetric flowrate along the right and left-hand side NETmix channels identified in Figure 6 was determined and normalised by the average outlet flowrate. Then, the variation of this normalised variable, Q^* , was analysed for different sets of inlet flowrates. In relation to flow dynamics, velocity fluctuations at the centre of the mixing chambers were analysed from power spectra representing the energy curve, E , versus wavenumber, λ , calculated as $\lambda = f/\bar{v}_{inj}$, where f is the frequency and \bar{v}_{inj} is the average fluid velocity of the inlets. Figure shows the CFD results for the case study of $Re_1 = 1200$ and $Re_2 = 120$. It can be observed in Figure a that the normalised flowrates in the same NETmix channel number become closer toward the downstream chambers and that the values are approximately one in the last rows of the mixer. Figure a and Figure c show a symmetric behaviour in the NETmix after channel 7. Hence, this mixer is able to equally distribute the flow inside its network, attaining the desirable condition of similar outlet flowrates when operated with different inlet flow regimes. Figure c shows that in the rows closer to the inlets have higher velocities in the right side, while in the last chambers there is a more homogenised velocity distribution.

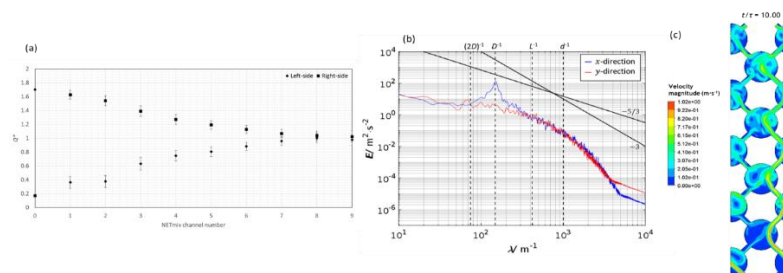


Figure 2. (a) Variation of Q^* along the NETmix channels, (b) power spectrum for chamber C8 and (c) velocity magnitude contour map for $t/\tau = 10$ for $Re_1 = 1200$ and $Re_2 = 120$.

The formation of eddies in chambers C4 to C8, associated with the high dynamics induced by Re_2 , contribute to the uniformity of the flowrate in the following channels. The power spectrum depicted in Figure b shows a slope change from $\lambda^{-5/3}$ to λ^{-3} at a wavenumber close to d^{-1} marking the energy injection scale. This slope and trends change was also observed for 2D and 3D simulations in NETmix for an equal Re at the two inlets above the critical value (Torres 2017). This indicates that the chaotic flow regime is also attained when different flowrates are considered at the two inlets.

4. Conclusions

The analysis of the flow distribution and dynamics in a NETmix operated with different flow regimes at the two inlets showed that this mixer rapidly homogenises the flowrates over the network. The homogenisation of the flow is due to the formation of eddies in chambers C4 to C8. Finally, the power spectrum of the velocity at the midpoint of chamber C8 proved that a fully developed chaotic flow regime was attained. These results show a good potential for the application of the NETmix technology for the production of struvite from the liquid fraction of digestates.

References

- Achilleos, P., K. R. Roberts, and I. D. Williams. 2022. "Struvite precipitation within wastewater treatment: A problem or a circular economy opportunity?" *Heliyon* 8 (7):e09862. doi: <https://doi.org/10.1016/j.heliyon.2022.e09862>.
- Alewell, Christine, Bruno Ringeval, Cristiano Ballabio, David A. Robinson, Panos Panagos, and Pasquale Borrelli. 2020. "Global phosphorus shortage will be aggravated by soil erosion." *Nature Communications* 11 (1):4546. doi: <https://doi.org/10.1038/s41467-020-18326-7>.
- Di Capua, Francesco, Simona de Sario, Alberto Ferraro, Andrea Petrella, Marco Race, Francesco Pirozzi, Umberto Fratino, and Danilo Spasiano. 2022. "Phosphorous removal and recovery from urban wastewater: Current practices and new directions." *Science of The Total Environment* 823:153750. doi: <https://doi.org/10.1016/j.scitotenv.2022.153750>.
- Prasad, Rishi, and Debolina Chakraborty. 2019. *Understanding Phosphorus Forms and Their Cycling in the Soil*. edited by Alabama Cooperative Extension System. Alabama: Alabama A&M and Auburn Universities.
- Torres, José Pedro Nunes da Silva. 2017. "Proper Orthogonal Decomposition of Turbulent Flows." Master, Chemical Engineering Department, University of Porto.

Acknowledgments

This work was financially supported by LA/P/0045/2020 (ALiCE), UIDB/50020/2020 and UIDP/50020/2020 (LSRE-LCM), funded by national funds through FCT/MCTES (PIDDAC).

P13. Photocatalytic H₂O₂ generation and pollutant degradation by nonmetal doped carbon nitride

Amanda Fujita^{1,2*}, André Torres-Pinto^{1,2}, Maria J. Sampaio^{1,2}, Cláudia G. Silva^{1,2}, Joaquim L. Faria^{1,2}, Adrián M.T. Silva^{1,2}

¹ LSRE-LCM - Laboratory of Separation and Reaction Engineering – Laboratory of Catalysis and Materials, Faculty of Engineering, University of Porto, Rua Dr. Roberto Frias, 4200-465 Porto, Portugal

² ALiCE - Associate Laboratory in Chemical Engineering, Faculty of Engineering, University of Porto, Rua Dr. Roberto Frias, 4200-465 Porto, Portugal

*Presenting author (up201900480@edu.fe.up.pt)

Abstract

Graphitic carbon nitride (GCN) has emerged as a widely employed photocatalyst due to its excellent electronic and photo-responsive properties. GCN materials often present a relatively narrow band gap, allowing the use of visible light irradiation; however, they also show a fast rate of charge carrier recombination. In this way, there are increasing attempts to overcome this drawback by modifying these materials, such as doping. In this work, our focus was doping GCN photocatalyst with metal-free atoms (*e.g.*, P, B, O and S) to assess the photoactivity towards the selective generation of H₂O₂ as well as the degradation of organic pollutants. The P-doped catalysts presented higher production rates of H₂O₂ in a methanol aqueous solution and faster removal of selected pharmaceutical substances compared to the bare GCN material.

Author Keywords. carbon nitride, doping, hydrogen peroxide, photocatalysis, pharmaceutical substances

 Open Access  Peer Reviewed  CC BY

1. Introduction

The fabrication of sustainable nanomaterials has developed into one of the most highly explored topics in scientific research. The synthesis of photocatalytic materials is becoming more and more investigated, specifically carbon-based catalysts such as graphitic carbon nitride (GCN), due to its excellent electronic and photo-responsive properties (Ong *et al.* 2016). GCN materials generally present a relatively narrow band gap, allowing the use of visible light irradiation, but also show a fast rate of charge carrier recombination. To overcome this limitation, these materials have been modified by doping, exfoliation or heterostructuring (Ong *et al.* 2016, Torres-Pinto *et al.* 2019). This work focuses on incorporating metal-free atoms (*e.g.*, P, B, O and S) in the GCN matrix during the thermal polymerisation of an earth-abundant and readily available precursor. The use of metal-free atoms was important to reinforce the overall sustainability of the process (Jiang *et al.* 2017, Torres-Pinto *et al.* 2019, Chen *et al.* 2022). The photocatalytic reactions were performed with sacrificial agents as proton donors (methanol, ethanol and isopropanol) to investigate the H₂O₂ production. It was also studied the possibility of using pharmaceuticals as sacrificial agents. So, at the same these contaminants were being degraded, H₂O₂ was being produced. These pharmaceuticals are considered contaminants of emerging concern (CEC) and are persistent and refractory in surface water, hence the importance of removing them from drinking water and wastewater.

2. Materials and Methods

GCN was synthesised by adding urea in semi-closed quartz crucibles placed in a microwave muffle furnace (Phoenix, CEM Corporation) for thermal polymerisation according to a previously reported procedure (Torres-Pinto *et al.* 2022). For the doped materials, urea was diluted in 20 mL of ultrapure water and for each doped element (P, B, O and S), the respective molar percentage was also added into the aqueous solution (in the form of precursors) and then transferred to semi-closed quartz crucibles.

The photocatalytic reactions were performed under visible light irradiation using four 10 W light-emitting diodes (LEDs) with an emission line peak at 417 nm, located symmetrically from the outside at 4.0 cm from the reactor wall. For H₂O₂ generation, different sacrificial agents - methanol, ethanol, and isopropanol - were used with different volume percentages (10, 50, 90, and 100 %). Then, the degradation reactions were performed with different concentrations of organic

contaminants in an aqueous solution: diclofenac (DCF), metoprolol (MTP) and venlafaxine (VEN) were tested at an initial concentration of 50 ppm. H₂O₂ was measured by a colourimetric method, and the pharmaceuticals' concentration was followed by high-performance liquid chromatography (HPLC).

3. Discussion

Each material was tested individually for H₂O₂ generation in a 10% (v/v) methanol solution. Notably, the P-doped catalysts presented a much higher production of H₂O₂ after 2 hours of reaction with a 10% (v/v) methanol aqueous solution compared to bare GCN. This can be explained by the characterisation results, such as photoluminescence intensity decrease and hypsochromic shifts in the visible absorbance range compared to the bare catalyst. Moreover, the 1%wt. P-doped GCN evolved 6 times more H₂O₂ than GCN and allowed for faster degradation and mineralisation rates of the selected pharmaceutical substances.

4. Conclusions

The doped materials increased the production of H₂O₂ compared to bare GCN, using a 10% (v/v) methanol solution. In particular, the P-doped GCN material produced more H₂O₂ in the diluted methanol solution than in pure isopropanol. The three assessed contaminants were degraded faster with the 1%wt. P-doped GCN compared to bare GCN, showing that this type of doping is a good approach to improve not only selective H₂O₂ production but also water treatment. Further characterisation is necessary to study the impact of doping or co-doping of GCN to explain the newly incorporated defects in the GCN matrix that are beneficial or derogatory to the photocatalytic activity.

References

- Chen, J., Kang, N., Fan, J., Lu, C. and Lv, K. 2022. "Carbon nitride for photocatalytic water splitting to produce hydrogen and hydrogen peroxide." *Materials Today Chemistry* 26 DOI: 10.1016/j.mtchem.2022.101028.
- Jiang, L., Yuan, X., Pan, Y., Liang, J., Zeng, G., Wu, Z. and Wang, H. 2017. "Doping of graphitic carbon nitride for photocatalysis: A review." *Applied Catalysis B: Environmental* 217: 388-406 DOI: 10.1016/j.apcatb.2017.06.003.
- Ong, W. J., Tan, L. L., Ng, Y. H., Yong, S. T. and Chai, S. P. 2016. "Graphitic Carbon Nitride (g-C₃N₄)-Based Photocatalysts for Artificial Photosynthesis and Environmental Remediation: Are We a Step Closer To Achieving Sustainability?" *Chemical Reviews* 116(12): 7159-7329 DOI: 10.1021/acs.chemrev.6b00075.
- Torres-Pinto, A., Sampaio, M. J., Silva, C. G., Faria, J. L. and Silva, A. M. T. 2019. "Recent strategies for hydrogen peroxide production by metal-free carbon nitride photocatalysts." *Catalysts* 9(12) DOI: 10.3390/catal9120990.
- Torres-Pinto, A., Silva, C. G., Faria, J. L. and Silva, A. M. T. 2022. "The effect of precursor selection on the microwave-assisted synthesis of graphitic carbon nitride." *Catalysis Today*, in press DOI: 10.1016/j.cattod.2022.08.010.

Acknowledgments

This work was financially supported by LA/P/0045/2020 (ALiCE), UIDB/50020/2020 and UIDP/50020/2020 (LSRE-LCM), and by project 2022.08738.PTDC (DRopH2O), funded by national funds through FCT/MCTES (PIDDAC), and by Project NORTE-01-0145-FEDER-000069 (Healthy Waters) supported by NORTE 2020, under the PORTUGAL 2020 Partnership Agreement, through ERDF. A.T-P. acknowledges FCT for his scholarship SFRH/BD/143487/2019. M.J.S. thanks FCT funding under the Scientific Employment Stimulus - Institutional Call (CEECINST/00010/2021).

P14. Recycling of printed circuit board (PCB) waste as a catalyst in advanced water treatment

Marta A. P. Azevedo^{1,2}, Cátia A. L. Graça^{1,2}, Márcia A. D. Silva³, Liliana M. Martelo³, Helena M.V.M. Soares³, Adrián M. T. Silva^{1,2}

¹ LSRE-LCM - Laboratory of Separation and Reaction Engineering - Laboratory of Catalysis and Materials, Faculty of Engineering, University of Porto, Rua Dr. Roberto Frias, 4200-465 Porto, Portugal

² ALiCE – Associate Laboratory in Chemical Engineering, Faculty of Engineering, University of Porto, Rua Dr. Roberto Frias, 4200-465 Porto, Portugal

³ REQUIMTE/LAQV, Department of Chemical Engineering, Faculty of Engineering, University of Porto, Rua Dr. Roberto Frias, 4200-465 Porto, Portugal

*Presenting author (up201806423@up.pt)

Abstract

This study evaluates a recycled material, printed circuit boards (PCBs), as a catalyst in the wet peroxide (H_2O_2) water treatment process due to its abundance of copper – Cu. The PCBs were thermally treated at different temperatures: 400 °C and 800 °C under air, or 400 °C, 500 °C and 800 °C under nitrogen (N_2); and tested at two pH: natural (~6.8) and 2.8. PCBs treated at 500 °C under N_2 allowed the fastest removal of the target contaminant (venlafaxine) at natural pH, with low Cu leaching. Moreover, some impurities in the original PCBs, which promote water contamination due to leaching, were removed with this thermal treatment.

Author Keywords: circular economy; electronic waste; heterogeneous catalysts; Fenton-like; water treatment.

 Open Access  Peer Reviewed  CC BY

1. Introduction

Water quality and scarcity is one of the major global environmental issues affecting people worldwide, which has led to a growing demand for cost-effective water and wastewater treatment solutions. Catalytic wet peroxide oxidation (CWPO) is one of these options, in some particular cases known as Fenton-like process. Printed circuit boards (PCBs) are electronic waste (e-waste) that can be used as catalysts (Rahman *et al.* 2022; Wang *et al.* 2019), since these residues are rich in copper and fiber glass, among other metals that can be recycled for other purposes in line with the sustainable management of resources. This study focuses on the temperature screening for treating and recycling PCBs as catalysts in CWPO to degrade venlafaxine (VFX) as a model contaminant in water, which is an antidepressant substance detected in Portuguese surface waters (Sousa *et al.* 2020).

2. Materials and Methods

PCBs were obtained from obsolete electronic devices collected from a local electronics store. The PCBs were firstly dismantled manually from the waste of electronic devices and then, separated into their main constituents (mainly, gold, fiber glass and copper laminates) by performing an organic swelling in a low pressure sealed reactor as described by Sousa *et al.* (2022). The residue that remains after this process (hereafter referred to original) is mostly made of fiber glass and copper (Cu) laminates plus other metals such as aluminum and zinc. This residue was used in CWPO experiments, both in its original form and thermally treated under N_2 or air atmosphere, by mixing 2.34 g in a solution containing 250 $\mu\text{g L}^{-1}$ of VFX and 2.2 mmol L^{-1} of H_2O_2 . In some experiments, the pH of the solution was adjusted to 2.8 with H_2SO_4 (5 mol L^{-1}). The solution was kept under constant stirring for 60 min and aliquots of 1 mL were withdrawn over time. To separate the PCBs from the solution, the aliquots were centrifuged for 10 min at 4500 rpm. The VFX concentration along the reaction was monitored by high-performance liquid chromatography (HPLC) equipped with a fluorescence detector (FD). Total organic carbon (TOC) analyses were performed in a Shimadzu TOC

analyzer. The content of leached metals was determined by using an inductively coupled plasma-optical emission spectrometer (ICP-OES, thermo scientific, model iCAP 7000 Series).

3. Results and Discussion

As preliminary experiments (i.e., without H₂O₂), both original and thermally treated materials were left overnight in ultrapure water for 15 h, under constant stirring, to verify if the thermal treatment enabled removing the impurities present in the original sample. After that period, the supernatant was removed by centrifugation and analyzed in terms of TOC and copper contents. A TOC in liquid phase of 189.2 mg L⁻¹ was determined after the contact with the original PCB sample, which can be attributed to the organic solvents used in the swelling procedure and that can remain in the material. The TOC release was negligible for all the thermally treated materials, indicating that this treatment was effective in removing these impurities that are released in carbon from the solid to the liquid phase. In terms of Cu leaching, increasing the temperature of the thermal treatment, less Cu is leached in these preliminary experiments, both at natural and acidic media, independently of the atmosphere used in the treatment (N₂ or air). In this way, the material that released less Cu was PCB treated at 800 °C and tested at natural pH.

Regarding the CWPO experiments (i.e., adding H₂O₂), all tested PCBs were able to degrade VFX in 60 min, the best performing material being selected based on the higher apparent first-order reaction rate constant (*k*), and also considering the results discussed above, i.e. a low TOC release from the material and low Cu leaching. Among all the catalyst samples, the PCB treated at 500 °C under N₂ showed the fastest removal of VFX from water, regardless of the pH tested (natural or acidic). It is also observed that the concentration of Cu in water at acidic pH is around twice (with some exceptions) that quantified at natural pH. This means that, in order to have less Cu released from the solid to the liquid phase during the CWPO process, the use of natural pH should be considered, which has additional economic and environmental advantages. Given the above observations, the best performance is attributed to PCB treated at 500 °C under N₂ and tested at natural pH.

4. Conclusions

VFX was effectively degraded by CWPO using PCBs as catalysts. It is also found that lower pH promotes a higher Cu leaching, and that the thermal treatment of the material is necessary and beneficial for the CPWO performance, because less TOC is released. The results showed that the best performance is obtained with PCB treated at 500 °C under N₂ and tested at natural pH, because it presents the best compromise between a higher reaction rate, less release of TOC and low Cu leaching.

References

- Rahman, K. O., Aziz, K.H.H., 2022. "Utilizing scrap printed circuit boards to fabricate efficient Fenton-like catalysts for the removal of pharmaceutical diclofenac and ibuprofen from water", *Journal of Environmental Chemical Engineering*, 10(6), 109015, <https://doi.org/10.1016/j.jece.2022.109015>.
- Wang, C-H., Jiang, X-Y., Huang, R., Cao, Y-J., Xu, J., Han, Y-F., 2018. "Copper/carbon composites from waste printed circuit boards as catalysts for Fenton-like degradation of Acid Orange 7 enhanced by ultrasound", *AIChE Journal*, 65(4): 1234-1244, <https://doi.org/10.1002/aic.16519>.
- Sousa, J.C.G., Barbosa, M.O., Ribeiro, A.R.L., Ratola, N., Pereira, M.F.R., Silva, A.M.T., 2020. "Distribution of micropollutants in estuarine and sea water along the Portuguese coast", *Marine Pollution Bulletin*, 154, 111120, <https://doi.org/10.1016/j.marpolbul.2020.111120>.

Sousa, P.M.S., Martelo, L.M., Marques, A.T., Bastos, M.M.S.M., Soares, H.M.V.M., 2022. "A closed and zero-waste loop strategy to recycle the main raw materials (gold, copper and fiber glass layers) constitutive of waste printed circuit boards", *Chemical Engineering Journal*, 134604, <https://doi.org/10.1016/j.cej.2022.134604> .

Acknowledgments

This work was financially supported by: LA/P/0045/2020 (ALiCE), UIDB/50020/2020 and UIDP/50020/2020 (LSRE-LCM), and by project PTDC/CTA-AMB/3489/2021 (RECY-SMARTE) funded by national funds through FCT/MCTES (PIDDAC).

P15. H₂O₂-assisted photocatalytic degradation of pharmaceuticals in surface waters

Thalita Tavares^{1,2*}, André Torres-Pinto^{1,2}, Cláudia G. Silva^{1,2}, Joaquim L. Faria^{1,2}, Adrián M.T. Silva^{1,2}

¹ LSRE-LCM - Laboratory of Separation and Reaction Engineering – Laboratory of Catalysis and Materials, Faculty of Engineering, University of Porto, Rua Dr. Roberto Frias, 4200-465 Porto, Portugal

² ALiCE - Associate Laboratory in Chemical Engineering, Faculty of Engineering, University of Porto, Rua Dr. Roberto Frias, 4200-465 Porto, Portugal

*Presenting author (up201901674@edu.fe.up.pt)

Abstract

Nanotechnology has been one of the fastest developing fields of science. In particular, the synthesis of nanostructured catalysts derived from graphitic carbon nitride (GCN) is considered very promising due to the material's intrinsic conductivity and photoactivity, essential for a variety of catalytic applications, such as photocatalytic treatment of contaminated waters. In this work, several photolysis and heterogeneous photocatalysis experiments were conducted, using three different materials to evaluate their photocatalytic activity. Furthermore, to increase the effectiveness of the treatment, photocatalytic peroxidation reactions were also performed using hydrogen peroxide (H₂O₂). River water was employed as matrix to assess a realistic application of the visible-light photocatalytic system and to study the impact of organic and inorganic matter. The complete removal of carbamazepine and acetaminophen was achieved in 60 min at the optimised reaction conditions.

Author Keywords. photocatalysis, carbon materials, advanced oxidation processes (AOPs), organic contaminant, pharmaceutical substances

 Open Access  Peer Reviewed  CC BY

1. Introduction

Developing sustainable nanomaterials with effective and innovative characteristics has been increasingly researched in recent years. In particular, the synthesis of graphitic carbon nitride (CN) derived catalysts is well documented for different applications (Ismael 2020). This family of materials shows an interesting particularity compared to other photocatalysts due to its ability to simultaneously remove organic pollutants and activate oxidising agents, such as hydrogen peroxide - H₂O₂ (Torres-Pinto *et al.* 2020). Therefore, the exploration of these unique potentialities was attempted in this work to remove carbamazepine (CBZ) and acetaminophen (ACP) by photocatalysis and photocatalytic peroxidation.

A previous work explored the combination of H₂O₂, photoactivated CN and dissolved iron species to promote photo-Fenton-like conditions for the removal of phenolic compounds, and it was observed that CN alone could efficiently activate H₂O₂ removing the need to externally add iron to the media (Torres-Pinto *et al.* 2020). With this knowledge, we will herein explore the H₂O₂-assisted photocatalytic removal of refractory micropollutants from waters. We employed dicyandiamide and urea to synthesise CN and compared the resulting materials with a benchmark material of titanium dioxide (TiO₂). The reactions were performed on model solutions (ultrapure water) and spiked river waters. The impact of inorganic anions and organic matter was investigated to understand the degradation mechanism in representative matrices. Therefore, we aim for a better understanding of the overall system operability to improve the removal of organic pollutants in different water compartments, through the use of a metal-free CN photocatalyst and the addition of innocuous concentrations of H₂O₂ as added oxidising agent.

2. Materials and Methods

The CN materials were synthesised by calcination in a microwave furnace (Phoenix, CEM Corporation), using either dicyandiamide or urea as the precursor, resulting in CN-D and CN-U, respectively, following a previously reported procedure (Torres-Pinto *et al.* 2022). TiO₂ was a commercial sample (Degussa P25).

The photo-activated reactions were performed in a glass reactor equipped with four visible-light emitting diodes (LEDs). Different dosages of H₂O₂ (0 – 2.5 mmol L⁻¹), initial concentrations of

contaminants and organic/inorganic interferents (*e.g.*, nitrates, sulphates, chlorides and humic acids) were studied. The concentration of the contaminants was followed by high-performance liquid chromatography (HPLC), and the concentration of H₂O₂ was determined by a colourimetric approach.

3. Discussion

The degradation of the contaminants (CBZ and ACP) was attempted individually and in a mixture using the different catalysts (CN-D, CN-U and TiO₂). The best removal results were obtained with CN-U, owing to the increased surface area and enhanced charge transfer abilities seen by photoluminescence studies. The degradation of the studied pharmaceuticals was vastly improved with the addition of H₂O₂, achieving complete removal in less than 60 min, with the first-order reaction rate constants being 4.7 times higher than those obtained with photocatalysis only. When employing different inorganic anions (*i.e.*, Cl⁻, SO₄²⁻, and HCO₃⁻) the degradation rates were slightly enhanced owing to the higher conductivity of the solutions, which can facilitate redox reactions. The same behaviour was observed in surface water as a matrix, owing to its natural composition in inorganic matter.

4. Conclusions

The removal of two recalcitrant pharmaceutical compounds in a mixture was easily achieved when employing the CN-U material under visible light irradiation. The addition of H₂O₂ proved to be very effective in improving the abatement of these molecules, with complete removal under 1 h of irradiation. Both photocatalysis and photocatalytic peroxidation reactions were enhanced in the presence of inorganic matter since those ions provide higher conductivity to the matrix and enable faster removal of the organic molecules and their degradation by-products.

References

- Ismael, M. 2020. "A review on graphitic carbon nitride (g-C₃N₄) based nanocomposites: Synthesis, categories, and their application in photocatalysis." *Journal of Alloys and Compounds* 846: 156446.
- Torres-Pinto, A., Sampaio, M. J., Teixo, J., Silva, C. G., Faria, J. L. and Silva, A. M. T. 2020. "Photo-Fenton degradation assisted by in situ generation of hydrogen peroxide using a carbon nitride photocatalyst." *Journal of Water Process Engineering* 37: 101467.
- Torres-Pinto, A., Silva, C. G., Faria, J. L. and Silva, A. M. T. 2022. "The effect of precursor selection on the microwave-assisted synthesis of graphitic carbon nitride." *Catalysis Today*.

Acknowledgments

This work was financially supported by LA/P/0045/2020 (ALiCE), UIDB/50020/2020 and UIDP/50020/2020 (LSRE-LCM), and by project 2022.08738.PTDC (DRopH2O), funded by national funds through FCT/MCTES (PIDDAC), and by Project NORTE-01-0145-FEDER-000069 (Healthy Waters) supported by NORTE 2020, under the PORTUGAL 2020 Partnership Agreement, through ERDF. A.T-P. gratefully acknowledges FCT for his scholarship SFRH/BD/143487/2019.

P16. Evaluation of temperature and nitrogen modified activated carbons as catalysts in the ozonation of emerging pollutants

Cátia A. L. Graça^{1,2}, Riccardo Zema³, Carla A. Orge^{1,2}, João Restivo^{1,2}, Juliana Sousa³,
Manuel F. R. Pereira^{1,2}, Olívia S. G.P. Soares^{1,2}

¹ Laboratory of Separation and Reaction Engineering - Laboratory of Catalysis and Materials (LSRE-LCM), Faculdade de Engenharia, Universidade do Porto, Rua Dr. Roberto Frias, 4200-465 Porto, Portugal (catiaalgraca@fe.up.pt) ORCID [0000-0001-7811-6765](https://orcid.org/0000-0001-7811-6765)

² ALiCE – Associate Laboratory in Chemical Engineering, Faculty of Engineering, University of Porto, Rua Dr. Roberto Frias, 4200-465 Porto, Portugal

³ INL, International Iberian Nanotechnology Laboratory, Avenida Mestre José Veiga s/n, 4715-330 Braga, Portugal. (juliana.sousa@inl.int) ORCID [0000-0002-8941-786X](https://orcid.org/0000-0002-8941-786X)

Abstract

This study evaluated the effectiveness of temperature and nitrogen modified activated carbons (ACs) as catalysts in the ozonation of an emerging pollutant: salicylic acid, a metabolite of the worldwide consumed pharmaceutical aspirin. The modified activated carbons were prepared using a combination of high-temperature treatment and reductive atmosphere (H₂) or nitrogen doping with precursors. The results showed that the modified activated carbons had a significant effect on the degradation of salicylic acid, with those with the highest mesoporous surface area showing the best performance.

Author Keywords. Carbon catalysts; catalytic ozonation; salicylic acid;; water treatment.

• Open Access  Peer Reviewed   CC BY

1. Introduction

Contaminants of emerging concern (CECs) are gaining great attention because even though they are found in very low concentrations in water bodies, their increased presence might lead to negative impacts on human and environmental health. Resistance to conventional water treatment methods is one of the reasons behind the persistence of CECs in waters, being urgent the development of advanced alternatives. Ozonation has been successfully explored for this purpose, but it still presents limitations towards some oxidant-resistant pollutants. To surpass this, the conversion of ozone (O₃) into more reactive species is required, which can be accomplished using catalysts. Carbon catalysts, such as activated carbons (ACs), represent an eco-friendlier option than traditional metal-based catalysts, with the advantage of their textural and surface properties being easily modified for activity improvement. In this study, two different sources of ACs were tested in the catalytic ozonation of a frequently detected CEC: salicylic acid (SalAc). These ACs were submitted to thermal treatment under a reductive atmosphere or doped with nitrogen groups, to induce changes in their surface properties and verify if these influence the catalytic activity of the material.

2. Materials and Methods

The ACs, provided by Cabot, namely Norit GCN 1240 Plus and Norit GAC 1240 Plus M-2059 (samples AC-GCN and AC-GAC, respectively), were used as catalysts with and without different treatments. According to the information made available by the supplier, AC-GCN is obtained by the steam activation of coconuts, while AC-GAC is produced from coal. The introduction of N-containing groups onto the surface of these materials was made by using a N-precursor. For that, the carbon samples (1.0 g) were mixed with 1 M solution of melamine (monomer, 98.0 %, TCI Chemicals) in ethanol (98.0 %, Honeywell) and stirred at room temperature overnight until solvent evaporation. The functionalized materials were dried in an oven at 80 °C, followed by thermal treatment under an inert atmosphere. The thermal treatment under a reductive atmosphere consisted of placing 1 g of the activated carbon in the vertical furnace and heating up to 1000 °C for 2 h under H₂/N₂ (5:95) flow. The materials were characterized by N₂ equilibrium adsorption/desorption isotherms, thermogravimetric analysis (TG), X-ray photoelectron spectroscopy (XPS), Fourier transform infrared spectroscopy (FTIR), and scanning electron microscopy (SEM).

Both neat and treated materials were tested for the catalytic ozonation of SalAc. For that, 50 mg of sample was mixed with 100 mL of SalAc (20 mg L⁻¹), under a constant O₃ stream (50 mg L⁻¹ at 20 cm³ min⁻¹), in a closed stirred tank reactor. O₃ was produced from pure oxygen in a BMT 802X ozone generator, and its concentration in the gas stream was quantified in an ozone analyser (BMT 964). O₃ that is not transferred to the liquid phase escapes at the top of the reactor to an O₃ destroyer device (2 % KI solution). The SalAc concentration along the reaction was monitored by High-Performance Liquid Chromatography with Diode-Array Detection (HPLC-DAD).

3. Results and Discussion

3.1. Materials characterization

The specific surface area (S_{BET}) of the samples treated with melamine is lower than the original ones due to the introduction of surface groups that may partially block the access of N₂ to the small pores during the measurement. Samples treated under H₂/N₂ show a general tendency to increase the mesopore surface area (S_{meso}) and, consequently, the average pore diameter.

3.2. Application of the modified activated carbons in the ozonation of Salicylic Acid

The ACs under study were tested in the catalytic ozonation of SalAc. Control experiments in the absence of catalysts indicate that O₃ by itself is capable of removing the pollutant below the LOQ in less than 30 min. Another set of control experiments in the absence of O₃ also revealed that all the ACs under study are capable of adsorbing the target pollutant, which is a feature that cannot be ignored when evaluating the catalytic activity of each material.

When both neat and modified ACs are combined with O₃, a much faster degradation of SalAc is obtained compared to that observed for ozonation or adsorption performed individually, indicating that these materials are catalyzing the reaction. SalAc concentration decay promoted by catalytic ozonation followed a pseudo-first-order reaction for all the catalysts tested, being the apparent first-order rate constant (k'), as well as k' normalized by the S_{BET} (k'/S_{BET}) presented in Table 1: Average k' and k'/S_{BET} of catalytic ozonation reactions. The latter was considered for a fairest comparison between catalytic activities (Graça *et al.*, 2020). Based on this, it can be stated that functionalized and thermally treated AC-GCN samples do not present a statistically different performance compared to pure GCN (*t*-test). Regarding AC-GAC samples, AC-GAC-1000-H₂ presents the best performance of all, even when compared with AC-GCN samples. Although modified AC-GAC samples do not reveal k'/S_{BET} values statistically different between each other (*t*-test), they present faster degradations than AC-GCN samples in average. In terms of textural differences that could justify this observation, the most evident one is the S_{meso} value, which is generally higher in AC-GAC samples, especially in AC-GAC-1000-H₂. There are evidence in the literature that this feature is favorable for the catalytic ozonation of organic pollutants (Orge *et al.*, 2009).

Sample	Average $k' \pm$ standard deviation (min^{-1})	$k'/S_{\text{BET}} \times 10^4$ ($\text{g m}^{-2} \text{min}^{-1}$)
None (sole ozonation)	0.098 ± 0.022 ($R^2 = 0.97$)	n.a.
AC-GCN	0.281 ($R^2 = 0.97$)	2.55
AC-GCN-M-800	0.19 ± 0.019 ($R^2 = 0.93$)	1.75 ± 0.25
AC-GCN-1000-H ₂	0.27 ± 0.047 ($R^2 = 0.95$)	2.73 ± 0.64
AC-GAC	0.307 ± 0.067 ($R^2 = 0.97$)	4.10 ± 1.27
AC-GAC-M-800	0.337 ± 0.040 ($R^2 = 0.97$)	5.26 ± 0.88
AC-GAC-1000-H ₂	0.88 ± 0.073	12.8 ± 1.5

Table 1: Average k' and k'/S_{BET} of catalytic ozonation reactions

4. Conclusions

SalAc, a non-degradable compound by conventional treatments, was effectively degraded by ozonation. Its removal was further accelerated in the presence of either neat or modified ACs. The introduction of N-groups was successfully attained by the doping with melamine precursor. However, the best catalytic performance was achieved by the AC thermally treated at 1000 °C under a reductive atmosphere derived from coal (AC-GAC-1000-H₂).

References

- Graça, C. A.L., Mendes, M.A., Teixeira, A.C.S.C. and Velosa, A.C. 2020. "Anoxic degradation of chlorpyrifos by zerovalent monometallic and bimetallic particles in solution", *Chemosphere*, 244, 125461: 1-11, DOI: 10.1016/j.chemosphere.2019.125461.
- Orge, C.A., Sousa, J.P.S., Gonçalves, F., Freire, C., Órfão, J.J.M. and Ferreira, M.F.R. 2009. "Development of Novel Mesoporous Carbon Materials for the Catalytic Ozonation of Organic Pollutants". *Catalysis Letters*, 132: 1–9, DOI: 10.1007/s10562-009-0029-5

Acknowledgments

This work was financially supported by: NORTE-01-0247-FEDER-069836, co-financed by the European regional development fund NORTE2020; LSRE-LCM associated laboratory funding (UIDB/50020/2020), ALiCE associated laboratory funding (LA/P/0045/2020) and Programmatic-UIDP/50020/2020 (FCT/MCTES national funds PIDDAC). O. S. Soares thanks FCT funding under the Scientific Employment Stimulus – Institutional Call CEECINST/00049/2018. C. A. Orge acknowledges FCT funding under DL57/2016 Transitory Norm Programme. C.A.L. Graça thanks FCT funding under the Scientific Employment Stimulus – Individual Call 2022.08029.CEECIND.

P17. Generation of sulphate radical through heterogeneous catalysis for wastewater remediation

Alba Giráldez^{1*}, Marta Pazos¹, Ángeles Sanromán¹

¹BIOSUV Research Group, CINTECX, University of Vigo, As Lagoas Marcosende s/n, Vigo, Spain

*Presenting author (alba.giraldez.rodriguez@uvigo.gal) ORCID (0009-0002-8226-6621)

Abstract

Traditional methods of wastewater treatment have been shown to be inefficient in removing pathogens in large quantities from wastewater. Currently, Advanced Oxidation Processes (AOPs) are very attractive because they have proven to be able to remove microorganisms and toxic compounds. In this study, the process of generating sulphate radicals is used for the removal of pathogens. For this purpose, it uses peroxymonosulphate (PMS) activated by a heterogeneous catalyst, a Metal Organic Framework (MOF) with catalytic and disinfection properties (copper-based). In order to improve the handling of the MOF and facilitate the scale-up of this process, different methods of immobilisation are evaluated using alginate or polyacrylonitrile (PAN) as support material. The obtained results show that after the immobilisation of the MOF, maintains its catalytic properties and after the disinfection process, the presence of pathogens is eliminated from the wastewater.

Author Keywords. MOF, HKUST-1, disinfection, immobilization, PMS, AOP.

 Open Access  Peer Reviewed  CC BY

1. Introduction

The presence of huge amounts of pathogens in wastewater, as well as resistant microorganisms and other resistant compounds, is one of the main issues that concern our society nowadays, and the need to find an effective method to remove them in Wastewater Treatment Plants (WWTPs). The majority of these plants still use conventional systems such as activated sludge to treat these waters, but they are only able to remove easily degradable organic matter (Valdivia et al. 2023). Recent studies consider as a possible solution to this problem the application of AOPs (process using photonic excitation, ozonisation, etc.) in WWTPs (Valdivia et al. 2023).

The aim of this study is to facilitate the handling of these nanomaterials, as well as to facilitate the possible scaling up of the process. Consequently, a heterogeneous catalyst (MOF HKUST-1) will be immobilised on a solid support material, which will activate the PMS and produce sulphate radicals that will eliminate these pathogens.

2. Materials and Methods

Pathogenic microorganisms such as *Escherichia coli* (*E. coli*) or *Pseudomonas aeruginosa* (*P. aeruginosa*), among others, from the *Colección Española de Cultivos Tipo (CECT)* were used as pathogenic agents. The heterogeneous catalyst used was the MOF HKUST-1 (Sigma-Aldrich), which is characterised by being copper-based.

The immobilisation was performed following different procedures, the main ones being using PAN (Riley et al. 2020) and sodium alginate (Poza-Nogueiras et al. 2018) for the entrapment of the HKUST-1.

The disinfection tests were carried out using a synthetic water simulating wastewater, inoculated with the pathogen (10^{10} - 10^{11} colony forming unit per millilitre; CFU/mL), and adding the corresponding amount of PMS and the immobilized catalyst (Fdez-Sanromán, Pazos, and Sanroman 2022). These flasks were incubated in an orbital shaker (80 rpm, 25°C and without light) and samples were removed from time to time and seeded in a Petry dish by extension seeding. In addition, samples of the treated wastewater were analysed by inductively coupled plasma mass spectrometry to determine the presence of released metals.

3. Discussion

Initially, the concentrations of PMS and HKUST-1 (in powder) were optimised in the disinfection tests with both pathogen agents. The optimal values were 60.5 mg/L HKUST-1 and 0.1 mM PMS

obtained. In addition, by immobilization of HUSKT-1 in PAN (HKUST-PAN beads) and in alginate (HKUST-ALGINATE fibres), it was observed that the catalytic and disinfectant action persisted, obtaining a complete elimination of cell growth after 24h (Figure). Moreover, the amount of released copper was reduced with respect to the HKUST-1 in powder, from 7 mg/L (HKUST-1 in powder) to 0.7 mg/L (HKUST-ALGINATE fibres) and to 0.15 mg/L (HKUST-PAN beads). Therefore, based on their high stability, the reuse of this catalyst was evaluated, and cell growth was also eliminated, as shown in Figure .

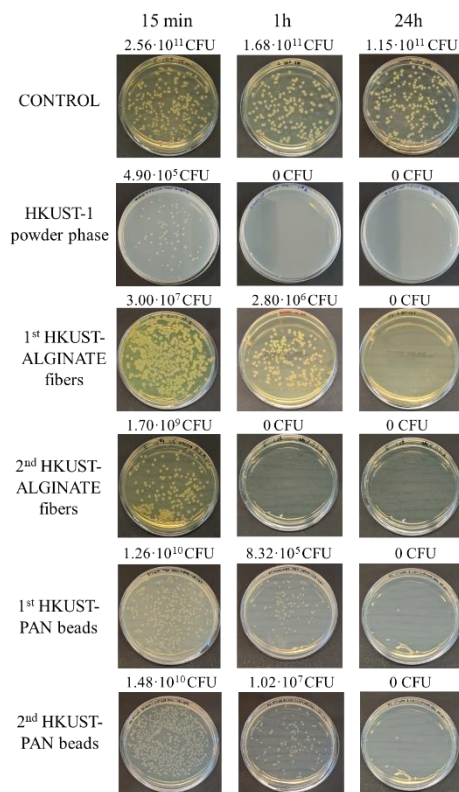


Figure 1: *P. aeruginosa* growth in Petri dish after disinfection tests using HUSKT-1 as catalyst without immobilising and immobilised, as well as the subsequent reuse of this immobilised catalyst.

Afterwards, this process was scaled up to a continuous system and a total of 400 mL of wastewater with a high microbiological loaded was treated (Figure).

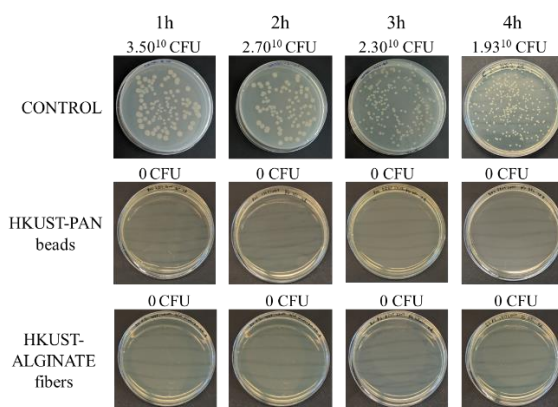


Figure 2: Evaluation of the continuous system in disinfection tests using HKUST-1 as a catalyst immobilized on beads and in fibres.

4. Conclusions

According to the results presented, the heterogeneous catalysis system designed has excellent potential for scaling to an industrial level, due to the fact that by the use of immobilised HKUST-1 (PAN beads or ALGINATE fibres), it was possible to operate in a flow system in continuous mode. It

is highlighted that under these conditions, the designed systems maintain their catalytic and disinfectant properties, thus facilitating the handling of these heterogeneous catalysts in the system. Moreover, it has been able to reuse these catalysts with great results, as well as to reduce the amount of copper released into the environment.

References

- Fdez-Sanromán, Antía, Marta Pazos, and Angeles Sanroman. 2022. 'Peroxymonosulphate Activation by Basolite® F-300 for Escherichia Coli Disinfection and Antipyrine Degradation'. *International Journal of Environmental Research and Public Health* 19 (11). <https://doi.org/10.3390/ijerph19116852>.
- Poza-Nogueiras, Verónica, María Arellano, Emilio Rosales, Marta Pazos, Elisa González-Romero, and M. Ángeles Sanromán. 2018. 'Heterogeneous Electro-Fenton as Plausible Technology for the Degradation of Imidazolium-Based Ionic Liquids'. *Chemosphere* 199 (May): 68–75. <https://doi.org/10.1016/J.CHEMOSPHERE.2018.01.174>.
- Riley, Brian J., Saehwa Chong, Wenbin Kuang, Tamas Varga, Ahmed S. Helal, Mitchell Galanek, Ju Li, Zayne J. Nelson, and Praveen K. Thallapally. 2020. 'Metal-Organic Framework-Polyacrylonitrile Composite Beads for Xenon Capture'. *ACS Applied Materials and Interfaces* 12 (40). <https://doi.org/10.1021/acsami.0c13717>.
- Valdivia, Manuel Thomas, Mark A. Taggart, Sabolc Pap, Alistair Kean, Sharon Pflieger, and Ian L. Megson. 2023. 'Photocatalytic Metallic Nanomaterials Immobilised onto Porous Structures: Future Perspectives for at-Source Pharmaceutical Removal from Hospital Wastewater and Potential Benefits over Existing Technologies'. *Journal of Water Process Engineering*. <https://doi.org/10.1016/j.jwpe.2023.103553>.

Acknowledgments

This research has been financially supported by Project PDC2021-121394-I00 funded by MCIN/AEI/10.13039/501100011033 and by the European Union Next Generation EU/PRTR, Project PID2020-11GBI00 funded by MCIN/AEI/10.13039/501100011033 and Xunta de Galicia and the European Regional Development Fund (ED431C 2021-43).

P18. Towards the development of a simple molecularly imprinted electrochemical sensor for the detection of carbamazepine

Verónica Poza-Nogueiras^{1,2*}, João G. Pacheco², Cristina Delerue-Matos²

¹BIOSUV research group, Department of Chemical Engineering, University of Vigo, As Lagoas-Marcosende, 36310 Vigo, Spain

²REQUIMTE/LAQV, Instituto Superior de Engenharia do Porto, Instituto Politécnico do Porto, Rua Dr. António Bernardino de Almeida, 431, 4200-072 Porto, Portugal

*Presenting author (vpoza@uvigo.gal) ORCID [0000-0002-7869-3850](https://orcid.org/0000-0002-7869-3850)

Abstract

The development of fast and inexpensive detection techniques for monitoring the occurrence of pharmaceuticals in water bodies is imperative. Hence, in this study, the elaboration of a novel molecularly imprinted polymer (MIP) sensor using disposable screen-printed carbon electrodes (SPCEs) was evaluated for the detection of carbamazepine (CBZ). Surface imprinting was carried out by electropolymerization, using 3,4-Ethylenedioxythiophene (EDOT) as the functional monomer in the presence of CBZ. The effect of key process parameters on the MIP response was evaluated and compared with non-imprinted control sensors (NIPs). Promising results were obtained, demonstrating the viability of the developed MIP electrochemical sensor.

Author Keywords. Carbamazepine, pharmaceutical, molecularly imprinted polymer, electrochemical detection, screen-printed carbon electrode.

 Open Access  Peer Reviewed  CC BY

1. Introduction

Carbamazepine (CBZ) is an antiepileptic and mood stabilizing drug widely prescribed. Unfortunately, it is recalcitrant to conventional wastewater treatments. Consequently, it ends up being released into the environment. The long-term exposure to pharmaceuticals like CBZ may cause a negative impact on public health and aquatic life. Hence, the monitoring of these pollutants in water bodies has become a pressing issue. Different analytical methods have been investigated for the detection of CBZ, mostly chromatographic techniques, whereas less attention has been paid to voltametric techniques. However, electroanalytical methods overcome the drawbacks of chromatographic techniques (*i.e.* time-consuming sample preparation, long analysis time, expensive equipment) and can be performed in portable devices, allowing the on-site monitoring of environmental water samples (Veiga et al. 2010).

Among different strategies, the development of electrochemical sensors based on molecularly-imprinted polymers (MIP) has demonstrated to be a promising technique. MIPs are built to create cavities on the electrode surface that are complementary to the analyte in shape, size and functional groups. As a consequence, highly selective sensors, which allow the specific recognition of the desired molecule, are obtained (Seguro et al. 2022).

With this in mind, the present work aims at developing a low-cost, disposable MIP-based sensor using screen-printed carbon electrodes (SPCE) for the detection of CBZ in water media.

2. Materials and Methods

2.1. Reagents and solutions

CBZ and 3,4-Ethylenedioxythiophene (EDOT) were purchased from Sigma-Aldrich. Chlorhydric acid, sodium hydroxide, methanol and acetonitrile were obtained from Fluka, Merck, Romil and Sigma-Aldrich, respectively. Phosphate buffer saline (PBS) solution, 0.1 M and pH 7, was prepared with KH_2PO_4 and K_2HPO_4 (Riedel-de-Haën). Water used throughout all assays was ultra-pure (18.2 M Ω cm), obtained from a Millipore water purification system.

2.2. Electrochemical measurements

In this study, cyclic voltammetry (CV) and differential pulse voltammetry (DPV) techniques were performed with a Metrohm Autolab PGSTAT 101 potentiostat/galvanostat controlled by Nova 1.10 software. All measurements were carried out at room temperature using commercial SPCEs (DRP-

110, Dropsens), which consist of a circular carbon working electrode (4 mm of diameter) surrounded by a carbon counter electrode and a silver pseudo-reference.

2.3. MIP sensor preparation

Different MIP fabrication conditions were tested. Firstly, an electropolymerization step was performed by CV using 40 μL of the polymerization solution containing 1 mM of CBZ as the template and different concentrations of EDOT (1.8, 2.7, 3.6, 4.5 mM) as the monomer in PBS. CV was performed from 0.0 to 1.4 V at 100 mV/s during 10 cycles. Then, the electrode was washed with deionized water and air dried. The control non-imprinted polymer (NIP) sensor was prepared under the same conditions, but in the absence of the template.

Afterwards, the extraction of the entrapped CBZ was carried out by placing 40 μL of the extraction solution (80 ACN/20 H₂O, 80 MeOH/20 H₂O, HCl 0.1 M or NaOH 0.1 M in 80 H₂O/20 MeOH) on the SPCE for 5 min. This step was performed twice.

Finally, the rebinding of CBZ molecules was performed by incubating the sensor with 40 μL of a 0.1 mM CBZ solution in PBS for 15 mins. The elaboration of the sensor was monitored stepwise by carrying out a DPV measurement using 40 μL of PBS after each fabrication step, scanning from 0.4 to 1.4 V at 50 mV/s.

3. Discussion

3.1. Molecularly imprinting of CBZ

Firstly, the imprinting of the template molecules on the SPCE surface was tested. Figure a shows the electrochemical polymerization process. The current intensity of the peaks decreased as the PEDOT polymer (poly(3,4-ethylenedioxythiophene)) was formed on the NIP and MIP sensors. However, differences were observed: whereas two peaks were detected during the formation of the MIP (at *ca.* 1.0 V and 1.2 V, ascribed to the oxidation of EDOT and CBZ, respectively), only the oxidation peak of the EDOT was observed on the NIP, with a reduced intensity. The successful incorporation of the template on the MIP sensor during the polymerization step was corroborated by DPV, as demonstrated by the CBZ oxidation peak observed in Figure b, which is not present in the case of the NIP.

After the entrapment of the template on the MIP, the extraction of CBZ molecules from the sensor is key to ensure the formation of the specific cavities. As depicted in Figure b, the CBZ peak completely disappeared after the extraction, indicating that this step was successfully achieved.

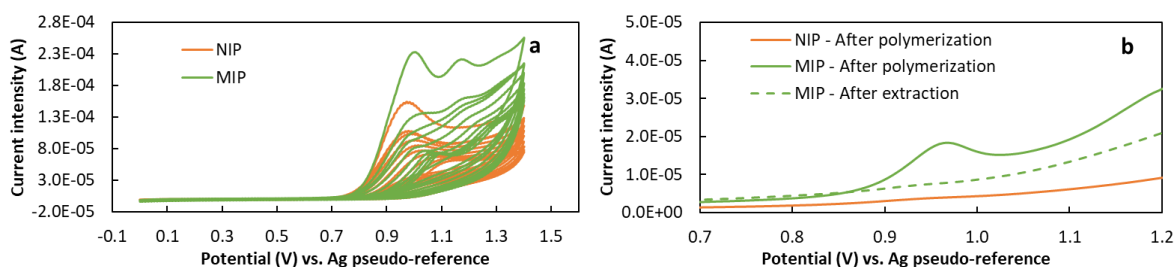


Figure 1: (a) CVs of electropolymerization of NIP and MIP sensors (b) DPV analysis of NIP and MIP after polymerization and extraction with NaOH 0.1 M.

3.2. Optimization of experimental conditions

Experimental parameters used during MIP fabrication greatly impact the sensor performance. Hence, the process should be optimized in order to maximize the signal provided by CBZ at the MIP after the incubation step, while at the same time enhancing the difference between the peak intensity of MIP and NIP sensors. Figure a and b show the results obtained when optimizing the extraction solution and the monomer concentration, respectively.

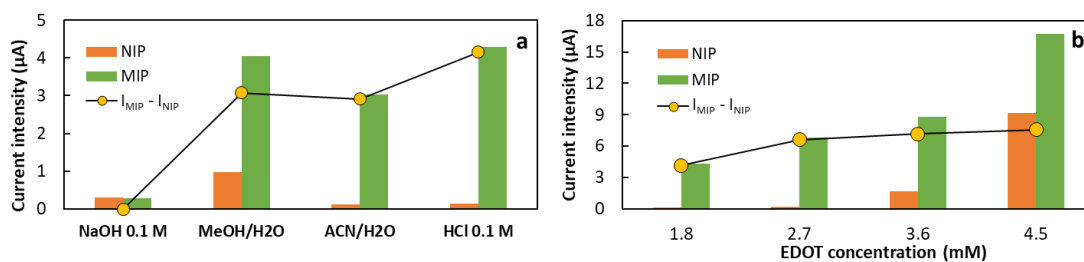


Figure 2: Effect on the post-incubation response of different **(a)** extraction solutions (1.8 mM EDOT), and **(b)** EDOT concentrations (extraction with HCl 0.1 M)

4. Conclusions

The feasibility of fabricating MIP-based SPCEs sensors for the detection of CBZ has been demonstrated and key process parameters were optimized. The promising results obtained pave the way for the future development of a suitable sensor for environmental water samples. With that in mind, future work will involve further optimizations and selectivity tests.

References

- Veiga, Alfredina, Ana Dordio, A.J. Palace Carvalho, Dora Martins Teixeira, and Jorge Ginja Teixeira. 2010. "Ultra-sensitive voltammetric sensor for trace analysis of carbamazepine". *Analytica Chimica Acta* 674:182-189. DOI: 10.1016/j.aca.2010.06.031.
- Seguro, Isabel, Patrícia Rebelo, João G. Pacheco, and Cristina Delerue-Matos. 2022. "Electropolymerized, Molecularly Imprinted Polymer on a Screen-Printed Electrode—A Simple, Fast, and Disposable Voltammetric Sensor for Trazodone". *Sensors* 22:2819. DOI: 10.3390/s22072819.

Acknowledgments

This work received financial support from PT national funds (FCT/MCTES, Fundação para a Ciência e Tecnologia and Ministério da Ciência, Tecnologia e Ensino Superior) through UIDB/50006/2020 and PTDC/QUI-QAN/3899/2021. This research was also funded through the 2019-2020 Biodiversa & Water JPI joint call for research proposals, under the BiodivRestore ERA-Net COFUND program, DivRestore/0002/2020, and with the funding organisation FCT, Portugal. Authors also acknowledge Xunta de Galicia (Consellería de Cultura, Educación y Universidad) for the financial support granted to V. Poza-Nogueiras (ED481B-2022-077).

P19. Phytotoxicity Testing of Sewage Sludge and Individual Emerging Contaminants in Agricultural Soil

Ana Sofia Fernandes^{1,2,*}, Filipe Rocha^{1,2}, Thiago Silva^{1,3}, Vera Homem^{1,2}

¹LEPABE - Laboratory for Process Engineering, Environment, Biotechnology and Energy, Faculty of Engineering, University of Porto, Rua Dr. Roberto Frias, 4200-465 Porto, Portugal

²ALiCE - Associate Laboratory in Chemical Engineering, Faculty of Engineering, University of Porto, Rua Dr. Roberto Frias, 4200-465 Porto, Portugal



³Instituto Federal de Educação Ciência e Tecnologia do Tocantins - Campus Araguatins, Povoado Santa Tereza, Km 05 S/N Zona Rural, 77950-000, Tocantins, Brasil

*Presenting author (up201605385@edu.fe.up.pt) ORCID 0000-0002-90750117

Abstract

Phytotoxicity tests were carried out in order to identify possible risks from agricultural application of sewage sludge as fertilizer. Rapid tests with garden cress, sorghum and mustard plants grown in soils amended with sewage sludge at 4 application rates or spiked with emerging contaminants were performed. After 3 days, germination and root growth inhibition were determined. These experiments showed that sewage sludge toxicity may be greatly dependent on plant species, and that sludge application rate may influence root growth inhibition, yet further testing is required to conclude which contaminants are responsible for the observed effects.

Author Keywords. Sewage sludge, phytotoxicity, germination and root growth inhibition.

 Open Access  Peer Reviewed  CC BY

1. Introduction

Agricultural application of sewage sludges from wastewater treatment plants (WWTPs) is an increasingly appealing valorization option, due to sludge's richness in essential plant nutrients, as well as organic matter and water (Seleiman, Santanen and Mäkelä, 2020). Although sewage sludge is applied to agricultural soils to improve crop growth and productivity, the wide range of contaminants present may have unwanted phytotoxic effects, such as germination and plant growth inhibition (Oleszczuk, 2006). In this work, a first approach to phytotoxicity testing using rapid test kits is presented. Three plants (*Sorghum saccharatum* (sorghum), *Lepidium sativum* (garden cress) and *Sinapis alba* (mustard)) and two different contaminant soil input vectors were tested (sewage sludge soil-amendment and direct soil spiking). For the spiked soil tests, 5 contaminants commonly detected in sludge (galaxolide (HHCB), tonalide (AHTN), and volatile methylsiloxanes D4, D5 and D6) with noticeable knowledge gaps on phytotoxicity and fate within soil-plant systems were selected to assess their possible contributions to overall toxicity to plants.

2. Materials and Methods

Phytotoxkit microbiotest kits for solid samples (Microbiotests, Ghent, Belgium) were used to perform the intended tests. Agricultural soil collected from Campus Agrário de Vairão was used in all tests and sewage sludge was collected from a local urban WWTP. Initial experiments tested 4 sewage sludge application rates to soil (A1: 4, A2: 9, A3: 18, A4: 30 ton ha⁻¹). The prepared sludge and soil mixtures were placed in the kit test plates, smoothed into flat surfaces and saturated with distilled water before 10 plant seeds were sown. In the soil spiking experiments a similar procedure was done but using water solutions with the selected contaminants to saturate the soils. The target concentrations in the saturated soils (HHCB – 550 ng g⁻¹ dw, AHTN – 87.50 ng g⁻¹ dw, D4 – 1.55 ng g⁻¹ dw, D5 – 90.60 ng g⁻¹ dw, D6 – 26.04 ng g⁻¹ dw) corresponded to those found in the soils amended with the 30 ton ha⁻¹ sludge. Control groups included a reference soil group (to assure validity of tests), a group of unamended agricultural soils (sludge amendment tests) and unamended agricultural soils with added acetone (spiked soil tests). All plates were closed and incubated in an upright position in an incubator for a 72-hour period at 25 ± 1°C in darkness. After incubation the number of germinated seeds was counted, and photographs of each plate were taken to perform root measurements using the ImageJ software. Germination and root growth are the only two

parameters contemplated by the kits. The collected data was used to calculate germination and root growth inhibition percentages. Statistical data analysis, including descriptive statistics and hypothesis testing was performed with IBM SPSS Statistics v 28.0.

3. Discussion

Germination of all 3 plant species was not affected by sludge or soil spiking, with no significant differences in number of germinated seeds across test groups and their respective control plates (results not shown). Root growth results varied according to the tested plant (Table). In sludge amendment tests, roots of garden cress were significantly shorter ($p < 0.05$) in the two highest application rates, when compared with the controls. Roots of mustard revealed a similar trend, although differences in mean root length were not significant. The inhibition of sorghum root growth did not follow a clear pattern. Plant uptake may have been more limited in sorghum and/or the plant may be more resilient to contaminant-induced stress.

Treatment Group	Garden Cress		Mustard		Sorghum		
	Root Length	Growth Inhibition	Root Length	Growth Inhibition	Root Length	Growth Inhibition	
Sludge	Control	53.2 ± 0.3a	-	61 ± 4a	-	38 ± 7a	-
	S1	45 ± 6ab	15.84%	56 ± 20a	7.95%	37 ± 6a	1.81%
	S2	48 ± 3a	9.36%	53 ± 1a	13.59%	44 ± 7a	-15.14%
	S3	37 ± 3bc	29.79%	33 ± 5a	45.48%	38 ± 2a	0.32%
	S4	29 ± 2c	45.70%	36 ± 8a	41.28%	36 ± 11	5.02%
Spike	Control	58 ± 4a	-	56 ± 15a	-	40 ± 4	-
	D4	57 ± 3a	1.30%	49 ± 10a	12.94%	37 ± 6a	5.14%
	D5	39 ± 20a	33.56%	56 ± 3a	-0.09%	41 ± 7a	-2.66%
	D6	57 ± 2a	1.78%	58 ± 8a	-3.17%	41 ± 9a	-4.85%
	HHCb	54 ± 5a	7.67%	54 ± 12a	3.26%	42 ± 5a	-6.10%
	AHTN	58 ± 4a	0.26%	56 ± 2a	0.15%	41 ± 4a	-4.00%

Table 1: Mean root lengths (mm) and calculated root growth inhibition % of tested soil groups. Different letters show statistical differences between groups ($p < 0.05$).

In the spiked soil tests some inhibition of garden cress and mustard root growth was observed, mostly in the soils spiked with HHCb, D4 and D5, but these differences in root length were not statistically significant due to high standard deviations across triplicates. While phytotoxic effects have been observed for some of the targets (Jiang et al. (2021)) differences between spiked and amended soil experiments could be due to the wide range of contaminants present in sludges (e.g., heavy metals) or faster dissipation from soil in the absence of sludge.

4. Conclusions

A first approach for sewage sludge phytotoxicity testing was conducted yielding some primary results. The application of sewage sludge to agricultural soil in 4 different application rates revealed different root growth inhibition percentages, which appear to be largely influenced by the plant tested and application rate. The highest application rates yielded statistically significant inhibition of garden cress root growth when compared to the unamended soil controls. Soil spiking with singular emerging compounds present in the sludge did not yield statistically significant effects, possibly due to the wide range of contaminants present in soil and/or greater contaminant dissipation in the absence of sludge. Further testing is needed to fully understand which contaminants caused the observed effects, the influence of inter-contaminant interactions on toxicity and the risks of sludge application to terrestrial plants.

References

- Jiang, Lisi, Qianru Zhang, Jianmei Wang, and Wan Liu. "Ecotoxicological Effects of Titanium Dioxide Nanoparticles and Galaxolide, Separately and as Binary Mixtures, in Radish (*Raphanus Sativus*)." *Journal of Environmental Management* 294 (2021): 112972. <https://doi.org/10.1016/j.jenvman.2021.112972>.
- Oleszczuk, Patryk. "Phytotoxicity of Municipal Sewage Sludge Composts Related to Physico-Chemical Properties, Paks and Heavy Metals." *Ecotoxicology and Environmental Safety* 69, no. 3 (2008): 496–505. <https://doi.org/10.1016/j.ecoenv.2007.04.006>.
- Seleiman, Mahmoud F., Arja Santanen, and Pirjo S.A. Mäkelä. "Recycling Sludge on Cropland as Fertilizer – Advantages and Risks." *Resources, Conservation and Recycling* 155 (2020): 104647. <https://doi.org/10.1016/j.resconrec.2019.104647>.

Acknowledgments

This work was financially supported by: i) LA/P/0045/2020 (ALiCE) and UIDB/00511/2020 - UIDP/00511/2020 (LEPABE) funded by national funds through FCT/MCTES (PIDDAC); ii) Project PTDC/ASP-PLA/29425/2017 - POCI-01-0145-FEDER-029425, funded by FEDER funds through COMPETE2020 – Programa Operacional Competitividade e Internacionalização (POCI) and by national funds (PIDDAC) through FCT/MCTES; iii) Project "S4Hort_Soil&Food - Sustainable practices for Soil health & horticultural products quality improvement in the Entre Douro e Minho Region", with reference NORTE-01-0145-FEDER-000074, supported by Norte Portugal Regional Operational Programme (NORTE 2020), under the PORTUGAL 2020 Partnership Agreement, through the European Regional Development Fund (ERDF); iv) Project "HealthyWaters – Identification, Elimination, Social Awareness and Education of Water Chemical and Biological Micropollutants with Health and Environmental Implications", with reference NORTE-01-0145-FEDER-000069, supported by Norte Portugal Regional Operational Programme (NORTE 2020), under the PORTUGAL 2020 Partnership Agreement, through the European Regional Development Fund (ERDF); v) V. Homem thanks national funds through FCT, under the Scientific Employment Stimulus—Individual Call - CEECIND/00676/2017. PhD Studentship 2020.09041.BD (Filipe Rocha), financed by FCT with funds from the State Budget and by the European Social Fund (ESF).

P20. CFD Design of a Raceway Pond Reactor: Overall geometry improvement

Margarida L.R. Peixoto^{1,2*}, Margarida S.C.A. Brito^{1,2}, Ricardo J. Santos^{1,2}, Vítor J.P. Vilar^{1,2}

¹Laboratory of Separation and Reaction Engineering – Laboratory of Catalysis and Materials (LSRE-LCM), Faculty of Engineering, University of Porto, Rua Dr. Roberto Frias, 4200-465 Porto, Portugal

²ALiCE – Associate Laboratory in Chemical Engineering, Faculty of Engineering, University of Porto, Rua Dr. Roberto Frias, 4200-465 Porto, Portugal

*Presenting author (up201806245@up.pt)

Abstract

In this work, a configuration of a raceway pond reactor (RPR) was designed and optimised through computational fluid dynamics (CFD). The best geometry regarding the overall flow design comprises the implementation of flow deflectors on the RPR curve. Its application has been shown to improve fluid mixing and reduce the stagnant fluid zones in the reactor.

Author Keywords. Raceway pond reactor, CFD, Design, Flow deflectors.

 Open Access  Peer Reviewed  CC BY

1. Introduction

Raceway pond reactors (RPRs) are extensive non-concentrating photoreactors, with a very low construction cost, consisting of open channels forming a raceway where the stream is set in motion by a paddlewheel. They have been widely used for large-scale production of microalgae and more recently for disinfection of secondary effluents in WWTPs (Inostroza et al. 2021; Peralta Muniz Moreira et al. 2021).

The application of this type of reactor is very promising, given its innumerable advantages. For example, their configuration provides a large area of solar exposure, which can be very useful for radiation dependent uses. Besides that, they can be suitable for processes that highly depend on the effects caused by mechanical forces, such as shear stresses. Moreover, they generally present a low construction cost and low energy consumption, being able to yield high productivity rates, as they present an easy scale-up (Liffman et al. 2013; Mendoza et al. 2013). In this sense, the design of these reactors is crucial, since it may interfere with several variables, such as the degree of mixing, and the existence of property gradients, such as temperature, solar penetration, dissolved oxygen concentration, among others. To optimise the design, some aspects like the geometry, the configuration of bends, and the specific design of the paddlewheel have to be taken into account, as they may affect both the mass transfer and the hydrodynamic behaviour of the reactor (Inostroza et al. 2021).

In this work, the overall RPR design, concerning the setup of flow deflectors, and some aspects that affect the reactor performance were analysed using Computational Fluid Dynamics (CFD).

2. Materials and Methods

CFD simulations were performed using the ANSYS 2022 R2 software. Figure shows the computational domain geometry that represents a 2D configuration of the raceway top view. It should be noted that only half of the reactor has been considered, as there is a symmetry axis on the *inlet/outlet* plan. The CFD domain is described as $L_{in} = 1$ m, $L_{out} = 1$ m, $L_w = 10$ m, $L_m = 0.15$ m, and $R = 1$ m.



Figure 1: Geometry of the overall 2D domain.

Reynolds Average Navier-Stokes equations were used to simulate the turbulent flow and Standard $k-\epsilon$ model was set for the subgrid modeling. The working fluid was set as water at 20 °C, where $\rho = 998.2 \text{ kg}\cdot\text{m}^3$ and $\mu = 1.003 \text{ mPa}\cdot\text{s}$. The inlet velocity was defined at $0.3 \text{ m}\cdot\text{s}^{-1}$ and at the walls a no-slip condition was established. Regarding the near-wall treatment, scalable wall functions were set. The convergence criteria were defined as the residuals below 10^{-6} .

The setup of flow deflectors on the reactor U-turn was investigated according to Figure . This aimed to improve the fluid mixing and reduce the recirculation zones in the reactor. The dimensions x_1 , x_2 , L_1 and L_2 were under analysis to optimise the geometry.

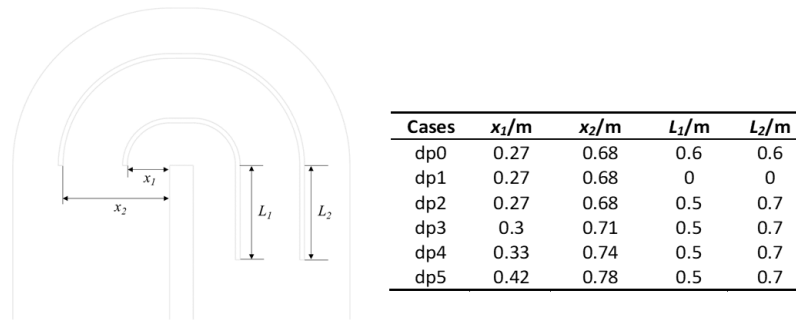


Figure 2: Flow Deflectors 2D geometry and values of x_1 , x_2 , L_1 and L_2 for the cases analysed.

3. Discussion

Figure shows the streamline maps before and after the implementation of flow deflectors. In addition, the velocity profiles at the outlet were also compared in Figure .

Figure shows a clear reduction in the recirculation zones after the inclusion of the flow deflectors, which results in a more uniform and stable flow, as can be proven by the velocity profiles in Figure . Comparing cases dp0 and dp1, it turns out that the extension of the deflectors at the end of the raceway curve make the flow profiles more uniform. Moreover, comparing cases dp0 and dp2, where the difference is related to lengths L_1 and L_2 , the case where the length of the baffle near the inner wall is greater presents a slightly more uniform velocity at the outlet. Cases dp3, dp4 and dp5 show a progressive leftward movement since the velocity at the outlet is higher on the side of the outer wall. This modification makes the velocity at the outlet much more uniform, being practically constant for dp5. Nonetheless, for these last three cases, additional stagnant areas are generated near the baffles, which may cause the accumulation of deposits and sedimentation in these regions, creating problems for the flow.

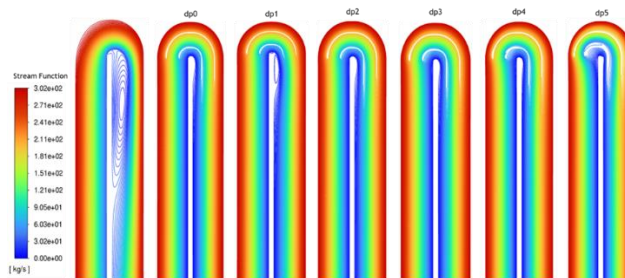


Figure 3: Flowrate streamlines before, left, and after the implementation of flow deflectors for the different configurations studied.

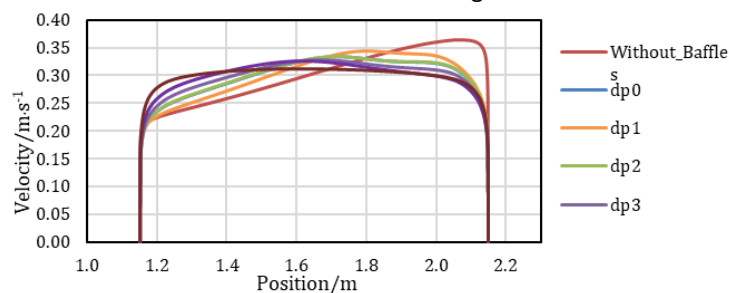


Figure 4: Velocity profiles at the outlet for the different configurations studied.

4. Conclusions

The setup of flow deflectors on the RPR U-turn has proven to be a good strategy to improve the flow distribution and reduces the dead zones in the reactor. Furthermore, among the cases studied, dp2 seems to be the most appropriate, presenting the best compromise between the uniformity of the velocity at the outlet and the presence of stagnant fluid zones. As future work, the vertical mixing in the reactor and the specific design of the paddlewheel will be assessed.

References

- Inostroza, Cristian, Alessandro Solimeno, Joan García, José M. Fernández-Sevilla, and F. Gabriel Acién. 2021. "Improvement of real-scale raceway bioreactors for microalgae production using Computational Fluid Dynamics (CFD)." *Algal Research* 54: 102207. <https://doi.org/10.1016/j.algal.2021.102207>.
- Liffman, Kurt, David A. Paterson, Petar Liovic, and Pratish Bandopadhyay. 2013. "Comparing the energy efficiency of different high rate algal raceway pond designs using computational fluid dynamics." *Chemical Engineering Research and Design* 91 (2): 221-226. <https://doi.org/doi.org/10.1016/j.cherd.2012.08.007>.
- Mendoza, J. L., M. R. Granados, I. de Godos, F. G. Acién, E. Molina, C. Banks, and S. Heaven. 2013. "Fluid-dynamic characterization of real-scale raceway reactors for microalgae production." *Biomass and Bioenergy* 54: 267-275. <https://doi.org/doi.org/10.1016/j.biombioe.2013.03.017>.
- Peralta Muniz Moreira, Rodrigo, Alejandro Cabrera Reina, Paula Soriano Molina, José Antonio Sánchez Pérez, and Gianluca Li Puma. 2021. "Computational fluid dynamics (CFD) modeling of removal of contaminants of emerging concern in solar photo-Fenton raceway pond reactors." *Chemical Engineering Journal* 413: 127392. <https://doi.org/doi.org/10.1016/j.cej.2020.127392>.

Acknowledgments

This work was financially supported by LA/P/0045/2020 (ALICE), UIDB/50020/2020 and UIDP/50020/2020 (LSRE-LCM), funded by national funds through FCT/MCTES (PIDDAC).

P21. CO₂/N₂ separation using PDMS membranes with inorganic filler ZSM-5

Inês Rodrigues^{1,2*}, Lidia Martínez-Izquierdo^{3,4}, Carlos Téllez^{3,4}, Joaquín Coronas^{3,4}, Alírio Rodrigues^{1,2}, Vítor Vilar^{1,2}, Alexandre Ferreira^{1,2}

¹Laboratory of Separation and Reaction Engineering - Laboratory of Catalysis and Materials (LSRE-LCM), Department of Chemical Engineering, Faculty of Engineering, University of Porto, Rua Dr. Roberto Frias, 4200-465 Porto, Portugal;

*Presenting author (inesmr@fe.up.pt)

²ALiCE – Associate Laboratory in Chemical Engineering, Faculty of Engineering, University of Porto, Rua Dr. Roberto Frias, 4200-465 Porto, Portugal

³Institute of Nanoscience and Nanomaterials of Aragon (INMA), CSIC-University of Zaragoza, Zaragoza, Spain

⁴Chemical and Environmental Engineering Department, University of Zaragoza, Zaragoza, Spain

Abstract

By 2022, more than 36.8 Gt of global CO₂ energy-related emissions were registered, reaching a new record. Membrane-based CO₂ capture is one of several strategies being considered to minimize these emissions. This work studied polymeric PDMS membranes (symmetric and asymmetric) with the embedment of zeolite filler ZSM-5 for CO₂/N₂ separation. The optimum 10 wt.% loading of ZSM-5 resulted in a 47 % increase in CO₂ permeance and a CO₂/N₂ selectivity of 12 for PDMS/ZSM-5 membranes. When comparing PSf/PDMS/ZSM-5 to PDMS/ZSM-5, optimum ZSM-5 loading resulted in an 88 % increase in CO₂ permeance and no change in CO₂/N₂ selectivity (12). In conclusion, the synthesized membranes, especially the PDMS asymmetric membranes, proved to be efficient at separating CO₂ and decreasing CO₂ emissions.

Author Keywords. Carbon dioxide; Gas separation; Mixed matrix membrane; PDMS; ZSM-5

Open Access  Peer Reviewed  CC BY

1. Introduction

Greenhouse gas (GHG) emissions, particularly CO₂ emissions, are one of the most important of today's environmental concerns. The pandemic caused, in 2020, a decrease in energy use and emissions, which led to a rise of 6 % in worldwide CO₂ energy-related emissions in 2021. The growth was slightest in 2022, with 0.9 %, however, a new record of more than 36.8 Gt of worldwide CO₂ energy-related emissions was reached ("Global Energy Review 2021 – Analysis - IEA" 2023). Therefore, it is crucial to consider methods for reducing CO₂ emissions, such as membrane-based CO₂ capture. Polymeric membranes have been extensively explored and tested for gas separation due to their chemical resistance, high-pressure tolerance, operation over a wide temperature range, and low-cost manufacturing. Rubbery polymers, like Polydimethylsiloxane (PDMS), present a flexible structure, allowing the rotation around the main chain and the easy passage of gases. This led to high values of permeability and low values of selectivity, given the "trade-off" phenomenon between permeability and selectivity, founded by Robeson in 1991 (Haider et al. 2021; Robeson 2008). Fillers with stronger separation characteristics surrounded in polymeric membranes can reverse this tendency to create what is known as mixed matrix membranes (MMMs). For gas separation within MMMs, PDMS membranes embedded by MFI type zeolites, such as ZSM-5, have demonstrated promising results (Haider et al. 2021).

2. Materials and Methods

As an inorganic filler was used the zeolite ammonium ZSM-5 powder (280 SiO₂/Al₂O₃ mole ratio and particle size of ca. 3-5 μm) from Zeolyst. The Polysulfone (PSf) porous support was synthesized by immersion precipitation (phase inversion method), which involved pouring the PSf solution onto a Teflon plate using an automatic film applicator (knife thickness of 250 μm) and then submerging it in a water coagulation bath. The asymmetric membranes PSf/PDMS/ZSM-5 were formed by solvent evaporation after casting the polymeric solution containing the filler on the PSf porous support using the film applicator. For the symmetric membranes PDMS/ZSM-5, the PDMS solution embedded with ZSM-5 was placed in a metal petri dish, occurring the evaporation of the solvent, and the membrane was dried in an oven for 1 hour. Fourier transform infrared spectroscopy (FTIR) was performed in the synthesized membranes using a Bruker Vertex 70 FTIR spectrometer, and the crystalline phases of the membranes were analyzed by x-ray diffraction (XRD) using Panalytical

Empyrean equipment with CuK α radiation ($\lambda = 0.154$ nm). The gas permeation experiments were conducted on a flat module containing synthesized membranes (2.12 cm² effective area). The tests were performed for a CO₂/N₂ mixture (15/85 cm³ (STP) min⁻¹) and using helium as carrier gas (4.5 cm³ (STP) min⁻¹) at 35 °C and 1-3 bar. The permeances (in gas permeance unit (GPU) = 10⁻⁶ cm³(STP) cm⁻² s⁻¹ Pa⁻¹) were calculated using N₂ and CO₂ concentrations in the permeate stream examined by an Agilent 3000 A micro-gas chromatograph at 1 bar (Martínez-Izquierdo et al. 2021).

3. Discussion

The embedment of ZSM-5 in the PDMS symmetric membranes improved the performance of the membrane, with an increase of 26 % and 47 % in CO₂/N₂ selectivity (for 50 wt.% of ZSM-5) and CO₂ permeance (for 10 wt.% of ZSM-5), respectively. The 10 wt.% of ZSM-5 was considered the optimal wt.% since it presented the higher CO₂ permeance with a selectivity around 12. The FTIR spectra and XRD pattern of PDMS/ZSM-5 membranes, illustrated in Figure , proved that the inorganic filler was properly enclosed in the polymeric matrix and that the polymer and the filler exhibited good compatibility.

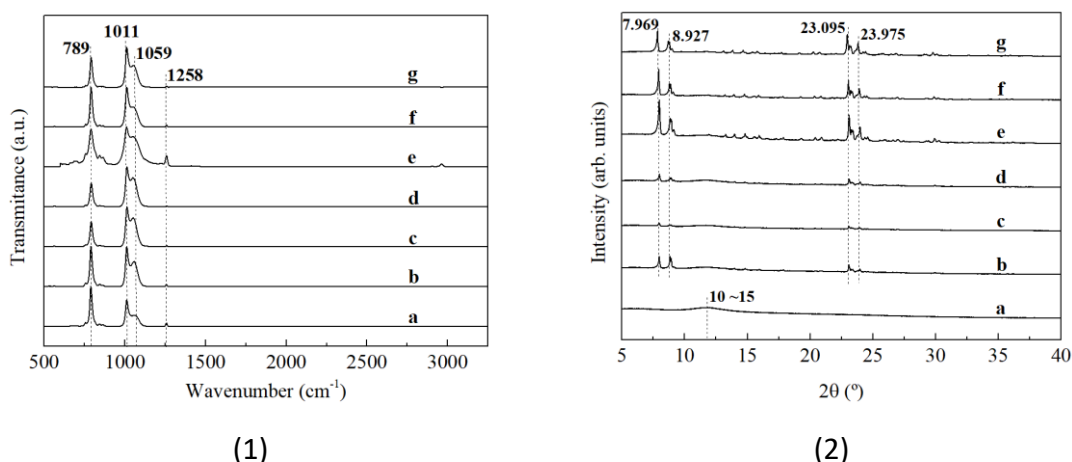


Figure 1: (1) FTIR spectra and (2) XRD patterns of PDMS/ZSM-5 membranes with different ZSM-5 content: (a) 0 wt% (pure PDMS membrane) (b) 5 wt% (c) 10 wt% (d) 20 wt% (e) 30 wt% (f) 40 wt% (g) 50 wt%.

Asymmetric membranes (PSf/PDMS) were prepared using a high wt.% of PDMS (80 wt.%) to ensure the complete embedment of micrometric ZSM-5 (3-5 μm size range). For the optimal 10 wt.%, PSf/PDMS/ZSM-5 showed to be superior compared with PDMS/ZSM-5, leading to an increase of 88 % in CO₂ permeance (from 11 to 92 GPU) while maintaining the selectivity result, as shown in Figure .

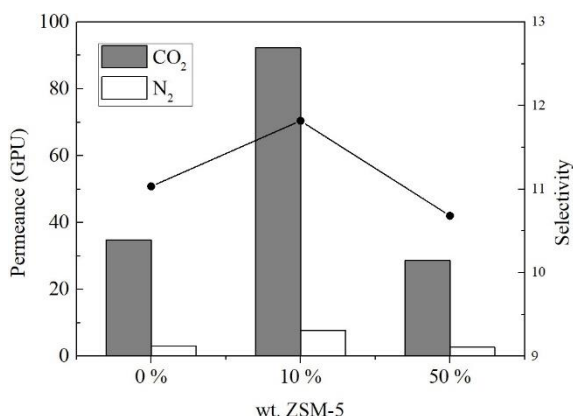


Figure 2: CO₂ and N₂ permeance (columns) and CO₂/N₂ selectivity (dots) results for PSf/PDMS (80 wt.%) asymmetric membranes with different ZSM-5 content.

4. Conclusions

With this work it was possible to conclude that the performance of PDMS symmetric and asymmetric membranes can be enhanced by embedding fillers, in particular ZSM-5. PSf/PDMS asymmetric membranes proved to be more efficient for using fillers due to their naturally smaller thickness and inherent higher permeance. However, both membranes could be used in CO₂/N₂ separation and carbon capture processes.

References

- Haider B., Dilshad M.R., Akram M.S., et al. 2021. "Novel Polydimethylsiloxane membranes impregnated with SAPO-34 zeolite particles for gas separation". *Chemical Papers* **75**: 6417–6431 (2021). Accessed 24 March, 2023. <https://doi.org/10.1007/s11696-021-01790-w>
- IEA (International Energy Agency). 2023. "CO₂ emissions in 2022". Accessed 27 March, 2023. <https://www.iea.org/reports/co2-emissions-in-2022>
- Martínez-Izquierdo L., Malankowska M., Téllez C., and Coronas J. 2021. "Phase inversion method for the preparation of Pebax® 3533 thin film membranes for CO₂/N₂ separation". *Journal of Environmental Chemical Engineering* **9**:105624. Accessed 24 March, 2023. DOI: <https://doi.org/10.1016/j.jece.2021.105624>
- Robeson L. M. 2008. "The upper bound revisited". *Journal of Membrane Science* **320**:390-400. Accessed 24 March, 2023. DOI: <https://doi.org/10.1016/j.memsci.2008.04.030>

Acknowledgments

This work is financially supported by national funds through the FCT/MCTES (PIDDAC), under the project PTDC/EAM-AMB/4702/2020 (OZONE4WATER), LA/P/0045/2020 (ALICE), UIDB/50020/2020 and UIDP/50020/2020 (LSRE-LCM). Inês Rodrigues acknowledges FCT for her PhD Research Scholarship (2022.10784.BD reference). Grants PID2019-104009RB-I00 funded by MCIN/AEI/10.13039/501100011033 is gratefully acknowledged (Agencia Estatal de Investigación (AEI) and MCIN (Ministerio de Ciencia e Innovación), Spain). Grants T43-20R and T68_23R financed by the Aragón Government is gratefully acknowledged. L. Martínez-Izquierdo also thanks the Aragón Government (DGA) for her PhD grant.

P22. Automatic monitoring and measurement system for electrodegradation processes

M. Rúa-Pereira^{1,*}, E. Soto³, E. González-Romero², M. Pazos¹, E. Rosales¹, M.A. Sanromán¹

¹Department of Chemical Engineering, University of Vigo, Isaac Newton Building, Campus As Lagoas Marcosende 36310, Vigo, Spain

²Department of Analytical and Food Chemistry, University of Vigo, Campus As Lagoas Marcosende, 36310, Vigo, Spain

³Department of Electronic Technology, University of Vigo, Campus As Lagoas Marcosende, 36310, Vigo, Spain

*Presenting author (mario.rua@uvigo.gal) ORCID [0009-0005-5481-3087](https://orcid.org/0009-0005-5481-3087)

Abstract

In wastewater electrodegradation processes, real-time analysis of data is key to facilitate the on-time decision making and following the process. This work presents the development of an automatic and portable monitoring system for autonomous evaluation of process parameters as pH, conductivity, the concentration of analytes of interest, temperature, flow and presents the on-time remote data consultation platform based on IOT (internet of things). The system provides the monitoring of the analytes concentration for different pollutants of interest and controls the flow and physical-chemical properties of the water system.

Author Keywords. Wastewater, electrodegradation, analyte concentration, IOT.

 Open Access  Peer Reviewed  CC BY

1. Introduction

Access to safe water sources, which is a key point for human health and well-being, is a current problem. Accordingly, United Nations aimed several objectives to ensure the availability of water for human consumption to the entire global population in the 2030 Agenda for Sustainable Development adopted in 2015.

Industrial, agricultural and livestock activities, and also human healthcare are increasing the water pollution, especially by micropollutants, in both surface and groundwater causing a loss in the water resources quality. Among these micropollutants, pharmaceutical drugs have been drawing attention due to the body only absorbs a small portion of them, being the vast majority excreted in the urine as primitive drugs (Li et al. 2023) and transported to wastewater treatment plants (WWTP). WWTP cannot board the quantification and treatment of micropollutants which demands the development of novel and complete treatment alternatives including a combination of monitoring, treatment (e.g. advanced oxidation processes) and control. To achieve rapid on-time data acquisition, monitoring and modulate the response of these new treatments, tailor-made monitoring systems are required (Bijlsma et al. 2021). The objective of this work is to develop an automatic real-time data acquisition system (DAS) capable of monitoring the micropollutants and their degradation during the treatment process. The system is designed to take measurements and automatically act in case of process deviations as well as to detect changes in the monitored properties to reduce the human intervention needs. The data acquisition parameters (time, frequency, etc.) are configurable and the obtained data is stored and easily consulted in remote mode. The robustness of the data acquisition and the system validation confirm its performance.

2. Materials and Methods

The selected treatment system involves an electrochemical reactor, pumps, and pipes as shown in Figure . pH, conductivity and temperature probes whose data is stored digitally and supplied to an Arduino Nano Probes and level sensors have been acquired to be connected in line.

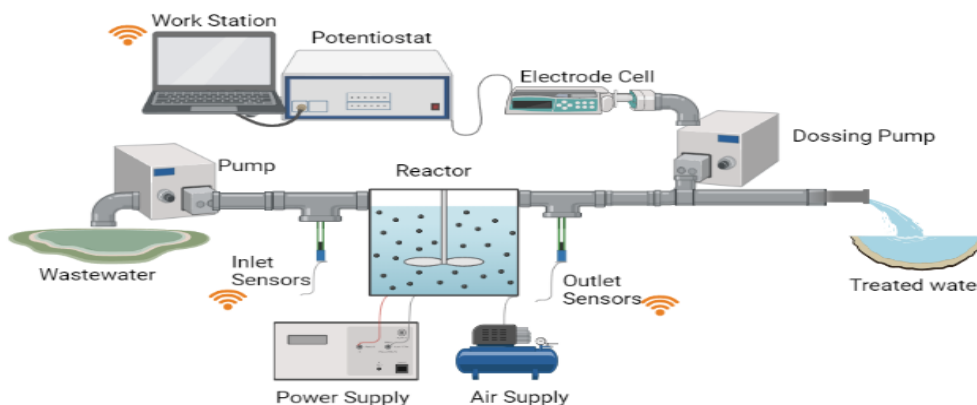


Figure 1: Treatment system scheme.

The monitoring of selected micropollutants is done by using a potentiostat. Each probe and sensor are connected to microcontrollers (ESP32) and these to a master microcontroller (ESP32) and transmits data through WIFI communication interface. The programming of the microcontrollers is developed in the Arduino® IDE programming software. The selected IOT platform is ThingSpeak™ (© The MathWorks) and this platform allows access to data in remote mode. Microsoft Power Automate, a SaaS platform by Microsoft, is selected to create and manage all aspects of the automation of recurring tasks from a central portal.

The monitoring of the selected pollutants (sulfamethazole and paracetamol) has been carried out using a potentiostat Autolab (Metrohm).

3. Discussion

The operational parameters of the system pH, temperature, conductivity, level of liquid and concentration of the pollutants have been identified as variables to be monitored before and during the treatment and treatment time as a response to modify. The response implies the modification of the volumetric flow by interacting with the peristaltic pumps.

For this purpose, input and output sensors and probes and also pumps were connected in line. The probes and sensor architecture are based on a slave-master configuration through an MQTT broker where the master can compare the data from the rest of the ESP32 slaves and then act if necessary. Each ESP32 works independently and measures the designated variable, but they also work together. The system design had a real handicap related to the integration of all the incoming data from the electrodegradation system and the operational parameters. The chosen IOT platform ThingSpeak™ can process both data transmissions, to print them in different graphics and allow remote consultation. The data can be consulted both on the smartphone or web. If the ESP32 master, through the broker, detects an out-of-specifications value variation on the water properties between the inlet and outlet of the reactor, the system activates the pumps to regulate the flow and set up the optimal conditions for the process. An overview of this communication system is presented in Figure 7(a). Also, the Figure 7(b) contains an example of the data representation on the IOT platform. The results show a continued decrease in the pollutant concentration during the process. Under the effect of the electric field of 1A, a degradation of 80% of the pollutant was detected compared to the initial detection peak (40 to 8 ppm) after 90 min.

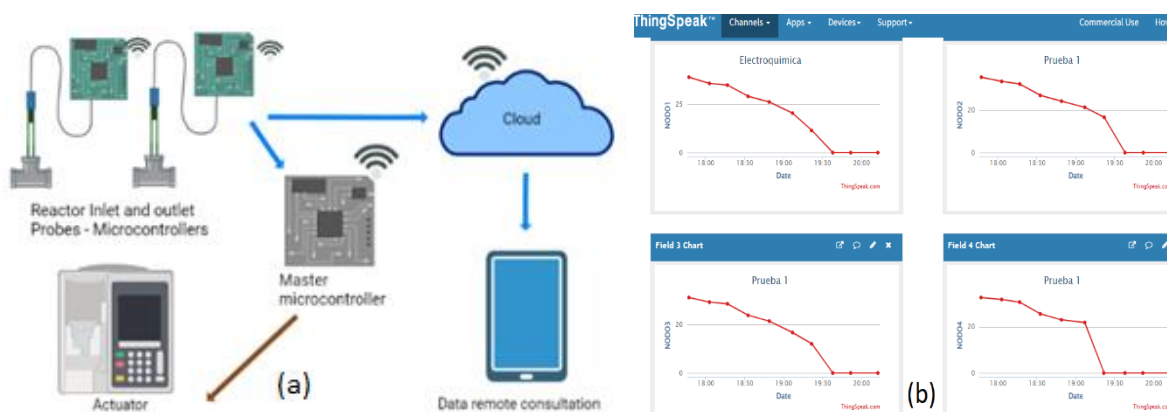


Figure 7: (a) Overview of the communication system, (b) Data from IOT platform

Once the DAS has been developed, the integrated degradation and monitoring system has been validated with recirculation and in a continuous flow. pH or conductivity online values from the inlet and the outlet of the reactor were validated by comparison with laboratory pH measurements. Three samples for each parameter present a <0.2 variation between them. In order to validate the online pollutant determination, another potentiostat was used to contrast. Two different drugs were compared in eight different analytes concentrations, from $10\mu\text{M}$ to $400\mu\text{M}$, all at pH 6. The operation was repeated three times and used also as a calibration. The analyte concentration values show no variation between the system data and the laboratory so it was determined that the cell of electrodes and the equipment are properly working and the DAS operating correctly. After the feasibility validation, the next validation needs to probe the robustness of the data acquisition. The system was configured in a 5-minute interval for the parameters measurements and the potentiostat was configured to provide analyte concentration every 15 minutes. There was no loss of data transmission during the process.

4. Conclusions

The system optimizes the data collection time and reduces the need for human intervention, facilitating on-time decision-making due to its automation. It only needs the preset of values and to select the technique for the analyte concentration calculations. Once is started, the system works independently if the Wi-Fi connection is stable. If there are loss of Wi-Fi or power supply the system stops and can't restart by itself. The obtained data is also stored in the IOT application. The system works with low energy consumption and monitors the process successfully with high reproducibility. The system can be articulated to evaluate parameters in different processes related to water quality and micropollutant degradation. The system has proven to control process parameters such as pH or conductivity in case of deviations.

Acknowledgments

This research has been financially supported by Project PDC2021-121394-I00 funded by the Spanish Ministry of Sciences and Innovation MCIN/AEI/10.13039/501100011033 and European Union Next Generation EU/ PRTR.

References

- Li, Xiaolin, Bin Wang, Feng Liu, and Gang Yu. 2023. "Occurrence and Removal of Pharmaceutical Contaminants in Urine: A Review." *Water* 15 (8): 1517. <https://doi.org/10.3390/w15081517>
- Bijlsma, Lubertus, Elena Pitarch, Eddie Fonseca, María Ibáñez, Ana María Botero, Javier Claros, Laura Pastor and Félix Hernández. 2021. "Investigation of pharmaceuticals in a conventional wastewater treatment plant: Removal efficiency, seasonal variation and impact of a nearby hospital." *Journal of Environmental Chemical Engineering* 9 (4): 105548. doi: <https://doi.org/10.1016/j.jece.2021.105548>.

P23. Evaluation of municipal sewage sludge compliance with Portuguese legislation for its agricultural use

Filipe Rocha^{1,2*}, Idalina Bragança^{1,2}, Nuno Ratola^{1,2}, Vera Homem^{1,2}

¹LEPABE - Laboratory for Process Engineering, Environment, Biotechnology and Energy, Faculty of Engineering, University of Porto, Rua Dr. Roberto Frias, 4200-465 Porto, Portugal

²ALiCE - Associate Laboratory in Chemical Engineering, Faculty of Engineering, University of Porto, Rua Dr. Roberto Frias, 4200-465 Porto, Portugal




*Presenting author (up201003084@up.pt) ORCID [0000-0003-1166-1990](https://orcid.org/0000-0003-1166-1990)

Abstract

Aiming at a more sustainable use of resources, current sewage sludge management trends encourage its reuse as a by-product of wastewater treatment plants (WWTPs). Its agricultural valorization is considered the most interesting and pragmatic disposal approach in many countries. However, municipal sewage sludge is susceptible to the accumulation of several contaminants, including pathogens, hence precautions must be taken to avoid contamination risks during its storage, transportation, and proper disposal.

In Portugal, concentration limits for heavy metals, some organic compounds, and pathogens in sewage sludge are regulated. In order to assess the quality of sewage sludge generated in the country concerning legislated parameters for its agricultural use, a total of 72 samples from 36 WWTPs were analyzed. Results revealed that most samples met legal requirements for heavy metals, polycyclic aromatic hydrocarbons (PAHs), and polychlorinated biphenyls (PCBs). But the occurrence of pathogens (*E. coli* and *Salmonella*) was above threshold values in most samples.

Author Keywords. Sewage sludge, heavy metals, pathogens, soil-amendment.

 Open Access  Peer Reviewed  CC BY

1. Introduction

Municipal sewage sludge offers great potential for resource and energy recovery, adding to a circular economy model. Since it contains large amounts of organic matter, minerals, and soil nutrients, its application to farming and forest soils has been encouraged as a more sustainable alternative for disposal than landfilling or incineration (Kanteraki et al. 2022).

Agricultural valorisation of sewage sludge has been related to improvements in soil structure and fertility, while reducing dependence on mineral- and chemical-based fertilizers. But negative aspects should also be considered, including odour release, greenhouse gas emissions due to fermentability and poor stabilization of organic matter added to soils, and acute or long-term impacts on farmland, groundwater and grown crops from pathogens and toxic contaminants present in sewage sludge (Collivignarelli et al. 2019).

The EU legislation on this matter (Council Directive 86/278/EEC) focuses only on the threat posed by heavy metals and is currently being revised to better address ongoing concerns related to the occurrence of contaminants in sludge. Some Member States have already implemented stricter values for heavy metals and established limits for some organic compounds and pathogens, as well as more stringent requirements regarding the degree of sewage sludge treatment, frequency of application, or location and purpose of receiving soils (Collivignarelli et al. 2019). In Portugal, Decree-Law No. 276/2009 regulates this practice. In addition to heavy metals, thresholds for pathogens (*Escherichia coli* and *Salmonella spp*) and maximum concentrations for a few organic contaminants (including PAHs and PCBs) have been restricted in sewage sludge to be used in soils. This work aims to assess the suitability of sewage sludge generated in Portuguese WWTPs to be used as soil-amendment, particularly regarding compliance with the legislated parameters.

2. Materials and Methods

Dewatered sewage sludge samples were collected at the final treatment stage of 36 WWTPs treating mostly domestic/urban effluents, distributed across mainland Portuguese territory, in 2 different sampling campaigns (June/July 2019 and February 2020).

Total solids were determined by drying a portion of sample at 105 °C to constant mass, and the dried aliquots were later heated up in a furnace at 550 ° for the determination of volatile solids

(indication of organic matter). Sample pH was measured with an electrode probe immersed in a suspension of sewage sludge in distilled water in a ratio of 1:5 (w/v). The nitrogen content was measured using the Kjeldahl method while other nutrients (P and K) and heavy metals determined by microwave-assisted digestion with nitric and chloridric acid (ratio 1:3, v/v), followed by inductively coupled plasma optical emission spectroscopy. PAHs and PCBs content in sludge were determined by solvent extraction with *n*-hexane, dichloromethane and ethyl acetate aided by ultrasounds, followed by a dispersive solid-phase clean up and analyzed by gas chromatography – mass spectrometry. Number of *E. coli* UCF in 1 g and occurrence of *Salmonella spp* in 50 g of sample were also measured. All these determinations were performed in triplicate, and results compared with National legislation.

3. Discussion

A total of 72 sewage sludge samples were analysed for their agronomical parameters (total solids, pH, organic matter, N, P, and K content) and occurrence of legislated contaminants (heavy metals, PAHs, PCBs, and pathogens). Anaerobic digestion was used as the sludge stabilization method in 22 sampled WWTPs (44 samples), with the remaining 12 (24 samples) only using gravitational thickening after wastewater treatment, with no further sludge stabilization. The overall results reported for thickened and anaerobically digested sewage sludge are presented in Table .

Anaerobic digested samples showed lower average values of organic matter and macronutrients than only thickened samples (consistent with the expected higher degree of organic matter stabilization), as well as a higher overall percentage of total solids and pH value. Regarding the levels of legislated contaminants in the sewage sludge, most samples fulfill Portuguese legislation requirements with respect to the concentration of heavy metals, PAHs, and PCBs. Copper was above the legal limits in 3 samples (2 from the same WWTP) and zinc in 2 samples (also in the same WWTP). PAHs were found in all sample with average values way below the threshold of 6 mg/kg_{dw}, only surpassing the concentration limit in 2 samples from the same WWTP, while PCBs were rarely detected. On the other hand, the presence of pathogens was a major nuisance in most samples, even in those stabilized by anaerobic digestion. *E. coli* was above legal limits in all but 1 thickened and 9 anaerobic digested samples, while *Salmonella* was reported in 71 and 67% of thickened and digested samples, respectively.

Parameter	Only Thickened min – max (mean)	Anaerobically digested min – max (mean)	Legislated Limits (DL 276/2009)	No. of non- compliances
Total Solids (%)	11.6 – 26.7 (18.6)	11.4 – 41.8 (21.1)	n.d.	
Organic Matter (% _{dw})	73.3 – 91.4 (83.2)	49.0 – 90.0 (72.3)	n.d.	
pH value	4.7 – 7.5 (6.5)	5.3 – 8.2 (7.2)	n.d.	
Nitrogen (g/kg _{dw})	42.2 – 97.0 (70.3)	30.7 – 82.0 (59.5)	n.d.	
Phosphorous (g/kg _{dw})	7.8 – 42.1 (20.5)	9.3 – 53.5 (22.8)	n.d.	
Potassium (g/kg _{dw})	1.8 – 11.9 (5.5)	1.4 – 9.7 (3.6)	n.d.	
Cadmium (mg/kg _{dw})	0.5 – 3.1 (1.1)	0.7 – 11.1 (2.9)	20	-
Copper (mg/kg _{dw})	78 – 339 (162)	107 – 4429 (423)	1000	3
Nickel (mg/kg _{dw})	8 – 115 (23)	8 – 206 (45)	300	-
Lead (mg/kg _{dw})	11 – 52 (22)	16 – 204 (44)	750	-
Zinc(mg/kg _{dw})	271 – 856 (507)	381 – 5120 (1086)	2500	2
Mercury (mg/kg _{dw})	0.4 – 0.8 (0.6)	0.4 – 1.4 (0.7)	16	-
Chromium (mg/kg _{dw})	10 – 100 (30)	15 – 919 (104)	1000	-
∑16PAHs (mg/kg _{dw})	0.1 – 17.5 (1.7)	0.1 – 2.2 (0.9)	6	2
∑7PCBs (mg/kg _{dw})	n.d. – 0.017 (0.008)	n.d. – 0.022 (0.007)	0.8	-
<i>Escherichia coli</i> (UCF/g _{ww})	760 – 240000 (43000)	100 – 430000 (46000)	<1000 UFC/g _{ww}	62
<i>Salmonella spp</i> (Occurrence in 50 g _{ww})	Present in 17 samples	Present in 32 samples	Absent in 50 g _{ww}	49

Table 3: Overview of agricultural parameters and contaminants load measured in 72 sewage sludge samples and comparison to Portuguese legislation (n.d. – not defined).

In general, no seasonal differences were found between samples collected from the same WWTP within the 6 months sampling window. The only exception is the contamination with pathogens, which was less frequently recorded in samples collected in the winter (*E. coli* was within legal thresholds in 22% of all samples collected in the winter vs 6% in summer, while *Salmonella* was absent in 56% of winter samples vs 8% in summer ones).

4. Conclusions

Most samples complied with Portuguese legislation requirements regarding the concentration of heavy metals, PAHs, and PCBs. However, occurrence and levels of pathogens were above legal thresholds in most samples, even in those stabilized by anaerobic digestion. These results suggest more attention should be given to pathogens elimination prior to agricultural valorization of sewage sludges, such as recurring to alternative stabilization processes to further treat sludge digestates, like co-composting or drying for pellet production.

References

- Collivignarelli, Maria Cristina, Alessandro Abbà, Andrea Frattarola, Marco Carnevale Miino, Sergio Padovani, Ioannis Katsoyiannis and Vincenzo Toretta. 2019. "Legislation for the Reuse of Biosolids on Agricultural Land in Europe: Overview". *Sustainability* 11 (21):6015. DOI: 10.3390/su11216015.
- Kanteraki, A.E., E.A. Isari, P. Svarnas and I.K. Kalavrouziotis. 2022. "Biosolids: The Trojan horse or the beautiful Helen for soil fertilization?". *Science of the Total Environment* 839:15270. DOI: 10.1016/j.scitotenv.2022.156270.

Acknowledgments

This work was financially supported by: (i) LA/P/0045/2020 (ALiCE) and UIDB/00511/2020 - UIDP/00511/2020 (LEPABE) funded by national funds through FCT/MCTES (PIDDAC); (ii) PTDC/ASP-PLA/29425/2017 - POCI-01-0145-FEDER-029425, funded by FEDER funds through COMPETE2020 - Programa Operacional Competitividade e Internacionalização (POCI) and by national funds (PIDDAC) through FCT/MCTES; (iii) PhD Studentship 2020.09041.BD (Filipe Rocha), financed by FCT with funds from the State Budget and by the European Social Fund (ESF); (iv) Vera Homem thanks national funds through FCT – Fundação para a Ciência e a Tecnologia, I.P., under the Scientific Employment Stimulus - Individual Call - CEECIND/00676/2017.

P24. Incorporation of *Moringa oleifera* leaf powder and extract in cereal-based foods

Teresa Ferreira^{1*}, Sandra M. Gomes^{2,3}, Anabela Leitão⁴, Arminda Alves^{2,3}, Lúcia Santos^{2,3}

¹FEUP - Faculty of Engineering, University of Porto, Rua Dr. Roberto Frias, 4200-465 Porto, Portugal

²LEPABE - Laboratory for Process Engineering, Environment, Biotechnology and Energy, Faculty of Engineering, University of Porto, Rua Dr. Roberto Frias, 4200-465 Porto, Portugal

³ALiCE - Associate Laboratory in Chemical Engineering, Faculty of Engineering, University of Porto, Rua Dr. Roberto Frias, 4200-465 Porto, Portugal

⁴LESRA—Laboratory for Separation Engineering, Chemical Reaction and Environment, Faculty of Engineering, University of Agostinho Neto, Edifício CNIC, Avenida Ho Chi Min 201, Luanda P.O. Box 815, Angola

*Presenting authors (up201806792@edu.fe.up.pt) ORCID: 0009-0003-4554-6058

Abstract

Moringa oleifera, which is rich in bioactive compounds, is a powerful source of antioxidants and nutrients and therefore has been extensively studied for its incorporation into cereal-based foods as a means to fortify them. In this work, the bioactive compounds were extracted from *M. oleifera* leaf powder by solid-liquid extraction. The antioxidant and antimicrobial activities of the extract were evaluated and its phenolic compounds were identified by HPLC-DAD. The results demonstrated that *M. oleifera* extract presented antioxidant activity, which can be explained by the main phenolics quantified in the extract (catechin, epicatechin and caffeic acid).

Author Keywords: *Moringa oleifera*, food fortification, phenolic compounds, antioxidant capacity

 Open Access  Peer Reviewed  CC BY

1. Introduction

Food fortification with natural products is fundamental since it provides essential vitamins, minerals, and antioxidants, particularly in cereal-based products that lack nutritional and bioactive compounds in their composition. Malnutrition remains a persistent challenge in developing countries, underlining the urgent need for the consumption of fortified food to address nutrient deficiencies and improve the health and well-being of vulnerable populations. *Moringa oleifera* is a tree commonly found in tropical and subtropical regions renowned for its numerous beneficial properties, such as high levels of vitamins, minerals and bioactive compounds such as antioxidants, as well as anti-inflammatory and antimicrobial properties. The countries where *M. oleifera* grows, mostly coincide with countries where malnutrition is prevalent such as Angola, India and Mozambique. (Oyeyinka and Oyeyinka 2018). Fortifying popular, relatively affordable, but nutrient-limited foods such as cereal-based products with *M. oleifera* leaf powder (MOLP) and extract, could contribute significantly to addressing malnutrition while contributing to reducing the carbon footprint associated with food production and distribution, as it eliminates the need for importing synthetic nutrients from distant sources. The objective of this project is to study the influence the incorporation of *M. oleifera* leaf powder and extract have on the antioxidant capacity of cereal-based foods such as bread as a means to increase its shelf life and improve its nutritional value. Some research has been done in this means, however this topic is still a growing field that lacks extensive research.

2. Materials and Methods

The phenolic compound-rich extract was obtained from *M. oleifera* leaf powder (MOLP) using a solid-liquid extraction technique with a Soxhlet extractor for 2 hours, using ethanol as solvent. Subsequently, a rotary evaporator was used to remove the ethanol from the samples with further use of nitrogen steam. The total phenolic content (TPC) of the extract was analysed using a protocol from Silva et al. (2007). Firstly, the extract solution (1000 mg/L in ethanol), water, and Folin-Ciocalteu reagent were added to a cuvette with the posterior addition of sodium carbonate solution. The mixture was incubated in the dark for 2 hours at room temperature and the absorbance was measured at 750 nm. The results were expressed in mg GAE (gallic acid equivalents) per gram of extract. The antioxidant activity of the extract was evaluated using two assays: α -diphenyl- β -picrylhydrazyl (DPPH) free radical scavenging method and 2,2'-azino-bis(3-

ethylbenzothiazoline-6-sulfonic acid) assay (ABTS). The DPPH assay was carried out according to Bobo-García et al. (2014). Briefly, the extract (1.5–8.0 g/L in ethanol) was incubated with DPPH solution for 40 min in the dark at room temperature and the absorbance was analysed at 515 nm with posterior calculation of the inhibition percentage of DPPH. Finally, the half maximal inhibitory concentration (IC₅₀) was determined. Regarding the ABTS assay, the procedure was executed following a literature protocol (Xiao et al. 2020). First, the extract (0.1–2.5 g/L in ethanol) was incubated with ABTS solution for 15 min in the dark at room temperature with the posterior measurement of the absorbance at 734 nm. To identify and quantify the phenolic compounds of the extract, high-performance liquid chromatography (HPLC_DAD) was performed. Analytes were identified by their retention time (RT) and measured accordingly to their maximum absorption wavelength. For the antibacterial activity testing against *Escherichia coli* and *Staphylococcus aureus*, the disk diffusion test was used. Extract solutions (0.5 g/mL and 1.0 g/mL) were prepared in 2% aqueous dimethyl sulfoxide (DMSO) and incubated with the bacteria in Plate Count Agar (PCA) media. The plates were incubated at 37 °C for 24 hours before measuring the diameter of the inhibition halos.

3. Results and discussion

The average extraction yield was (41.4 ± 9.7) %, which is very similar to the one found by Mohammadpour et al. (2019) of 43% for extraction for 11 h with the Soxhlet method. The extract was characterized regarding its total phenolic content (TPC), antioxidant and antibacterial properties. The obtained results are described in Table .

TPC (mg _{GAE} /g _{dried extract})	Antioxidant Capacity (IC ₅₀ —mg _{extract} /L)		Antibacterial Activity (d _{halo} —mm)	
	DPPH	ABTS	<i>E. coli</i>	<i>S. aureus</i>
138.2 ± 17.0	601.8 ± 10.9	115.2 ± 4.9	ND	ND

Table 1: Results from the bioactive characterization of *M. oleifera* extract (ND— not detected).

The *M. oleifera* leaf extract presented a TPC of 138.2 ± 17.0 mg_{GAE}/g_{dried extract}. Mohammadpour et al. (2019) obtained a TPC with the Soxhlet method of 49.1 mg_{GAE}/g_{extract}, a lower value than that obtained in the present study which can be due the use of a higher temperature for prolonged extraction time (11 h at 60°C) as this tends to deteriorate the bioactive compounds that contribute to the antioxidant activity of the extract. Many studies have proven that the compounds start to lose their antioxidant capacity at around 60°C. Furthermore, *M. oleifera* extract presents a higher antioxidant capacity towards ABTS in comparison to DPPH, however both values are higher than the ones found in the literature (Obboh et al. 2015). This can be due to the variability in extract composition, methodology and experimental conditions. In terms of antibacterial activity, no inhibitory halo was visible, however, this does not indicate that the extract cannot inhibit the growth of *E. coli* and *S. aureus* since the halo can be found beneath the disk. Regarding the HPLC analysis, the major phenolic compounds identified and quantified in the *M. oleifera* extract were catechin (1.24 mg/g_{dried extract}), epicatechin (0.09 mg/g_{dried extract}) and caffeic acid (0.07 mg/g_{dried extract}).

4. Conclusions

To conclude, the extraction of the phenolic compounds from MOLP was efficient considering a low extraction time (2 hours). The evaluation of the TPC and antioxidant capacity, as well as the HPLC analysis, showed that *M. oleifera* has the potential to be a natural source of antioxidant compounds and therefore a good candidate for the incorporation of its extract into cereal-based foods. It can potentially increase the shelf life as well as increase the vitamin and mineral content of the food to combat children’s malnutrition in developing countries. In future work, the extract and powder will

be incorporated into bread along with further analyses of its antioxidant capacity and contaminations to test the product's shelf life.

References

- Oyeyinka, Adewumi T., and Samson A. Oyeyinka. 2018. "Moringa Oleifera as a Food Fortificant: Recent Trends and Prospects." *Journal of the Saudi Society of Agricultural Sciences* 17 (2): 127–36. <https://doi.org/10.1016/j.jssas.2016.02.002>.
- Mohammadpour, Hossein, Seyed Mojtaba Sadrameli, Fatemeh Eslami, and Ali Asoodeh. 2019. "Optimization of Ultrasound-Assisted Extraction of Moringa Peregrina Oil with Response Surface Methodology and Comparison with Soxhlet Method." *Industrial Crops and Products* 131 (May): 106–16. <https://doi.org/10.1016/j.indcrop.2019.01.030>.
- Silva, Adrián M.T., Ekaterini Nouli, Nikolaos P. Xekoukoulotakis, and Dionissios Mantzavinos. 2007. "Effect of Key Operating Parameters on Phenols Degradation during H₂O₂-Assisted TiO₂ Photocatalytic Treatment of Simulated and Actual Olive Mill Wastewaters." *Applied Catalysis B: Environmental* 73 (1-2): 11–22. <https://doi.org/10.1016/j.apcatb.2006.12.007>.
- Bobo-García, Gloria, Gabriel Davidov-Pardo, Cristina Arroqui, Paloma Vírseda, María R Marín-Arroyo, and Montserrat Navarro. 2014. "Intra-Laboratory Validation of Microplate Methods for Total Phenolic Content and Antioxidant Activity on Polyphenolic Extracts, and Comparison with Conventional Spectrophotometric Methods." *Journal of the Science of Food and Agriculture* 95 (1): 204–9. <https://doi.org/10.1002/jsfa.6706>.
- Xiao, Fan, Tao Xu, Baiyi Lu, and Ruihai Liu. 2020. "Guidelines for Antioxidant Assays for Food Components." *Food Frontiers* 1 (1): 60–69. <https://doi.org/10.1002/fft2.10>.
- Oboh, Ganiyu, Adedayo O. Ademiluyi, Ayokunle O. Ademosun, Tosin A. Olasehinde, Sunday I. Oyeleye, Aline A. Boligon, and Margareth L. Athayde. 2015. "Phenolic Extract From Moringa Oleifera Leaves Inhibits Key Enzymes Linked to Erectile Dysfunction and Oxidative Stress in Rats' Penile Tissues." *Biochemistry Research International* 2015: 1–8. <https://doi.org/10.1155/2015/175950>.

Acknowledgments

This work was financially supported by: (i) Project MORfood (541163254/2019) funded by Foundation for Science and Technology (FCT), Aga Khan Development Network (AKDN) and (ii) LA/P/0045/2020 (ALICE), UIDB/00511/2020 and UIDP/00511/2020 (LEPABE), funded by national funds through FCT/MCTES (PIDDAC), and S4Hort_Soil&Food (NORTE-01-0145-FEDER-000074), supported by Norte Portugal Regional Operational Programme (NORTE 2020), under the PORTUGAL 2020 Partnership Agreement, through the European Regional Development Fund (ERDF)

P25. Tailoring photoelectrochemical stability of tantalum nitride for solar redox flow cells

Filipe Moisés M. Francisco^{1,2*}, Paula Dias^{1,2}, Adélio Mendes^{1,2}

¹LEPABE - Laboratory for Process Engineering, Environment, Biotechnology and Energy, Faculty of Engineering, University of Porto, Rua Dr. Roberto Frias, 4200-465 Porto, Portugal

²ALiCE - Associate Laboratory in Chemical Engineering, Faculty of Engineering, University of Porto, Rua Dr. Roberto Frias, 4200-465 Porto, Portugal

*Presenting author (up201307953@edu.fe.up.pt) ORCID [0000-0003-3172-4047](https://orcid.org/0000-0003-3172-4047)

Abstract

Harvesting and storing solar energy into electrochemical fuels using solar redox flow cells (SRFC) requires the development of efficient, stable, and cost-effective semiconducting photoelectrode materials. Tantalum nitride (Ta_3N_5), with a bandgap of *ca.* 2.1 eV, allows reaching photocurrents higher than $12.5 \text{ mA}\cdot\text{cm}^{-2}$; however, stability limits its practical application. The present work aims at understanding the role of underlayers of aluminium -doped titanium dioxide ($\text{Al}:\text{TiO}_2$) and zinc-doped tin oxide ($\text{Zn}:\text{SnO}_2$) on the performance of semi-transparent Ta_3N_5 photoelectrodes prepared by electrophoretic deposition. $\text{Al}:\text{TiO}_2$ and $\text{Zn}:\text{SnO}_2$ underlayers proved effective in improving the Ta_3N_5 stability.

Author Keywords. Ta_3N_5 photoelectrodes, Al-doped TiO_2 underlayer, Zn-doped SnO_2 underlayer, stability, solar energy storage, electrochemical fuels, solar redox flow cells.

 Open Access  Peer Reviewed  CC BY

1. Introduction

Solar redox flow cells (SRFCs) combine a photoelectrochemical (PEC) cell with a redox flow cell (RFC) for cost-effective solar energy harvesting and storage in electrochemical fuels. However, no PEC devices are still fulfilling the requirements of long-term stability, high efficiency, low cost, abundance, and scalability (Cao *et al.*, 2018). The photoabsorber material, which is responsible for photocharging the redox pairs dissolved in the supporting electrolyte, is the main component of a PEC cell. Tantalum nitride (Ta_3N_5) is probably the most promising semiconductor among the ones almost reaching their theoretical limit, but its low photovoltage and poor stability are current issues. Tandem configurations can generate sufficient photovoltage to achieve overall redox reactions with high efficiency, but the use of semi-transparent photoelectrodes is a prerequisite. Ta_3N_5 thin films fabricated on transparent conductive oxide (TCO) substrates, such as F-doped SnO_2 (FTO), were potentially applicable. Unfortunately, the adhesion between Ta_3N_5 and FTO substrate is challenging (Liu *et al.*, 2014). Previous studies have shown that the addition of under- and overlayers can improve the performance of Ta_3N_5 . Recently, this authors demonstrated a photocurrent of *ca.* $4.01 \text{ mA}\cdot\text{cm}^{-2}$ at $0.3 \text{ V}_{\text{Ag}/\text{AgCl}}$ for semi-transparent Ta_3N_5 films prepared by electrophoretic deposition (EPD), using Ta-doped TiO_2 underlayer; its stability had not surpassed 8 h of operation. The poor stability of Ta_3N_5 is usually attributed to structural changes in the semiconductor interface, where oxygen atoms progressively replace the nitrogen atoms during redox reactions. To avoid this, the use of co-catalysts and overlayers have been pointed to accelerate the redox reactions and simultaneously mitigate the photocorrosion of Ta_3N_5 . On the other hand, the influence of underlayers on Ta_3N_5 photoelectrodes is less studied. Al doping influences the optical properties of TiO_2 films, especially promoting a smoother surface suitable for a good adhesion of Ta_3N_5 particles; its high transparency in the visible range (81-94 %) favors back illumination (Aarik *et al.*, 2014). Zn-doped SnO_2 works as a good electron transport layer for perovskites, increasing the electron extraction and transfer capability; high transparency, uniformity, and dense film formation are also advantages of this layer (Yang *et al.*, 2021). Both layers proved to improve the photoactivity of some semiconductors. Therefore, this work aims at studying the role of $\text{Al}:\text{TiO}_2$ and $\text{Zn}:\text{SnO}_2$ underlayers for designing more efficient and stable semi-transparent Ta_3N_5 photoelectrodes. $\text{Al}:\text{TiO}_2$ underlayer promoted a better adhesion of the Ta_3N_5 film to the substrate and improved the electron back-contact transport.

2. Materials and Methods

2.1. Synthesis of Ta₃N₅ photoelectrodes

An atomic layer deposition (ALD) system was used to deposit the Ta:TiO₂ and Al:TiO₂ underlayers over fluorine-doped tin oxide (FTO) glass substrates, following the procedures of Hajibabaei *et al.* and Aarik *et al.*, respectively. For the Al:TiO₂ deposition, it was performed sequential pulses of precursor and water, followed by purges until reach 20 nm with different ratios. Zn:SnO₂ was prepared using a spin coater, adapting the procedure from Yang *et al.*, under different speed rates (100-300 rpm/s) and final speeds (1000-6000 rpm) over 30 s. Ta₃N₅ films were prepared by EPD, adapting the procedure reported elsewhere (Higashi *et al.*, 2011). At the end, the photoelectrodes were annealed under 100 mL·min⁻¹ NH₃ (99.9999 %) flow at 698 K for 30 min; heating and cooling ramps were 5 °C·min⁻¹.

2.2. Photoelectrochemical characterization

The photoelectrochemical characterization of the photoelectrodes was performed using a “Cappuccino” PEC cell filled with an electrolyte solution of 0.1 M K₄Fe(CN)₆ in 1 M KOH. A three-electrode configuration was used with Ag/AgCl Sat. KCl as reference electrode, and Pt wire as counter-electrode, in dark and under 1 Sun AM 1.5 G simulated sunlight (scan rate of 10 mV·s⁻¹), in back-side illumination mode (active area of *ca.* 0.283 cm²).

3. Discussion

Figure A shows the *J-V* curves of as-prepared Ta₃N₅ photoelectrodes employing the optimized underlayers of Ta:TiO₂, Al:TiO₂ and Zn:SnO₂. Different ratios of Al:TiO₂ were tested, but 1 cycle Al: 50 cycles TiO₂ seems to be the best ratio, allowing to reach a photocurrent density of *ca.* 3.5 mA·cm⁻² at 0.3 V_{Ag/AgCl}, which decreased 12.7 % when compared with the Ta:TiO₂ layer. Concerning the Zn:SnO₂ underlayer (deposited at 4000 rpm and 300 rpm/s over 30 s), the current is even lower, but a maximum power density of *ca.* 1.2 mW·cm⁻² was obtained, which is similar to the one obtained with Al:TiO₂ layer and higher than with Ta:TiO₂. This can be explained by the onset of the dark current at more anodic potentials that improves the generated photovoltage.

Stability under continuous illumination was also evaluated with a ferrocyanide solution (pH 14) - Figure B. After a period of initial equilibrium, Al:TiO₂ and Zn:SnO₂ underlayers proved to be stable for more than 24 h, while stability of less than 8 h was observed for Ta:TiO₂. To the best knowledge of the authors, this is the highest stability reported for such materials. The induced photocorrosion mitigation can be attributed to the formation of a good electron back-extraction layer. Therefore, an improvement on the charge separation in the space charge layer is also anticipated, which would led to reduction of the surface recombination. EIS tests are being pursued to understand these phenomena.

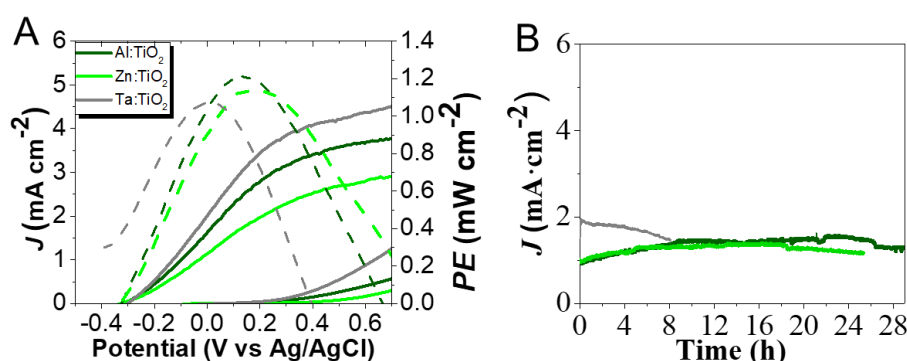


Figure 1: Performance of the as-prepared Ta₃N₅ photoelectrodes with Ta:TiO₂, Al:TiO₂ and Zn:SnO₂ underlayers, using 0.1 M K₄Fe(CN)₆ in 1 M KOH as electrolyte: A: *J-V* and power density curves; B: stability tests at 0 V.

4. Conclusions

Al:TiO₂ and Zn:SnO₂ underlayers revealed to be more effective on improving the stability of Ta₃N₅ than the commonly used Ta:TiO₂ layer. Considering their optical and conductive properties, both display acceptable transparency, which is important for SRFC applications. Al:TiO₂ showed to be the best underlayer studied, allowing to reach a photocurrent of *ca.* 3.5 mA·cm⁻² at 0.3 V_{Ag/AgCl} (*ca.* 1.2 mW·cm⁻²), with a very promising stability of 29 h. Despite the good stability provided by Zn:SnO₂, a slightly lower photocurrent of *ca.* 2.9 mA·cm⁻² at 0.3 V_{Ag/AgCl} was obtained. Understanding the contribution of these layers is critical for designing stable Ta₃N₅ photoelectrodes, thereby facilitating more efficient SRFCs.

References

- Cao, L., Skyllas-Kazacos, M., Wang, Da-Wei. "Solar Redox Flow Batteries: Mechanism, Design, and Measurement." *Advanced Sustainable Systems* 2, no. 8-9 (2018).
- Liu, G., J. Shi, F. Zhang, *et al.* "A Tantalum Nitride Photoanode Modified with a Hole-Storage Layer for Highly Stable Solar Water Splitting." *Angew Chem Int Ed Engl* 53, no.28 (2014): 7295-9.
- Aarik, L., Arroval, T., Rammula, R., *et al.* "Atomic Layer Deposition of High-Quality Al₂O₃ and Al-Doped TiO₂ Thin Films from Hydrogen-Free Precursors." *Thin Solid Films* 565 (2014): 19-24.
- Yang, C., Chen, M., Wang, J., *et al.* "Zn-Doped SnO₂ Compact Layer for Enhancing Performance of Perovskite Solar Cells". *International Journal of Photoenergy* (2021): 1-10.
- Hajibabaei, H., Zandi, O., Hamann., T. W. "Tantalum Nitride Films Integrated with Transparent Conductive Oxide Substrates Via Atomic Layer Deposition for Photoelectrochemical Water Splitting." *Chem Sci* 7, no. 11 (2016): 6760-67.
- Higashi, M., Domen, K., Abe, R. "Fabrication of Efficient Taon and Ta₃n₅ Photoanodes for Water Splitting under Visible Light Irradiation." *Energy & Environmental Science* 4, no. 10 (2011).

Acknowledgments

F. Francisco and P. Dias are grateful to FCT for funding (references: SFRH/BD/146338/2019 and CEECIND/02862/2018, respectively). This work has received funding from Project ASAPFuels - PTDC/EQU-EQU/4225/2021 funded by FEDER, through COMPETE2020 and by national funds, through FCT; and by LA/P/0045/2020 (ALICE), UIDB/00511/2020 and UIDP/00511/2020 (LEPABE), funded by national funds through FCT/MCTES (PIDDAC).

P26. Recent advancements in identifying sources of indoor air pollution using continuous monitoring methods

H. Chojer^{1,2a}, P.T.B.S Branco^{1,2}, F.G. Martins^{1,2}, S.I.V. Sousa^{1,2}

¹ LEPABE – Laboratory for Process Engineering, Environment, Biotechnology and Energy, Faculty of Engineering, University of Porto, Rua Dr. Roberto Frias, 4200-465 Porto, Portugal

² ALiCE – Associate Laboratory in Chemical Engineering, Faculty of Engineering, University of Porto, Rua Dr. Roberto Frias, 4200-465 Porto, Portugal

^a(hiten.chojer@fe.up.pt) ORCID: [0000-0001-6964-227X](https://orcid.org/0000-0001-6964-227X))

Abstract

Indoor air pollution (IAP) monitoring is important for understanding and mitigating the associated health risks. However, identifying the sources of pollutants is also crucial for effective mitigation. Traditional source-oriented and receptor models have been used for this purpose, but new methods using continuous monitoring data and low-cost sensors have emerged. This study critically analysed current trends in source identification with continuous monitoring and mitigation using IAP monitoring by reviewing studies from the last six years. The review focused on the types of pollutants monitored, methods of sample analysis, approaches to data analysis, and applicability of mitigation measures. Source identification using real-time continuous monitoring involved creating highly resolved spatio-temporal datasets. The review also proposes a hybrid approach using both samplers and continuous monitoring for preventive and reactive mitigation measures.

Author Keywords. indoor air quality, source identification, air quality monitoring, mitigation

 Open Access  Peer Reviewed  CC BY

1. Introduction

Indoor air quality (IAQ) has become an important area of research due to high pollution levels in indoor environments, where humans spend most of their time (Klepeis et al. 2001). Many studies have focused on monitoring IAQ to identify concentrations of pollutants and implement mitigation measures to reduce exposure to those pollutants. Accurately identifying indoor air pollution (IAP) sources is crucial to decreasing associated health risks, as sources can be of indoor as well as outdoor origins (attributed to outdoor infiltration). Recently, studies using devices with continuous monitoring capabilities for IAQ characterization and source identification have emerged (Men et al. 2021; Shen et al. 2021). The concentration data generated by these devices is used to identify pollution sources, highlighting the need for a critical review of recent advancements in source identification studies for indoor environments. The present study aims to review studies from the past six years on source identification based on continuous IAQ monitoring data.

2. Materials and Methods

The review included publications from Scopus, IEEE Xplore, and ScienceDirect, with no language restrictions, but all obtained publications were in English. The preliminary search included all articles published until December 2022. The search utilised four sets of keywords, resulting in 1053 conference or research articles. After screening the titles and abstracts, 60 studies were retained based on specific criteria, including the exclusion of studies that only conducted simulations with no real-world monitoring or identification, and the inclusion of studies focusing on indoor environments such as offices, homes, classrooms etc. Continuous monitoring studies published from the last six years were included for the final review that yielded eight papers.

3. Discussion

The projects studied environments like apartments, offices, school classrooms, university buildings. There was a significant variation in terms of the parameters monitored. Particulate Matter (PM) was the most commonly monitored pollutant. Some studies even used low-cost sensors (LCS) for

continuous monitoring and subsequent source identification and found sources such as chemical and fragrance products, combustion activity and outdoor infiltration (Mad Saad et al. 2017; Men et al. 2021; Zhang et al. 2022). While others used research grade devices from companies like TSI, GRIMM, etc. Some of the studies conducted both the traditional method of samples collection and laboratory analysis along with continuous real-time or near real-time monitoring.

The reviewed studies used highly time resolved data for source analysis. Mad Saad et al. (2017) and Tang, Chan, and Sohn (2021) used machine learning for source identification. Chan et al. (2018) and Men et al. (2021) used concentration peak analysis method. They identified the peaks to determine emission events upon conclusion of their monitoring campaigns. Shen et al. (2021) used the temporal and spatial variations with highly resolved datasets and found to cooking to be the major source of PM_{2.5}. Ouaret, Ionescu, and Ramalho (2021) used a GRIMM optical particle counter and applied matrix factorization to highly resolved particle concentrations time series data. They found pollutant sources like resuspension due to occupant activity and outdoor sources like road traffic among others. Zhang et al. (2022) applied principal component analysis based neural network models on environment and building correlation datasets and found sources like peeling paint, damaged walls and cracks, and other outdoor sources. Alameddine et al. (2022) ascertained indoor-outdoor ratios by placing two TSI DustTrak monitors, one indoor and the other outdoor.

4. Conclusions

The review shows a few different methods by which source identification has been done for IAP in the past few years using continuous monitoring devices. The use of LCS has strong implications as there is still much debate about the reliability of their data accuracy. Their utility in this field can have tremendous significance to provide mitigation of pollutant sources and improving the IAQ. Although, the reviewed 8 studies conducted real-time monitoring, the data analysis was done post-monitoring. Hence, the upcoming work in this field should put efforts in conducting real-time source identification.

References

- Alameddine, I., K. Gebrael, F. Hanna, and M. El-Fadel. 2022. "Quantifying indoor PM_{2.5} levels and its sources in schools: What role does location, chalk use, and socioeconomic equity play ?" *Atmospheric Pollution Research* 13 (4): 101375. <https://doi.org/10.1016/j.apr.2022.101375>.
- Chan, W. R., J. M. Logue, X. Wu, N. E. Klepeis, W. J. Fisk, F. Noris, and B. C. Singer. 2018. "Quantifying fine particle emission events from time-resolved measurements: Method description and application to 18 California low-income apartments." *Indoor Air* 28 (1): 89-101. <https://doi.org/10.1111/ina.12425>.
- Klepeis, Neil E., William C. Nelson, Ott Wayne R., John P. Robinson, Andy M. Tsang, Paul Switzer, Joseph V. Behar, Stephen C. Hern, and William H. Engelmann. 2001. "The National Human Activity Pattern Survey (NHAPS): a resource for assessing exposure to environmental pollutants." *Journal of Exposure Science & Environmental Epidemiology* 11 (3): 231–252. <https://doi.org/10.1038/sj.jea.7500165>.
- Mad Saad, Shaharil, Allan Melvin Andrew, Ali Yeon Md Shakaff, Mohd Azuwan Mat Dzahir, Mohamed Hussein, Maziah Mohamad, and Zair Asrar Ahmad. 2017. "Pollutant Recognition Based on Supervised Machine Learning for Indoor Air Quality Monitoring Systems." *Applied Sciences* 7 (8): 823. <https://doi.org/10.3390/app7080823>.
- Men, Yatai, Jianpeng Li, Xinlei Liu, Yaojie Li, Ke Jiang, Zhihan Luo, Rui Xiong, Hefa Cheng, Shu Tao, and Guofeng Shen. 2021. "Contributions of internal emissions to peaks and incremental indoor PM_{2.5} in rural coal use households." *Environmental Pollution* 288: 117753. <https://doi.org/10.1016/j.envpol.2021.117753>.

- Ouaret, Rachid, Anda Ionescu, and Olivier Ramalho. 2021. "Non-negative matrix factorization for the analysis of particle number concentrations: Characterization of the temporal variability of sources in indoor workplace." *Building and Environment* 203: 108055. <https://doi.org/10.1016/j.buildenv.2021.108055>.
- Shen, Huizhong, Weiying Hou, Yaqi Zhu, Shuxiu Zheng, Subinuer Ainiwaer, Guofeng Shen, Yilin Chen, Hefa Cheng, Jianying Hu, Yi Wan, and Shu Tao. 2021. "Temporal and spatial variation of PM2.5 in indoor air monitored by low-cost sensors." *Science of The Total Environment* 770: 145304. <https://doi.org/10.1016/j.scitotenv.2021.145304>.
- Tang, Hao, Wanyu Rengie Chan, and Michael D. Sohn. 2021. "Automating the interpretation of PM2.5 time-resolved measurements using a data-driven approach." *Indoor Air* 31 (3): 860-871. <https://doi.org/10.1111/ina.12780>.
- Zhang, He, Ravi Srinivasan, Xu Yang, Sherry Ahrentzen, Eric S. Coker, and Aladdin Alwisy. 2022. "Factors influencing indoor air pollution in buildings using PCA-LMBP neural network: A case study of a university campus." *Building and Environment* 225: 109643. <https://doi.org/10.1016/j.buildenv.2022.109643>.

Acknowledgments

This work was financially supported by: LA/P/0045/2020 (ALiCE) and UIDB/00511/2020 - UIDP/00511/2020 (LEPABE) funded by national funds through FCT/MCTES (PIDDAC); Project 2SMART - engineered Smart materials for Smart citizens, with reference NORTE-01-0145-FEDER-000054, supported by Norte Portugal Regional Operational Programme (NORTE 2020), under the PORTUGAL 2020 Partnership Agreement, through the European Regional Development Fund (ERDF). H. Chojer thanks the Portuguese Foundation for Science and Technology (FCT) for the individual research grant SFRH/BD/05092/2021.

P27. Understanding indoor air quality in private dwellings: a case study of Portuguese homes

Adhymaura Silva¹, Maria C. Pereira², Klara Slezakova³

¹Departamento de Engenharia Química, Faculdade de Engenharia, Universidade do Porto, Rua Dr. Roberto Frias, 4200-465 Porto, Portugal (up202009779@edu.fe.up.pt)

² LEPABE-Alice, Faculdade de Engenharia, Universidade do Porto, Rua Dr. Roberto Frias, 4200-465 Porto, Portugal (mcsp@fe.up.pt) ORCID 0000-0001-8505-3432

³LEPABE-Alice, Faculdade de Engenharia, Universidade do Porto, Rua Dr. Roberto Frias, 4200-465, Porto, Portugal (slezakok@fe.up.pt) ORCID 0000-0001-5265-4186

Abstract

As people spend a large part of their time at home, maintaining good indoor air quality (IAQ) in their respective environments is essential for their health and well-being. This study aimed to evaluate IAQ in private dwellings (H1-H4) situated in Oporto, MA. Particulate matter (PM₁₀, PM_{2.5}) was concurrently monitored indoors and outdoors for 24-76 h. The results showed low levels of pollution for PM₁₀ (range: 9–590 $\mu\text{g m}^{-3}$; median=14 $\mu\text{g m}^{-3}$) and PM_{2.5} (8–349 $\mu\text{g m}^{-3}$; 12 $\mu\text{g m}^{-3}$). Both indoor PMs were highly correlated ($r_s=0.887-0.976$). PM_{2.5} accounted for 87% of indoor PM; PM_{2.5} indoor-to-outdoor ratios (1.96–3.96), emphasized the contribution of indoor emission sources for fine fraction. Outdoor PM₁₀ was 1-3 times higher than indoors (18–772 $\mu\text{g m}^{-3}$; 41 $\mu\text{g m}^{-3}$) and 1-6 times lower for PM_{2.5} (3–38 $\mu\text{g m}^{-3}$; 6 $\mu\text{g m}^{-3}$). Outdoor PMs were weakly-moderately correlated ($r_s=0.389-0.780$), most likely due to meteorological conditions. Coarse particles accounted for the majority (82%) of ambient PM₁₀.

Author Keywords. Air pollution, indoor air quality (IAQ), particulate matter (PM), PM₁₀, PM_{2.5}, indoor/outdoor homes.

 Open Access  Peer Reviewed  CC BY

1. Introduction

Scientific concerns about air quality frequently focus on reducing ambient air pollution. However, there is an increasing awareness that the quality of the indoor environment affects human health and well-being. Exposure to poor indoor air has been linked with various adverse health outcomes, including respiratory and cardiovascular illness, allergic symptoms, cancer, premature mortality as well as cognitive performance (Vardoulakis, et al. 2020, Wang et al. 2021). Indoor pollution results from various combustion emission sources (heating systems and activities such as cooking, smoking, use of incense and candles burning, etc.), occupants and their activities (cleaning, domestic products, use of personal care products), as well as the design and material of interior spaces (paints, furnishes, etc.) (Vardoulakis, et al. 2020). As people spend a substantial part of their indoor exposure at home, maintaining good indoor air quality in these spaces is essential for the health and well-being of residents. Thus, this work aimed to assess indoor air quality in private dwellings.

2. Materials and Methods

Indoor air quality (IAQ) monitoring was conducted in four selected homes (H1-H4) that were situated in different urban zones in Oporto Metropolitan Area in August 2022. Indoor air sampling was conducted continuously (between 24 and 76 h in each home) in the living room as it was the place where occupants spent the majority of their awake time. Indoor PM₁₀ and PM_{2.5} was monitored by DustTrak™ II Aerosol Monitor (8532, TSI, Minnesota, USA). Particle number concentrations (N₂₀₋₁₀₀₀) were sampled by TSI P-Track™ particle counter (8525, TSI, Minnesota, USA). Concurrently, outdoor PM (N₃₀₀₋₂₅₀₀₀) was monitored by Handheld Airborne Particle Counter (3016/5016, Lighthouse Worldwide Solutions, Inc., Medford, USA). Data acquisition interval was 1 min for all pollutants/ places leading to a large amount of data (n=115 000). All statistical analyses were conducted in SPSS (IBM Statistics 27).

3. Discussion

Indoor PM₁₀ (Figure 1) ranged between 9–590 $\mu\text{g m}^{-3}$ (overall median 14 $\mu\text{g m}^{-3}$; medians per home range: 11–19 $\mu\text{g m}^{-3}$). The corresponding indoor PM_{2.5} ranged between 8 and 349 $\mu\text{g m}^{-3}$, while it was between 11 and 16 $\mu\text{g m}^{-3}$ (overall median of 12 $\mu\text{g m}^{-3}$) for the individual home medians. In outdoor air, PM concentrations were significantly higher ($p < 0.05$). Specifically, PM₁₀ levels were 1–3 times higher (overall median of 41 $\mu\text{g m}^{-3}$), with values between 18 and 772 $\mu\text{g m}^{-3}$; across H1–H4, PM₁₀ medians ranged between 37 and 45 $\mu\text{g m}^{-3}$. The corresponding outdoor PM_{2.5} were 1–6 times lower than indoors, with concentrations ranging between 2.6 and 38 $\mu\text{g m}^{-3}$. The observed medians per dwelling were between 11 and 16 $\mu\text{g m}^{-3}$ (overall 12 $\mu\text{g m}^{-3}$).

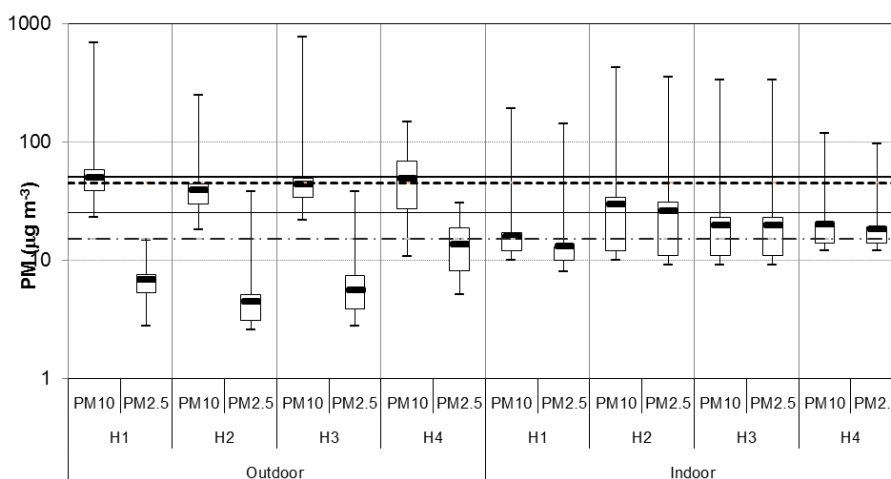


Figure 1: PM₁₀ and PM_{2.5} (■ median, □ 25–75%, ⊥ range) in indoor and outdoor air at four homes (H1–H4). The horizontal continuous and dashed lines represent, respectively, Portuguese protective thresholds for PM₁₀ (50 $\mu\text{g m}^{-3}$) and PM_{2.5} (25 $\mu\text{g m}^{-3}$) (Ordinance No. 138-G/2021).

Indoor PM fulfilled the respective PM₁₀ and PM_{2.5} protective thresholds designated in the Portuguese legislation on indoor air quality of public buildings (Ordinance No. 138-G/2021) (50 and 25 $\mu\text{g m}^{-3}$ for 8 h period, for PM₁₀ and PM_{2.5}, respectively; Figure 1, continuous lines). These values are based on the past WHO recommendations for PM in ambient air (2005 edition). Nevertheless, in 2021 WHO updated its recommendations with revised ambient air quality limits (AQL). Concerning 24 h, the guidelines are 45 and 15 $\mu\text{g m}^{-3}$ for PM₁₀ and PM_{2.5}, respectively (WHO 2021). Daily ambient air quality limit of the current EU legislative was met all homes (Directive 2008/50EU; PM₁₀: 50 $\mu\text{g m}^{-3}$; PM_{2.5}: 25 $\mu\text{g m}^{-3}$). Additionally, the observed levels showed that the 24 h AQL (Figure 1, dashed lines) for PM₁₀ proposed in the WHO 2021 was exceeded at 50% of homes (H1, H4), whereas AQL for PM_{2.5} was met at all H1–H4.

Both indoor PMs were highly and significantly correlated ($r_s = 0.887–0.976$), indicating that indoors both fractions originated from the same emission sources. Indoor fine particles accounted for the majority, i.e., 87%, of PM. PM_{2.5} is the predominant carrier for toxic components (such as carcinogenic compounds, organic pollutants and pathogenic microorganisms; Li et al. 2017), which may lead to additional health/ toxicological effects of the respective particles. In agreement, indoor-to-outdoor ratios (I/O) of PM_{2.5} ranged between 1.96–3.96 (median 2.75), thus further emphasizing the contribution of indoor emission sources for fine particles. On the contrary, median indoor I/O of coarse (i.e., PM_{10-2.5}) was 0.36 (range 0.301–0.51), suggesting penetrations of ambient emissions indoors. As expected, in ambient air, the correlations between both fine and coarse fractions were only weakly-moderately strong ($r_s = 0.389–0.780$), most likely due to the impact of the meteorological parameters. Coarse particles, in a form of resuspended dust, contributed the majority of ambient PM₁₀, as PM_{2.5} accounted for 18% of outdoor PM (range between 16–20%).

4. Conclusions

This study assessed IAQ in indoor air at four private dwellings H1-H4. The obtained data allowed for an understanding of possible exposure levels at private dwellings. Regarding PM, both PM₁₀ and PM_{2.5} levels were below the Portuguese protective thresholds at all four dwellings. However, more detailed information, namely for PM distribution and smaller-sized fractions (i.e. ultrafine), would be required in future assessments. Understanding their role in IAQ in homes, why and how they are emitted, their toxicity and health outcomes will allow for proper risk assessments and, consequently, the establishment of public health protection strategies.

References

- Directive 2008/50/EC. "Directive 2008/50EC of the European Parliament and of the Council of 21 May 2008 on ambient air quality and cleaner air for Europe". *Official Journal of the European Union*, L152: 1-44.
- Li, Z., Q. Wen and R. Zhang. 2017. "Sources, health effects and control strategies of indoor fine particulate matter (PM_{2.5}): a review". *Science of the Total Environment*, 586: 610–622. DOI: [10.1016/j.scitotenv.2017.02.029](https://doi.org/10.1016/j.scitotenv.2017.02.029).
- Ordinance No. 138-G/2021. "Saúde e ambiente e ação climática (in Portuguese)". *Diário da República*, 126/2021 (2º Suplemento): 128(2) – 128(6).
- Vardoulakis, S., E. Giagloglou, S. Steinle, A. Davis, A. Leeuwenhoek, K. Galea, K. Dixon. J. Crawford. 2020. "Indoor exposure to selected air pollutants in the home environment". *International Journal of Environmental Research and Public Health*, 17:1-24. DOI: [10.3390/ijerph17238972](https://doi.org/10.3390/ijerph17238972).
- Wang, C., F. Zhang, J. Wang, J.K. Doyle, P.A. Hancock, C.M. Mak and S. Liu. 2021. "How indoor environmental quality affects occupants' cognitive functions". *Building and Environment*, 193: 107647. DOI: [110.1016/J.BUILDENV.2021.107647](https://doi.org/10.1016/J.BUILDENV.2021.107647).
- WHO. 2021. *WHO global air quality guidelines: particulate matter (PM_{2.5} and PM₁₀), ozone, nitrogen dioxide, sulfur dioxide and carbon monoxide*. Geneva: World Health Organization.

Acknowledgements

This work was financially supported by LA/P/0045/2020 (ALiCE), UIDB/00511/2020 - UIDP/00511/2020 (LEPABE). Additional support was received from support by PTDC/CTA-AMB/3040/2021 from Fundação para a Ciência e a Tecnologia (FCT) through national funds.

P28. Impact of PM_{2.5} in schools on asthma-related symptoms

Juliana P. Sá^{1,2*}, Pedro T.B.S. Branco^{1,2}, Maria C.M. Alvim-Ferraz^{1,2}, Fernando G. Martins^{1,2},
Sofia I.V. Sousa^{1,2}

¹LEPABE - Laboratory for Process Engineering, Environment, Biotechnology and Energy, Faculty of Engineering, University of Porto, Rua Dr. Roberto Frias, 4200-465 Porto, Portugal



²ALiCE – Associate Laboratory in Chemical Engineering, Faculty of Engineering, University of Porto, Rua Dr. Roberto Frias, 4200-465 Porto, Portugal

*Presenting author (up201100656@up.pt) ORCID: 0000-0001-6011-8842

Abstract

Indoor air pollution has a greater impact on children than on adults due to their developing lungs and immune systems and higher inhalation rates. This study aimed to assess the impact of PM_{2.5} exposure on asthma-related symptoms in children attending urban nursery and primary schools. A microenvironmental modelling approach was used to assess individual PM_{2.5} exposure and information on health outcomes such as asthma, wheezing and dyspnea were collected from ISAAC questionnaires. Descriptive statistics and logistic regression models were used for data analysis. Results showed that approximately 40% of children were exposed to PM_{2.5} above the WHO guidelines. This study found evidence of an association between exposure to PM_{2.5} levels above World Health Organization guidelines and wheezing (aOR = 1.68, *p*-value = 0.038) and dyspnea (aOR = 2.07, *p*-value = 0.018). These findings highlight the potential respiratory health risks associated with PM_{2.5} exposure indoors for children in nursery and primary schools.

Author Keywords. PM_{2.5}, nursery and primary, children, asthma, wheezing, dyspnea.

 Open Access  Peer Reviewed  CC BY

1. Introduction

Children are more susceptible to the health effects of indoor air pollution (IAP) than adults due to their still developing lungs and immune systems and their relatively higher amount of air inhalation. Moreover, IAP affects children's respiratory health and it has been linked to respiratory symptoms and chronic diseases like asthma. Although children spend a great part of their day in school, there is still limited research on the effects of IAP exposure on childhood respiratory health. Specifically, concerning PM_{2.5}, previous studies in the literature highlighted its negative impact on human respiratory health (Nandasena, Wickremasinghe, and Sathiakumar 2013). Thus, this study mainly aimed to assess the impact of children's exposure to PM_{2.5} in urban nursery and primary schools on asthma-related symptoms.

2. Materials and Methods

The study population consisted of children in the early stages of education (aged 3 to 10), who attended 10 nursery and 10 primary schools located in metropolitan area of Porto. Based on previous studies (Branco et. al 2014), a microenvironmental modelling approach was followed to assess individual children's exposure to air pollution. This approach was based on continuous monitoring of PM_{2.5} in classrooms and time-location patterns obtained from the school timetable. Furthermore, continuous sampling of indoor PM_{2.5} levels was carried out over the first half of 2022 in 39 classrooms, during occupancy periods. PM_{2.5} exposure was dichotomized in "below" or "above" health protection levels, using the cut-off of 25 µg/m³ recommended by the World Health Organization (WHO) guidelines, for the association with respiratory health outcomes.

Simultaneously, a total of 649 questionnaires derived from the International Study of Asthma and Allergies in Childhood were completed, allowing to collect parent-reported individual information of sex, age, parental history of asthma, asthma previously diagnosed, and asthma-related symptoms (wheezing and dyspnea). Asthma previously diagnosed, and both active wheezing and dyspnea (reporting at least one episode in the previous year) were considered the main health outcomes in this study. Descriptive statistics were used to express the characteristics of individuals, PM_{2.5} exposure and health outcomes. Multivariate logistic regression models were used to estimate the odds ratio (OR) of the associations between PM_{2.5} exposure and each of the health outcomes

analysed, adjusted for parental history of asthma. Statistical analyses were performed with R Studio software. The level of statistical significance was set at 0.05.

3. Discussion

The findings of this study on children's daily indoor exposures to PM_{2.5} are consistent with previous literature (Branco et al 2019). The minimum, median, mean and maximum PM_{2.5} exposure levels observed were 13.4 µg/m³, 23.2 µg/m³, 28.1 µg/m³ and 127.4 µg/m³, respectively. Approximately 40% of the individuals (71.9% of preschoolers and 25.1% of primary school children) were exposed to PM_{2.5} levels above the threshold suggested by the WHO guidelines. Although the study population was well-balanced for gender, there was a higher proportion of primary school children (68.7%) compared to preschoolers (31.3%) involved in this study. Also, 20.8% of the study children had at least one asthmatic parent, and the prevalence of parent-reported asthma was 6.6%, both in accordance with previous studies, despite the variability in estimates of asthma prevalence among pediatric populations (Flores et al. 2022). The prevalence of ever wheezing and dyspnea (at least once in lifetime) was 30.7% and 13.1%, respectively, while the prevalence of active wheezing and dyspnea (at least one episode in the previous year) was 11.9% and 7.6%, respectively. Table 1 summarizes the results from the multivariate logistic regression models representing the association between exposure to PM_{2.5} and each studied health outcome.

Model / Health outcome	crude OR (95% CI)	crude p-value	adjusted OR (95% CI)	adjusted p-value
Asthma (reported)				
Exposure to PM _{2.5}	0.93 (0.49 - 1.76)	0.814	0.99 (0.51 - 1.91)	0.974
Parental history of asthma	4.81 (2.54 - 9.11)	< 0.001*	4.8 (2.53 - 9.11)	< 0.001*
Active wheezing				
Exposure to PM _{2.5}	1.58 (0.98 - 2.54)	0.062	1.68 (1.03 - 2.73)	0.038*
Parental history of asthma	2.88 (1.74 - 4.78)	< 0.001*	2.99 (1.8 - 4.98)	< 0.001*
Active dyspnea				
Exposure to PM _{2.5}	1.98 (1.09 - 3.61)	0.025*	2.07 (1.13 - 3.8)	0.018*
Parental history of asthma	2.57 (1.38 - 4.78)	0.003*	2.67 (1.43 - 5.01)	0.003*

*Significant at p-value < 0.05 calculated by likelihood ratio test.

Table 1: Crude and adjusted odds ratio (OR), and respective 95% confidence intervals (95% CI) and significance (p-value) of the associations between exposure to PM_{2.5} and reported asthma, as well as active wheezing and dyspnea.

Children's exposure to indoor PM_{2.5} in nursery and primary schools was not associated with reported asthma (aOR = 0.99, p-value = 0.974). However, concerning asthma-related symptoms, a statistically significant association with PM_{2.5} exposure above the threshold was found, revealing an increase in the odds of having active wheezing and dyspnea in childhood (aOR = 1.68, p-value = 0.038 and aOR = 2.07, p-value = 0.018, respectively). Evidence from prior studies in the literature demonstrated the negative impact of particulate matter on respiratory health, with children being particularly vulnerable. Specifically, short-term exposures to PM_{2.5} in schools have been associated with higher rates of hospital admissions and emergency department visits due to respiratory symptoms (Yang et al. 2019).

4. Conclusions

This study concluded that children were often exposed to PM_{2.5} levels higher than the WHO threshold inside nursery and primary schools. Moreover, it was identified statistically significant associations between PM_{2.5} exposure and respiratory health outcomes, specifically active wheezing and dyspnea, meaning an increased risk of respiratory symptoms in children exposed to PM_{2.5} concentration above WHO guidelines in schools. These findings highlight the importance of

studying IAP in schools and its potential impact on the respiratory health of children. Further research and interventions may be needed to reduce indoor PM_{2.5} exposure in schools. Also, the analysis should be extended to the PM_{2.5} exposure of a complete day, as well as to physician diagnosed respiratory health outcomes.

References

- Branco, P. T. B. S., M. C. M. Alvim-Ferraz, F. G. Martins, and S. I. V. Sousa. 2014. "The microenvironmental modelling approach to assess children's exposure to air pollution – A review." *Environmental Research* 135:317-332. doi: <http://dx.doi.org/10.1016/j.envres.2014.10.002>.
- Branco, Pedro T. B. S., Maria C. M. Alvim-Ferraz, Fernando G. Martins, and Sofia I. V. Sousa. 2019. "Quantifying indoor air quality determinants in urban and rural nursery and primary schools." *Environmental Research* 176:108534. doi: <https://doi.org/10.1016/j.envres.2019.108534>.
- Flores, Pedro, José E. Teixeira, Anna K. Leal, Luís Branquinho, Rui Brito Fonseca, Sandra Silva-Santos, Amanda Batista, Samuel Encarnação, António M. Monteiro, Joana Ribeiro, and Pedro Forte. 2022. "Asthma Prevalence in Adolescent Students from a Portuguese Primary and Secondary School." *Adolescents* 2 (3):381-388. doi: <https://doi.org/10.3390/adolescents2030029>..
- Nandasena, Sumal, Ananda Rajitha Wickremasinghe, and Nalini Sathiakumar. 2013. "Indoor air pollution and respiratory health of children in the developing world." *World journal of clinical pediatrics* 2 (2):6-15. doi: <https://doi.org/10.5409/wjcp.v2.i2.6>.
- Yang, Y., Z. Ruan, X. Wang, Y. Yang, T. G. Mason, H. Lin, and L. Tian. 2019. "Short-term and long-term exposures to fine particulate matter constituents and health: A systematic review and meta-analysis." *Environmental Pollution* 247:874-882. doi: <https://doi.org/10.1016/j.envpol.2018.12.060>.

Acknowledgments

This work was financially supported by: LA/P/0045/2020 (ALiCE) and UIDB/00511/2020 - UIDP/00511/2020 (LEPABE) funded by national funds through FCT/MCTES (PIDDAC). PTBS Branco thanks FCT for the financial support of his work contract through the Scientific Employment Stimulus - Individual Call – 2022.05461.CEECIND.

P29. Indoor air quality in vehicles: Can low-cost sensors be used as CO₂ indicators?

Ana Catarina T. Silva^{1,2*}, Pedro T.B.S. Branco^{1,2}, Sofia I.V. Sousa^{1,2}

¹LEPABE – Laboratory for Process Engineering, Environment, Biotechnology and Energy, Faculty of Engineering, University of Porto, Porto, Portugal




²ALiCE – Associate Laboratory in Chemical Engineering, Faculty of Engineering, University of Porto, Porto, Portugal

*Presenting author (up201605702@up.pt) ORCID (0000-0003-2847-7698)

Abstract

Exposure to elevated levels of CO₂ can impair driving performance and increase the risk of road accidents. This study evaluated the potential of low-cost sensors (LCS) of measuring and indicating CO₂ levels in vehicles. Data was collected in vehicles during 17 short and long trips, using LCS and reference instruments (ref). The performance of LCS was evaluated through Spearman correlation and by calculating the number of times that LCS detected CO₂ concentrations above the threshold (1376.5 mg/m³). Results showed that LCS captured a similar pattern of CO₂ levels as ref, though it registered higher peak concentrations during long trips. Of the 13% of CO₂ levels above the threshold, LCS detected 7%. The use of LCS can provide valuable insights into CO₂ levels in vehicles and help to reduce the associated risks of driving under high CO₂ exposure, yet future work should focus on LCS calibration to improve their accuracy.

Author Keywords. Indoor Air Quality, Vehicles, Transport, Low-cost Sensors, CO₂

 Open Access  Peer Reviewed  CC BY

1. Introduction

Indoor air pollution (IAP) is a significant health concern and carbon dioxide (CO₂) is one of the main concerns in enclosed spaces (Azuma et al., 2018). High levels of CO₂ in vehicles can lead to poor driving performance and increase the risk of road accidents, as it can impair cognitive functioning (Lohani et al., 2022). Despite the growing interest in IAP in many indoor environments, the literature in vehicles is still limited. Only a few studies have characterized IAP inside vehicles and its correlation with other variables such as ventilation (Chen et al., 2020; Hofman & Manna, 2020). However, to the best of the authors' knowledge, no studies have investigated the potential of low-cost sensors (LCS) as a tool for monitoring and controlling CO₂ levels in vehicles.

This study aimed to evaluate the reliability and potential of LCS in measuring CO₂ inside vehicles and their effectiveness as indicator tools for car occupants. This study compared the performance of LCS against research-grade reference instruments and evaluated the influence of journey duration on LCS measurements.

2. Materials and Methods

2.1. Data collection

Data was collected between February 16th and April 16th, 2021, from four similar diesel-fueled vehicles occupied only by the driver (always the same) over 17 trips. The trips were classified according to their duration as short (≤ 30 min, median of 17min) or long (> 30 min, median of 43min), resulting in 10 short and 7 long trips. The LCS AirVisual Pro (IQAir), herein referred as 'av1' (log time of 10s), and the research-grade reference instrument GrayWolf Advanced Sense BE (log time of 1min), herein defined as 'ref', were used to collect CO₂ data. Another similar AirVisual Pro, herein referred as 'av2', was collocated in 7 trips to validate av1 measurements. CO₂ concentrations obtained from LCS were averaged (1-min) to compare with ref.

2.2. Data analysis

Descriptive statistics were used to evaluate the performance of LCS in comparison to ref. Normality was evaluated using the Shapiro-Wilk test, and Spearman correlation was used to quantify the relationship between the two LCS (av1 and av2) and between those and reference instrument. The number of concentrations above the threshold considered (1376.5 mg/m³, 600 ppm) detected by LCS and reference instrument was also counted to determine if LCS can serve as an indicator tool. The cutoff CO₂ concentration of 1376.5 mg/m³ was chosen as threshold based on literature indicating no health effects below this concentration (Hudda & Fruin, 2018). These analyses were

performed using the R Studio software (version 4.2.1) (Team, 2022). The level of statistical significance was set at 0.05 (p -value < 0.05).

3. Discussion

3.1. CO₂ Characterisation

Overall, the average CO₂ concentrations measured by av1 and ref were similar (av1 = 1070 mg/m³, ref= 1090 mg/m³), and both instruments showed a similar pattern of CO₂ levels (Figure). Most of the time (87%), the median CO₂ levels remained between 800 mg/m³ to 1200 mg/m³, which is within the threshold of <1376.5 mg/m³. However, peak CO₂ concentrations (black dots) were observed a few times (exceeding this limit), especially during long trips. Analogous results were obtained for av2 (when collocated with av1).

3.2. LCS performance

The Spearman correlation showed a strong positive correlation between the two LCS ($\rho = 0.9$; p -value < 0.05), validating av1 measurements. A similar strong correlation between av1 and ref ($\rho = 0.8$; p -value < 0.05) was obtained.

Ref detected CO₂ concentrations above the safe threshold (1376.5 mg/m³) in 13% of the measurements (83/633). On the other hand, LCS was able to capture 7% of the times that CO₂ levels were above the threshold (44/633). Thus, LCS could detect 53% (44/83) of the concentrations that ref measured above the threshold.

4. Conclusions

The study results demonstrate the importance of implementing measures to reduce CO₂ levels in vehicles, as even with only one driver the CO₂ concentrations exceeded the safe threshold (1376.5 mg/m³) several times. Given that CO₂ is a byproduct of human metabolism, higher levels can be expected with more occupants in the vehicle. The LCS tool used in this study has the potential to serve as an indicator of CO₂ levels, as it was able to capture more than half of the times the concentrations that exceeded the threshold. However, further research is needed to improve the accuracy of LCS measurements, which may involve the calibration process and subsequent evaluation of their performance.

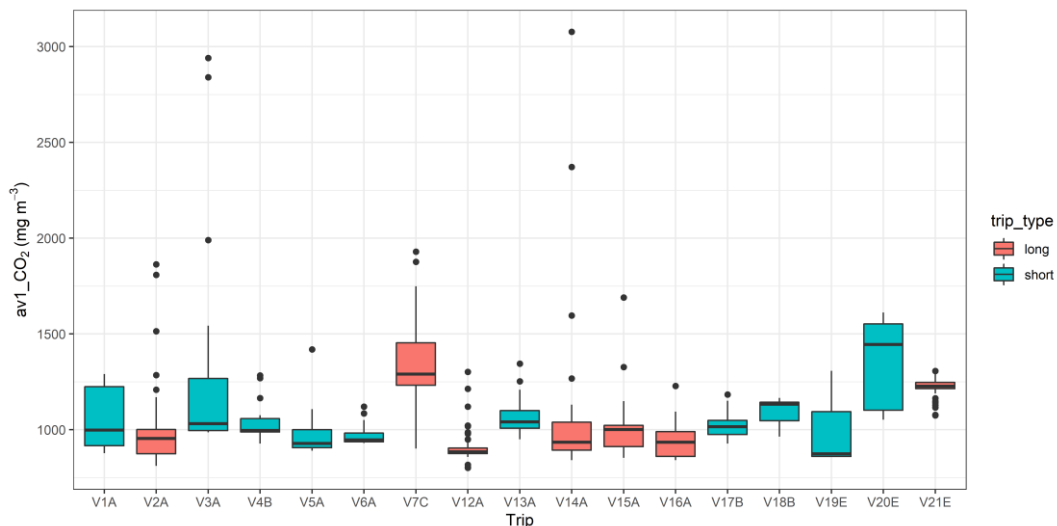


Figure 1: Boxplot representation of the CO₂ concentrations (in mg/m³) measured by the low-cost sensor AirVisual Pro (av1), per type of trip (short or long).

References

Azuma, K., Kagi, N., Yanagi, U., & Osawa, H. (2018). Effects of low-level inhalation exposure to carbon dioxide in indoor environments: A short review on human health and psychomotor

performance. *Environment International*, 121, 51-56.
<https://doi.org/https://doi.org/10.1016/j.envint.2018.08.059>

- Chen, R.-Y., Ho, K.-F., Chang, T.-Y., Hong, G.-B., Liu, C.-W., & Chuang, K.-J. (2020). In-vehicle carbon dioxide and adverse effects: An air filtration-based intervention study. *Science of The Total Environment*, 723, 138047. <https://doi.org/https://doi.org/10.1016/j.scitotenv.2020.138047>
- Hofman, J., & Manna, V. P. L. (2020, 25-28 Oct. 2020). The Air Quality Paradigm inside Car Microenvironments; Balancing between PM2.5 and CO2 Offsets. 2020 IEEE SENSORS,
- Hudda, N., & Fruin, S. A. (2018). Carbon dioxide accumulation inside vehicles: The effect of ventilation and driving conditions. *Science of The Total Environment*, 610-611, 1448-1456. <https://doi.org/https://doi.org/10.1016/j.scitotenv.2017.08.105>
- Lohani, D., Barthwal, A., & Acharya, D. (2022). Modeling vehicle indoor air quality using sensor data analytics [Article]. *Journal of Reliable Intelligent Environments*, 8(2), 105-115. <https://doi.org/10.1007/s40860-021-00137-2>
- Team, R. C. (2022). R: A language and environment for statistical computing. R Foundation for Statistical Computing. <https://doi.org/https://www.R-project.org/>.

Acknowledgments

This work was financially supported by LA/P/0045/2020 (ALiCE), UIDB/00511/2020 and UIDP/00511/2020 (LEPABE), funded by national funds through FCT/MCTES (PIDDAC) and Project 2SMART - engineered Smart materials for Smart citizens, with reference NORTE-01-0145-FEDER-000054, supported by Norte Portugal Regional Operational Programme (NORTE 2020), under the PORTUGAL 2020 Partnership Agreement, through the European Regional Development Fund (ERDF). PTBS Branco thanks the Portuguese Foundation for Science and Technology (FCT) for the financial support of his work contract through the Scientific Employment Stimulus - Individual Call – 2022.05461.CEECIND. Ana Catarina T. Silva thanks the Portuguese Foundation for Science and Technology (FCT) for the individual research grant 2022.11772.BD.

P30. Future shipping emissions – a review

Rafael A.O. Nunes^{1,2*}, Maria C.M. Alvim-Ferraz^{1,2}, Fernando G. Martins^{1,2}, Sofia I.V. Sousa^{1,2}

¹LEPABE – Laboratory for Process Engineering, Environment, Biotechnology and Energy, Faculty of Engineering, University of Porto, Rua Dr. Roberto Frias, 4200-465, Porto, Portugal

²ALICE – Associate Laboratory in Chemical Engineering, Faculty of Engineering, University of Porto, Rua Dr. Roberto Frias, 4200-465 Porto, Portugal

*Presenting author (raonunes@fe.up.pt) ORCID [0000-0002-0810-7916](https://orcid.org/0000-0002-0810-7916)

Abstract

In this work, 16 studies conducted since 2012 calculating and/or using future shipping emissions to assess their impacts on health or the environment were reviewed. The authors reported a general decrease in SO_x, NO_x, and PM_{2.5} concentrations due to emission regulations, but current regulatory energy efficiency policies may not compensate for the increase in traffic and resulting CO₂ emissions. The impacts on climate change of future ship-related emissions were rarely studied, and none of the studies considered external costs and International Maritime Organization target to reduce CO₂ emissions. Future studies should assess the impacts of future ship emissions on health and external costs, on climate change and include alternative fuels.

Author Keywords. Shipping emissions, Future scenarios, CO₂ IMO target

 Open Access  Peer Reviewed  CC BY

1. Introduction

Shipping traffic is an important source of air pollution, including emissions of carbon dioxide (CO₂), mainly in coastal regions (Ramacher et al. 2020). According to the projections, it is expected that shipping will grow by 50-250% until 2050 (Kalli et al. 2013; IMO 2015). International legal actions have been implemented by the International Maritime Organization (IMO) to lower ship-related emissions globally. Still, despite all the efforts, most scenarios for the next 20-30 years indicate that current regulatory policies may not be sufficient to outweigh an increase in traffic in terms of CO₂ reduction goals (Kalli et al. 2013; Ramacher et al. 2020; Jutterström et al. 2021). Considering the need for new studies on future emissions, the present study aims at providing a literature review that includes studies establishing future shipping emissions scenarios or using them to investigate the impact of future shipping emissions on air pollution, human health and climate.

2. Materials and Methods

This review analysed studies published in the last 10 years in the following databases: Science Direct, Scopus, PubMed, and Google Scholar, with no language restrictions. The search identified 16 articles that met the inclusion criteria: i) assessing future shipping emissions impacts on air pollution, and/or human health and or/and climate (Browse et al. 2013; Dalsøren et al. 2013; Winther et al. 2014; Jonson et al. 2015; Matthias et al. 2016; Sofiev et al. 2018; Chen et al. 2019; Ramacher et al. 2020; Zhao et al. 2020; Geels et al. 2021); ii) quantifying the contribution of future shipping emissions to pollutants deposition (Gong et al. 2018; Karl et al. 2019; Jutterström et al. 2021); and iii) considering the impact of emission control areas and specific measures to be implemented in the future (Kalli et al. 2013; Song and Shon 2014; Eiof Jonson et al. 2019).

3. Discussion

For the establishment of future scenarios, authors developed or adapted considerations regarding the growth and renewal of the ship fleet, percentage of sulfur in fuels, different implementation dates for NO_x tier III, implementation of abatement technologies, namely the use of exhaust gas cleaning systems, the use of liquefied natural gas as an alternative fuel, energy efficiency measures, implementation of emission control areas (ECAs) and the use of shoreside electricity. Most authors reported a general decrease in SO_x, NO_x, and PM_{2.5} concentrations and consequent reduction on the health impacts, due to the regulations adopted over the years. However, authors who studied CO₂ emissions reported that the current regulatory energy efficiency policies seem not be sufficient to compensate the increase of shipping traffic emissions in the next 20 to 30 years. IMO established

in 2018 a target to reduce CO₂ emissions from transport by 50 % by 2050 compared to 2008 levels. As far as known, the impacts on climate change were rarely studied, and none of the studies considered external costs and IMO's target. Figure summarizes the main results reported by the authors and outlines factors to be considered in future studies. Based on the findings, once emission factors are available for alternative fuels (such as ammonia and biofuels), it is recommended that future studies include them to reduce uncertainties regarding how maritime transport industry can achieve the necessary CO₂ reductions to meet IMO's target. It is also important to add estimations of external costs due to health impacts, and climate change assessment.

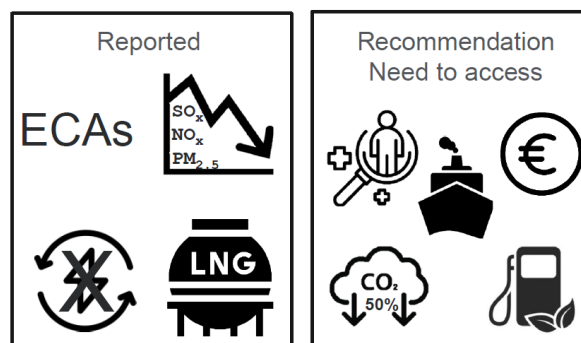


Figure 1: summarizes the main results reported by the authors and outlines the factors to be considered in future studies.

4. Conclusions

While regulations will help to reduce the impact of future ship emissions on air pollution and health, more research is needed to estimate external costs and climate change. Furthermore, it is recommended future studies consider alternative technologies, such as ammonia and biofuels, to investigate how maritime transport industry can achieve the required CO₂ reductions to meet the International Maritime Organization's target of reducing emissions by 50 % by 2050 compared to 2008 levels.

References

- Browse, J., et al. 2013. "Impact of Future Arctic Shipping on High-Latitude Black Carbon Deposition." *Geophysical Research Letters* 40 (16). DOI:10.1002/grl.50876.
- Chen, et al. 2019. "Ship Emission Impacts on Air Quality and Human Health in the Pearl River Delta (PRD) Region, China, in 2015, With Projections to 2030." *GeoHealth* 3 (9). DOI:10.1029/2019GH000183.
- Dalsøren, S. B., et al. 2013. "Environmental Impacts of Shipping in 2030 with a Particular Focus on the Arctic Region." *Atmospheric Chem. Phys.* 13 (4): 1941–55. DOI:10.5194/acp-13-1941-2013.
- Eiof J., et al. 2019. "Effects of Strengthening the Baltic Sea ECA Regulations." *Atmospheric Chem. Phys.* 19 (21). DOI:10.5194/acp-19-13469-2019.
- Geels, C., et al. 2021. "Projections of Shipping Emissions and the Related Impact on Air Pollution and Human Health in the Nordic Region." *Atmospheric Chem. Phys.* 21 (16). DOI:10.5194/acp-21-12495-2021.
- Gong, W., et al. 2018. "Assessing the Impact of Shipping Emissions on Air Pollution in the Canadian Arctic and Northern Regions: Current and Future Modelled Scenarios." *Atmospheric Chem. Phys.* 18 (22): 16653–87. DOI:10.5194/acp-18-16653-2018.
- IMO. (2015). Third IMO Greenhouse Gas Study 2014 - Executive Summary. 1–26.
- Jonson, J., et al. 2015. "Model Calculations of the Effects of Present and Future Emissions of Air Pollutants from Shipping in the Baltic Sea and the North Sea." *Atmospheric Chem. Phys.* DOI:10.5194/acp-15-783-2015.
- Jutterström, S., et al. 2021. "The Impact of Nitrogen and Sulfur Emissions from Shipping on the Exceedance of Critical Loads in the Baltic Sea Region." *Atmospheric Chem. Phys.* 21 (20).

DOI:10.5194/acp-21-15827-2021.

- Kalli, J., et al. 2013. "Atmospheric Emissions of European SECA Shipping: Long-Term Projections." *WMU Journal of Maritime Affairs* 12 (2). DOI:10.1007/s13437-013-0050-9.
- Karl, .M, et al. "Impact of a Nitrogen Emission Control Area (NECA) on the Future Air Quality and Nitrogen Deposition to Seawater in the Baltic Sea Region." *Atmospheric Chem. Phys.* 19 (3). DOI:10.5194/acp-19-1721-2019.
- Matthias, V., et al. 2016. "The Impact of Shipping Emissions on Air Pollution in the Greater North Sea Region-Part 2: Scenarios for 2030." *Atmospheric Chem. Phys.* 16 (2): 759–76. DOI:10.5194/acp-16-759-2016.
- Ramacher, M. O.P., et al. 2020. "The Impact of Ship Emissions on Air Quality and Human Health in the Gothenburg Area - Part II: Scenarios for 2040." *Atmospheric Chem. Phys.* 20 (17). DOI:10.5194/acp-20-10667-2020.
- Sofiev, M., et al. 2018. "Cleaner Fuels for Ships Provide Public Health Benefits with Climate Tradeoffs." *Nature Communications* 9 (1). DOI:10.1038/s41467-017-02774-9.
- Song, Sang Keun, and Zang Ho Shon. 2014. "Current and Future Emission Estimates of Exhaust Gases and Particles from Shipping at the Largest Port in Korea." *Environmental Science and Pollution Research* 21 (10): 6612–22. DOI:10.1007/s11356-014-2569-5.
- Winther, M., et al. 2014. "Emission Inventories for Ships in the Arctic Based on Satellite Sampled AIS Data." *Atmospheric Environment* 91: 1–14. DOI:10.1016/j.atmosenv.2014.03.006.
- Zhao, J., et al. 2020. "Projection of Ship Emissions and Their Impact on Air Quality in 2030 in Yangtze River Delta, China." *Environmental Pollution* 263. DOI:10.1016/j.envpol.2020.114643.

Acknowledgments

This work was financially supported by: LA/P/0045/2020 (ALiCE) and UIDB/00511/2020 - UIDP/00511/2020 (LEPABE) funded by national funds through FCT/MCTES (PIDDAC). RAO Nunes acknowledges FCT for the individual research grant SFRH/BD/146159/2019.

Alemi, Mahdi	29
Alves, Arminda	26, 35, 132
Alvim-Ferraz, Maria C.M.	144, 150
Amorim, Daniela	50
Azevedo, Marta A. P.	103
Bacelo, Hugo A.M.	38
Bastos, Margarida M.S.M.	38
Benniche, Salima	77
Bernárdez, Nuria	74
Bernárdez, Nuria	80
Bernardino, Raul	32
Bernardo, Fábio	26
Boaventura, Rui	86
Botelho, Cidalia	77, 86
Braga, Vasco	18
Bragança, Idalina	129
Branco, P.T.B.S	138, 144, 147
Brito, Inês	59
Brito, Margarida S.C.A.	120
Cabral, Sofia	18
Caetano, Nídia	56
Capitão, Jeffrey	44
Cereceda-Balic, Francisco	35
Chojer, H.	138
Coronas, Joaquín	123
Correia-Sá, Luísa	15
Cotrim, Luís	32
Cullen, Laura J. R.	98
Delerue-Matos, Cristina	15, 53, 114
Dias, Mafalda	23
Dias, Paula	44, 135
Dorosh, Olena	53
Esteves, Ana F.	65, 68
Fadic, Ximena	35
Faria, Joaquim L.	101, 106
Fdez-Sanromán, Antía	92
Fernandes, Ana Sofia	117
Fernandes, Isabel S.	98
Ferreira, Alexandre	123
Ferreira, Sara M.	59
Ferreira, Teresa	132
Ferreira, Tiago	35
Figueiredo, Sónia	56
Figueiredo, Sónia A.	15
Fonseca, André	32
Fontas, Claudia	77

Fraga, Carolina	23
Francisco, Filipe Moisés M.	135
Fujita, Amanda	101
Giráldez, Alba	111
Gomes, Ana I.	89
Gomes, Sandra M.	41, 132
Gonçalves, Ana L.	68
González-Romero, E.	126
Gouveia, Joana R.	47
Graça, Cátia A. L.	103, 108
Homem, Vera	26, 35, 117, 129
Ivanou, Dzmitry	44
Jafarzadeh, Sayedreza	29
Kebiche-Senhadji, Ounissa	77
Leitão, Anabela	132
Lima, Aías	56
Lomba, Bárbara	80
Lopes, Tânia	44
Loureiro, Joana A.	71
Maia, Carolina	71
Maia, Rodrigo	29
Manaia, Célia M.	18
Martelo, Liliana M.	38, 103
Martínez-Izquierdo, Lidia	123
Martins, Fernando G.	50, 138, 144, 150
Martins, Rúben A.	68
Matiazzo, Tatiana	95
Mendes, Adélio	44, 135
Mesquita, Sara	23
Miranda, Rita	41
Miranda, Sandra M.	95
Montes, Rosa	89
Moreira, Manuela M.	53
Neto, Belmira	47
Nobre, Maria L.F.	23
Nunes, Olga C.	18
Nunes, Rafael A.O.	150
Oliveira, Bruna	23
Oliveira, Catarina M.	23
Oliveira, Luís	47
Orge, Carla A.	108
Pacheco, João G.	114
Padoin, Natan	95
Pazos, Marta	74, 80, 83, 92, 111, 126
Peixoto, Margarida L.R.	120
Pereira, Manuel F. R.	108
Pereira, Maria Carmo	71, 141
Pintor, Ariana	77

Pires, José C.M.	23, 50, 65, 68, 71
Poza-Nogueiras, Verónica	80, 114
Quintana, José B.	89
Ramísio, Paulo	56
Ramos, Larissa	71
Ratola, Nuno	26, 35, 129
Remor, Paula V.	15
Restivo, João	108
Ribeirinho-Soares, Sara	18
Rocha, Filipe	117, 129
Rodil, Rosário	89
Rodrigues, Alírio	123
Rodrigues, Inês	123
Rodrigues, Leonardo	44
Rodrigues, Mafalda	86
Rodrigues, Maria	32
Rosales, Emilio	74, 83, 92, 126
Rúa-Pereira, M.	126
Sá, Juliana P.	144
Salgado, Eva	65, 68
Sampaio, Maria J.	101
Sánchez-Soberón, Francisco	26
Sanromán, M. Ángeles	74, 80, 83, 92, 111, 126
Santos, Carla S.	89
Santos, Lúcia	41, 59, 132
Santos, Ounísia	32
Santos, Ricardo J.	98, 120
Santos, Sílvia	86
Sebastião, Fernando	32
Silva Lopes, Telmo da	44
Silva, Adhymaura	141
Silva, Adrián M.T.	101, 103, 106
Silva, Ana Catarina T.	147
Silva, Cláudia G.	101, 106
Silva, Márcia A.D.	38, 103
Silva, Tânia F. C. V.	95
Silva, Thiago	117
Slezakova, Klara	141
Soares, Cíntia	95
Soares, Cristina	15
Soares, Helena M.V.M.	38, 103
Soares, Olívia S. G.P.	108
Soto, E.	126
Sousa, Juliana	108
Sousa, S.I.V.	138, 144, 147, 150
Sousa, Sara	65
Tavares, Daniel	23
Téllez, Carlos	123

Terrón, Daniel	83
Thalita Tavares	106
Tomasi, Isabella	86
Torres-Pinto, André	101, 106
Vaz, Daniela	32
Vieira, Judite	32
Vilar, Vítor J.P.	15, 18, 89, 95, 98, 120, 123
Zema, Riccardo	108



ISBN: 978-972-752-301-6



9 789727 523016 >

🏠 www.fe.up.pt/dce

✉ dce@fe.up.pt